# 6. Site 1171[1]

Shipboard Scientific Party[2]

## PRINCIPAL RESULTS

Site 1171 is located in lower bathyal water depths of ~2150 m on a gentle southwesterly slope on the southernmost South Tasman Rise (STR), ~550 km south of Tasmania and 270 km southeast of Site 1170. At 48°30′S, Site 1171 lies in subantarctic waters between the Subtropical Convergence and the Subantarctic Front. In this area, very strong surface and bottom currents are associated with the Antarctic Circumpolar Current. The major objectives were to (1) core and log an Oligocene to Holocene pelagic carbonate section to evaluate expected major paleoceanographic and paleoclimatic effects resulting from the opening of the Tasmanian Gateway near the time of the Eocene/Oligocene boundary and later development of deep Antarctic Circumpolar Current flow; (2) core and log an expected underlying detrital sedimentary Eocene sequence to evaluate paleoenvironmental conditions during rifting of the STR from Antarctica; and (3) obtain high-resolution sedimentary records from critical subantarctic latitudes to better understand the role of the Southern Ocean in climate changes during the Neogene.

Site 1171 is located on thinned continental crust, just west of the strike-slip boundary between the central and eastern STR blocks that moved with Antarctica until 66 Ma. The boundary is the Balleny Fracture Zone, which extends southward to Antarctica. Seismic and other data indicate that during the Late Cretaceous to Paleocene, the blocks themselves were cut by strike-slip faults that developed as Australia moved northwestward, and later northward, past Antarctica. Basins that formed in association with this tectonism are filled with ~1000 to 2000 m of Cretaceous through Eocene rift sediments deposited during steady subsidence.

Site 1171 is in a small north-south oriented rift basin, bounded to the east by the Balleny Fracture Zone. The middle Eocene fast seafloor spreading and opening to the south strengthened the basin's connec-

tion to the Pacific Ocean and its difference in setting to that of Site 1170 in the Australo-Antarctic Gulf. Seismic profiles and regional correlations suggest that the site was subject to steady deposition of prograded siliciclastic deltaic sediments through the Cretaceous into the Eocene and hemipelagic sedimentation grading to pelagic sedimentation thereafter (Fig.F1). Much of the siliciclastic detritus must have come from the high, subaerial bounding blocks of continental crust and also along the basin from the higher northern areas. The southwestern tip of the STR cleared Antarctica during the early Oligocene and deep antarctic circumpolar circulation became established. Site 1171 was selected because of its extreme southern location on the STR, in sufficiently shallow water to provide a carbonate sequence unaffected by dissolution. Thus, the site was designed to provide critical data about STR subsidence and on the timing of the initial surface water, and later deep-water flow, through the opening of the Tasmanian Gateway between Australia and Antarctica.

At Site 1171 we cored two advanced hydraulic piston corer (APC) holes, one APC/XCB (extended core barrel) hole, and a rotary cored hole (Table T2, p. 94, in the "Leg 189 Summary" chapter). Because weather conditions were good during the APC drilling, construction of a composite section of the total triple-cored portion of the sedimentary sequence was possible to 118 mbsf (late Miocene). Beyond that, there are limited gaps, but core recovery averaged 81.8%. Hole 1171A was APC cored to 124 mbsf with 94.5% recovery, Hole 1171B was APC cored to 109 mbsf with 98.1% recovery, and Hole 1171C was APC/XCB cored to 275 mbsf with 89.4% recovery. Hole 1171D was rotary cored from 248 to 959 mbsf with 73.9% recovery. The interbedded hard and soft beds from 265 to 440 mbsf greatly reduced recovery of both the XCB and rotary core barrel (RCB) drilling and stopped XCB coring earlier than desired. Because of operational problems, wireline logging was conducted only with the triple-combo string over most of Hole 1171D.

Site 1171, with a total sediment thickness of 959 m, ranges in age from late Paleocene (58 Ma) to Quaternary. The Neogene section is largely complete except for a hiatus in the uppermost Miocene. The Paleogene record from the early middle Eocene to the latest Oligocene is cut by five hiatuses, and the Oligocene is poorly represented. The older sequence consists broadly of ~616 m of rapidly deposited shallow-water silty claystone of late Paleocene to late Eocene age (lithostratigraphic Units V and VI) overlain by 67 m of diatom-bearing claystone of late Eocene age (lithostratigraphic Unit IV) and 6 m of shallow water, glauconitic siltstone, deposited slowly during the latest Eocene (Unit III). Unit III is overlain by 67 m of slowly deposited, deep-water nannofossil chalk and ooze of early Oligocene to early Miocene age (Unit II); limestone and siliceous limestone beds are in the base of the Oligocene section. Unit I consists of 234 m of deep-water foraminifer-bearing nannofossil ooze and chalk of early Miocene to Holocene age. The lithostratigraphic sequence has been divided into six units and a number of subunits.

Lithostratigraphic Unit I (0–253 mbsf), of early Miocene to Pleistocene age, has been divided into two subunits: Subunit IA to 41 mbsf and Subunit IB to 253 mbsf. Subunit IA is a white to light gray foraminiferal nannofossil ooze and foraminifer-bearing nannofossil ooze, whereas Subunit IB is a nannofossil ooze and chalk, which is distinguished from Unit IA by decreasing foraminiferal content. Carbonate content averages 93 wt% and organic carbon is very low (<0.2 wt%) in Unit I. Average sedimentation rates were low.

**F1.** Postdrilling interpretation for local seismic profile AGSO 202-5, across Site 1171, p. 65.
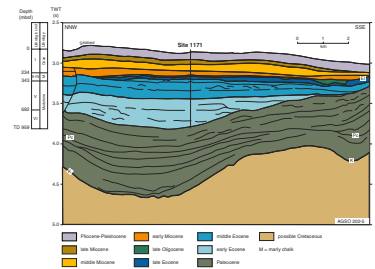
Lithostratigraphic Unit II (253–270 mbsf), of late Oligocene age, is a white to light greenish gray nannofossil chalk characterized by a downsection increase in the detrital components (e.g., glauconite, quartz, and mica) and a decrease in the biogenic fraction. Organic carbon content is low, and carbonate content decreases from 95 wt% at the top to 75 wt% at the base. Sedimentation rates were very low.

Lithostratigraphic Unit III (270–276 mbsf) is ~6 m of dark greenish gray to blackish green glauconitic sandy to clayey glauconitic siltstone of late Eocene age. Carbonate content decreases from 77 wt% at the top of the unit to 0.4 wt% at the base. Organic carbon content is extremely low and approaches zero.

Lithostratigraphic Unit IV (276–343.5 mbsf) is a middle to upper Eocene nannofossil-bearing diatomaceous silty claystone that darkens downsection from olive gray to dark gray and bottoms in a black chert. Carbonate content is low (5 wt%) and organic carbon averages 0.4 wt%.

Lithostratigraphic Unit V (343.5–692.5 mbsf) is composed of claystones and silty claystones of middle Eocene age and is divided into three subunits. Subunit VA consists of dark greenish gray or dark olive-gray claystone and nannofossil-bearing claystone. Carbonate content averages 14 wt%, and organic carbon content is 0.5 wt%. Subunit VB is a dark gray claystone, occasionally organic matter–bearing, and is distinguished from Subunit VA by a lower nannofossil abundance, darker color, and higher organic carbon content (average = 1 wt%). Carbonate content is very low (1 wt%). Subunit VC is olive gray to dark olive-gray silty claystone with higher nannofossil abundance and lower organic carbon (0.5 wt%) than the overlying subunit. Carbonate content averages 8 wt%. Sedimentation rates fluctuated between 4–12 cm/k.y.

Lithostratigraphic Unit VI (692.4–958.8 mbsf) is early Eocene to late Paleocene in age and has been divided into two subunits. Subunit VIA is lower Eocene greenish gray nannofossil-bearing silty claystone in the upper part and silty claystone in the lower part. Carbonate nodules and pressure solution seams are sporadic through the subunit. Carbonate content is low, averaging 2 wt%, and organic carbon is 0.5 wt%. Subunit VIB is lowermost Eocene to upper Paleocene silty claystones that give way to dark grayish brown, organic matter–bearing clayey siltstones in the lower part. The bottom ~40 m of the subunit is pervasively laminated. Carbonate content is <1 wt% and organic carbon content (0.9 wt%) is higher than in Subunit VIA. Sedimentation rates average 4 cm/k.y.

In general, calcareous nannofossils at Site 1171 are abundant in the Neogene and Oligocene, highly variable in abundance in the Eocene (where they are also absent in many intervals), and rare in the Paleocene. The Neogene and Oligocene are marked by highly abundant and well-preserved calcareous nannofossils and planktonic foraminifers and relatively abundant radiolarians and diatoms. In contrast, the Eocene has many intervals barren of calcareous microfossils, especially planktonic foraminifers. Radiolarians and diatoms are rare to absent throughout much of the Eocene, although neritic planktonic and benthic diatoms are common in the upper Eocene. The shallow-water Eocene siliciclastics are distinguished by a continuous record of abundant organic dinoflagellate cysts and pervasive pollen and spores, which are critical for biostratigraphic subdivision of this interval and provide a rich paleoenvironmental record. The Paleocene sediments also contain abundant assemblages of organic palynomorphs, but only rare to few calcareous nannofossils. Planktonic foraminifers, radiolarians, and diatoms are absent. Benthic foraminifers, which have provided critical in-

formation on benthic environments, are largely present throughout the entire sequence and are noticeably more abundant in the Eocene.

Sedimentation rates determined from the fossil record were rapid (4–12 cm/k.y) during the Paleocene to middle Eocene. Biostratigraphic datums indicate four brief hiatuses (~2 m.y.) interspersed with brief periods of slow sedimentation (<1 cm/k.y.) through the late Oligocene to the middle Eocene. Sedimentation rates were low, fluctuating between 0.7–2.0 cm/k.y. in the early and middle Miocene, increased to 3.8 cm/k.y across the middle/late Miocene boundary, and decreased again to a very low 0.5 cm/k.y. during the late Miocene. The Miocene/Pliocene boundary is marked by a hiatus of at least 1.6 m.y., followed by slow sedimentation (1.3 cm/k.y.) in the Pliocene–Pleistocene.

A major result of the coring was the discovery that the unconformity separating flat-lying strata from gently dipping strata in seismic profiles corresponds to the Paleocene/Eocene boundary. This means that tectonism in this small basin, bounded by the major strike-slip fault system of the Balleny Fracture Zone, ended at ~55 Ma. This strongly suggests that the driving force for the strike-slip motion, the separation of Australia and Antarctica, no longer affected this part of the STR from that time, accurately defining the age of the onset of seafloor spreading to the south as 55 Ma. It is surely no coincidence that uplift of the western and eastern onshore margins of Tasmania occurred in the late Paleocene to early Eocene (O'Sullivan and Kohn, 1997).

Similar to Site 1168 on the west Tasmania margin, and Site 1170 on the eastern STR, pore-water freshening (13% decrease in $Cl^-$ relative to seawater) is also observed at Site 1171 below ~320 mbsf, which is coincident with the onset of methanogenesis, but unexpectedly below the interpreted bottom-simulating reflector. Organic matter is immature through most of the cored interval, with maturity increasing with depth. However, organic matter is mature toward the base of the cored interval, and gases have a thermogenic signature, although total gas quantities are low. Characterization of the organic matter (hydrogen index) indicates three intervals of upwardly increasing marine influence in the early to middle Eocene.

The wireline logs were confined to a single complete run of the triple-combo tool in Hole 1171D because of technical and hole stability problems. Logging data display a strong cyclicity, especially the Th spectrum of the natural gamma-ray log in the middle Eocene section. Variability in log data also may record alternating marine and terrestrial influences. Distinct spikes in resistivity and density are observed in middle Eocene sediments, which likely correlate with indurated carbonates and/or glauconite and tend to be directly above Th and K peaks, indicating increased input of terrestrial clays.

The Paleogene (late Paleocene through Oligocene) depositional history is one of increasing ventilation and a major, rapid increase in water depths that began to occur near the Eocene/Oligocene boundary. This deepening causes transformation from shallow (neritic) to deep open-ocean conditions. Late Paleocene sediments were deposited in near anoxic conditions in near-shore highly sheltered environments, with resulting high organic carbon content. Early to middle Eocene neritic sediments show evidence of being less restricted as reflected by pervasive, well-developed sediment bioturbation and increasing abundance of calcareous nannofossils.

The Eocene–Oligocene transition at Site 1171 is marked by a series of distinct stepwise environmental changes, reflecting increasingly cool conditions and coeval rapid deepening of the basin. By the earliest

Eocene, a change had occurred from inner neritic environments with freshwater influences and sluggish circulation, to outer neritic environments with increased ventilation and bottom-current activity. Concomitant cooling is indicated by episodic increases of endemic antarctic dinocyst taxa, a trend that continued through the late Eocene to earliest Oligocene (~34.0–33.3 Ma). Sediments and biota indicate increasing bottom-water ventilation and more productive surface waters at slightly deeper depths (outer neritic to upper bathyal depths), with increasingly cold conditions. This trend culminated in the early Oligocene (33–30 Ma) with a distinct increase in open-ocean upwelling and rigorous ventilation that precluded accumulation of organic matter, despite the overall higher surface-water productivity. At this time, slow deposition of silica-rich calcareous sediments commenced in lower bathyal depths.

As at Site 1170, the sedimentary succession of Site 1171 records three major phases of paleoenvironmental development that are consistent with the hypothesis that initial development and evolution of the middle and late Cenozoic cryosphere resulted from thermal isolation of the Antarctic by the development of the Antarctic Circumpolar Current and the Southern Ocean:

1. Late Paleocene to early late Eocene rapid deposition of shallow-water (neritic) siliciclastic sediments during rifting between Antarctica and the STR. This was a time of minimal or no connection between the Pacific Ocean, in which these sediments were deposited, and the Australo-Antarctic Gulf in the southern Indian Ocean.
2. A relatively brief transitional interval of slow sedimentation with shallow-water late Eocene glauconitic siliciclastic sediments changing suddenly to earliest Oligocene deeper water clayey biogenic carbonates. Deposition of the glauconitic sediments represents initiation of moderate current activity as the Tasmanian Gateway opened to shallow (neritic) waters. Deposition of the overlying carbonates heralds the development of open-ocean conditions in the Gateway and initiation of circumpolar circulation.
3. Oligocene through Quaternary deposition of pelagic carbonate sediments in increasingly deep waters and in increasingly open-ocean conditions as the Southern Ocean developed and expanded with the northward flight of the STR and the Australian continent.

Although the history of sedimentation at Sites 1171 and 1170 exhibits the same broad regional trends, strong evidence exists that, up until the late Eocene, sediments accumulated in separate basins isolated by the Tasmanian land bridge. This is most clearly shown by the poorly ventilated depositional environment at Site 1170 vs. the relatively more ventilated environment at Site 1171. This is consistent with the interpretation of highly restricted marine conditions at the easternmost end of the Australo-Antarctic Gulf, as is also suggested by the Eocene sediment record at Site 1168 off western Tasmania.

Climatic implications resulting from interpretations of data from Site 1170 and other locations on the STR include the following:

1. The rapid transformation from Eocene siliciclastic sediments to Oligocene pelagic carbonates near the Eocene/Oligocene boundary in the STR region seems to have resulted largely from major

cooling of Antarctica that caused greatly reduced rainfall, weathering, and erosion and, hence, greatly reduced siliciclastic supply. Siliciclastic sediment starvation appears to have occurred broadly at this time around the Antarctic margin.

2. No evidence for glaciation has yet been observed in the Oligocene sediments of Sites 1171 and 1170, the two southernmost sites drilled during Leg 189. This and other supporting evidence suggests that this Antarctic margin was warmer than other sectors.

3. A strong meridional climatic gradient appears to have existed during the Oligocene between the STR margin of Antarctica and the Ross Sea at Cape Roberts (77°S), where early Oligocene diamictites were deposited (Cape Roberts Science Team, 2000).

4. Antarctica was clearly marked by strong regional climatic differences during the Oligocene, well before a unifying Neogene circumpolar influence had developed.

5. It is unlikely that continent-wide ice sheets of proportions typical of the Neogene developed in the Oligocene.

# BACKGROUND AND OBJECTIVES

Site 1171 is located near the southernmost tip of the STR ~550 km south of Tasmania and 270 km southeast of Site 1170 in a water depth of 2150 m on a gentle slope to the southwest (Fig. F3, p. 68, in the "Leg 189 Summary" chapter). At 48°30′S, Site 1171 lies in subantarctic waters south of the present-day position of the Subtropical Front and north of the Subantarctic Front. The major objectives were to (1) core and log an Oligocene to present-day pelagic carbonate section to evaluate expected major paleoceanographic and paleoclimatic effects resulting from the initial opening of the Tasmanian Gateway in the early Oligocene, followed by later development of deep-water Antarctic Circumpolar Current flow; (2) core and log an expected underlying detrital sedimentary sequence of Eocene age, deposited during rifting of the STR from East Antarctica, for paleoenvironmental information; and (3) obtain high-resolution sedimentary records from critical subantarctic latitudes to better understand the role of the Southern Ocean in processes of climatic change during the Neogene on Milankovitch time scales.

Site 1171 is located on thinned continental crust of the STR in the central part of the eastern terrain that was believed to be attached to both Antarctica and Australia until 66 Ma (Royer and Rollet, 1997) (Figs. F4, p. 69, F5, p. 70, in the "Leg 189 Summary" chapter). The block is rhombohedral shaped,~100 km across, and bounded by north-south sheared margins (Exon et al., 1997). During the Late Cretaceous to Eocene, the block was broken up into sub-blocks and several complex transtensional sub-basins by strike-slip faults that developed as Australia slid northward past Antarctica (Fig. F2). The faults, some of which have throws of several thousand meters, probably trend northwest-southeast or north-south, and the resultant sub-basins are filled with ~1000 to 2000 m of Cretaceous through Eocene rift sediments.

During the Paleogene, stretching and thinning of the STR led to steady subsidence. By the early late Eocene, initial marine transgression migrated onto the shallow part of the rise as documented in Deep Sea Drilling Project (DSDP) Site 281, 150 km to the northwest of Site 1171 (Kennett, Houtz, et al., 1975). We assumed initially that Site 1171 was probably at the far eastern end of the restricted Australo-Antarctic Gulf

**F2.** Regional cross section through time across Site 1171, p. 66.
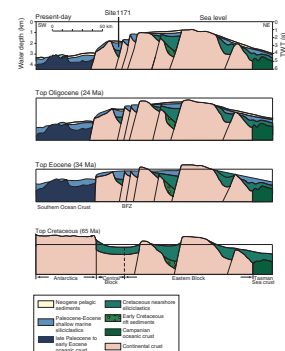
and separated from the Pacific Ocean by the Tasmanian land bridge. Drilling showed that it was, in fact, east of the land bridge and in the Pacific Ocean. By late Oligocene times, the sub-basins had filled, most of the high blocks were covered, detrital sedimentation had ceased, pelagic sedimentation could not keep up, and much of the STR had sunk to bathyal depths. The southern tip of the STR cleared Antarctica during the Oligocene (Cande et al., 2000; S.C. Cande et al., unpubl. data), at which time deep-water antarctic circumpolar circulation became established. Site 1171 was selected because of its extreme southern location on the STR, which is nevertheless in sufficiently shallow-water depths to provide a carbonate sequence suitable for studies of Cenozoic biostratigraphy and chemostratigraphy. Thus, the site should provide critical data on the subsidence of the STR during the Oligocene, on the timing of the initial flow of surface water, and the later flow of deep water through the opening Tasmanian Gateway. The site might also provide a record of ice-rafted detritus, valuable in further understanding of the development of the antarctic cryosphere (Miller et al., 1991).

Earlier drilling of two sites (DSDP 281 and 280) has provided critical information about the sedimentary succession in the STR region. DSDP Site 281 (Kennett, Houtz, et al., 1975) was drilled on a basement high of quartz-mica schist of latest Carboniferous age near the southwestern tip of the STR in 1591 m water depth. The 169-m-thick cored sequence includes upper Eocene conglomerate and glauconitic sandy mudstone immediately overlying basement, upper Oligocene glauconite-rich detrital sand, Miocene foraminifer-nannofossil ooze, and Pliocene–Pleistocene foraminifer-nannofossil ooze. The site was sufficiently shallow throughout for preservation of the calcareous microfossils so valuable for paleoenvironmental interpretations. Evidence from the recovered intervals suggests that the site had subsided to middle bathyal depths by the Miocene.

The other nearby, relevant DSDP Site is Site 280 (Kennett, Houtz, et al., 1975), drilled in 4176 m of water on oceanic crust, southwest of the STR and 150 km southwest of Site 1171. The site penetrated a veneer of upper Miocene to upper Pleistocene clay and ooze and was underlain, beneath a sampling gap, by 55 m of siliceous lower Oligocene sandy silt. The lower part of the sequence consists of 428 m of middle Eocene to lower Oligocene sandy silt, containing chert in the upper 100 m, and glauconite and manganese micronodules in the lower succession. The lower 200 m is rich in organic carbon (0.6–2.2 wt%). The middle to late Eocene carbonaceous sequence contains only dinoflagellates and agglutinating foraminifers in the lowest 360 m (Crouch and Hollis, 1996). The environment of deposition during this interval may have been similar to that of the late Eocene at Site 1168. The base of the site is a basaltic sill believed to be associated with oceanic crust, but it is possible that water depths were shallower than abyssal at the onset of rapid seafloor spreading in the middle Eocene.

Site 1171 is located at the intersection of multichannel seismic profiles AGSO 202-05 (Fig. F3) and -06 in an area of flat-lying Cenozoic sediments near a structural low in the Cretaceous sequence. The basement unconformity is possibly at 2.5 s two-way traveltime (TWT) below the seafloor, the top of the Cretaceous may be at ~1.7 s, the top of the Paleocene is at ~0.9 s, and two younger seismic boundaries are at ~0.58 and 0.31 s.

The site was designed to penetrate 0.31 s (~270 m) of ooze and chalk above a very strong reflector, possibly an unconformity, which drilling proved to be an unexpectedly shallow Oligocene/Eocene boundary.

**F3.** Portion of seismic profile AGSO 202-05 through Site 1171, p. 67.
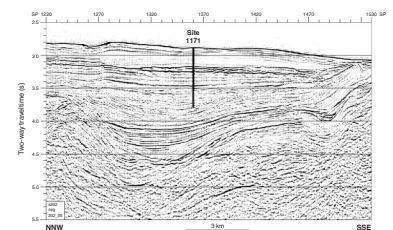
This sequence is seismically semitransparent, but it does contain evidence of large sediment waves and downlaps the unconformity. Below the reflector, we planned to drill 0.1 s (~100 m) of highly reflective sediments, which proved to be interbedded hard and soft siliciclastics of Eocene age. Low in this reflective sequence, at ~0.38 s, a possible bottom-simulating reflector might have represented the base of a zone of gas hydrates, but drilling gave no evidence of hydrates. Below the reflective section is a seismically semitransparent 0.2-s-thick section (~175 m) that proved to be Eocene mudstone. Below this sequence is an unconformity at 0.58 s, within the Eocene section.

Below the unconformity within the Eocene (0.58 s), a sequence of older Eocene siliciclastic sediments (0.6 s thick) is poorly and irregularly bedded. Below an unconformable top at 0.92 s (~900 mbsf) are prograded sediments proven to be of Paleocene age. Planned penetration was to a total depth of 940 m, but we had permission to drill as deeply as 1100 m, if appropriate.

Site 1171 was also designed to recover upper Neogene sedimentary sequences of sufficiently high resolution to conduct critically needed paleoclimatic investigations for the subantarctic region. The nutrient dynamics of the subantarctic region are important for better understanding of global carbon cycling, because of effects on atmospheric $CO_2$ and because a majority of the world's intermediate and deep waters are ventilated in the Southern Ocean (Ninnemann and Charles, 1997). The increased biological productivity of the surface ocean needed to decrease atmospheric $CO_2$ may have occurred in the subantarctic region (Mortlock et al., 1991). Stable isotopic and other geochemical records at Site 1171 are expected to assist with such evaluations.

# OPERATIONS

## Transit to Site 1171

To avoid excessive rolling caused by the southwesterly 5.5-m swell, the captain elected to pursue an east-southeast course that had the ship approach Site 1171 from the northeast. The chosen course added 54 nmi to the transit for a total distance of 202 nmi, which required 18.8 hr. As the ship approached the location, the thrusters and hydrophones were lowered, and a beacon was deployed at 0645 hr on 12 April, initiating Site 1171.

### Hole 1171A

An APC/XCB bottom-hole assembly (BHA) was run to near the precision depth recorder depth of 2176.4 mbrf, and Hole 1171A was spudded with the APC at 1415 hr on 12 April. The seafloor depth was calculated to be 2159.4 mbrf, or 2148.2 mbsl, based on recovery of the first core. Piston coring advanced to 111.6 mbsf (mean recovery = 98%), where Core 12H could not be retrieved from the sediment with 80 kips overpull, requiring drilling over the core barrel to release it from the sediments. Piston cores were oriented starting with Core 3H and continued through to Core 12H. Heat-flow measurements were obtained with the Adara cutting shoe at 35.6 mbsf (Core 5H) and 54.6 mbsf (Core 7H).

The XCB system was used to deepen the hole to 124.4 mbsf, with 62% recovery. The original operational plan called for the hole to be

cored as deeply as possible with the XCB. Because of unusually calm sea conditions, we decided to stop XCB coring after two cores and to continue piston coring the remaining two of the three planned APC holes to potentially avoid weather-dependent core disturbance that we had previously encountered.

## Hole 1171B

The vessel was offset 20 m north of Hole 1171A. To obtain a stratigraphic overlap with the cores recovered from Hole 1171A, the bit was positioned 3 m shallower, and Hole 1171B was spudded with the APC at 0530 hr on 13 April. The estimated seafloor depth of 2159.2 mbrf (2148 mbsl) was calculated based on recovery of the first core. Piston coring advanced to 108.8 mbsf with an average recovery of 98% (Table T1), and cores were oriented starting with Core 3H. The bit was pulled clear of the seafloor at 1545 hr on 13 April, ending Hole 1171B.

## Hole 1171C

The vessel was offset 20 m to the east, and Hole 1171C was spudded with the APC at 1630 hr. To maintain appropriate stratigraphic overlap with the two previous holes, the bit was lowered 6 m from the spud-in depth of Hole 1171B. The seafloor depth was estimated to be 2159.0 mbrf, or 2147.8 mbsl. Piston coring advanced without incident to the depth objective of 104.5 mbsf, with an average recovery of 101%. Cores were oriented beginning with Core 3H, and one Adara deployment was made at 38.0 mbsf (Core 5H).

The XCB system was used to deepen Hole 1171C from 104.5 to 274.8 mbsf, where a glauconitic sandstone was encountered. When the rate of penetration (ROP) slowed to 1.5 m/hr, the refusal depth of the XCB system was declared and coring terminated. The average recovery of the XCB portion of this hole was 82%, with a total average recovery of 89% for Hole 1171C (Table T1).

## Hole 1171D

Following the recovery of the last core from Hole 1171C, the drill string was recovered, a RCB BHA was made up, and the ship was offset 20 m east of Hole 1171C. Hole 1171D was spudded at 0400 hr on 15 April and drilled ahead with a center bit to 100 mbsf. The center bit was recovered by wireline and the Davis-Villinger temperature probe (DVTP) deployed to obtain a temperature measurement at this depth. Following the recovery of the DVTP, the center bit was dropped again and drilling resumed to the depth objective of 247.6 mbsf. The average ROP for the drilled interval was 62 m/hr, excluding the time expended on the DVTP measurement. At 1235 hr on 15 April, RCB coring was initiated and advanced with increasing recovery to the depth objective of 958.8 mbsf (Table T1). The average recovery for this hole was 74%, with an average ROP of 17 m/hr for the 711-m cored interval. There were no stability problems encountered while drilling and coring in this hole.

Following an 11-hr wiper trip and hole preparation that included the release of the bit at the bottom of the hole, the pipe was raised to the logging depth of 162.2 mbsf. Three tool string runs were planned for this hole; the triple combination (triple-combo) tool string, the geological high-sensitivity magnetic tool (GHMT)-sonic, and the Formation MicroScanner (FMS). The first logging run with the triple combo

reached the target depth of 958.8 mbsf, and excellent quality data were collected from the entire section of open hole. While running in with the second log, the GHMT-sonic, the tool string bridged out at ~291 mbsf, near the transition from nannofossil chalk to Eocene glauconitic sandstones. Apparently while running in with this logging suite, power was lost to the GHMT-sonic tool when the unit became caught on this bridge. The tool string was returned to the rig floor, where ~600 m of damaged logging cable was removed and the logging line was reterminated.

In an attempt to clear the bridge in the formation, the drill string was lowered with the objective of clearing all hole obstructions to ~300 mbsf. Perhaps as a result of the 4- to 5.5-m heave, the open end of the BHA became plugged with sediment after traversing less than one stand of pipe at 190 mbsf. The drill string was worked free with 150,000 lb of additional tension after working the drill string for 45 min. Because the bottom of the pipe was plugged and we believed that the drill string had apparently meandered into the side of the borehole, no further logging could be undertaken.

While we retrieved the drill string, the primary beacon was recovered. The alternate beacon was also successfully released; however, the flasher apparently did not activate upon surfacing, and the beacon drifted off into the dark and could not be located. The drilling equipment was secured by 0645 hr on 22 April as the ship departed for the next site. The errant beacon was observed on the surface as the vessel left location, but when the ship came about to recover the unit, it could not be found in the 4.5-m swell.

# LITHOSTRATIGRAPHY

A total of 958.8 m of sediments ranging in age from Pleistocene through latest Paleocene was penetrated at Site 1171 (Fig. F4). Of the four holes drilled at Site 1171 (see "Operations," p. 8), the sedimentary succession recovered at Holes 1171C and 1171D will be the focus of this lithologic report. Holes 1171A and 1171B recovered strata from the Pleistocene through latest Miocene, which are also present in Hole 1171C. Core recovery at Site 1171 was generally good to excellent (89.4% mean, 93.6% median in Hole 1171C), except for an upper Eocene section in Hole 1171D that contained interbedded lithified and unlithified strata (73.8% total mean, 91.4% mean, and 97.5% median excluding the lithified interval in Hole 1171D). This included an exceptional middle Eocene to upper Paleocene interval, which contained an expanded section, fair to excellent preservation of the calcareous microfossils, and apparent color cyclicity. The triple APC-drilled cores of Holes 1171A, 1171B, and 1171C also contained almost no drilling disturbances, which allows for the construction of a composite section of Holes 1171A, 1171B, and 1171C to a depth of 70 mbsf that contains spectrophotometric reflectivity cycles (See "Composite Depths," p. 43). Except in a few intervals, biscuiting and fracturing caused by drilling disturbances varied from absent to moderate (disturbance B0–B3) in the lower part of Hole 1171C and throughout Hole 1171D (Fig. F5).

The sedimentary succession at Site 1171 has been divided into six lithostratigraphic units, with Units I, V, and VI being further subdivided into two, three, and two subunits, respectively (Table T2). These lithostratigraphic units and subunits are at the 10- to 100-meter scale. These

**F4.** Summary of lithostratigraphic units, biozonation, carbonate content, and physical properties, p. 68.
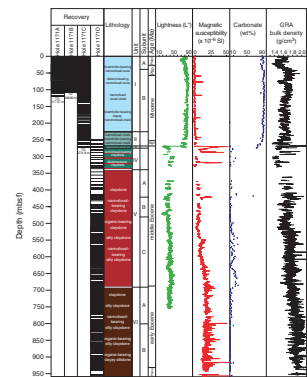
**F5.** Detailed summary for the 0–958.8 mbsf interval, p. 69.
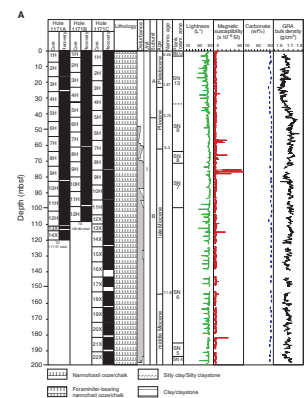
**T2.** Lithostratigraphic summary, p. 129.

units often show an internal cyclic structure at the decimeter to meter scale (in the sense of a systematic repetition of lithologies within the succession). Units and subunits were identified by integrating megascopic core inspection and smear slide examination. The identification of these units was supported by reflectance spectrophotometry, bulk density, magnetic susceptibility, and carbonate content.

Unit I is a biogenic ooze and chalk that was divided into two subunits based on microfossil content. Subunit IA consists of Pleistocene to Pliocene foraminiferal nannofossil ooze and diatom-bearing foraminiferal nannofossil ooze. Subunit IB is composed of nannofossil ooze and foraminifer-bearing nannofossil ooze that represent a fairly continuous section of lower Pliocene to lowermost Miocene succession. The subunit is characterized by having lower foraminifer abundances (ranging between 5% and 15%) than Subunit IA (20%–50%), increased carbonate content (86.5 to 96.8 wt%; average = 94.0 wt%) (Fig. **F5A, F5B**), and rare to occasional silt-sized detrital glauconite. Unit II is Oligocene in age and represents the transition from the pelagic sediments of Unit I to the predominately siliciclastic sediments in Unit III. Overall, Unit II consists of a foraminifer-bearing nannofossil chalk that downsection contains increasing glauconite, clay, accessory minerals, quartz, radiolarians, bioclasts, sponge spicules, and volcanic glass as well as a decrease in carbonate content. Glauconite generally increases in size and abundance to 272.8 mbsf in Hole 1171C and 269.8 mbsf in Hole 1171D, where the most dramatic lithologic change at this site is found.

Unit III is a thin (6.4 m) uppermost Eocene sequence consisting of glauconitic sandy silt and clayey glauconite silt. Unit IV is an upper Eocene diatomaceous claystone and nannofossil-bearing diatomaceous silty claystone (Fig. **F5B**). Unit V is a middle Eocene nannofossil claystone to silty claystone to organic-bearing silty claystone. Sediments of Unit V can be grouped into two general types: lighter-colored nannofossil-bearing claystones and darker-colored silty claystones containing more organic debris. Unit V is divided into three subunits based on the distributional patterns of these sediment types at the decimeter scale (Fig. **F5C, F5D**). However, higher frequency changes at the meter scale also are observed throughout this unit. Subunit VA is a claystone and nannofossil-bearing claystone that increases in nannofossil content and lightens in color downsection. Subunit VB is a claystone, occasionally organic debris-bearing, that contains an overall pattern of lower nannofossil abundance and higher organic debris in the upper and lower sections, separated by a slightly elevated nannofossil content and the absence of organic matter between these two intervals. Subunit VC is a claystone with increasing nannofossils in the lower portion.

In contrast, Unit VI is characterized by nannofossils becoming rare to absent and increasing quartz silt and organic matter. Overall, it can be characterized as nannofossil-bearing claystone, clayey siltstone, and organic matter–bearing siltstone. Subunit VIA consists of nannofossil-bearing claystones overlying silty claystones and is marked by a further downsection decrease in nannofossils and increase in quartz silt and organic matter. Subunit VIB is a silty claystone in the upper portion, grading to an organic matter–bearing clayey siltstone in the lower portion (Fig. **F5E**). Bioturbation, often common in the overlying siliciclastic units, decreases in the last two cores of Subunit VIB and is replaced by laminated strata. Between Cores 189-1171D-72R and 73R (920.0–939.5 mbsf), the boundary between the Paleocene and Eocene was identified by organic dinocyst biostratigraphy. Little to no apparent sedimentological change occurred across this boundary.

## Description of Lithostratigraphic Units

### Unit I

Depth: 0 to 253.4 mbsf
Age: Holocene to earliest Miocene
Intervals: Cores 189-1171A-1H to 14X; Cores 189-1171B-1H to 5H;
    and Cores 189-1171C-1H to 26H
Thickness: 253.4 m

Unit I consists of white, light greenish gray, light bluish gray, and light gray pelagic nannofossil ooze, foraminifer-bearing nannofossil ooze, and occasional intervals of foraminiferal nannofossil ooze with minor siliceous biogenic, calcareous biogenic, and terrigenous materials. Sediments are generally massive, with thin, faintly laminated intervals. This unit is divided into two subunits. Subunit IA contains more foraminifers, less carbonate, and has higher reflectance values than Subunit IB (Fig. **F5A, F5B**).

### Subunit IA

Depth: 0 to 41.0 mbsf
Age: Holocene to Pliocene
Intervals: Cores 189-1171A-1H to 5H; Cores 189-1171B-1H to 5H;
    and Cores 189-1171C-1H to 5H
Thickness: 41.0 m

Subunit IA is Holocene to Pliocene in age and consists of a nannofossil foraminiferal ooze that grades downsection into a foraminiferal nannofossil ooze and foraminifer-bearing nannofossil ooze. The subunit is characterized by an overall decrease in foraminiferal content (20%–50% in the upper portion to 5%–15% at the base; Fig. **F6**). Clay minerals, quartz grains, diatoms, radiolarians, and sponge spicules are present in minor amounts. Pyrite stains are frequent, together with occasional silt-sized glauconite grains. From 0 to 19 mbsf, sediment color ranges from white (N 8, 5Y 8/1) to light greenish gray (5Y 7/2, 10Y 8/1 to 7/1) to light bluish gray (10PB 8/1) to light gray (5YR 7/1). From 19 to 41 mbsf, sediments are generally white (N 8) and massive, with occasional faint light greenish gray (5G 7/1) and light bluish gray (5PB 7/1) laminations. A small increase in siliceous material (diatoms and radiolarians; average of 5%–15%) coincides with the change to more massive sediments. Bioturbation is occasionally moderate to common and appears more prevalent in darker intervals; this appearance may relate to the lack of color contrast in the white ooze. The carbonate content (see **"Organic Geochemistry,"** p. 44) is variable in the upper 27 m, with two major decreases to ~86 wt% at 10.82 and 23.32 mbsf. Gamma-ray attenuation (GRA) bulk density data increase from 0 to 10 mbsf, followed by decreasing values for the rest of the subunit (Fig. **F5**) (see **"Physical Properties,"** p. 54). Subunit IA may correlate to Subunit IA at Site 1168, Subunit IA at Site 1169, and the upper portion of Unit I at Site 1170.

### Subunit IB

Depth: 41.0 to 233.7 mbsf
Age: early Pliocene to earliest Miocene

**F6.** Lithologic composition of Holes 1171A, 1171B, and 1171C sediments, p. 75.
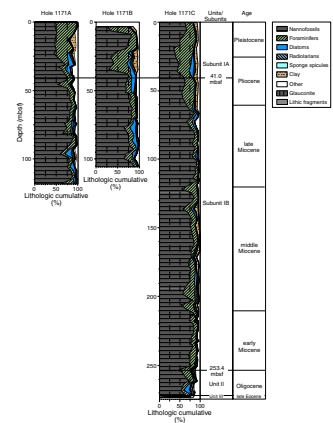
Intervals: Cores 189-1171A-6H to 14X; Cores 189-1171B-6H to 12H; and Cores 189-1171C-6H to 26X
Thickness: 212.4 m

Subunit IB is lower Pliocene to lowermost Miocene in age and consists of white (5Y 8/1 and N 8) nannofossil ooze and foraminifer-bearing nannofossil ooze that grades into chalk at ~211 mbsf. Subunit IB is distinguished from Subunit IA by having a lower foraminiferal content (5%–15%) and a higher and less variable carbonate content (90.2 to 96.9 wt%; average = 94 wt%). Minor variable components include clay minerals, quartz, diatoms, radiolarians, sponge spicules, and bioclasts. Bioturbation is rarely visible. Sediments are generally massive with laminated intervals (10 to 150 cm thick) present that are spaced at meters to decameters. Laminations range in color from light greenish gray (5G 8/1), to light bluish gray (5PB 8/1) and light gray (N 6 and N 7); laminated intervals are occasionally followed by an abrupt color change.

A minor increase in the foraminiferal content coincides with occasional silt-sized pyrite and glauconite grains between 115 and 210 mbsf. GRA bulk density is a relatively constant unit (1.7–1.8 g/cm³) from 41 to 141 mbsf. Silt-sized glauconite is clearly visible throughout the unit. Subunit IB is correlated to Subunits IB and IIA at Site 1168, Subunit IB at Site 1169, Unit II at Site 1170, and the lower portion of Subunit IB at Site 281 (Kennett, Houtz, et al., 1975).

## Unit II

Depths: 233.7 to 269.8 mbsf
Age: late Oligocene
Intervals: Cores 189-1171C-26X through 30X and Cores 189-1171D-1R through 3R
Thickness: 16.4 m

Unit II is late Oligocene in age and is characterized by a foraminifer-bearing nannofossil chalk and a general downsection decrease in carbonate percent (89.7–74.1 wt%) and increases (2–11 wt% increase) in glauconite, clay, accessory minerals, quartz, radiolarians, bioclasts, sponge spicules, volcanic glass, and silt-sized particles. This unit marks the transition from the pelagic sediments of Unit I to the predominately siliciclastic sediments of Unit III. Unit II is distinguished from Subunit IB by (1) lower calcium carbonate percentages (from 89.7 wt% at 252.62 mbsf to 84.2 wt% at 259.30 mbsf), (2) lower reflectivity, and (3) higher abundances of glauconite, radiolarians, bioclasts, sponge spicules, clays, accessory minerals, and volcanic glass. The upper unit boundary also coincides approximately with the Oligocene/Miocene boundary (see **"Biostratigraphy,"** p. 25).

Smaller-scale features in Unit II may represent paleoenvironmental changes. A relatively thin interval containing alternating light greenish gray (10GY 8/1) to white (N 8) color is observed in Cores 189-1171C-29X and 189-1171D-2R (257–268 mbsf). In two instances, the transition from the lighter to darker strata downsection is abrupt and contains a well-defined surface. In contrast, cycles in Unit I are typically marked by a change from darker to lighter sediments.

A distinct surface marked by foraminifer-bearing chalk above, and nannofossil chalk below, is located 12 cm above the base of Unit II (272.68–272.80 mbsf in Hole 1171C; Fig. **F7;** interval 189-1171D-3R, 17–30 cm). Glauconite begins to increase downsection both in abun-

**F7.** Close-up photograph of the striking lithologic contact between Units II and III, p. 76.
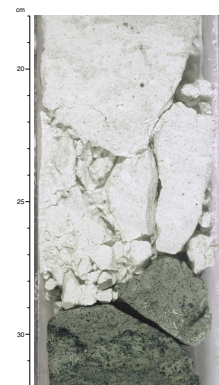
dance and size from ~40 cm above this surface (272.28 mbsf in Hole 1171C) often reaching sand size. Rip-up clasts (~1 cm) are observed up to a few centimeters above the surface. The strata below contain considerably less glauconite and consist of massive white (N 8) nannofossil chalk. This thin (12 cm) chalk is terminated by the abrupt lithologic change at 272.68 mbsf in Hole 1171C and 269.8 mbsf in Hole 1171D.

Transitional units are recognized at all of the deeply drilled sites from Leg 189, as well as at sites from Leg 29 (Kennett, Houtz, et al., 1975) and may correspond to Unit II at Site 1171. At Site 1168, Subunits IIB and IIC can be interpreted as an extended transitional unit (130 m thick) dated as late Oligocene (see "Lithostratigraphy," p. 8, in the "Site 1168" chapter). The transitional unit at Site 1170, Unit III, also roughly correlates to Unit II of Site 1171 and may represent an intermediary between the thicker, more clay-rich transitional Subunits IIB and IIC at Site 1168 (130 and 120 m thick, respectively) and Unit II of Site 1171. Subunit IA and Unit III of DSDP Site 281 may also be equivalent to Unit II of Site 1171 (Kennett, Houtz, et al., 1975).

## Unit III

Depths: 269.8 to 276.2 mbsf
Age: latest Eocene
Intervals: Cores 189-1171C-30X and 31X and Core 189-1171D-3R
Thickness: 6.4 m

Unit III is uppermost Eocene in age and consists of 6.4 m of dark greenish gray (5GY 4/1) to blackish green (5G 2.5/1) glauconitic sandy siltstone and clayey glauconitic siltstone. This is a distinct transition (at 269.8 and 272.8 mbsf in Holes 1171C and 1171D, respectively) from the overlying lower Oligocene white nannofossil chalk of Unit II. Visual observations, bulk density, magnetic susceptibility, spectrophotometer, and coulometric carbonate data sets all indicate a major change across this surface (Fig. F5B) (see "Physical Properties," p. 54). The interval immediately below this transition (0–0.34 m) is highly bioturbated with *Zoophycos* visible throughout. Quartz and glauconite increase as the color changes from dark greenish gray (5GY 4/1) to blackish green (5G 2.5/1) downsection. Bioturbation is abundant to common, with a decrease in intensity downsection. Calcium carbonate decreases sharply from 77.3 wt% immediately above the surface to 0.41 wt% below. This agrees with the smear-slide data, where calcareous nannofossils number only a few percent. Small intervals with laminations and individual beds are observed in the upper part of the unit, marked by very high glauconite content, and some clay clasts. Unit III may correlate to Unit IV at Site 1168 and Unit IV at Site 1170.

## Unit IV

Depth: 276.2 to 343.5 mbsf
Age: late to middle Eocene
Interval: Cores 189-1171D-4R to 11R
Thickness: 67.3 m

Unit IV is late to middle Eocene in age, containing 67 m of nannofossil-bearing diatomaceous silty claystone, silty claystone, and diatomaceous claystone. It is distinguished from Unit III by a major lithologic change from clayey glauconitic siltstone to diatomaceous silty clay-

stone, a slight lightening in color, an increase in carbonate content from 0.41 wt% in Unit III to 6.96 wt% at the top of Unit IV (with the unit averaging 4.67 wt%), and bulk density falling from 1.7 g/cm³ at the base of Unit III to 1.35 g/ cm³ at the top of Unit IV. The unit is characterized by an abrupt increase in siliceous biogenic components, with 20%–40% diatoms and lesser sponge spicules and radiolarians. Foraminifers are generally absent. Minor quartz, opaque, and accessory minerals are present throughout. Glauconite content varies (2%–15%) with a marked decrease below 300 mbsf. However, abundant glauconite (20%) reoccurs together with quartz (25%) in a 1-m interval from 317.7 to 318.7 mbsf. Bioturbation is common to abundant with *Zoophycos, Chondrites,* and burrows of unknown origin.

The color darkens downsection at 276.2 mbsf, from olive-gray (5Y 5/2) to dark gray (5Y 4/1) to black (5Y 2.5/1) silty claystone at ~300 mbsf. The sediment is characterized by increased quartz and glauconite, and there is little biogenic material except for 5% nannofossils. The second downsection darkening succession is slightly lighter in color because of a higher content of diatoms, nannofossils, and sponge spicules. It grades from pale olive (5Y 6/3) at 276.2 mbsf to olive (5Y 5/2 and 4/3) to black (5Y 2.5/2), with quartz and opaque grains at the bottom of the unit.

The lowest values of calcium carbonate (0 and 1.61 wt%) are reached at 294 and 334 mbsf, respectively, in the unit. Between the two minima the values increase to 7.9 and 14.9 wt%; the generally higher values correspond to higher nannofossil content. Unit IV correlates to Unit V at Site 1168, Unit IV at Site 1170, and Units III through V at Site 281 (Kennett, Houtz, et al., 1975).

## Unit V

Depth: 343.5 to 692.5 mbsf
Age: middle Eocene
Interval: Cores 189-1171D-11R through 48R
Thickness: 348.99 m

The sediments of Unit V are middle Eocene claystones and silty claystones with occasional minor amounts of nannofossils. Unit V is differentiated from Unit IV by the general absence of siliceous microfossils, the increase in volcanic glass and opaque and accessory minerals, and occasional mica. This unit is divided into three subunits based on nannofossil content, organic matter content, and visual color.

## Subunit VA

Depth: 343.5 to 421.6 mbsf
Age: middle Eocene
Interval: Cores 189-1171D-11R to 20R
Thickness: 78.1 m

Subunit VA generally consists of an upper middle Eocene light greenish gray (10Y 6/1), olive (5Y 5/3), dark greenish gray (10Y 4/1), and dark olive-gray (4/13/2) claystone and nannofossil-bearing claystone. Although the upper part of the subunit is interbedded with hard and soft strata, resulting in low drilling recovery (343.50–394.83 mbsf), a satisfactory lithostratigraphic framework was created. Claystone extends from the top to 411.6 mbsf, where nannofossils increase to a minor modifier

and carbonate content increases downward. In well-recovered intervals, there is a pervasive alternation in color, from olive (5Y 5/3) to dark olive gray (5Y 3/2) or dark greenish gray (10Y 4/1), with average cycles ranging from 0.6 to 1.5 m long. Typically, darker intervals contain fewer calcareous microfossils than lighter colored intervals, and the cycles may represent high-frequency oscillations ($10^4$–$10^5$ yr) in the depositional environment. Site 1168 did not penetrate to equivalent-age sediments. This unit roughly correlates to Subunit VA at Site 1170 and to Units IV and V at Site 281 (Kennett, Houtz, et al., 1975).

## Subunit VB

Depth: 421.6 to 485.7 mbsf
Age: middle Eocene
Interval: Cores 189-1171D-20R to 26R
Thickness: 64.1 m

Subunit VB is a middle Eocene dark greenish gray (10Y 4/1) to very dark gray (5Y 3/1) claystone to an organic-bearing claystone. A bioturbated contact at 421.6 mbsf separates the glauconitic interval at the base of Subunit VA from Subunit VB. This subunit differs from Subunit VA in its lower nannofossil abundance, generally darker color, and higher organic content (Fig. F8). Organic content reaches minor modifier levels in the upper (421.6–440.0 mbsf) and lower sections (469.33–485.70 mbsf). Between these intervals, nannofossils are slightly more abundant (4%–7%). Photospectrometry data indicate that positive or red color in chromaticity coordinate a* (associated with a browner color) correlates with higher total organic carbon (TOC) in the upper and lower parts. A shift to negative values (green color) is associated with the lower organic content and higher nannofossil abundances in the middle part (Fig. F9). Subunit VB roughly correlates to Subunit VB at Site 1170. The nearby DSDP Site 281 records glauconitic silty clays, sand, and basal breccia in the upper Eocene, above a Paleozoic quartz-mica schist basement (Kennett, Houtz, et al., 1975).

## Subunit VC

Depth: 485.7 to 692.5 mbsf
Age: middle Eocene
Interval: Cores 189-1171D-26R to 48R
Thickness: 206.79 m

Subunit VC is middle Eocene in age and is characterized by silty claystone, with nannofossil content increasing downsection from a minor to occasionally major modifier. The upper boundary of this subunit is identified by (1) an increase in nannofossils, (2) a color change from very dark gray (5Y 3/1) to dark gray (5Y 4/1), and (3) less organic matter (Fig. F10). Subunit VC can be characterized by the following lithologic criteria:

1. Color generally lightens downsection while alternating at the decimeter to meter scale from dark gray (5Y 4/1) and dark olive gray (5Y 3/2) in the upper part to greenish gray (10Y 5/1) and dark greenish gray (10Y 4/1) in the lower part.
2. Nannofossil abundance generally increases downsection, from <1% just above the top of the subunit to 1%–10% in the darker-

**F8.** Lithologic composition of Hole 1171D sediments, p. 77.
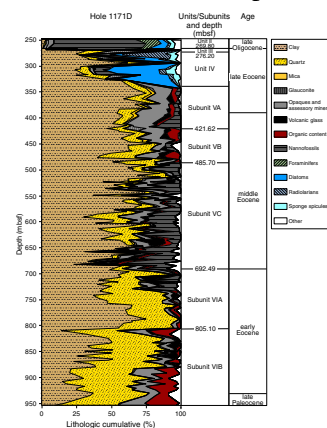
**F9.** Comparison of chromaticity coordinate a* from the photospectrometer to carbonate content and the nannofossil percent, 400–500 mbsf, p. 79.
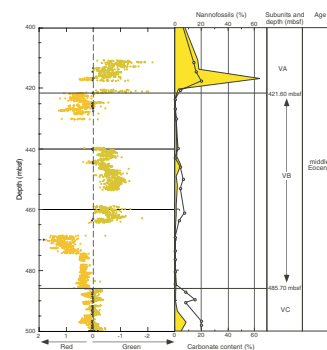
**F10.** Comparison of chromaticity coordinate a* from the photospectrometer to carbonate content and the nannofossil percent, 450–700 mbsf, p. 80.
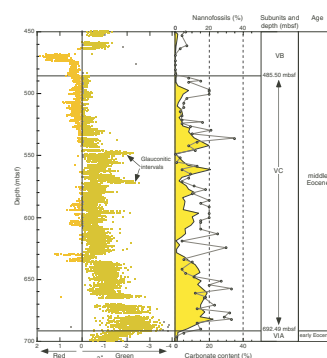
colored intervals and up to 20%–33% in the lighter-colored strata. This trend correlates well with chromaticity coordinate a* (green vs. red) and calcium carbonate percentages (Fig. F10).

3. Organic matter is low to absent for most of this subunit. In contrast, Subunit VB and Unit VI generally contain more organic matter.

Higher-frequency lithologic changes are observed in most of this unit (521.00–692.49 mbsf), although the upper 40 m of Subunit VC consists of mainly homogeneous olive-gray and dark olive-gray (5Y 4/2 and 5Y 3/2) nannofossil-bearing claystone to silty claystone containing occasional lignite fragments. A cyclic color pattern, of light greenish gray (10Y 5/1 and 5Y 6/2) to dark greenish gray to olive gray (10Y 4/1 to 5Y 4/2), begins at 521 mbsf. The cycle length varies from 65 to 90 cm. The transition from darker to lighter sediments becomes sharper with depth, and an increase in glauconitic silt and fine sand is associated with darker sediment. Carbonate content and color begin to increase at ~521 mbsf (Fig. F10). Bioturbation is common to locally abundant, often obscuring most sedimentary structures as well as the transition between darker and lighter sediments. However, by 530.0 mbsf, sharp surfaces separate the darker strata above from the lighter strata below. There is a particularly distinct surface at 548.90 mbsf with glauconite-filled burrows below the contact surface (Fig. F11).

These cycles continue to 579.47 mbsf, where they are replaced by generally more massive light greenish gray (10Y 5/1) sediments. This change is marked by a thin (6 cm), black (N 2.5) interval containing abundant shells (Fig. F12). Nannofossil abundance generally increases downsection, and calcium carbonate increases from ~1 wt% above 630 mbsf to more than 20 wt% near the base of the subunit (5.8 to 22.5 wt%; average = 14.1 wt%; N = 14). These increases suggest a generally less restrictive and more open marine setting for the lower part of the subunit. Two thin sandstone beds are observed at the base of this subunit in Core 189-1171D-48R (689.90–690.30 mbsf).

## Unit VI

Depth: 692.5 to 958.8 mbsf
Age: early Eocene to late Paleocene
Interval: Core 189-1171D-48R through 75R
Thickness: 266.40 m

The sediments of Unit VI are lower Eocene to upper Paleocene clayey siltstones and silty claystones with organic matter increasing downsection to minor and occasional major modifiers. In contrast to Unit V, carbonate content decreases to a few percent in Subunit VIA and then to trace amounts in Subunit VIB (Fig. F5E). Spectrophotometry data also indicate a sharp color change at the upper boundary of Unit VI. Unit VI was subdivided into Subunits VIA and VIB based on changes in sediment components such as quartz, clay, organic debris, and nannofossils and supported by calcium carbonate content and physical properties data.

## Subunit VIA

Depth: 692.5 to 805.1 mbsf
Age: early Eocene
Interval: Core 189-1171D-48R through 59R
Thickness: 112.61 m

F11. Close-up photograph of a sharp bioturbated surface, p. 81.

F12. Close-up photograph of a thin black sediment bed containing abundant shells, p. 82.
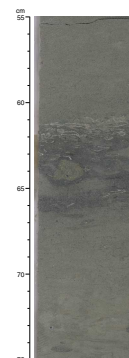
Subunit VIA consists mainly of lower Eocene greenish gray to dark greenish gray (5GY 5/1 to 10Y 4/1) nannofossil-bearing silty claystone in the upper part (692.49–729.01 mbsf) and silty claystone in the lower part (729.01–805.10 mbsf). Throughout the subunit, sediment texture is massive with common small-scale bioturbation of unknown origin, and rare *Chondrites* and *Zoophycos* are present throughout. Occasionally, burrows contain lighter greenish rings.

Carbonate content in sediment averages 2.1 wt% with a maximum of 9.5 wt% at 801.51 mbsf. The carbonate is mainly derived from nannofossils, which are more frequent between 700 and 730 mbsf (Cores 189-1171D-49R to 52R), with an average of 7% in smear-slide observations. Nannofossil content decreases considerably at 738 mbsf, and nannofossils disappear completely at 780 mbsf. The dominant sediment components are clay (average of 42%) and quartz (average of 38%), with quartz increasing and clay decreasing downsection. Small lignite fragments (<1 cm) are sporadic throughout the unit.

Pressure solution seams are sporadic and filled with quartz, microsparite, or clay. Other postdepositional textural features include a few microfaults (Fig. F13) and calcareous and occasionally siliceous veins. Light yellowish brown (2.5Y 4/2) nodules that range in diameter between 1 and 2.5 cm are sporadic throughout Subunit VIA. According to X-ray diffraction (XRD) results (from Core 189-1171D-50R), the nodules consist mainly of diagenetic minerals (siderite, apatite, and calcite). In the entire subunit, siliceous white tubes of unknown origin are very rare. Two distinct ash layers were found in Cores 189-1171D-51R and 59R.

## Subunit VIB

Depth: 805.1 to 958.8 mbsf
Interval: Core 189-1171D-60R through 75R
Age: earliest Eocene to late Paleocene
Thickness: 153.70 m.

Subunit VIB consists of lower Eocene dark olive-gray (5Y 3/2) to dark greenish gray (10Y 4/1) silty claystone and clayey siltstone in the upper section, giving way at 870.00 mbsf to lower Eocene to upper Paleocene dark grayish brown (2.5Y 3/2) organic matter-bearing clayey siltstones in the lower part. Sediment texture throughout the entire subunit is massive, and small-scale bioturbation is common. *Chondrites, Zoophycos,* and burrows of unknown origin, often containing lighter green rings, are sporadic throughout. Pressure solution seams are rare and filled with quartz, microsparite, or clay. Light yellowish brown (2.5Y 4/2) nodules continue into Subunit VIB and are most abundant between 805.1 and 814.65 mbsf in Core 189-1171D-60R. According to XRD results, the nodules consist mainly of calcite, apatite, and siderite, with minor quartz. In the entire subunit, siliceous white tubes of unknown origin are very rare.

Carbonate content is extremely low in Subunit VIB, rarely exceeding 1 wt%. However, from 910 mbsf downward (Core 189-1171D-71R), calcium carbonate increases slightly with spot maxima at 912.01 mbsf (9.2 wt%) and at 949.21 mbsf (5.10 wt%). Clay decreases from 40% to 20% downsection, whereas quartz increases from 38% to 48%. Subunit VIB is uniquely characterized by a downward increase of organic debris (below 865 mbsf; Core 189-1171C-66R). In Section 189-1171D-71R-2, a distinct surface separates a massive, very dark grayish brown (2.5Y 3/2) clay above from a heavily glauconitic, dark grayish brown (2.5Y 4/2)

**F13.** Close-up photograph of microfaults with an offset cutting bioturbated claystone, p. 83.
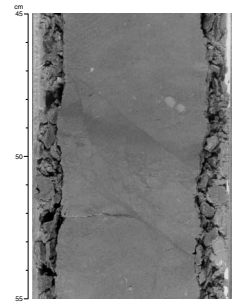
clay below (Fig. F14). Glauconite decreases downward until Section 189-1171D-71R-4, where a lighter colored extensively bioturbated layer is found (Fig. F15). Below this interval, color darkens downsection and laminated sediments are found down to the bottom of the hole. Limestone layers 2 to 12 cm thick are present between 812.35 and 904.12 mbsf. Thin sections show a micritic texture with extremely rare bioclasts (radiolarian ghosts and sponge spicules), a few small, angular quartz grains, and organic matter. Signs of late diagenetic dissolution and deformation are present.

## Discussion and Interpretations

Primary objectives of Site 1171 were to develop a better understanding of the pre-, syn-, and postdepositional history of the opening of the Tasmanian Gateway and its role in Southern Ocean development and climatic processes during the Paleogene and Neogene. Preliminary lithologic results provide evidence that sediments recovered at Site 1171 may hold critical information for unlocking many of the paleoceanographic questions related to the opening of the Tasmanian Gateway. These observations include clear sedimentological evidence of major long-term lithologic changes (scale of tens of meters) during and after the opening and decimeter- to meter-scale cyclic changes in the lithology before the opening of the gateway (lower to middle Eocene), which are suggestive of high-frequency ($10^4$–$10^5$ yr) cyclicity. They indicate that the paleoenvironmental history of Site 1171 is one of slowly increasing ventilation during the Paleocene and Eocene, a transition to a fully open marine regime during the Eocene–Oligocene transition and throughout the Oligocene, and winnowing caused by vigorous bottom-water circulation during the Neogene.

## Paleoenvironmental Changes during the Late Paleocene and Eocene: Increasing Ventilation on the South Tasman Rise

The depositional history of the late Paleocene to the Eocene at Site 1171 is one of increasing ventilation and water deepening. Embedded within this long-term trend are higher frequency oscillations. The mechanisms of long-term change include local subsidence, opening of the Tasmanian Gateway, deep-water circulation changes, local productivity changes, regional and global climatic changes, and eustasy. The drilling, in combination with the seismic profiles, indicates that most local tectonic activity occurred at the Paleocene/Eocene boundary. This suggests that derivation of sediment from the local fault blocks associated with the Balleny Fracture Zone would have peaked at ~55 Ma. Because of the preliminary nature of this volume, we will not speculate on which are the primary mechanism(s) for the long-term changes. Postcruise studies should be able to address many of these questions. The evidence for increasing ventilation includes an increase of lighter colored claystones with more nannofossils upward and less quartz and organic matter. Lighter colored claystones are interpreted as deposited in more open-marine and less restricted environments, and the darker-colored clayey siltstones and silty claystones in more restricted and less open marine environments.

Late Paleocene sediments are laminated siltstones containing high organic matter and quartz. The presence of laminations and absence of any bioturbation indicate near anoxic conditions. This suggests poor

**F14.** Close-up photograph of a distinct surface that separates a massive very dark grayish brown clay from a glauconitic dark grayish brown clay, p. 84.

**F15.** Close-up photograph of the surface of Section 189-1171D-71R-2, p. 85.
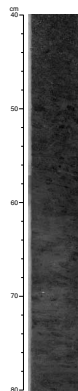
ventilation and may represent a shallow-marine sheltered marginal environment or an extreme shallowing of the oxygen minimum zone. A stratigraphic surface associated with a glauconite layer in Core 189-1171D-71R (912.70–914.90 mbsf) may indicate a larger environmental change or stratigraphic break and corresponds to the Paleocene/Eocene boundary.

The upper part of Subunit VIB (early Eocene) contains increasing clay and decreasing quartz and organic matter, which suggests steadily decreasing input of coarse terrestrial sediment. This trend continues in Subunit VIA, where nannofossil content slowly increases, suggesting a more open ocean regime. Several thin micritic limestone beds between 812.35 and 904.12 mbsf may have been transported into the basin as tempestites, either as a result of tectonic activity or during storm events. If these are storm events, then water depths for Subunit VIA were below fair weather wave base and above storm wave base.

There is a sharp lithologic change at the lower to middle Eocene boundary (Subunit VIA and Unit V boundary). Quartz rapidly decreases and nannofossils increase, indicating a more open marine paleoenvironment. A distinct surface at this boundary also suggests a water-depth change, based on the glauconite above the surface (typical in transgressive phases) and upward increases in nannofossil abundance. In fact, Subunit VC contains the highest carbonate and nannofossil abundances observed in the middle Eocene, indicating more open marine conditions. Generally, from ~500 to 340 mbsf, nannofossil and organic matter abundances vary inversely at the meter to tens of meter scale, indicative of high frequency and longer-term changes in the ventilation history at Site 1171. There is an overall trend within Subunits VA and VB of generally less ventilation than in Subunit VC.

There are several thin sandstone beds in Subunit VC that may represent storms (690.78–692.44 mbsf). Paleogeographic reconstructions and local seismic sections suggest a constricted basin during this time, resulting in relatively low-wave energy. Thus, the storm-wave base level may have been in water as shallow as 30 m. A thin (6 cm) black interval with abundant mollusk shells (Fig. F12) is also interpreted to be a storm lag or sequence boundary (i.e., a change in sea level). In either case, early to middle Eocene water depths were generally above storm-wave base level (30–60 m water depth). These units also had relatively high sedimentation rates, suggesting that subsidence was also high.

The transition from claystone to diatomaceous claystone within the late Eocene (Subunit VA to Unit IV) is associated with diatom assemblages, which suggest an increase in water depth, from inner neritic to outer neritic (see "Biostratigraphy," p. 25). The dissolution of the calcareous microfossils in Unit IV is probably caused by the presence of acid pore waters in the sediments, which have 0.2–0.5 wt% TOC. Upper Eocene siliceous biogenic units (i.e., diatoms and radiolarians) are also identified at Sites 1170 and 1172 (see "Lithostratigraphy," p. 10), indicating that there were similar depositional conditions on both sides of the Tasmanian Gateway. Similar dissolution of calcareous microfossils occurred in other southern ocean sites (e.g., Sites 689 and 690; Thomas et al., 1995) during the late Eocene.

In Unit III, glauconite increases upsection and becomes a major modifier. In situ glauconite indicates low sedimentation rates and sediment-starved depositional environments (McRae, 1972) and represents a major change at Site 1171 from the high sedimentation rates that characterize the middle Eocene. Possible mechanisms for these lower rates could be decreasing sediment input, reduction in the area of eroding

landmasses, decreasing weathering rates caused by climatic cooling, or winnowing by currents.

The lithology of the Eocene/Oligocene transition indicates sweeping changes in both water masses and water depth at Site 1171. Glauconitic silts and clays indicative of neritic to upper bathyal conditions are replaced at 272.8 mbsf (Hole 1171C) by foraminifer-bearing nannofossil chalks. Although this change could be caused in part by a rapid decrease in sedimentation rates and an increase in productivity, benthic foraminiferal studies indicate a rapid water-depth increase across this transition (see "Biostratigraphy," p. 25).

The depositional history after the opening of the Tasmanian Gateway at Site 1171 is one of winnowing by strong bottom-water currents and the establishment of a well-ventilated environment. Evidence for strong bottom-water currents is found 12 cm above the Eocene–Oligocene transition, where rip-up clasts overlie a distinct, probably erosional, surface (Fig. F7). Detrital glauconite, clay, accessory minerals, quartz, radiolarians, bioclasts, sponge spicules, and volcanic glass content decrease upsection to minor and trace amounts. Silt-sized glauconite is interpreted as detrital based on the small size and roundness of the grains and the lack of glauconite infillings in foraminifers. They continue upsection into the Pliocene-age sediments (up to 41 mbsf) indicating that bottom currents were able to transport silt-sized particles. Evidence for well-ventilated bottom water includes good to excellent preservation of the calcareous microfossils indicating noncorrosive waters and a relatively high diversity (for southern ocean sites) of foraminifers and nannofossils (see "Biostratigraphy," p. 25). This pattern has continued into the Holocene. During the Pleistocene and Holocene, foraminifers increase to major modifier, suggesting increased winnowing caused by stronger bottom-water currents of the Antarctic Circumpolar Current.

## Middle Eocene Sequence Stratigraphic Interpretations

During the middle Eocene, a persistent alternating pattern was observed at the meter and tens of meters scale. These possible cycles in Unit V contain two basic sedimentary types: lighter-colored nannofossil-bearing claystones interpreted as being deposited during better ventilated, more open marine periods, or marine highstands, and darker-colored silty claystones containing more organic matter, interpreted as being deposited during more restricted, less open marine periods, or marine lowstands.

Several expanded cycles also contain distinct and sharp basal surfaces as well as sedimentological evidence of possible sea level changes, allowing sequence stratigraphic terminology to be applied, albeit at a very preliminary stage. For example, from ~392 to 421.62 mbsf in Subunit VA, a distinct sedimentary succession contains a well-defined basal surface (Fig. F16) and is interpreted as a stratigraphic sequence. This sequence is characterized by the following:

1. The sharp but bioturbated basal surface at 421.62 mbsf with large (2 cm) glauconite-filled burrows extends as much as 10 cm below the basal surface.
2. Across the surface, glauconite increases dramatically from 2% below the basal surface (423.80 mbsf) to 16% above it (420.8 mbsf) and continues upward for ~1 m.
3. Glauconite content decreases upsection to 3% by 417.60 mbsf, whereas carbonate content dramatically increases from 2.8% at

**F16.** Close-up photograph of a distinct well-defined surface at the base of Subunit VA, which is interpreted as a basal sequence boundary, p. 86.
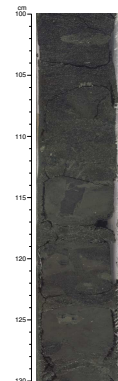
420.4 mbsf to 64.4% at 416.88 mbsf. Nannofossils also show a similar upward increase (4% to 20%). Nannofossil and carbonate contents remain relatively high until ~410 mbsf. This increase in carbonate is interpreted as reflecting increased marine conditions and higher sea levels.

4.  Darker-colored claystones, containing lower nannofossil abundance and carbonate content (5% and 3.2 wt%, respectively), represent less marine conditions (lower sea level).

This succession may correspond to a sequence boundary, a transgressive system tract, a condensed section, and a highstand system tract, respectively.

Numerous lithologic successions are bounded by distinct surfaces in Subunit VC. Typically, the base contains a bioturbated surface with glauconite-filled burrows below the contact. This is overlain by abundant glauconitic dark greenish gray strata that lighten upward to light greenish gray strata. The lighter strata often contain abundant nannofossils. An example of this is in Subunit VC between 545.50 and 548.90 mbsf. It contains a sharp, although heavily bioturbated and irregular surface (interval 189-1171D-33R-3, 5–45 cm; Fig F17). The surface at 548.90 mbsf is interpreted as the sequence boundary; the dark-colored glauconitic unit above is the transgressive systems tract, and the lighter strata are assigned to the marine flooding unit (condensed section). Thinner, less-defined successions, containing less distinct surfaces and less contrast in color and glauconite abundance, could be interpreted as parasequences with the surfaces interpreted as flooding surfaces. However, these changes in lithology and biogenic material may also be caused solely by climatically related water-mass changes and may have little to do with changes in sea level (as implied by the sequence stratigraphic terms).

## Clay Mineralogy

X-ray diffraction analyses were completed on 58 samples from Holes 1171A, 1171C, and 1171D (Fig. F18). The purpose of the clay mineral studies at Site 1171 was to (1) recognize the major variations of the paleoenvironment, as expressed by the clay mineral assemblages at a sampling interval of one every two cores and (2) compare the clay mineral assemblages with those recognized at Sites 1168 and 1170 drilled in similar water depths on the west Tasmania margin, the western STR, and with other areas of the Southern Ocean.

### Results

The clay minerals identified include smectite, random mixed-layered clays, illite, chlorite, and kaolinite. Based on the relative abundance of the clay minerals, five units were identified for Site 1171. These were designated Units C1 to C5 (Fig. F18).

Unit C1, which extends from the seafloor to 40 mbsf, has a clay mineral assemblage that consists of abundant smectite (45% to 85%) and common to abundant random mixed-layered clays (15% to 40%) accompanied by illite (0% to 15%) and kaolinite (0% to 5%). Unit C1 ranges in age from late Pliocene to Pleistocene and correlates to lithostratigraphic Subunit IA. Unit C2 extends from 40 to 273 mbsf and is characterized by abundant random mixed-layered clays (10% to 100%) and smectite (0% to 75%) accompanied by illite (0% to 20%) and ka-

**F17.** Close-up photograph of a sharp, although heavily bioturbated and irregular, surface, p. 87.



**F18.** Clay mineral units, p. 88.
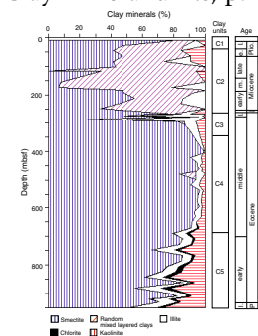
olinite (0% to 15%). Because of the low clay content in the nannofossil oozes and chalks of lithostratigraphic Subunit IA and Unit II, percentages of random mixed-layered clays >50% are probably overestimated. Unit C2 ranges in age from early Oligocene to early Pliocene. Unit C3 extends from 273 to 340 mbsf and exhibits alternation of abundant smectite (25% to 95%) and illite (5% to 50%) accompanied by random mixed-layered clays (0% to 25%) and kaolinite (0% to 5%). Unit C3 is middle to late Eocene in age and correlates to lithostratigraphic Units III and IV. Unit C4 extends from 340 to 690 mbsf and is characterized by largely predominant smectite (85% to 100%) accompanied by minor amounts of illite and kaolinite (0% to 5% each) and sporadic random mixed-layered clays (~10%). Sporadic trace amounts of chlorite are present below 420 mbsf. Unit C4 is middle Eocene in age and correlates to lithostratigraphic Unit V. Unit C5 extends from 690 mbsf to the bottom of Hole 1171D. Unit C5 is characterized by kaolinite (5% to 25%) and illite (5% to 20%) increasing with depth and minor amounts of chlorite (0% to 5%). However, smectite is still abundant in this unit (50% to 85%), and its content decreases with depth. Unit C5 is late Paleocene to early Eocene in age and correlates to lithostratigraphic Unit VI.

## Paleoenvironmental Interpretation of Clay Assemblages

The predominance of smectite and kaolinite indicates that warm climatic conditions and intense chemical weathering prevailed in sediment source areas. Smectite predominates in areas of low relief with alternating periods of precipitation and aridity, its formation being enhanced on basic volcanic substrates. Kaolinite is typical of warm areas with high precipitation during at least part of the year and good drainage conditions (Chamley, 1989; Weaver, 1989). Clay assemblages with predominant smectite were widespread in most oceanic areas off passive continental margins during the early Paleogene, including southern high-latitude locations of the Weddell Sea (Robert and Maillot, 1990) and Kerguelen Plateau (Ehrmann, 1991). Illite and chlorite are derived from erosion of substrates and characterize the environments of strong physical weathering. Such conditions prevail in cold and/or dry areas as well as in areas of steep relief, where active erosion prevents full development of soils (Chamley, 1989; Weaver, 1989). As illite and chlorite are associated with dominant smectite and abundant kaolinite, their presence in Paleocene to lower Eocene Unit C5 is probably not climatically induced but rather results from intense erosion of steep relief areas. Although significant amounts of kaolinite have already been observed in calcareous biogenic chalks of Maud Rise (Weddell Sea) in relation with the episode of extreme warmth of the Paleocene/Eocene boundary, it lasted for ~150 k.y. only (Robert and Kennett, 1994). Continuous occurrence of significant amounts of kaolinite from the late Paleocene throughout the entire early Eocene as observed at Site 1171 is unusual in the antarctic region.

Site 1171 is located in one of several transtensional sub-basins that developed on the STR from the Late Cretaceous to the Eocene as Australia moved northward (see "Background and Objectives," p. 6). The lithology of the corresponding prograded Paleocene and onlapping Eocene seismic units consists of clayey siltstone and silty claystone. The clay particles are therefore considered of local origin principally, supplied through runoff from adjacent emerged areas. Such emergence was almost certainly caused by the coeval tectonic uplift on nearby faults,

associated with the culminating movements on the Balleny Fracture Zone. The clay assemblage would have been derived from weathering and erosion of adjacent steep continental areas occurring at the end of the Cretaceous to Eocene stage of tectonic activity (Royer and Rollet, 1997) that led to the final formation of local transtensional sub-basins in the late Paleocene (see "Tectonic Evolution," p. 45, in "Discussion and Conclusions" in the "Leg 189 Summary" chapter). Identical clay assemblages in similar structural and sedimentological settings have been observed in the South Atlantic during warm Cretaceous intervals of tectonic activity related to early stages of ocean opening (Robert, 1987). In these areas, tectonic activity resulted in steep relief, whereas precipitation and drainage ensured chemical weathering and erosion of soils (kaolinite) and substrates (illite and chlorite).

The large predominance of smectite characterizes middle Eocene Unit C4, together with decreased contents of kaolinite and illite and the lack of chlorite. The siliciclastic sediment consists of claystone and silty claystone, and the clay particles are most probably derived from adjacent emerged areas as in Unit C5. Largely predominant smectite still points to warm climatic conditions with alternating humid and dry intervals. The clay assemblage of Unit C4 is very similar to that in coeval sediments of Site 1170 (see "Lithostratigraphy," p. 9, in the "Site 1170" chapter). In the middle Eocene, clay assemblages dominated by smectite also prevailed in areas off the passive Antarctic margins on the Maud Rise (Robert and Maillot, 1990) and Kerguelen Plateau (Ehrmann, 1991). However, the increasing trend of smectite, beginning in the upper part of Unit C5, and correlative decrease of kaolinite, illite, and chlorite suggest that the continental relief decreased from the late early to the middle Eocene. A similar evolution of the clay assemblage is observed in Cretaceous sediments from the South Atlantic, where it is related to the phase of subsidence and transgression of the continental margins that follows the early stages of ocean opening (Robert, 1987). The transition to almost exclusively smectite in Unit C4 probably resulted from a stage of tectonic relaxation and subsidence after tectonic activity ceased in that part of the STR (see "Tectonic Evolution," p. 45, in "Discussion and Conclusions" in the "Leg 189 Summary" chapter).

Distinct increases of illite (and random mixed-layered clays) in middle to upper Eocene Unit C3 are indicative of strong physical weathering and erosion of substrates in the source areas. Coeval increases of illite (up to 100%) also occurred at Site 1170 on the western STR (see "Lithostratigraphy," p. 9, in the "Site 1170" chapter). However, such an occurrence of illite has not been observed in other areas of the middle and late Eocene Southern Ocean and Tasman Sea, where the clay assemblage consisted largely of smectite (Robert et al., 1985; Robert and Maillot, 1990; Ehrmann, 1991). It is inferred that illite in Unit C3 is derived from physical weathering and erosion of substrates in the emerged parts of the STR area. Lower illite content at Site 1171 than at Site 1170 (see "Lithostratigraphy," p. 9, in the "Site 1170" chapter) also suggests that physical weathering and erosion were more intense in the western part of the STR. There, steep relief developed during the late middle to late Eocene stage of tectonic activity that preceded the separation of the STR from Antarctica, when strike-slip tectonism formed at the ridge of the Tasman Fracture Zone on the western edge of the STR (Royer and Rollet, 1997). This interval of tectonic activity is associated with a slight decrease of chemical weathering on the emerged Antarctic margins and expansion of cool antarctic waters in the Southern Ocean

(Robert and Kennett, 1992; see "Lithostratigraphy," p. 9, in the "Site 1170" chapter).

A drastic decrease of smectite is the most typical feature of Unit C2, which spans the Oligocene to early Pliocene. Significant amounts of illite and random mixed-layered clays result from erosion of poorly weathered substrates in the sediment's source area. The clay assemblage of Unit C2 at Site 1171 strongly differs from that at Site 1168 on the west Tasmania margin, where relatively high kaolinite content is found together with minor illite and an absence of random mixed-layered clays (see "Lithostratigraphy," p. 8, in the "Site 1168" chapter). However, it closely resembles that of Unit C2 at Site 1170 (see "Lithostratigraphy," p. 9, in the "Site 1170" chapter). The C2 clay assemblages at both sites of the STR most probably derived from a range of continental areas and expresses average weathering conditions on the emerged margins of the Southern Ocean.

Unit C1 of late Pliocene to Pleistocene age is marked by significantly increased smectite (up to 80%) and minor amounts of illite and kaolinite (<10%). Coeval sediments at Sites 1168 and 1170 (see "Lithostratigraphy," p. 8, in the "Site 1168" and "Lithostratigraphy," p. 9, in the "Site 1170" chapter) and in the adjacent Tasman Sea (Stein and Robert, 1986) contain significantly higher amounts of kaolinite (15% to 45%). Therefore, the clay assemblage of Unit C1 does not principally reflect either dust transport from Australia or weathering conditions of antarctic or subantarctic areas, as illite, chlorite, and random mixed-layered clays account for ~50% of the clay fraction in these areas (Robert and Maillot, 1983, 1990; Ehrmann, 1991). It may rather result from erosion of ancient sediments containing high proportions of smectite. Such sediments are frequent from the Cretaceous to the Paleogene in Southern Ocean margins and basins (Robert and Maillot, 1990; Ehrmann, 1991), including the STR (Fig. F18; see "Lithostratigraphy," p. 9, in the "Site 1170" chapter). As Cretaceous and early Paleogene sediments outcrop on the flanks of strike-slip basins and ridges of the STR (see "Background and Objectives," p. 6), their erosion by submarine currents may have provided ancient reworked smectite to the late Pliocene–Pleistocene Unit C1 of Site 1171.

## BIOSTRATIGRAPHY

Sediments ranging in age from late Paleocene (~56 Ma) to Quaternary were recovered at Site 1171. Triple APC coring of a relatively undisturbed upper Neogene sequence made it possible to construct a composite stratigraphy using biostratigraphic and physical properties data. Thus, stratigraphic coverage and resolution was greatly enhanced for Cores 189-1171A-1H through 14H. The age-depth model used to calculate sedimentation rates (Fig. F19) is plotted in meters composite depth (mcd).

The Neogene sequence is largely complete except for a hiatus at the Miocene/Pliocene boundary. The hiatus is evidenced by the absence of several planktonic foraminiferal zones, which indicate that the lowermost Pliocene and much of the upper Miocene is missing at Site 1171 (see "Planktonic Foraminifers," p. 29). A similar hiatus was identified across the Miocene/Pliocene boundary at Sites 1169 and 1170, but not at Site 1168. The lower upper and upper middle Miocene interval, by contrast, appears to be expanded, showing sedimentation rates approaching 4 cm/k.y.

**F19.** Age-depth plot and linear sedimentation rates, p. 89

Although sedimentation rates decrease, the biostratigraphic succession continues relatively uninterrupted across the Oligocene/Miocene boundary. Another hiatus is inferred farther downsection at the base of the upper Oligocene (~28.5 Ma). In all likelihood, the uppermost part of the lower Oligocene has been truncated as well (see "Planktonic Foraminifers," p. 29). Multiple lines of biostratigraphic evidence (planktonic foraminifers, calcareous nannofossils, and diatoms) corroborate the presence of a hiatus at the upper/lower Oligocene boundary (see Fig. F20).

The completeness of the Eocene–Oligocene transition, as recorded at Site 1171, remains unresolved. There is a sharp sedimentological break in Section 189-1171D-3R-3, 28 cm, which juxtaposes limestone and green siliciclastic sediments (see "Lithostratigraphy," p. 10). This abrupt lithologic change is well expressed as a precipitous decline in the percent $CaCO_3$ record (see Fig. F30). Calcareous nannofossils from near the base of the overlying limestone (Sample 189-1171D-3R-3, 20 cm) yield a maximum age of ~32.3 Ma, placing the limestone firmly within the early Oligocene (see "Calcareous Nannofossils," p. 27). Furthermore, the stratigraphic ranges of three calcareous nannofossil taxa terminate within a relatively short interval just below the limestone (Samples 189-1171D-3R-3, 20 cm, and 3R-CC), suggesting that the sequence is condensed and/or the presence of a hiatus.

However, examination of smear slides taken from the upper meter of "green sands," directly beneath the limestone, revealed this interval to be barren of calcareous nannofossils. Study of the associated core-catcher sample (189-1171D-3R-CC) yielded a suite of palynomorphs containing the dinocysts *Areophaeridium diktyoplokum* and *Enneadocysta partridgei.* This association of dinocysts constrains the age of the core-catcher sample between 33 to 37 Ma (see "Palynology," p. 36). This finding has added significance because the last occurrence (LO) of *A. diktyoplokum* demarcates the Eocene/Oligocene boundary (Brinkhuis and Biffi, 1993). Sample 189-1171D-2R-CC was found to be barren of palynomorphs. Thus, the actual position of this important datum (the LO of *A. diktyoplokum*) is not precisely known but must fall somewhere between Sample 189-1171D-3R-CC and the abrupt lithologic change at Sample 189-1171D-3R-3, 28 cm. The precise stratigraphic position of the Eocene/Oligocene boundary and whether the upper stratigraphic range of *A. diktyoplokum* is truncated by the base of the upper Oligocene limestone needs further investigation.

Sedimentation resumes temporarily in the upper middle Eocene, but it is possible that yet another hiatus is present within the middle middle Eocene. This may be the oldest in a series of closely spaced unconformities and its presence is indicated by the coincidence of several calcareous nannofossil datums (see "Calcareous Nannofossils," p. 27). An alternative interpretation can be formulated using a biochronology based upon the middle Eocene palynological record (see "Palynology," p. 36). The sedimentation model yielded by dinocyst datums is equally viable and indicates that sedimentation resumes in the upper middle Eocene and continues uninterrupted until the lower middle Eocene. Finally, several lines of evidence (palynological, physical properties, organic geochemistry, and magnetostratigraphy) suggest the presence of a stratigraphic gap within the lower middle Eocene as well.

The lowermost part of the recovered section (Samples 189-1171D-70R-CC through 75R-CC) contains rare to few calcareous nannofossils and is barren of planktonic foraminifers, radiolarians, and diatoms. No age-diagnostic nannofossil taxa are present in this interval, although

F20. Combined biostratigraphic interpretation of the Eocene–Oligocene transition, p. 90.
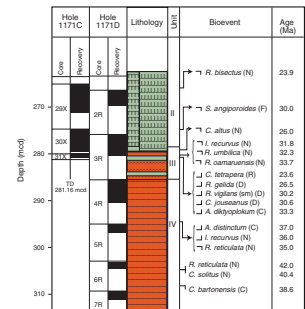
there are rare, possibly reworked, Paleocene taxa within the depauperate nannofloras. In contrast, the stratigraphic succession of palynological datums and bioevents observed over this same interval clearly indicate that sediments below Sample 189-1171D-73R-CC are of late Paleocene age. There is marked shift in the composition of these palynological assemblages between Samples 189-1171D-72R-CC and 74R-CC, suggesting that there may be a hiatus at, or near, the Paleocene/Eocene boundary.

Calcareous nannofossils and planktonic foraminifers dominate the Oligocene and Neogene carbonate sequences recovered at Site 1171. Siliceous microfossil groups (i.e., radiolarians and diatoms) are relatively abundant and well preserved throughout much of the same ~272 m of carbonates. Benthic foraminifers are well preserved throughout this interval but are sparse relative to their planktonic counterparts. Benthic foraminiferal faunas are characterized as having affinities for bathyal to abyssal water depths, reflecting an open-ocean environment with well-ventilated bottom waters. The Oligocene to Quaternary section is largely devoid of dinoflagellate cysts.

The thick (~670 m) Eocene sequence recovered at Site 1171 contrasts starkly with the younger carbonate sequences. The smectite-enriched glauconitic siltstones of the Eocene not only differ sedimentologically from the younger carbonates, but paleontologically as well. The Eocene sequence is punctuated by numerous intervals barren of calcareous microfossils. This holds true particularly for the planktonic foraminifers, which are absent across the Eocene–Oligocene transition. Siliceous microfossils are rare to absent throughout much of the Eocene as well, although benthic and neritic planktonic diatoms are common in the upper part of the Eocene section. Benthic foraminifers become significant contributors to sediment production in the Eocene, composing up to 50% of the >125-µm-size fraction in some samples. Another striking difference is that palynomorphs are very abundant throughout the Eocene, providing much needed biochronological control.

In general, the microfossil groups (planktonic foraminifers, radiolarians, dinocysts, diatoms, and calcareous nannofossils) are dominated by temperate to subantarctic species. Given that Site 1171 is south of the modern Subtropical Front and is the most southerly location drilled during Leg 189, this observation is expected. The decreases in abundance recorded in both the calcareous and siliceous microfossil groups in the Eocene sequence appear to have been caused by harsh paleoenvironmental conditions, rather than poor preservation. This interpretation is supported by various lines of independent evidence. Both the diatom floras and benthic foraminiferal faunas indicate that Eocene sediments were deposited in a neritic setting. This paleoenvironmental signal is consistent with the dinocyst biofacies. The palynological evidence also indicates that the Eocene "green sands" were deposited in a eutrophic, neritic environment (see **"Palynology,"** p. 36). Furthermore, planktonic foraminifers, although rare in Eocene sediments, do not exhibit conspicuous signs of shell dissolution and/or fragmentation. Thus, it appears that marginal marine conditions, stemming from local and global variations in tectono-eustasy, prevailed during the Eocene.

## Calcareous Nannofossils

All core-catcher samples, plus additional samples from some critical intervals, were examined for calcareous nannofossils at Site 1171. Calcareous nannofossil abundance decreases downcore with many barren

samples below 770 mbsf (Table T3). Preservation is generally good to moderate. Nannofossil diversity is lower at Site 1171 than previous sites cored during Leg 189, reflecting its higher latitude. Some calcareous nannofossil zones/subzones could not be differentiated because of the lack of marker species. The nannofossil biostratigraphy for the middle Eocene through the Pleistocene presented in Table T4 was based on all the nannofossil bioevents recognized. Holes 1171A, 1171B, and 1171C had excellent core recovery and provide an overlap record down to ~11 Ma (Fig. F21).

The first occurrence (FO) of *Emiliania huxleyi* was not recorded in the first core-catcher sample at any of the three holes, indicating an age of older than 0.26 Ma for these samples. The LO of *Pseudoemiliania lacunosa* (0.46 Ma) was recognized, which helps subdivide the Pleistocene epoch (see Table T5 for occurrence intervals in Holes 1171A, 1171B, and 1171C).

The rarity of discoasters in all holes prevented the recognition of several subzones and necessitated the use of alternative markers to recognize epoch boundaries. The LO of *Calcidiscus macintyrei* (1.67 Ma) is used to approximate the Pliocene/Pleistocene boundary in the absence of *Discoaster brouweri*. The LO of *Reticulofenestra psuedoumbilica* (and its cooler water form *Reticulofenestra gelida*) (3.65 Ma) is used to mark the lower/upper Pliocene boundary.

The traditional marker for the Pliocene/Miocene boundary is *Discoaster quinqueramus,* which was not observed at this site. The LO of *Triquetrorhabdulus rugosus* (5.3 Ma) is used to approximate this boundary. The middle/late Miocene marker *Discoaster hamatus* was not encountered at any of the Leg 189 sites. The LO of *Coccolithus miopelagicus* (11.0 Ma) and the LO of *Cyclicargolithus floridanus* (11.9 Ma) are used to here to bracket the boundary.

The FO of *Calcidiscus premacintyrei* (17.4 Ma) is located between Samples 189-1171C-22X-CC and 23X-CC. The acme of *Cyclicargolithus abisectus,* observed between Samples 189-1171C-27X-CC and 28X-CC, marks the beginning of Subzone CN1b in the earliest Miocene (~23.2 Ma).

The LO of *Reticulofenestra bisecta* (23.9 Ma) was recognized between Samples 189-1171C-28X-CC and 29X-CC. The Oligocene/Miocene boundary is generally placed just above this datum. Another Oligocene nannofossil datum, the LO of *Chiasmolithus altus* (26.1 Ma), is one core lower between Samples 189-1171C-29X-CC and 30X-CC.

The first core from Hole 1171D stratigraphically overlaps with Core 189-1171C-29X. Both core-catcher samples contain similar nannofossil assemblages with an age range of 23.9–26.1 Ma. The LO of *C. altus* is located between Samples 189-1171D-2R-CC and 3R-CC.

Three nannofossil datums are truncated between Samples 189-1171D-3R-3, 20 cm, and 3R-CC. These datums are the LO of *Reticulofenestra umbilica, Isthmolithus recurvus,* and *Reticulofenestra oamaruensis,* indicating a hiatus that correlates to at least 32.3 to 33.7 Ma (Fig. F19) (i.e., the uppermost Eocene to the lowermost Oligocene is missing; Fig. F21).

*Isthmolithus recurvus* is present down to Sample 189-1171D-4R-CC and thus suggests an age of 36.0 Ma between Samples 189-1171D-4R-CC and 5R-CC. Both *I. recurvus* and *R. oamaruensis,* which are excellent stratigraphic markers in southern high latitudes, were easily recognized at Site 1171 but are missing at the previous Site 1170. This is most likely the result of missing more sections at Site 1170 than at Site 1171 over the Eocene–Oligocene transition.

T3. Identification and abundances of nannofossils, p. 130.

T4. Calcareous nannofossil datum levels, p. 138.

F21. Correlations between Holes 1171A, 1171B, and 1171C based on calcareous nannofossil biostratigraphy, p. 91.
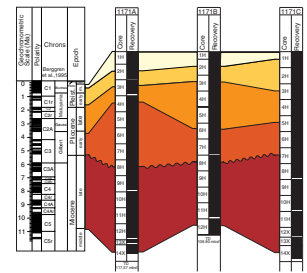


T5. Range chart of planktonic foraminifers, p. 139.

Similar to Site 1170, the LO of *Chiasmolithus solitus* (40.4 Ma) coincides with the FO of *Reticulofenestra reticulata* (42.0 Ma) between Samples 189-1171D-6R-CC and 7R-1, 25 cm. A hiatus is therefore indicated here (Fig. F21). We note that this same middle Eocene hiatus at Site 1170 was called into question because of the lack of evidence for significant lithologic change. Further study is needed to resolve this issue.

The FO of *R. umbilica* (43.7 Ma) is located between Samples 189-1171D-26R-CC and 27R-CC. Assuming that the age for this datum is valid at this site, this would suggest a sedimentation rate of >10 cm/k.y. between Cores 189-1171D-7R and 26R.

*Discoaster kuepperi* was sporadic from Samples 189-1171D-45R-CC to 56R-CC. This suggests an age range of ~48–53 Ma for the samples. Because samples below this stratigraphic interval are generally barren of nannofossils, the true FO of *D. kuepperi* (~53 Ma) could not be determined.

*Prinsius bisulcus* and small *Reticulofenestra* were found in Samples 189-1171D-64R-CC and 67R-CC. The former species is generally limited to the Paleocene, whereas the latter taxon is generally limited to the Eocene or younger sediments. A consistent age cannot be assigned to these samples based on these nannofossil taxa. Furthermore, the co-occurrence of taxa of different ages suggests sediment reworking.

## Planktonic Foraminifers

Sediments bearing planktonic foraminifers ranged in age from middle Eocene to Quaternary at Site 1171. The planktonic foraminiferal assemblages are typical of cool temperate to subantarctic regions, although they occasionally exhibit a temperate-water influence. Consequently, the subantarctic zonal scheme of Stott and Kennett (1990) rather than that of Jenkins (1993a, 1993b) is used to discuss the Eocene to lower Oligocene sediments at Site 1171. Most of the Neogene to the late Oligocene biozones are recognized at Site 1171, with the notable exception of the lower Pliocene/upper Miocene boundary where Zones SN10, SN11, and Subzone SN12a are missing. The absence of the late Oligocene Subzone SP14a indicates another stratigraphic break. Beneath this is the early Oligocene Zone AP13, which is followed by an upper to lower Eocene sequence. The sequence, including the hiatuses, is similar to that found at Site 1170.

Planktonic foraminifers provide little biostratigraphic control throughout much of the Paleogene sequence recovered at Site 1171. However, notable exceptions are found in the lower Oligocene and within discrete intervals in the upper Eocene to middle Eocene. In the lower Eocene, planktonic foraminiferal assemblages are often depauperate, but sporadic assemblages are present in the section. Within the Eocene, the assemblages are separated by a series of barren intervals, with all samples barren of planktonic foraminifers below Sample 189-1171D-65R-CC. The lower Eocene at this site contains the most diverse of the Eocene assemblages, but these assemblages are still relatively sparse. Furthermore, evidence derived from other microfossil groups (e.g., dinocysts and calcareous nannofossils) suggests the presence of an unconformity separating the middle and lower Eocene (Samples 189-1171D-32R-CC and 33R-CC). This complication, plus the ecological exclusion of key marker species such as *Acarinina primitiva* and *Globigerinatheka index* combined with the many barren intervals, will undoubtedly result in considerable refinement to the Eocene biostratigraphy discussed herein.

Stratigraphic distributions for Oligocene and Neogene species are given in Table T5. The core depths of the various planktonic foraminiferal datums at Site 1171 are given in Table T6. A brief discussion of the salient biostratigraphic findings is provided below.

## Quaternary

The base of the Quaternary, as defined by the FO of *Globorotalia truncatulinoides,* is confined between the two uppermost cores in Holes 1171A and 1171B (Samples 189-1171A-1H-CC to 2H-CC). Curiously, the FO of *G. truncatulinoides* is not recognized in Hole 1171C (Sample 189-1171C-1H-CC; 9.65 mbsf). This appears to be another instance where the FO of *G. truncatulinoides* is an unreliable datum in the STR region (for further discussion see "Biostratigraphy," p. 19, in the "Site 1170" chapter). The well-preserved assemblages are primarily subantarctic in character and dominated by such cool-water species as *Globigerina bulloides, Globorotalia crassaformis, Globorotalia inflata,* and *Neogloboquadrina pachyderma* (sinistral).

## Pliocene

The late Pliocene Zone SN13, as well as the upper part of Subzone SN12b, are well represented at Site 1171 (see Table T5). The well-preserved faunas are dominated by specimens belonging to the *Globorotalia puncticulata/Globorotalia inflata* plexus. In contrast, the lower Pliocene (Subzone SN12a) and much of the upper Miocene (Zones SN10 and SN11) appear to be missing. There is a conspicuous break in the stratigraphic sequence at the Miocene/Pliocene boundary (Samples 189-1171A-6H-CC and 7H-CC). Preservation within Samples 189-1171A-6H-CC and 7H-CC deteriorates with increased carbonate dissolution and shell fragmentation.

## Early Pliocene/Late Miocene Hiatus

Subzone SN12b corresponds to a succession ~25 to 30 m thick at Site 1171, which is relatively thin compared to the same subzone at Sites 1168 and 1169. Thus, the lower part of Subzone SN12b may also be missing given the evidence for carbonate dissolution. Subzone SN12b unconformably overlies the early late Miocene Zone SN9, which, in turn, is itself thin (10 to 20 m). The assemblages within Zone SN9 have been strongly affected by dissolution. Given that one of the missing zones (SN10) is by definition a gap zone, it is possible that its absence is, in part, a stratigraphic aberration caused by migratory shifts in the biogeographies of the marker taxa. A conservative estimate of the amount of time missing is ~2.5 m.y. This estimate should be treated as a minimum because it is likely that the uppermost part of the underlying Zone SN9 has also been removed. This same hiatus is present at Sites 1169 and 1170.

## Middle Miocene

Zones SN5 to SN8, which are within the middle Miocene, are recognized with no conspicuous breaks. Planktonic foraminifers are typically abundant throughout the interval bounded by Zones SN7 to SN8. Warm-water species with subtropical affinities (e.g., *Globorotalia limbata*) are present in low abundances throughout much of Zone SN8 (see

Table T5). Many foraminifers show varying degrees of dissolution with taxa, such as *Orbulina universa* being rare to absent. The lower zones (SN5 and SN6) have better-preserved assemblages, and foraminifers are abundant.

## Early Miocene

All early Miocene zones (SN1 to SN4) are recognized at Site 1171. Planktonic foraminifers are abundant and well preserved throughout the lower Miocene. However, determination of the base of Zone SN1, which coincides with the Oligocene/Miocene boundary, was problematic. The FO of *Globoquadrina dehiscens* (23.3 Ma) approximates the Oligocene/Miocene boundary. Unfortunately, the stratigraphic distribution of this marker species is quite erratic at Site 1171. The scarcity of this thermophilic species probably reflects the cold surface waters that bathed Site 1711 during the earliest Miocene. Consequently, the Oligocene/Miocene boundary is tentatively placed between Samples 189-1171C-26X-CC (237.56 mbsf) and 27X-CC (247.33 mbsf).

## Late Oligocene/Early Miocene Boundary

The transition from the lower Miocene (Zone SN1) to the upper Oligocene (Subzone SP14b) is confined to the interval between Samples 189-1171C-26X-CC (237.56 mbsf) and 27X-CC (247.33 mbsf). Much like at Sites 1168 and 1170, the biostratigraphic succession across the boundary appears to be relatively complete at Site 1171. However, Subzone SP14b is only ~26 m thick, as opposed to nearly 300 m at Site 1168. The presence of a hiatus at the base of Subzone SP14b is indicated by the appearance of *Subbotina angiporoides* in Sample 189-1171C-30X-CC (272.87 mbsf). Thus, the lower upper Oligocene (Subzone SP14a), which encompasses some 1.5 m.y., is missing at Site 1171. A similar hiatus was also recorded at Site 1170. Thus, Sample 189-1171C-30X-CC, and the bottom of Hole 1171C, is assigned to the early Oligocene Zone AP13. The uppermost core-catcher sample from Hole 1171D, Sample 189-1171D-1R-CC, overlaps with Hole 1171C in the late Oligocene Subzone SP14b.

## Early Oligocene

The lower Oligocene at Site 1171 is much thicker (160 m) than at Site 1170 (40 m). The early Oligocene is represented by the *S. angiporoides* Zone (AP13), which is bounded by unconformities at Site 1171. The base of Zone AP13 appears to grade down into a barren interval in Sample 189-1171D-3R-CC (271.34 mbsf). The interval from Samples 189-1171D-2R-CC to 3R-CC is also associated with a precipitous decline in overall carbonate content (see "Organic Geochemistry," p. 44). In general, the overall character of the lower Oligocene stratigraphic succession, with its numerous barren intervals and with Zone AP13 directly overlying a barren interval, is similar to that at Site 1170. The uppermost occurrence of *Chiloguembelina cubensis* was in Sample 189-1171C-30X-CC (272.87 mbsf), where it coexists with *S. angiporoides,* indicating that these sediments belong to Zone AP13. The early Oligocene assemblages are characterized by low (trace) numbers of specimens to abundant planktonic foraminifers in the upper parts.

## Eocene/Oligocene Boundary

Much like the section at Site 1170, the Site 1171 Eocene–Oligocene transition (Sample 189-1171D-3R-CC) is barren of planktonic foraminifers. The absence of planktonic foraminifers is believed to be caused by unfavorable ecological conditions, as opposed to poor carbonate preservation. A few samples (Samples 189-1171D-4R-CC, 7R-CC, and 8R-CC) contain *Subbotina angiporoides* only and so can be no younger than Zone AP13. Sample 189-1171D-4R-CC contains the calcareous nannofossil *I. recurvus* (see "Calcareous Nannofossils," p. 27) and is assigned a late Eocene age. Thus, Sample 189-1171D-4R-CC is believed to belong to Zone AP11. Samples 189-1171D-4R-CC, 7R-CC, and 8R-CC are older but still within Zone AP12, above the FO of *S. linaperta.*

## Late to Middle Eocene

Below the barren Eocene/Oligocene boundary interval, the stratigraphic sequence between Samples 189-1171D-14R-CC to 31R-CC (353.28–533.73 mbsf) is marked by numerous barren intervals that occasionally give way to discrete horizons containing impoverished assemblages. The co-occurrence of *Pseudohastigerina micra* and *Subbotina linaperta,* particularly in Sample 189-1171D-31R-CC, constrains the age of this interval to the late middle to early late Eocene (Zones AP9 to AP11).

There are sporadic assemblages between Samples 189-1171D-34R-CC and 46R-CC that contain such species as *Acarinina collactea, Acarinina bullbrooki, Acarinina pentacamerata,* and, in rare instances, *Morozovella spinulosa.* Similar faunas have been reported (Huber, 1991; Berggren, 1992) from the Kerguelen Plateau region and assigned to the early middle to late middle Eocene (Zones AP8 to AP10).

## Early Eocene

As with the rest of the Eocene, planktonic foraminifers are only sporadically present. The section between Samples 189-1171D-47R-CC and 65R-CC is within the stratigraphic range of *Globanomalina australiformis,* indicating the lower portion of this interval is no older than earliest Eocene (~55.5 Ma). The two lowermost samples (189-1171D-64R-CC and 65R-CC) contain specimens referable to *Globanomalina ovalis* and *G. australiformis,* placing these sediments into Zone AP6. Below this level, all samples are barren of planktonic foraminifers. Preservation in the lower Eocene section ranges from poor to moderate.

# Benthic Foraminifers, Ostracodes, and Bolboforma

Similar to Site 1170, benthic foraminiferal assemblages at Site 1171 document a profound change from a shallow-water fauna in the Paleocene–Eocene to a bathyal to abyssal fauna in the Oligocene and Neogene (Fig. F22). The transition from water depths of <100 to >1000 m was accomplished by the end of the early Oligocene. Another aspect that distinguishes the intervals before and following the Eocene/Oligocene boundary is that for most of the Eocene, benthic foraminifers are abundant, accounting for as much as 50% of the material in the >125-µm fraction. In the Oligocene and Neogene sections, however, abundances are very low.

**F22.** Benthic foraminiferal assemblages and inferred paleodepths, p. 92.

Samples 189-1171D-75R-CC to 70R-CC are dominated by the occurrence of the finely agglutinating *Spiroplectammina* spp., which is present together with a limited variety of coarsely agglutinating species. This interval includes the Paleocene with its upper limit possibly postdating the Paleocene/Eocene boundary. The lowest interval in the lowermost Eocene (Samples 189-1171D-69R-CC through 64R-CC) is marked by very low abundances of agglutinating foraminifers and occasional traces of calcareous species. The middle lower Eocene is an interval of alternating assemblages, the main feature of which is the presence or absence of *Spiroplectammina* spp. (Samples 189-1171D-63R-CC through 57R-CC). The remainder of the lower Eocene features low abundances of agglutinating foraminifers, such as *Reophax* spp. and of some calcareous species (Samples 189-1171D-56R-CC through 48R-CC). Most of the middle Eocene is characterized by highly abundant benthic foraminifers. Calcareous species were clearly dominant during this interval, with *Elphidium* and *Lenticulina* spp. being most important during the interval from Sample 189-1171D-47R-CC through 20R-CC. The interval 189-1171D-19R-CC to 7R-CC shows slightly lower abundances and is marked by the additional occurrence of calcareous *Nonion deceptrix* and agglutinating *Eggerelloides* spp. Faunal assemblages in the Paleocene and Eocene suggest neritic (~50–100 m) water depths. Preservation is moderate, with most tests showing signs of diagenetic alteration.

Samples 189-1171D-5R-CC and 3R-CC are glauconitic siltstones mainly barren of benthic foraminifers. But within this interval (Sample 189-1171D-4R-CC), rare and mostly calcareous foraminifers are present, suggesting upper- to middle-bathyal water depth (~200–1000 m) based on the presence of *Cibicidoides* spp. The top samples in Hole 1171D (189-1171D-2R-CC and 1R-CC) and the bottom samples in Hole 1171C (189-1171C-30X-CC through 27X-CC) show increased numbers of *Karreriella bradyi,* which was not observed at previous sites. The assemblages suggest middle to lower bathyal water depths (~600–1500 m) for the late Oligocene based on the presence of *Bulimina* and *Melonis* spp., and lower bathyal to abyssal water depths (~1500–2500 m) during the early Miocene as reflected by the presence of *Cibicidoides mundulus* and *Nuttalides umbonifera.*

By the middle Miocene, sediments were being deposited in upper abyssal depths (~2000–3000 m), as suggested by the presence of *Epistominella exigua.* The entire Neogene and Pleistocene section is marked by low abundances and reduced diversities of benthic foraminifers, when compared to all the previous sites. Both *C. mundulus* and *Fontbotia wuellerstorfi* disappear at the lower to upper Pliocene boundary (Sample 189-1171A-5H-CC). *Melonis* spp. are present in the Neogene, but they are never abundant. The topmost sample (189-1171A-1H-CC) shows traces of *Chilostomella oolina,* similar to Sites 1169 and 1170. Preservation of tests is generally good in the Neogene and Pleistocene section.

The benthic foraminiferal assemblages suggest that the most significant interval of subsidence occurred during the late Eocene–early Oligocene (i.e., the transition from water depths of <100 m to depths of >1500 m). This period is marked by numerous hiatuses interspersed with intervals of extremely low sedimentation, which makes a precise age control difficult. The lower Miocene might still have been shallower than the middle Miocene at this site, but the deepening to upper abyssal depths could have been concluded by the time of the early early Miocene.

Most samples in the biogenic carbonate sequence (189-1171C-30X-CC to 15X-CC and 189-1171A-14X-CC to 1H-CC) contain a few ostracode carapaces, whereas the Eocene interval is marked by only sporadic traces. *Bolboforma* spp. were identified in Samples 189-1171C-29X-CC and 21X-CC and were notably abundant in Samples 189-1171A-13X-CC through 11H-CC.

## Radiolarians

Radiolarians are generally common and well preserved in the Quaternary through lowermost Miocene, generally rare to common and poorly preserved in the Oligocene, whereas the Eocene is barren with a few exceptions. The datum, age, and sample intervals recognized at Site 1171 are shown in Table T7. Some remarks on selected radiolarian events are presented below.

Samples 189-1171A-1H-CC through 3H-CC, 189-1171B-1H-CC through 3H-CC, and 189-1171C-1H-CC through 3H-CC are Quaternary through early Pliocene in age. The boundary between the lower and upper Pliocene is placed between the LO and FO of *Pseudocubus vema*. The lower Pliocene is recognized in Samples 189-1171A-4H-CC through 6H-CC, 189-1171B-4H-CC through 6H-CC, and 189-1171C-4H-CC. The base of the Pliocene is approximated by the last consistent occurrence (LCO) of *Stichocorys delmontensis* (5.18–6.9 Ma).

The upper Miocene is recognized in Samples 189-1171A-7H-CC through 11H-CC, 189-1171B-7H-CC through 11H-CC, and 189-1171C-5H-CC through 11H-CC, respectively. Similar to Site 1170, the upper Miocene *Stichocorys peregrina* abundance zone at Site 1171 is recognized (Samples 189-1171A-7H-CC through 10H-CC, 189-1171B-7H-CC through 10H-CC, and 189-1171C-6H-CC through 9H-CC). *Amphymenium challengerae* has an age range of 6.8 to 6.1 Ma and is recovered from Sample 189-1171A-7H-CC only. The base of the upper Miocene is placed between Samples 189-1171A-11H-CC and 12H-CC, 189-1171B-11H-CC and 12H-CC, and 189-1171C-11H-CC and 12X-CC, based on the last abundant occurrence (LAO) of *Cyrtocapsella japonica,* for which a tentative age of 11.6 Ma has been derived from a cursory age-depth model at Site 1170.

The middle Miocene is recognized from Samples 189-1171A-12H-CC through 14X-CC, 189-1171B-12H-CC, and 189-1171C-12X-CC through 20X-CC. The boundary between middle and lower Miocene is placed between Samples 189-1171C-20X-CC and 23X-CC and is characterized by the FO of *Lychnocanoma nipponica nipponica* at 15.7 Ma and the LO of *Cenosphaera coronata* at 16.7 Ma. The lower Miocene radiolarian faunas at Site 1171 are marked by abundant *C. coronata* and *Cenosphaera coronataformis.* The FO of *Cyrtocapsella tetrapera* between Samples 189-1171C-25X-CC and 26X-CC and 189-1171D-2R-CC and 3R-CC approximates the base of lower Miocene.

Samples 189-1171C-26X-CC through 28X-CC are correlated to the latest Oligocene because the FO of *Cenosphaera coronataformis* at 24.4 Ma, calculated from the Site 1170 age-depth model, was recorded in Sample 189-1171C-28X-CC. Samples 189-1171D-1R-CC through 2R-CC are assigned to the early Oligocene as indicated by the presence of *Lychnocanoma conica* (FO between 32.6 and 33.1 Ma) and *Eucyrtidium spinosum* (LO between 32.6 and 33.1 Ma) in Sample 189-1171D-3R-CC. Samples 189-1171D-7R-CC through 10R-CC contain many well-preserved radiolarians but lack age-diagnostic radiolarians. Samples 189-1171D-11R-CC through 75R-CC are barren. Poorly preserved radiolarians are

**T7.** Core depths of selected radiolarian datums, p. 144.

common in Samples 189-1171D-11R-CC, 17R-CC, 18R-CC, 23R-CC, 27R-CC, and 28R-CC.

## Diatoms, Silicoflagellates, and Sponge Spicules

All core-catcher material from Holes 1171A and 1171D, most samples from Holes 1171C, and selected samples from Hole 1171B were analyzed for diatoms, silicoflagellates, and sponge spicules. Smear slides were examined to assess overall relative abundance. For full assemblage analysis, additional material was treated with 40% HCl to remove the carbonate component.

Well-preserved diatoms are abundant throughout Hole 1171A, except for Samples 189-1171A-5H-CC through 7H-CC, which contain a poor to moderately preserved in situ flora along with reworked diatoms of Oligocene (e.g., *Rocella vigilans*) and middle Miocene (e.g., *Actinocyclus ingens* var. *nodus*) age. Reworking of shallow-water sediments (probably from the STR) is also implied in these three samples by the rare occurrences of neritic diatoms such as *Paralia*. Diversity generally decreases downhole. Likewise, diatoms are mostly abundant in every sample studied from Hole 1171C. Samples 189-1171D-1R-CC through 11R-CC contain common to abundant diatoms (except Sample 189-1171D-5R-CC, where diatoms are rare). Samples 189-1171D-12R-CC through 36R-CC contain trace to few diatoms, and below this level diatoms are mostly absent. The sharp decrease in abundance of diatoms between Samples 189-1171D-11R-CC and 12R-CC is reflected in a sharp decrease in the concentration of pore-water silica in Hole 1171D (see "Inorganic Geochemistry," p. 50). Relative abundance data for diatoms, sponge spicules, and silicoflagellates are presented in Tables **T8** and **T9.**

Twenty-six age-diagnostic diatom bioevents are recognized in Holes 1171A, 1171C, and 1171D. These are presented in Table **T10.** The LO of *Actinocyclus ingens* var. *ovalis* (6.27 Ma) is recognized in Hole 1171C between Cores 189-1171C-6H and 7H (at a mean depth of 62.29 mbsf). This datum is difficult to place in Hole 1171A, however. As for Site 1170, the oldest diatom bioevents at Site 1171 are present above the Eocene/Oligocene boundary. At Site 1171, these represent the FO of *Rocella vigilans* (small form) (30.24 Ma) and the FO of *Cavitatus (Synedra) jouseanus* (30.62 Ma). Both events are between Samples 189-1171D-2R-CC and 3R-CC. The FO of *R. gelida* (26.50 Ma) also is between these samples, suggesting a hiatus representing ~4 m.y. across the early/late Oligocene boundary.

Below the Eocene/Oligocene boundary, diatoms are not age diagnostic (i.e., long-ranging taxa are present such as *Stephanopyxis turris* and benthics such as *Actinoptychus*). Eocene markers, such as those documented from the high southern latitudes (e.g., Fenner, 1984) and the eastern Indian Ocean (Fourtanier, 1991), are not encountered at Site 1171.

In terms of paleobathymetry, a similar geological setting to that inferred for Site 1170 is inferred at this site. The Eocene is marked by robust, neritic diatoms including eutrophic indicators such as resting spores of *Chaetoceros*. In the uppermost Eocene (Samples 189-1171D-3R-CC and 4R-CC), there is a low but noteworthy abundance (~<5% of the total assemblage) of more oceanic taxa (e.g., *Coscinodiscus*). The lowermost Oligocene yields mostly neritic diatoms along with some indicative of an increasingly open marine influence. Diversity also markedly increases in the lowermost Oligocene. Fully open ocean conditions

**T8.** Relative abundance of selected diatom taxa, sponge spicules, and silicoflagellates, p. 145.

**T9.** Relative abundance of selected diatom taxa, sponge spicules, and silicoflagellates, Hole 1171D, p. 149.

**T10.** Diatom bioevents identified, Holes 1171A, 1171C, and 1171D, p. 150.

are attained after the inferred early/late Oligocene hiatus. Neritic diatoms in the Eocene and lower Oligocene are considered to be in situ (i.e., not reworked) because of their high abundance and the absence of any other data to support major reworking. However, upper Oligocene through middle Miocene samples (189-1171C-27X-CC through 22X-CC) also contain common neritic diatoms. Reworking is inferred in this case since other data suggest an open marine setting for Site 1171 during this interval (e.g., see **"Benthic Foraminifers, Ostracodes, and Bolboforma,"** p. 32). Such reworking is probably associated with rising sea levels. Samples 189-1171C-21X-CC and above contain almost exclusively open-ocean diatoms with only ~5% reworked neritic types (e.g., *Paralia sulcata* var. *crenulata*).

The Neogene section is marked largely by an endemic subantarctic flora. However, the common occurrence of warm-water diatoms (mainly *Hemidiscus cuneiformis*) suggests a warming or the influence of warmer waters during the early late Miocene (Sample 189-1171A-8H-CC) and middle to late Pliocene (Samples 189-1171A-4H-CC through 5H-CC). Assemblage diversity also markedly increases from the lower upper Miocene onward.

## Palynology

Onboard palynological analysis of a selection involved core-catcher samples from Site 1171, comprising a few from Holes 1171A and 1171C and a suite from Hole 1171D. Of the samples from Hole 1171A, only the topmost Sample 189-1171A-1H-CC yields a few (Pleistocene) dinoflagellate cysts, which are dominated by *Spiniferites miriabilis*. The remainder of the investigated samples from the Neogene and upper Paleogene are palynologically barren. Analysis of samples from Hole 1171C was therefore limited to the presumed Eocene–Oligocene transition and involved Samples 189-1171C-30X-CC and 31X-CC only. Results are similar to the correlative interval of 1171D (i.e., Samples 189-1171D-2R-CC and 3R-CC) (viz., Sample 189-1171C-30X-CC was found to be barren, whereas the palynological composition of Sample 189-1171C-31X-CC is almost identical to Sample 189-1171D-3R-CC; see **"Hole 1171D,"** p. 9, in "Operations").

Recovery of palynomorphs is generally excellent in Hole 1171D, and they are assigned to the upper Paleocene to lower Oligocene on the basis of combined biostratigraphic information. Only the uppermost two core-catcher samples of Hole 1171D (189-1171D-1R-CC and 2R-CC) proved to be devoid of acid-resistant organic matter.

### Hole 1171D

Palynomorphs are consistently present in great abundance from Sample 189-1171D-3R-CC down. Unfortunately, the uppermost two core-catcher samples are completely barren (189-1171D-1R-CC and 2R-CC). This record is similar to the top of Hole 1170D and, thus, provides further evidence of the inception of the influence of well-oxygenated (bottom) water masses, which are responsible for the oxidation of organic matter in the early Oligocene apparently all along the Antarctic margin.

Dinocysts are generally the most abundant category of palynomorphs in productive samples from Hole 1171D, assigned to the upper Paleocene to lower Oligocene. In addition, pollen, spores, foraminifer organic linings, and acritarchs are present, albeit generally in low rela-

tive abundances. Only in the lowermost portion of Hole 1170D, in the upper Paleocene section, are sporomorphs quantitatively significant (Table T11). Paleocene assemblages throughout are indicative of (very) warm climates. The few identified sporomorph taxa may be compared with established records from New Zealand and Australia and indicate cooling and increasing humidity from the middle middle Eocene into the late Eocene. Moreover, as stated for previous sites, they are comparable to those reported by Mohr (1990) from the approximate age-equivalent sediments across Antarctica.

Palynomorphs are generally well preserved and dinocyst concentrations high, possibly on the order of 200,000 cysts/g in many samples, except for the interval between Samples 189-1171D-60R-CC to 50R-CC and in Sample 189-1171D-73R-CC. Recovered dinocyst assemblages are often of relatively low diversity for the Eocene and may be totally dominated by a single taxon. In terms of quantitative distribution patterns, the middle to upper Eocene interval is quite comparable to the correlative succession of Hole 1170D.

The dinocyst assemblages throughout are indicative of the latest Paleocene to earliest Oligocene (i.e., pre-O1b isotopic event of Zachos et al., 1996). Notably the middle and upper Eocene assemblages are composed of a mix of cosmopolitan and endemic taxa, with *Enneadocysta partridgei, Deflandrea phosphoritica,* and allied morphotypes (including the presumed endemic *Deflandrea antarctica* and, occasionally, *Deflandrea cygniformis*), and/or *Thalassiphora pelagica* dominating the assemblages. High abundances of typical high-latitude Eocene representatives of *Vozzhennikovia, Alterbidinium,* and/or *Spinidinium,* possibly indicative of cool episodes, were found notably in the upper part of Hole 1171D (cf. Wrenn and Hart, 1988) (Table T11). Hence, the middle to upper Eocene interval is quite comparable to the correlative succession of Hole 1170D.

## Dinocyst Stratigraphy

Middle to upper Eocene (and lowermost Oligocene?) Hole 1171D assemblages are quite comparable to those reported from age-equivalent records from nearby sites and even to nearly coeval successions recovered from the other side of Antarctica, as well as those from Northern Hemisphere high-latitude sites (see "Palynology," p. 30, in the "Site 1170" chapter). Little is known from the upper Paleocene and lower Eocene in terms of southern high-latitude dinocysts. Most meaningful information has been derived from the New Zealand sites (e.g., Wilson, 1988). However, these dinocyst successions still await sound chronostratigraphic calibration. The dinocyst events applied are listed in Table T12. For the middle to upper Eocene, the dinocyst datums are reasonably consistent with results from the calcareous nannofossil results in Hole 1171D. For the upper Paleocene to middle middle Eocene interval, dinocysts are the sole source of biostratigraphic information (see also Fig. F19).

## Eocene–Oligocene Transition

Somewhat differently from the situation encountered at Site 1170, the dinocyst and nannofossil biostratigraphies are in harmony for the Eocene–Oligocene transition (viz., the interval from Samples 189-1170D-6R-CC through 3R-CC). In the case of Hole 1171D, nannofossil distribution indicates a major hiatus between the youngest siliciclastic

**T11.** Distribution of organic walled dinocysts and palynomorph percentages, p. 151.

**T12.** Selected dinocyst events, p. 153.

sediments and the inception of silica-rich limestones overlying them. This contrasts to the situation in Hole 1170D, where such a hiatus was inferred to be present, on nannofossil grounds, within the "green sand" (lithostratigraphic Unit III) just below the limestone interval. The youngest palynologically productive sample of Hole 1171D (189-1171D-3R-CC) still contains the duo *Areosphaeridium diktyoplokum* and *Enneadocysta partridgei,* as well as *Alterbidinium distinctum* and *Stoveracysta ornata*. The co-occurrence of these taxa constrains the age of the sample to 37.0–33.3 Ma. (see "Palynology," p. 30, in the "Site 1170" chapter). Overlying samples are barren, and so no statements can be provided on possible missing sections. However, a conspicuous incoming taxon in the topmost productive sample from Hole 1170D is *Stoveracysta kakanuiensis*. This species has a FO in the regional New Zealand Runangan Stage (G.J. Wilson, pers. comm., 2000), which is equated to the uppermost part of the late Eocene. Since *S. kakanuiensis* is absent in the available (core catcher) material from this interval at Hole 1171D, it is possible that the (very) uppermost Eocene–lowermost Oligocene interval is extremely condensed or missing altogether. Obviously, as shown at other sites, the precise positioning of the onboard analyzed samples influences these kind of preliminary interpretations; postcruise work should provide more detail in this matter. Other leg sites consistently show that the "green sand episode" represents ~3 m.y., which may be as condensed as <1 m (e.g., see "Biostratigraphy," p. 22, in the "Site 1172" chapter and "Palynology," p. 30, in "Biostratigraphy," in the "Site 1170" chapter).

Comparison of the qualitative and quantitative dinocyst distribution in Sample 189-1171D-3R-CC with the uppermost samples from Hole 1170D would suggest correlation to Samples 189-1170D-7R-CC and/or 8R-CC. This is notable in view of the abundance of *Vozzhennikovia* spp. in all these samples.

## Middle Eocene

The middle Eocene is recognized at the top by the FO of *A. distinctum* (between Samples 189-1171D-5R-CC and 4R-CC; ~37 Ma) and at the base by the LO of *Charlesdowniea coleothrypta* and *Charlesdowniea edwardsii* (between Samples 189-1171D-44R-CC and 40R-CC; ~48 Ma). Although sample spacing leaves much to be desired in this interval, there is no obvious gap in the succession between Samples 189-1171D-44R-CC and 5R-CC. There may well be a more condensed section and/or a hiatus between Samples 189-1171D-35R-CC and 29R-CC on the basis of the proximity of the LO of *Membranophoridium perforatum* and the inception of the *Enneadocysta* acme sensu Raine et al. (1997). The known/inferred ages of these events suggests that the larger part of the lower middle Eocene (Lutetian) interval is missing or condensed (cf. Fig. F19).

## Paleocene/Eocene Boundary

The Paleocene/Eocene boundary is recognized between the FO of *A. homomorphum* (between Samples 189-1171D-74R-CC and 73R-CC; ~56 Ma) and the FO of frequent *Deflandrea phosphoritica* group (in this case the *D. antarctica* morphotype, between Samples 189-1171D-73R-CC and 72R-CC; ~55 Ma following Wilson's [1988] correlation). It is believed to coincide with a minor hiatus, discussed below. Another important bioevent is the FO of *Dracodinium waipawaense,* part of the classic early Eocene *Wetzeliella* lineage, between Samples 189-1171D-71R-CC and

70R-CC. This event may be placed at ~53.5 Ma (middle early Eocene). The FO of the *D. phosphoritica* group is somewhat arbitrarily placed, since specimens are present in underlying samples. This is thought to be caused by contamination, as overlying samples yield massive concentrations of this taxon. The dinocyst succession from Samples 189-1171D-75R-CC through 73R-CC shows the established pre–late Paleocene suite from the LO of *Spinidinium densispinatum* and *Cassidium fragile* to the FO of *A. homomorphum* (Wilson, 1988). However, it should be noted that it is conceivable that the entire lower part of Hole 1171D is, in fact, early Eocene in age and that the latter represents reworked specimens.

A possible hiatus is indicated by the abrupt compositional change of the palynological association between Samples 189-1171D-74R-CC and 72R-CC, where dominating sporomorphs give way to dominating dinocysts (Sample 189-1171D-73R-CC has only few palynomorphs). This hiatus would also support the view that the underlying interval represents the late Paleocene. In addition, the classic globally identified oldest *Apectodinium* acme was not recorded in the available material (or any *Apectodinium acme*). This event is indicative for the interval containing the well-known negative $\delta^{13}C$-excursion, marking the base of the Eocene (e.g., Bujak and Brinkhuis, 1998).

## Paleoenvironment

The quantitative dinocyst distribution in the Paleocene–lower Oligocene generally indicates somewhat restricted, eutrophic, neritic conditions throughout the succession. A generally eutrophic, restricted setting (possibly related to freshwater influences and/or coastal upwelling) may be indicated by (1) the relatively low species diversity (for Eocene times), (2) the high dominance of a single taxon in most samples, (3) the frequent dominance of peridinioid dinocysts like *D. phosphoritica* and *Vozzhennikovia* spp. (considered to represent mainly heterotrophic dinoflagellates; Brinkhuis et al., 1992), and (4) the near absence of typically open-marine coastal/neritic cysts such as *Glaphyrocysta* spp., *Cordosphaeridium* spp., and so forth. The few open-marine taxa like *Impagidinium* and *Spiniferites* spp. are quite rare. For further discussion, see "Palynology," p. 30, in "Biostratigraphy" in the "Site 1170" chapter because the assemblages are comparable.

The rather abrupt change in palynological associations between Samples 189-1171D-74R-CC and 72R-CC, with downhole dominant sporomorphs, may reflect even more shallow, restricted marine conditions. This would also explain the poor palynological contents of Sample 189-1171D-73R-CC.

## Age Model and Sedimentation Rates

The combined nannofossil, foraminifer, diatom, radiolarian, and dinocyst biostratigraphy at Site 1171 yielded 91 bioevents with age significance. Principal trends through this section are shown in Figure F19. Datums are from the combined microfossil bioevents from Holes 1171A, 1171C, 1171D, and 25 magnetic polarity datums (see "Paleomagnetism," p. 40). The bioevents (Table T13) consist of 39 FO events, 49 LO events, 1 first abundant occurrence (FAO), and 2 last abundant occurrence (LAO) events. All events are plotted according to their observed composite depths at Site 1171 and by their ages as defined in "Biostratigraphy," p. 9, in the "Explanatory Notes" chapter. The FO

events may have been estimated to be too shallow, and the LO events may have been estimated deep, based on the limited sampling interval. Stratigraphic position of these datums will be refined with further study. See individual microfossil group discussion for more detailed bio-event data.

A detailed age-depth curve was constructed for the last 12 m.y. at Site 1171 utilizing the composite section (see "Composite Depths," p. 43) created from the top 14 cores (Fig. F23). Sedimentation rates of 1.3 cm/k.y. through the Pliocene–Pleistocene section are truncated by a hiatus of 1.6 m.y. at the Miocene/Pliocene boundary. The LO of foraminifer *Paragloborotalia continuosa* (8.0 Ma) at 65.2 mcd indicates a longer hiatus of 2.7 m.y. in duration. Physical properties measurements indicate a break at ~65 mcd of <2 m.y. (see "Physical Properties," p. 54). *Paragloborotalia continuosa* persists across the Zone SN9/SN10 boundary (Kennett and Srinivasan, 1983), and we suggest that the last common occurrence may be a more useful datum. Sedimentation rates for the late Miocene were quite low (0.5 cm/k.y.), increasing to 3.8 cm/k.y. across the middle/late Miocene boundary (10 Ma). Early and middle Miocene sedimentation rates fluctuated between 0.7 to 2.0 cm/k.y at the Oligocene/Miocene boundary.

Combined biostratigraphic datums may indicate up to four brief hiatuses (~2 m.y.) interspersed with brief periods of sedimentation (<1 cm/k.y.) through the late Oligocene to the middle Eocene. Nineteen foraminifer, nannofossil, radiolarian, diatom, and dinoflagellate cyst datums, spanning ~15 m.y., are within ~42 m of sediment (Fig. F19).

Sedimentation rates through the middle Eocene to Paleocene were dramatically higher compared to the Neogene portion of Site 1171, ranging from 4.4–12.5 cm/k.y. The age-depth curve through the bottom 600 m is based primarily on dinoflagellate cyst datums. Nannofossils and foraminifers are present down to ~870 mcd and provide an age datum. Radiolarians are sporadic below 340 mcd, and diatoms are present to 580 mcd but provide environmental data only. Dinoflagellate cyst datums between Cores 189-1171D-29X and 35X (Table T13) indicate a hiatus of ~2 m.y. at ~550 mcd. A spike in the hydrogen index (HI) and the percentage of total organic contents (see "Organic Geochemistry," p. 44), along with changes in density measurements from downhole logging (see "Downhole Measurements," p. 56) indicate the hiatus at ~530 mcd. Paleomagnetic interpretations also indicate a gap in the middle Eocene (see "Paleomagnetism," p. 40).

Sedimentation patterns from the Pleistocene through the Paleocene have been interpreted on the combined biostratigraphic data supplemented with information from other shipboard laboratories. The Eocene/Oligocene boundary interpretation and the middle Eocene hiatus are discussed in "Organic Geochemistry," p. 44, and "Paleomagnetism," p. 40.

# PALEOMAGNETISM

## Introduction

After alternating-field (AF) demagnetization, the natural remanent magnetization (NRM) of whole-core sections from Site 1171 was measured at 5-cm intervals using the pass-through cryogenic magnetometer. An exception was made for cores whose liners or end caps were deformed, because these could damage the magnetometer. These

**F23.** The age-depth plot and linear sedimentation rates for the composite sections for the last 12 m.y., p. 93.
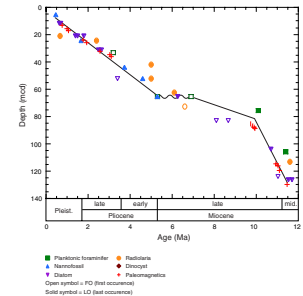
deformed cores were measured as archive-half cores. The AF of 20 mT applied for Holes 1171A and 1171B did not completely remove the strong drilling overprint, so for Hole 1171C an AF of 30 mT was used, which provided a relatively good magnetic record. In view of these results, demagnetization of 30 mT was used for Hole 1171D and the remaining sites. The nonmagnetic core barrel assembly was again employed for even-numbered cores in Holes 1171A and 1171C and for odd-numbered cores in Hole 1171B, starting with Core 3H. The comparison between results from cores collected with the nonmagnetic corer and with those from the standard corer is discussed in the "Appendix" chapter, as are results of experiments investigating the effect of core splitting on magnetization and other coring-related magnetic experiments. The Tensor tool is usually used to orient the APC cores beginning with the third core at each hole, but the poor determination of the declination values of the cores at this site precluded the orientation of cores.

Discrete oriented samples were routinely collected from Holes 1171A, 1171C, and 1171D. These samples were used to aid in the interpretation of the long-core magnetization record by providing additional measurements of polarity and basic magnetic characterization. Most of them were demagnetized at 5, 10, 15, 20, 30, 40, and 50 mT to permit principal component analysis. For rock-magnetic characterization, anhysteretic remanent magnetization (ARM) was given in 0.2-mT DC and 200-mT alternating-current fields and isothermal remanent magnetization (IRM) in a DC field of 1 T. Discrete samples were also progressively saturated up to 1 T to study the hardness of the IRM.

# Results

## Long-Core Measurements

The long-core measurements for the cores are presented in Figures F24 and F25, which show inclination and intensity for Holes 1171A, 1171B, and 1171C. A new, larger drill bit was used in the APC BHA and appears to have induced a strong magnetic overprint, recognizable by abnormally high intensities. Thus, all measurements with an intensity higher than $10^{-4}$ mA/m or lower than $10^{-6}$ mA/m (the sensitivity limit of the cryogenic magnetometer) were excluded. In fact, the intensity of magnetization was very constant between $10^{-5}$ and $10^{-4}$ mA/m. Even if measurements approached the noise level of the instrument and the background noise from core liners, a record could be interpreted for most of Hole 1171C. GRA bulk density measurements (see "Physical Properties," p. 54) allowed us to obtain a good depth correlation that showed a very small shift among Holes 1171A, 1171B, and 1171C. Furthermore, some individual features on the magnetic records could be recognized from one hole to another, which confirmed the absence of a major depth shift.

In the upper part of Hole 1171C, the onset of the Brunhes Chron (C1n), the Jaramillo Subchron (C1r.1n), the Olduvai Subchron (C2n), and the termination of the Gauss Chron (C2r.1r) are clearly identified providing a useful magnetostratigraphy down to 35 mbsf. The section between 35 and 80 mbsf was marked by a succession of sequences of reversals that could not be matched to the geomagnetic polarity time scale.

**F24.** Long-core measurements from 0 to 120 mbsf, p. 94.
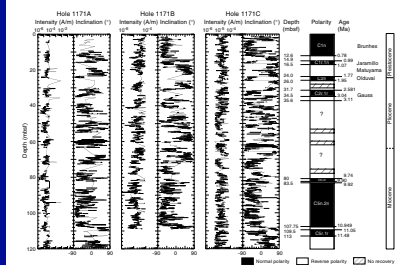


**F25.** Long-core measurements from 120 to 240 mbsf, Hole 1171C, p. 95.
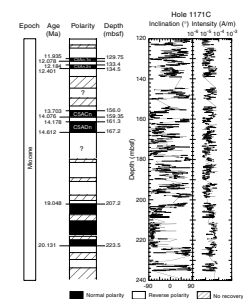
Between 83.5 and 107.75 mbsf, a long normal magnetozone was identified as Subchron C5n.2n with two short reversed magnetozones above and below.

Below 120 mbsf, where there was only core from Hole 1171C, we found the onset of Subchron C5An.1n at 130.06 mbsf, the onset of Subchron C5An.2n at 134.5 mbsf, the onset of Subchron C5Acn at 159.35 mbsf, and the onset of Subchron C5ADn at 167.2 mbsf. At deeper depths, between 207.2 and 223.5 mbsf, the particularly distinctive long normal Chron C6n was recognized (Table T14).

In Hole 1171D, poor recovery precluded any further interpretation of magnetostratigraphy until a depth of nearly 450 mbsf was reached. Between 450 and 950 mbsf, the magnetic record (Fig. F26) was marked by long magnetozones suggesting a high sedimentation rate. However, suspicious sequences of stable inclination around –40°, and weaker values of reverse inclination compared with normal, suggested a strong remagnetization in the normal direction. This remagnetization was not caused by the standard drill overprint, which was largely removed by 30 mT of demagnetization but was probably carried by the soft material surrounding and between biscuits. To minimize this effect, the data were filtered and only sections that ranked <2 in the 0–5 scale of soft intervening material between the biscuits (see "Lithostratigraphy," p. 10) are shown in Figure F26. However, it was very difficult to identify these magnetozones reliably in the absence of biostratigraphic control (see "Biostratigraphy," p. 25). In our interpretation, we recognized the onset of Chron C20r at 523 mbsf, the onset of Chron C21n at 571 mbsf, and the onset of Chron C24r between 773 and 889 mbsf. This interpretation is consistent with the biostratigraphic constraints of 43.7 Ma at 482 mbsf and 53.5 Ma at 908 mbsf from the nannofossils, but requires a significant hiatus between Chrons C21r and C24r. The normal-moment bias may have obscured the magnetic record, so shore-based investigations will be required to determine if a reliable magnetostratigraphy of the Eocene can be definitely established.

## Discrete Samples

The discrete samples were routinely subjected to NRM, ARM, and IRM demagnetization and progressive IRM acquisition. NRM demagnetization results were, for the most part, disappointing. Figure F27 shows the variation of the intensity of ARM and IRM downhole. There is progressive increase of about an order of magnitude in both, which reflects the increase of terrigenous input (see "Lithostratigraphy," p. 10). Some anomalous values near 200 mbsf are still not interpreted and do not appear to correlate with any major features observed in the core description. The normalized difference between IRM (20 mT) to IRM (Fig. F27) increases downcore, indicating an increase in the softest magnetic fraction and suggesting an increase of grain size of the magnetic fraction downhole. The normalized difference between IRM at 200 and 500 mT does not vary systematically downcore and suggests that the magnetic mineralogy does not change significantly downcore. However, there must be some component present other than magnetite to account for the very high coercivity of the hardest fraction, which is far greater than that of single domain magnetite.

Overall, the rock magnetic characteristics are similar from one lithostratigraphic unit to another and seem to characterize the same detrital source. In particular, they do not show the strong change of sedimen-

**T14.** Magnetostratigraphic results, p. 156.

**F26.** Long-core measurements from 400 to 950 mbsf, Hole 1170D, p. 96.
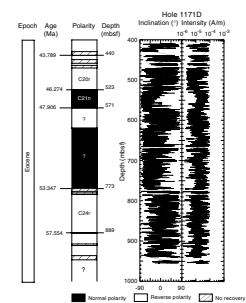


**F27.** Variation of magnetic properties, Holes 1171A, 1171C, and 1171D, p. 97.
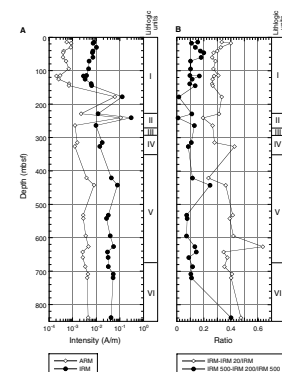
tary environment marked by the nannofossil ooze/silty claystone contact.

## Magnetostratigraphy and Age-Depth Estimates

The relatively good magnetic record of Hole 1171C (Table T14) allowed us to generate an age-depth curve (Fig. F28). From the Holocene down to early Pliocene and from the early Miocene down to the late Miocene, the sedimentation rate is relatively constant (10 m/m.y.). However, the position of Chron C5n in the record suggests the presence of a hiatus from the early Pliocene until the late Miocene, which is confirmed by biostratigraphic datums. Unfortunately, the absence of reliable magnetostratigraphy in this part of the record precludes the determination of its exact duration. Chron C5n represents a condensed section just before the hiatus, where the sedimentation rate reaches 25 m/m.y.

In comparison with the upper part of the record, the sedimentation rate is high in the Eocene section, as recorded in Hole 1171D. Whatever the interpretation of the magnetic record may be, these long magnetozones give a sedimentation rate of at least 25 m/m.y. If we base our estimation upon Chron C24r between 773 and 889 mbsf, we obtain a sedimentation rate of 45 m/m.y. The final estimates of these sedimentation rates will be made in conjunction with the biostratigraphic data (see "Biostratigraphy," p. 25).

# COMPOSITE DEPTHS

Multisensor track (MST) and spectral reflectance (L*) data collected from Holes 1171A, 1171B, and 1171C were used to determine depth offsets in the composite section. Magnetic susceptibility, gamma-ray attenuation (GRA) bulk density, and spectral reflectance measurements were the primary parameters used for core-to-core correlation at Site 1171. GRA bulk density and magnetic susceptibility data were collected at 2-cm intervals on all APC cores recovered from Holes 1171A, 1171B, and 1171C and at 2- to 4-cm intervals on XCB cores from Holes 1171A, 1171B, and 1171C. Spectral reflectance data were collected at 2-cm intervals on cores from Holes 1171A, 1171B, and 1171C (see "Physical Properties," p. 54, and "Lithostratigraphy," p. 10, for details about MST and spectral reflectance data).

The data used to construct the composite section and determine core overlaps are presented on a composite depth scale in Figure F29. The depth offsets that comprise the composite section for Holes 1171A, 1171B, and 1171C are given in Table T15. The composite data show that the APC cores from Site 1171 provide a continuous overlap to 118 mcd (base of Core 189-1171A-12H). GRA bulk density data were the primary basis for interhole correlation. Spectral reflectance measurements were used in the upper 50 mcd to provide additional support for composite construction. The interhole correlations (Fig. F29) show that ~50 cm to 1 m of material is missing between cores in each hole.

Stretching and compression of sedimentary features in aligned cores indicate distortion of the cored sequence. Because significant distortion occurred within individual cores on depth scales of <9 m, it was not possible to align every feature in the MST and color reflectance records accurately by simply adding a constant to the mbsf core depth. Core-scale changes will require postcruise processing to align smaller sedi-

**F28.** Age-depth relationship from paleomagnetic data for the Neogene, Hole 1171C, p. 98.
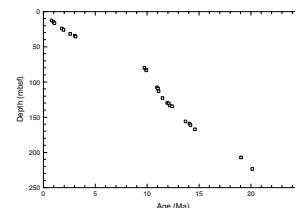
**F29.** Smoothed GRA bulk density and spectral reflectance data for the upper 118 mcd, Holes 1171A, 1171B, and 1171C, p. 99.
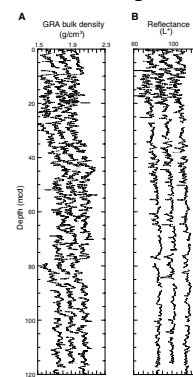
**T15.** Composite depth section, p. 157.

mentary features. Only after allowing variable adjustments of peaks within each core can an accurate estimate of core gaps be made.

Following construction of the composite depth section for Site 1171, a continuous spliced record was assembled for the aligned cores over the upper 120 mcd (base of Core 189-1171A-12H). Intervals having significant disturbance or distortion were avoided. The Site 1171 splice (Table T16) can be used as a sampling guide to recover a single sedimentary sequence between 0 and 120 mcd. The splice primarily utilizes cores from Holes 1171A and 1171B, except for a short interval around 32 mcd (Core 189-1171A-4H), where the splice was constructed from cores from Holes 1171B and 1171C. The variations in GRA bulk density, magnetic susceptibility, and spectral reflectance data from Core 189-1171A-4H do not match the data from equivalent cores and depths in Holes 1171B and 1171C. The cause of this difference in data quality is problematic as Core 189-1171A-4H does not contain any significant disturbance. Because of this apparent data mismatch, the sampling splice does not include Core 189-1171A-4H.

# ORGANIC GEOCHEMISTRY

The shipboard organic geochemistry program at Site 1171 included studies of volatile hydrocarbons, total organic and inorganic carbon, total nitrogen, total sulfur, and hydrogen and oxygen indexes. Rock-Eval pyrolysis and gas chromatography were performed (see "Organic Geochemistry," p. 20, in the "Explanatory Notes" chapter) on headspace residues sampled at one per core. The CNS analysis and carbon coulometry (see "Organic Geochemistry," p. 20, in the "Explanatory Notes" chapter) were performed on samples taken from Sections 1, 3, and 5 in each core.

## Sedimentary Geochemistry

### Results

Carbonate ($CaCO_3$) content for the strata sampled at Site 1171 ranges from 0 to >95 wt% (Fig. F30; Table T17). In general, the carbonate distribution exhibits a two-tiered profile. Sediments from ~270 to 955 mbsf commonly contain <10 wt% $CaCO_3$ (with a distinct excursion of ~60 wt% at ~415 mbsf and a broader zone from ~500 to 680 mbsf with values up to >20 wt%), whereas the carbonate content abruptly increases to mostly >90 wt% above 270 mbsf. Within the upper high–carbonate content strata, carbonate content values are consistently ~90 wt% from ~200 to 270 mbsf. From ~50 to 200 mbsf, carbonate content is mostly >90 wt%, with a slight decrease to ~85 wt% at ~108 mbsf. From ~50 mbsf, carbonate content values range from ~85 to 95 wt%.

The total organic carbon (TOC) content for most intervals at Site 1171 is <1 wt% (Fig. F30; Table T17). Note that the TOC content values determined by Rock-Eval pyrolysis and CNS analysis mostly provide similar TOC content profiles, although the absolute values differ for each method. In the upper 100 mbsf, however, the CNS results determined by difference indicate TOC content values up to >1 wt%, whereas Rock-Eval pyrolysis results indicate very little organic carbon content in this part of the section. Total nitrogen content ranges from 0 to 0.16 wt% (Fig. F30; Table T17), with the highest values occurring below ~800 mbsf; nitrogen content covaries with the TOC content (Fig.

F30). From 955 to ~760 mbsf, total sulfur content displays an overall decrease from 2 to 0.1 wt% (Fig. F31; Table T17). From ~760 to 500 mbsf, the total sulfur profile varies from 0.1 to ~1 wt%. At 500 mbsf, total sulfur content increases to >2 wt%. From ~370 to 500 mbsf, sulfur content remains generally high, ranging from 0.6 to >3 wt%. Above ~370 mbsf, total sulfur values gradually decrease to values ranging from 0 to 1.2 wt%. No reliable total sulfur data were obtained above ~270 mbsf. We calculated the C/S ratios for strata below ~270 mbsf at the site assuming that all of the sulfur exists as pyrite. The C/S values <2 are generally considered representative of marine environments, whereas the C/S values >5 indicate relatively fresh water settings (Berner and Raiswell, 1984). The implications of these ratios are discussed below.

Organic matter type was assessed using Rock-Eval pyrolysis and CNS analyses. A discussion of this methodology is included in "Organic Geochemistry," p. 37, in the "Site 1168" chapter and "Organic Geochemistry," p. 40, in the "Site 1170" chapter. The HI values from Rock-Eval pyrolysis range from 0 to 1000 mg of hydrocarbon per gram of TOC at Site 1171 (Fig. F30; Table T18). The highest HI values are at ~520 and 790 mbsf. Oxygen index (OI) values vary between 0 and 7000 mg of $CO_2$ per gram of TOC. The $T_{max}$ values obtained from Rock-Eval pyrolysis range from 301° to 597°C (Fig. F32), although the most reliable $T_{max}$ values cluster between 420° and 430°C. The $T_{max}$ provides an estimate of organic matter thermal maturity, with values of <435°C indicative of immaturity relative to petroleum generation. The "oil window" is generally considered to range between $T_{max}$ values of 435° and 465°C, whereas values of >465°C are indicative of thermogenic gas zones (Espitalié et al., 1977; Peters, 1986). Note that some of the Rock-Eval pyrolysis data (particularly the low HI values) below ~850 mbsf may not be reliable because of instrument malfunction during analysis of those samples.

The extremely low TOC content values obtained from Rock-Eval pyrolysis in the upper ~270 mbsf at Site 1171 lower the reliability of HI and OI values in this interval. We performed replicate analyses on many of the samples to validate the results. The HI values and C/N ratios (discussed immediately below) exhibit similar trends, which suggests that most of our results are consistent and valid for interpretation. However, total nitrogen contents above ~270 mbsf in the core are very low, so the C/N ratios must also be considered with care. The generally high OI values through much of the core are attributed to the thermal degradation of calcium carbonate during pyrolysis and are not considered in this interpretation.

## Discussion

The high carbonate content of Oligocene through Holocene sediments at Site 1171 primarily reflects dominance of calcareous nannofossils; foraminifers are secondary in importance (see "Biostratigraphy," p. 25). This observation is similar to those made for Sites 1168, 1169, and 1170. The overall upward increase in carbonate content through the sequence is again (as at previous sites) a direct consequence of a change from shallow marine to pelagic open-ocean conditions. Here, the transition from carbonate-poor to carbonate-rich sediments is abrupt at ~270 mbsf. This observation is similar to and coeval with the distribution of carbonate observed at Site 1170, and it implies either a rapid change in depositional environments or the presence of an unconformity and condensed section in the stratigraphic record.

F31. Total sulfur content compared to C/S ratios, p. 101.

T18. Results of Rock-Eval pyrolysis analyses, p. 163.

F32. $T_{max}$ values generated from Rock-Eval pyrolysis analyses of organic matter, p. 102.

As with Sites 1168 and 1170, two modes of carbonate and total organic carbon preservation are apparent in sediments from Site 1171 (Fig. **F30**). High carbonate content values generally correspond to sediments with low TOC content values, whereas low–carbonate content sediment contains a range of TOC content values including the highest values observed at the site. Upper Paleocene through lower Oligocene sediments with relatively elevated TOC and low $CaCO_3$ contents exist between ~270 mbsf and the base of Hole 1171AD. Here, mostly common to abundant ichnofossils (see **"Lithostratigraphy,"** p. 10) and Th/U ratios mostly >2 (see **"Downhole Measurements,"** p. 56) indicate dysoxic to oxic conditions, although short episodes of anoxia may have affected the seafloor (discussed immediately below). Through this interval, as at Sites 1168 and 1170, most of the high TOC–low $CaCO_3$ sediments may represent enhanced burial efficiency of organic matter.

The organic matter type encountered provides some insight into depositional processes. Three intervals in HI values are observable on Figure **F30.** Paleocene through lowermost Eocene sediments (from ~780 mbsf to the base of the hole) show alternations between horizons containing marine and terrestrial organic matter, all overlain by an extremely high HI horizon. The C/N ratios, however, indicate dominantly marine organic matter preservation. In this case, the HI values appear to have more faithfully recorded organic matter type since abundant terrestrial palynomorphs have been described from the base of the interval (see **"Biostratigraphy,"** p. 25). As described previously, these sediments contain generally low $CaCO_3$ content and some of the highest TOC content values from the site. The total sulfur content through the interval is also amongst the highest observed at Site 1171, although it decreases upward through the interval; the C/S ratios indicate deposition under marine conditions. The Th/U values <2 (see **"Downhole Measurements,"** p. 56) suggest an episode of anoxia at the seafloor at ~920 mbsf. This observation is supported by the pervasively laminated sediments visible below ~910 mbsf in the core (see **"Lithostratigraphy,"** p. 10). Interestingly, this anoxic horizon contains terrestrially derived organic matter. Apparently, large quantities of terrestrial organic matter were, at times, deposited on the seafloor. This organic matter provided a sufficient substrate for bacterial sulfate reduction, pore- and/or bottom-water oxygen consumption, and pyrite formation as organic matter was remineralized.

A second interval (lower to middle Eocene) with distinct organic matter type exists from ~500 to 780 mbsf at Site 1171. Here, the organic matter is either mixed terrestrial-marine or marine-oxidized marine (an observation supported by the C/N ratios), although it is more marine in character and the amplitude of organic matter type variation is less pronounced than in the underlying interval. Total sulfur content here is lower than in the underlying sediment, whereas carbonate content is generally higher and displays a pronounced increase from ~500 to 680 mbsf. The C/S ratios suggest deposition under alternating marine to brackish conditions from ~660 to 780 mbsf and under marine conditions from ~500 to 660 mbsf. Using the method of Adams and Weaver (1958), the Th/U values indicate anoxic conditions exist from ~570 to 580 mbsf.

The overall trend from mixed terrestrial-marine organic matter in the lower interval to more marine organic matter facies in the overlying interval suggests an overall relative sea-level rise. Within the interval from ~500 to 680 mbsf, calcareous nannofossils are abundant to common

(see "Biostratigraphy," p. 25), whereas below, the nannofossil content is mostly rare with occasional intervals showing common to abundant nannofossils. These paleontological observations are compatible with an overall rise in sea level through the lower middle Eocene section of the core and can account for the carbonate content within these sediments. The record of brackish pore-water conditions (from the C/S ratios) may be difficult to resolve within this framework, however. Perhaps, overall conditions in the seaway were subject to a relative deepening, but fluctuations in climate (wet–dry cycles) were sufficient to cause episodes of relative "freshening" of the water column and/or sediment pore waters. This hypothesis may explain the mixed terrestrial-marine organic matter signature in the lowermost portions of the core and is supported by the overall paucity of calcareous nannofossils and foraminifers through this time. Alternatively, a diminished capacity for pyrite formation because of undefined limitations in iron or sulfate availability may have lead to a brackish water signature in the C/S values, which actually represent periods of decreased pyrite formation. In either case, more analyses will be needed to understand the significance of the geochemical record from this interval.

The second organic matter type interval is overlain by the highest HI interval at the site (>1000 mg of hydrocarbon per gram of TOC at ~520 mbsf). Here, density and *P*-wave velocity (and other downhole logging and physical properties) (see "Downhole Measurements," p. 56) display an abrupt downhole increase, although no abrupt change in lithologic character was noted (see "Lithostratigraphy," p. 10). Interestingly, a hiatus representing up to 2 m.y. of missing section was identified between ~515 and 560 mbsf (see "Biostratigraphy," p. 25). In addition, the Th/U ratios <2 (see "Downhole Measurements," p. 56) suggest anoxic seafloor conditions during deposition of the interval from ~460 to 520 mbsf. These characteristics are highly suggestive of a middle Eocene disconformity overlain by a marine flooding surface and condensed section.

A third interval in organic matter type is visible from ~270 to 500 mbsf at Site 1171. Through this middle Eocene to lower Oligocene interval, the organic matter is best characterized as marine to oxidized marine (an observation supported by the C/N ratios), although it is more marine in character than organic matter in the second interval. The total sulfur values include the highest values recorded at this site, and the C/S ratios indicate deposition under fully marine conditions. These trends are remarkably similar to those observed at Site 1170 and are highly suggestive of regional scale changes in seafloor redox conditions. Here, three subintervals in organic matter type are recorded. These subintervals are defined by zones of relatively high HI values (labile marine organic matter) separated by discrete horizons of relatively lower HI values (oxidized marine). The lowermost subinterval (from ~420 to 480 mbsf) contains some of the highest TOC and total sulfur content from the hole and includes Th/U values suggesting anoxic seafloor conditions; this subinterval corresponds to lithostratigraphic Subunit VA (see "Lithostratigraphy," p. 10). Barren to abundant calcareous nannofossils are reported through this interval (see "Biostratigraphy," p. 25). This subinterval is overlain by a discrete peak in carbonate content visible on the carbonate profile at ~415 mbsf. This carbonate peak exists in a similar stratigraphic position to a discrete limestone at Site 1170 and may represent a regionally correlative upper middle Eocene marker bed.

In the uppermost HI subinterval (from ~330 to 270 mbsf and corresponding to lithostratigraphic Unit IV; see "Lithostratigraphy," p. 10), the C/S ratios indicate an episode of late Eocene brackish water conditions. Admittedly, the relative availability of reduced iron or sulfate may have played a role in the C/S signature recorded here. However, this brackish water signature was recorded in the upper Eocene at Sites 1168 and 1170, suggesting that the interpretation may be correct. This change from marine to brackish conditions may easily be described by regional shoreline progradation. This regional-scale base-level fall interpretation is, however, not compatible with our interpretation of an overall relative sea-level rise during this time. Therefore, the increase in the C/S ratios may represent a regional change in seawater salinity (see also "Palynology," p. 36). Here, increases in carbonate content are visible and calcareous nannofossil assemblages are common to abundant (see "Biostratigraphy," p. 25). In coeval strata at Site 1170, relatively carbonate-rich horizons within a mostly carbonate-poor marine section were considered to suggest higher-frequency fluctuations in organic matter type than those resolved by our analyses.

Above ~270 mbsf, the extremely high carbonate contents (up to 95 wt%) represent either a reduction in clastic input or enhanced carbonate preservation and may indicate enhanced biogenic productivity (as observed at Sites 1168, 1169, and 1170). The extremely low TOC content values and low dinoflagellate cyst content (see "Biostratigraphy," p. 25) through the Oligocene to Holocene portion of the core may record settling of organic matter through a well-mixed water column and/or to a well-oxygenated seafloor (as observed at Sites 1168, 1169, and 1170). The apparent variations in organic matter type may record variations in seafloor redox conditions, although we cannot discount the possibility of limited terrestrial input to the system. Of note are the elevated total organic carbon values (>1 wt%) above ~110 mbsf on the CNS profile, an observation also made for a similar interval at Site 1170.

## Summary

The similarity between geochemical parameters from Sites 1171 and 1170 is significant because it suggests regional-scale changes in seafloor and water-column conditions. Both sections record a mostly shallow and dysoxic Eocene seafloor. At Site 1170, the average Th/U ratios are lower than those obtained from coeval strata at Site 1171. This observation suggests that the seafloor oxygenation state within the Australo-Antarctic Gulf at Site 1170 was, in general, less well ventilated than the seafloor at Site 1171. In addition, however, the Th/U values are more variable, and evidence for late Paleocene and middle and late Eocene anoxic episodes are most pronounced at Site 1171, perhaps associated with deposition influenced by the Paleogene Pacific Ocean. These anoxic episodes may represent impingement of an open Pacific Ocean oxygen minimum zone on the shallow to bathyal marine setting of Site 1171 Eocene–Oligocene sediments. A stepwise change in Eocene organic matter facies from mixed terrestrial marine to dominantly marine is suggestive of an overall relative sea-level rise through this time. This overall rise culminated in an abrupt change to deep well-oxygenated conditions in the early Oligocene.

## Volatile Hydrocarbons

### Results

Concentrations of volatile hydrocarbon gases were measured from every core, using the standard ODP headspace-sampling technique and gas chromatographic analysis. Profiles of methane content and various methane and heavier volatile hydrocarbon ratios are presented in Figure **F33** (also see Table **T19**). Within the upper ~490 m of the cored sediment section, methane only occurred in minor concentrations (2–393 ppmv). However, equipment failure likely led to erroneous values from ~320 to 490 mbsf; 320 mbsf (middle Eocene) likely represents the approximate onset of methanogenesis in the section based on the pore-water sulfate profile (see **"Inorganic Geochemistry,"** p. 50). A peak in methane concentration at ~490 mbsf is followed by an overall decrease in values to ~580 mbsf. Below 580 mbsf, methane concentrations exhibit a gradual increase to values >50,000 ppmv at ~650 mbsf and then steadily decrease to ~2100 ppmv at a depth of ~720 mbsf. From here, methane concentrations again exhibit a gradual increase to high values for Hole 1171D of >63,000 ppmv at ~860 mbsf. Methane concentrations range from ~5000 to 26,000 ppmv from here to the base of Hole 1171D. The ratio of methane vs. ethane plus propane ($C_1/C_2+C_3$) shows maximum values from ~490 to 700 mbsf and decrease gradually to ~11 at ~940 mbsf. Percent wetness is below 15% through the core, thus falling below the range of values typical for economically viable gas reservoirs.

### Discussion

The low gas content of the uppermost 480 or 320 mbsf (measured and assumed, respectively) of Site 1171 is nearly identical to those in the stratigraphically equivalent headspace-gas profiles generated for Sites 1168, 1169, and 1170. At those sites, the low gas content was suggested to be a function of very little organic matter as a source of gas and pore-water profiles with sulfate-reduction processes limiting the onset of methanogenesis.

Below ~480 (320) mbsf at Site 1171, methane content increases to a broad multipeaked zone of high concentrations through to the base of the hole. The $C_1/C_2+C_3$ ratios from ~480 to 700 mbsf suggest a biogenic origin. From ~700 to 900 mbsf, the $C_1/C_2+C_3$ ratios indicate a mixed biogenic/thermogenic origin for the gases, whereas below 900 mbsf the gases have been generated by thermogenic processes. Headspace samples analyzed on the natural gas analyzer from ~520 mbsf to the base of the hole include butane ($C_4$), pentane ($C_5$), and hexane ($C_6$), likely indicative of a thermogenic origin for this gas (Hunt, 1996). Hinz et al. (1986) postulated an early to middle Eocene source rock for thermogenic gas observed on the west Tasmanian continental slope, which is consistent with the Paleocene to middle Eocene age (see **"Biostratigraphy,"** p. 25) of the thermogenic gas-containing strata at Site 1171.

The $T_{max}$ values obtained from Rock-Eval pyrolysis are interpreted to represent mostly immature organic matter (Fig. **F32**). In the upper ~460 mbsf, the $T_{max}$ values fluctuate through the maximum possible range observed at Site 1171. This wide range is attributed to extremely low TOC content values and the mixed marine-oxidized character of organic matter, which can generate an erroneously large range in $T_{max}$ values. Below 460 mbsf, the $T_{max}$ values display a sloping linear trend from



**F33.** Methane and dissolved sulfate concentrations, methane vs. ethane plus propane ratio, and percent wetness from headspace gas analysis, p. 103.
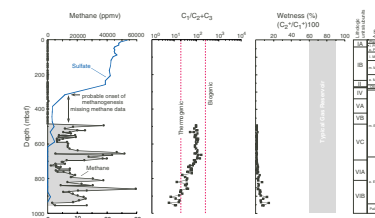
**T19.** Headspace gas composition, p. 165.

~420° to 430°C with depth. Within this trend are numerous elevated values, which were obtained from samples exhibiting double $S_2$ peaks on the Rock-Eval pyrograms. Double $S_2$ peaks have been attributed to the presence of bitumen (Clementz, 1979). The likely presence of bitumen and thermogenic gases suggests that the lower portions of Hole 1171 have been subject to some thermal maturation. We consider the sloping trend as probably most valid because the values were obtained from horizons containing at least 0.5 wt% TOC and do not display the double $S_2$ peak characteristic. The $T_{max}$ values approaching 435°C at the base of Hole 1171D are indicative of the top of the "oil window." The depths in the core at which maturation is postulated to have occurred are as shallow as at Sites 1168 and 1170, again suggesting an alternate heat source to burial maturation.

# INORGANIC GEOCHEMISTRY

Shipboard interstitial water (IW) analyses were performed on 39 of 58 whole-round samples taken from Hole 1171A (12 of 23 samples), Hole 1171C (5 of 13 samples), and Hole 1171D (22 samples). Samples were taken at the frequency of three per core in the upper ~50 mbsf, one per core from 50–100 mbsf, and one every third core to total depth in Hole 1171A. In Hole 1171C, samples were collected at two per core between 50 and 80 mbsf. Below, one whole-round core every third core to total depth was taken, continuing in Hole 1171D at one whole-round core every third core down to the bottom of the hole. Table **T20** and Figures **F34, F35, F36, F37,** and **F38** present the results of interstitial water geochemistry. The balance of the samples was archived for shore-based investigations.

## Chloride, Sodium, and Salinity

Based on the conservative parameters salinity and chloride (Cl$^-$), the downcore record at Site 1171 can be separated into three units. The uppermost ~270 mbsf shows little change in salinity (34 to 35) (Table **T20**) and Cl$^-$ (554–564 mM; Fig. **F34**). The Cl$^-$ concentrations are close to seawater concentrations although they increase by ~1% to a maximum of 564 mM at ~50 mbsf. In the second unit from ~270 to ~600 mbsf, salinity and Cl$^-$ decrease to 30–31 and 544–551 mM, respectively. Below ~600 mbsf in the lowermost unit, both parameters decrease to lower values (salinity 27–28; Cl$^-$ below ~520 mM). Chlorinity values exhibit a 13% decrease from seawater values. Sodium (Na$^+$) generally follows the same pattern as salinity and Cl$^-$, with concentrations ranging between ~465 and ~485 mM in the uppermost ~350 mbsf and increasing to 475–490 mM from ~350 to ~600 mbsf. Below ~600 mbsf, Na$^+$ concentrations become highly variable (~440 to ~490 mbsf) and are mostly below seawater values.

The ~1% increase in Cl$^-$ within the upper ~40–60 mbsf was also observed at Sites 1168, 1169, and 1170. The slight chlorinity change may be attributed to a salinity increase during the last glacial maximum as proposed by McDuff (1985) and Schrag et al. (1996). Farther downcore, a Cl$^-$ decrease provides evidence of deep pore-water freshening at this site. Note that in contrast to the Na$^+$ profile, the Na$^+$/Cl$^-$ downcore record exhibits gradually increasing values from 0.84 at the surface to 0.98 at depth.

**F34.** Concentration-depth profile of Cl$^-$ compared to methane and Na$^+$ compared to Na$^+$/Cl$^-$ ratios, p. 104.



**F35.** Concentration-depth profiles of SO$_4^{2-}$, pH, alkalinity, and NH$_4^+$, p. 105.



**F36.** Concentration-depth profiles of Sr$^{2+}$, Ca$^{2+}$, and Li$^+$, p. 106.



**F37.** Concentration-depth profiles of Mg$^{2+}$ and K$^+$, p. 107.

The advection of meteoric waters as a possible source of low-Cl⁻ interstitial waters (e.g., Austin, Christie-Blick, Malone, et al., 1998) can be ruled out because of the isolated location of Site 1171 on the STR. The Cenozoic sequence is mostly absent between the STR and the Tasmanian shelf, so there is no readily conceivable aquifer link to Tasmania. We suspect that as at Site 1170, the presence of low-Cl⁻ fluids implies internal processes such as gas hydrate dissociation, dehydration reactions of hydrous minerals (e.g., clay minerals and biogenic opal), and/ or clay-membrane ion filtration (e.g., Kastner et al., 1991; Hesse and Harrison, 1981; Paull, Matsumoto, Wallace, et al. 1996). Similar to Sites 1168 and 1170, pore-water freshening is restricted to older strata and apparently coincides with the onset of methanogenesis (Fig. F34). Whether the ongoing maturation of organic matter affects the freshening of pore water is not yet answered.

## Sulfate, pH, Alkalinity, and Ammonium

The sulfate-concentration profile can be differentiated into two units. From 0 to ~ 270 mbsf (a zone with ~90% $CaCO_3$ and low organic matter content), sulfate concentrations gradually decrease from near-seawater values (26–27 mM) at the top of the hole to ~18–19 mM at ~270 mbsf (~30% decrease) (Fig. F35). The decrease in interstitial water $SO_4^{2-}$ concentrations at Site 1171 exhibits the same amount of depletion through comparable depths as observed at Site 1169. Below ~270 mbsf, $SO_4^{2-}$ sharply decreases to values close to zero, coincident with a distinct increase in methane (the onset of methanogenesis unfortunately was not documented as a result of technical problems but likely occurred at ~320 mbsf; see "Volatile Hydrocarbons," p. 49, in "Organic Geochemistry").

The pH and alkalinity reveal a three-step downcore change. The pH decreases from ~7.6 at the top to <7.2 at ~70–80 mbsf. Subsequently, pH increases and stays nearly constant at 7.4–7.5 between 80 and 270 mbsf (Fig. F35). From ~270 to ~520 mbsf, pH increases from ~7.5 to ~7.7, below which the pH increases to ~8.3 and remains high to the bottom of the hole. This pH increase corresponds to an increase in methane content.

Titration alkalinity values from surface-sediment pore waters are ~3.1 mM and show a slight increase to ~4.0–5.5 mM within the upper ~270 mbsf of calcareous ooze (Fig. F35). From 270 to ~500 mbsf, alkalinity varies considerably from 4 to 7 mM. Below ~500 mbsf, the values decrease sharply to minimum values of 1.5–2.6 mM. Ammonium ($NH_4^+$) steadily increases from 10 µM at the surface to a maximum of ~3.0 mM at ~930 mbsf, thus reaching considerably higher values than at previous sites (Fig. F35).

The downcore change in $SO_4^{2-}$, alkalinity, and $NH_4^+$ is most likely the result of organic matter remineralization. The nearly complete exhaustion of $SO_4^{2-}$ below the carbonate-rich sediment sequence (lithostratigraphic Units I and II) should be immediately followed by the onset of methanogenesis (e.g., Claypool and Kaplan, 1974). Bacterial methane production, which normally proceeds by the mechanism of $CO_2$ reduction in marine environments, at the same time tends to raise the pH and also favors carbonate precipitation (Claypool and Kaplan, 1974) by the following generalized formula: $Me^{2+} + 2HCO_3^- + 8H^+ \rightarrow CH_4 + MeCO_3 + 3H_2O$.

F38. Concentration-depth profile of dissolved silica within interstitial water, p. 108.

## Strontium, Calcium, and Lithium

The calcareous lithostratigraphic Units I to III at Site 1171, which cover the uppermost ~ 270 mbsf, have relatively constant $Ca^{2+}$ concentration. Apart from the topmost sample where $Ca^{2+}$ concentrations are close to seawater values (Fig. **F36**), $Ca^{2+}$ concentrations increase to an average of 11.6 mM with a maximum of 12.3 mM at ~90 mbsf. In the underlying siliciclastic unit (lithostratigraphic Units IV and V), $Ca^{2+}$ concentrations exhibit a wider variability from 10.3 to 11.8 mM but still are close to seawater values. Below ~700 mbsf within lithostratigraphic Unit IV, $Ca^{2+}$ concentrations significantly decrease to minimum values of 5.6 mM at the bottom of the hole.

Strontium ($Sr^{2+}$) concentrations gradually increase with depth from 117 µM at the seafloor to ~420 µM at ~80 mbsf and, subsequently, decline to 178 µM at the base of the hole (Fig. **F36**). The distribution of $Li^+$ is inverse to that of $Sr^{2+}$. Concentrations vary between ~17 and 50 µM with minimum values in the uppermost sediments and gradually and steadily increase downcore. Maximum values of ~600 µM are observed at ~930 mbsf. Normalizing to $Cl^-$ to account for the downcore pore-fluid freshening does not affect the records of either $Ca^{2+}$, $Sr^{2+}$, or $Li^+$.

The slight increase in $Ca^{2+}$ and $Sr^{2+}$ concentrations and $Sr^{2+}/Ca^{2+}$ ratios within the calcareous ooze are most likely the result of dissolution and reprecipitation of calcite. A release of strontium into interstitial fluids is likely caused by the recrystallization and/or dissolution of biogenic carbonate to diagenetic low-Mg calcite (e.g., Manheim and Sayles, 1974; Baker et al., 1982).

The significantly increasing $Li^+$ concentrations below the carbonate sequence suggest that silicate phases may act as a major source for $Li^+$, which at the same time removes $Mg^{2+}$ and $K^+$. Volcanic matter alteration could be an alternative mechanism to describe increased $Li^+$ pore-water concentrations.

## Magnesium and Potassium

The downcore magnesium ($Mg^{2+}$) and potassium ($K^+$) profiles exhibit steadily decreasing concentrations from the uppermost sample to the bottom of Hole 1171D (Fig. **F37**). The uppermost $Mg^{2+}$ and $K^+$ concentrations of 51.3 and 10.0 mM, respectively, are close to normal seawater concentrations, decreasing by ~86% to 7.8 and 1.7 mM at depth, respectively. Note, however, that below ~270 mbsf (lithostratigraphic Unit III) $Mg^{2+}$ and $K^+$ concentrations decrease more rapidly. Normalizing these values to $Cl^-$ (Fig. **F37**) indicates that the elemental downcore gradients are much greater than can be attributed to pore-water salinity changes. The change in concentration of both elements is highly correlated ($r = 0.98$), as in the previous sites, and suggests that both elements are being removed from pore waters by similar processes. Most likely, basement alteration and/or ion-exchange reactions associated with clay minerals (Gieskes, 1983; De Carlo, 1992) take place below the drilled sequence and drive the $Mg^{2+}$ and $K^+$ distribution within the noncarbonate lithostratigraphic Units IV–VI. For example, the conversion of kaolinite to montmorillonite will remove varying amounts of $Mg^{2+}$ and $K^+$ from pore fluids (Loughnan, 1969). Additional processes within the calcareous oozes may act as sinks for $Mg^{2+}$ and $K^+$, although these processes have yet to be identified.

## Silica

Dissolved silica concentrations ($H_4SiO_4^0$) range from ~100 to 1100 µM. Within the upper ~300 mbsf (lithostratigraphic Units I–III and part of Unit IV), $H_4SiO_4^0$ exhibits a near-continuous increasing downward profile (Fig. F38) with the highest concentrations (>900 µM) in the lower part of lithostratigraphic Subunit IB and within Units II–IV (~170 to 320 mbsf). Below, silica concentrations decrease in a two-step manner: to ~500–700 µM (mainly restricted to lithostratigraphic Subunits VA and VB) and to ~100–200 µM (below 500 mbsf within lithostratigraphic Subunit VC and Unit VI).

The dissolved silica concentrations within the calcareous oozes (lithostratigraphic Units I–III) at Site 1171 are comparable to the concentrations found in the carbonate sequences of Sites 1169 and 1170 while being consistently higher than those at Site 1168. The lowest $H_4SiO_4^0$ values of ~100 to 200 µM within the siliciclastic deposits below ~500 mbsf compare to $H_4SiO_4^0$ concentrations below the diffusional boundary at Site 1170. In contrast to Site 1170, we observe a gradation in $H_4SiO_4^0$ between the calcareous oozes and the underlying siliciclastic deposits.

The distinct $H_4SiO_4^0$ variations are likely a response to the abundance of biogenic silica and the formation of opal-CT. Most silica dissolution is apparently in sediments rich in biogenic silica, and $H_4SiO_4^0$ concentrations are a reflection of the opal content of the sediments, as seen in the previous Leg 189 sites. A significant removal of $H_4SiO_4^0$ from pore waters, in contrast, may be induced by the recrystallization of opal-A to opal-CT (e.g., Baker, 1986). The highest abundance of siliceous fauna estimated from smear slides are present within lithostratigraphic Unit IV at Site 1171 (see "Lithostratigraphy," p. 10), whereas above and below, the abundance of biogenic silica is significantly lower. These trends are compatible with observed dissolved silica concentrations in the pore waters. Furthermore, increased radiolarian abundance (see "Biostratigraphy," p. 25) matches peaks in the dissolved silica record. X-ray diffraction analysis shows the existence of opal-CT between ~480 and 520 mbsf (Fig. F38; see "Lithostratigraphy," p. 10), coincident with a significant dissolved silica drop. Gieskes (1981), however, suggested that a significant change in $H_4SiO_4^0$ does not occur until the transition of opal-CT to quartz.

## Summary

Site 1170 provided valuable insight into the location of sources and sinks for many of the pore-water constituents because of the presence of a distinct and probably low-permeable lithologic change, which acts as a diffusional boundary (see "Inorganic Geochemistry," p. 46, in the "Site 1170" chapter). Although the geochemistry is characterized by a similar abrupt lithologic change from upper Oligocene to Pleistocene carbonate oozes to mainly Eocene siliciclastic deposits, a diffusional boundary is not present at Site 1171. Nevertheless, mechanisms for the distribution of various pore-water constituents become apparent by comparing sites.

At Site 1171, concentrations and the progressive removal of $Mg^{2+}$ and $K^+$ downcore compare with Site 1168 and 1170, suggesting that $Mg^{2+}$ and $K^+$ are most likely being consumed by silicate reactions (e.g., basement alteration and/or ion-exchange reactions associated with clay

minerals) either within the siliciclastic sediments or below the cored section.

The increasing $Sr^{2+}$ and $Ca^{2+}$ concentrations within the pore waters of the pelagic calcareous oozes (observed at Sites 1168–1171) and the continuous loss of $Sr^{2+}$ within the underlying siliciclastic sections point to dissolution and/or reprecipitation of calcite. The significant loss of $Ca^{2+}$ at depth, which is similar to observations of Site 1168, is most likely attributed to silicate reactions. Pore-water $Li^+$ concentrations from the calcareous oozes of Site 1171 resemble those of Sites 1168 and 1170, suggesting that an effective $Li^+$ sink is present within the nannofossil ooze and chalks.

In general, sulfate reduction is complete within or below the calcareous oozes and is followed at depth by the onset of methanogenesis. Coincident with increasing methane concentrations, pore waters become distinctly fresher as deduced from decreasing $Cl^-$ values, whereas pH increases. Whether pore-water freshening is caused by organic matter maturation, dehydration reactions of hydrous minerals, clay-membrane ion filtration, and/or gas hydrate dissociation is not yet answered.

$H_4SiO_4^0$ downcore variations reflect the abundance of biogenic opal and opal-CT within the sediments. Most silica dissolution apparently is present in sediments enriched in biogenic opal, leading to higher pore-water $H_4SiO_4$ concentrations. In contrast, the diagenetic conversion of opal-A to opal-CT may extract $H_4SiO_4$ from the interstitial fluids.

# PHYSICAL PROPERTIES

The physical properties program at Site 1171 included MST and thermal conductivity measurements of whole-round cores and compressional wave (*P*-wave) velocity, moisture and density (MAD), and vane shear-strength measurements of split cores. The Adara tool was deployed once each in Holes 1171A and 1171B for in situ temperature measurements.

## Multisensor Track

All core sections from Holes 1171A, 1171B, 1171C, and 1171D were routinely measured on the MST (for magnetic susceptibility, *P*-wave velocity, and GRA density) at 2- to 3-cm intervals. *P*-wave velocities were recorded only in APC cores from Holes 1171A, 1171B, and 1171C.

Variations in magnetic susceptibility (Fig. F39A) correlate with lithologic changes downcore. Magnetic susceptibility remains low through high-carbonate intervals (lithostratigraphic Units I and II), while the glauconite-rich sediments of Unit III are characterized by a sharp increase in magnetic susceptibility. Units III and IV are characterized by alternating lithified and unlithified intervals, associated with high and low values of magnetic susceptibility respectively. Magnetic susceptibility increases through Subunit VC and remains high through Unit VI.

Density generally increases between the seafloor and 950 mbsf as a result of normal sediment compaction and dewatering trends (Fig. F39B). Although the first-order GRA and discrete density trends are similar, GRA-density and discrete density values show some downcore offset. GRA values are higher than discrete values in carbonate-rich sections (between ~40 and 270 mbsf). Because the MST is optimized for mixed sediments, the calibration procedure overestimates densities in

**F39.** Magnetic susceptibility, GRA density, and wet bulk density vs. depth, Hole 1171A, p. 109.
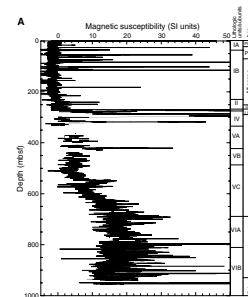
carbonate-rich sediments. MAD measurements are higher than recorded GRA-density values from Hole 1171D (390 mbsf to total depth [TD]). The RCB cores in Hole 1171D did not fill the core liner; therefore, this difference in measured density is expected because GRA processing assumes the core diameter equals the liner diameter.

At ~520 mbsf, there is a large positive shift in GRA and discrete density that corresponds to an increase in *P*-wave velocities (Fig. F32, p. 90, in the "Site 1172" chapter) and magnetic susceptibility, but does not appear to correspond to a compositional change. These changes in core physical properties correspond to variations seen in the downhole density, Th, and U logs (see "Downhole Measurements," p. 56), and dinocyst biostratigraphy (see "Biostratigraphy," p. 25), which all suggest a hiatus is present. At this same interval, low-TOC and high-HI values are observed (see "Organic Geochemistry," p. 44), suggesting the interval is a condensed section.

## Acoustic Velocity

Compressional velocities were obtained on the split-core sections at a sampling interval of one per section through the Pliocene sediments, and three to four per core below the Pliocene sediments in cores from Hole 1171A, the XCB sections from Holes 1171C and 1171D to a depth of ~754 mbsf (PWS3; x-direction) (Figs. F40, F41). When possible, discrete velocity was measured in longitudinal directions (PWS1; z-direction down to ~ 220 mbsf in Hole 1171A).

A comparison of the MST velocity profile and the discrete velocity values for the interval between 0 and 120 mbsf is shown in Figure F40. All the data sets correlate fairly well, with most values within the range of 1550–1700 m/s. Velocities >3000 m/s correspond to intervals with well-lithified sediments (Units III and IV, Subunit VA, and Unit VI). Average velocities vary from 1550 m/s in the soft-surface sediments to 2400 m/s in the more consolidated sediments (PWS3; Table T21; Fig. F41).

## Thermal Conductivity

Thermal conductivity was measured on Section 3 of each core in Hole 1171A to a depth at which induration prevented insertion of the needles (~110 mbsf) (Fig. F42; Table T22). Values increase rapidly at ~50 mbsf then slowly decrease with depth.

## In Situ Temperature Measurements

The Adara tools were deployed three times at Site 1171 and this deployment yielded two acceptable temperature records. The temperature at the seafloor (2.95°C) was determined using the mudline stops. Examination of the penetration temperature records indicates a normal deployment (see "Physical Properties," p. 45, in the "Site 1168" chapter).

### Heat Flow

The geothermal gradient determined by least-squares regression is 62°C/km (Fig. F43), compared to 58°C/km at Site 1168 and 52°C/km at Site 1170 (see the "Physical Properties," p. 45, in the "Site 1168" chapter and "Physical Properties," p. 49, in the "Site 1170" chapter). Data for all sites show higher values than the Cape Sorell No. 1 exploration

F40. *P*-wave velocities measured for discrete samples and in whole cores vs. depth, p. 111.
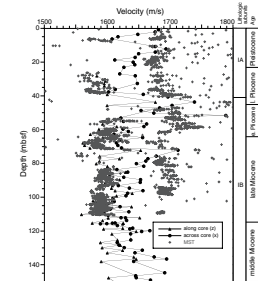


F41. *P*-wave velocities measured for discrete samples vs. depth, p. 112.
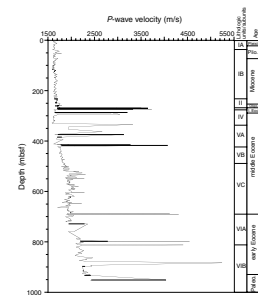


T21. *P*-wave velocities measured at discrete intervals, p. 167.

F42. Thermal conductivity vs. depth, p. 113.
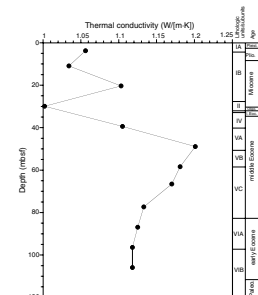


T22. Thermal conductivity measured on whole-core sections, Hole 1171A, p. 170.

well (27°C/km) on the continental shelf 100 km to the northeast of Site 1168 (Willcox et al., 1989). The average of the thermal conductivities measured from 0 through 108 mbsf in Hole 1171C is 1.112 W/(m·K). Using the average conductivity and the geothermal gradient yields a heat flow of 68 mW/m².

This heat-flow value is twice the values reported from sedimentary basins and slopes near western Tasmania north of Site 1168 and Mesozoic continental margins in the mid-Atlantic (~40 mW/m 2; see "Physical Properties," p. 45, in the "Site 1168" chapter).

## Undrained Shear Strength

One measurement per section of vane shear strength was taken in Hole 1171A to the depth at which induration prevented insertion of the vane for shear strength (~120 mbsf; the ooze–chalk transition). A clear trend in shear strength is not observed (Fig. F44; Table T23). The values are variable and fluctuate around an average value of ~13 kPa from 0 to 90 mbsf and at ~8 kPa from 90 to 120 mbsf.

## Moisture and Density

Bulk density generally increases with depth below seafloor, whereas porosity and water content decrease (Table T24). Several changes in the MAD gradients with depth are present throughout the section. These gradient changes are usually bounded by offsets that roughly correlate with the boundaries between lithostratigraphic units (see "Lithostratigraphy," p. 10) and with changes in sedimentation rates (see "Biostratigraphy," p. 25). The discrete wet bulk density data (Fig. F45) correlate very well with the GRA data and can be used to calibrate and correct GRA density (see "Multisensor Track," p. 54; Fig. F39B). Large fluctuations occur in the MAD records in lithostratigraphic Unit IV, corresponding to alternating intervals of lithified and unlithified sediments (see "Lithostratigraphy," p. 10).

# DOWNHOLE MEASUREMENTS

## Logging Operations

Downhole logging was conducted in Hole 1171D after it had been drilled to a depth of 959 mbsf with a 9.785-in drill bit. The basal 711.4 m was cored, whereas the upper 247.6 m of the hole was drilled ahead with a center bit (see "Operations," p. 8). After a wiper trip (see "Downhole Measurements," p. 47, in the "Site 1168" chapter) and displacing the hole with sepiolite mud, the RCB bit was released and the pipe was set at 151 mbsf in preparation for logging. Three tool-string runs were planned; the triple combo, the GHMT-sonic, and the FMS-sonic. However, operational difficulties only allowed triple-combo measurements to be obtained (see below).

There was substantial and increasing heave throughout the logging operations. The wireline heave compensator (WHC) stroked out on three occasions while logging with the triple combo near the base of the hole. A repeat pass of the triple combo, with no failures of the WHC, was conducted between 761 and 959 mbsf (Fig. F46), and the results from both passes have been spliced together to produce a composite depth-corrected data set.

**F43.** Temperature vs. depth, p. 114.
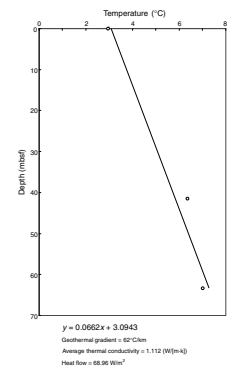
**F44.** Undrained shear strength from miniature vane-shear measurements vs. depth, Hole 1171A, p. 115.
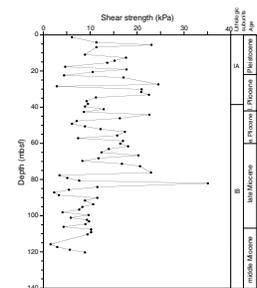
**T23.** Undrained shear strength from miniature vane-shear measurements, Hole 1171A, p. 171.

**T24.** Moisture and density measured at discrete intervals, p. 172.

**F45.** Wet bulk density, water content, and porosity measured at discrete intervals vs. depth, p. 116.
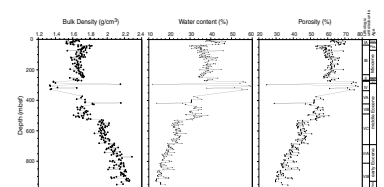
While running in with the GHMT-sonic, heaves of ~9 m were recorded at the rig floor. During the transit of this tool down through the open formation, the WHC frequently stroked out and, possibly as a result of the extreme heave, the head-tension gauge malfunctioned. Shortly afterward, downhole telemetry with the tool string was also lost, so we decided to pull out of the hole. While pulling the tool back toward the rig floor, it became apparent that the tool had sat, bridged out, at ~280 mbsf. The tool was returned to the rig floor. To try and clear the bridge in the formation, the drillers attempted to push the open pipe down to ~294 mbsf. Unfortunately, after adding one stand of drill pipe, the end of the pipe deviated from the hole and became clogged with soft sediment. No further logging was possible.

## Results/Data Quality

The principal results are shown in Figures **F47** and **F48.** The borehole was generally smooth, with diameters of ~12 in below 272 mbsf and ~19 in above 250 m (Fig. **F47**). Despite the washed out conditions in the upper section of the hole, the pad contact tools (HLDS and APS) appear to have produced good-quality data. The raw spherically focused resistivity (SFLU) results contain anomalous spikes (9700 Ωm) between ~294 and 308 mbsf. These data have been edited out.

There is generally good agreement between log density and core density values, with both data showing a stepwise variation downhole (Fig. **F49**). However, although the log densities are almost the same as the core densities near the top of the logged section (e.g., 170–270 mbsf; log densities = 1.72 ± 0.04 g/cm³; core densities = 1.67 ± 0.04 g/cm³), toward the base of the hole log densities are slightly higher and less variable than the core densities (e.g., 845–845 mbsf; log densities = 2.3 ± 0.03 g/cm³; core densities = 2.17 ± 0.07 g/cm³). This disparity most likely results from postcoring sediment expansion affecting the core densities.

Log porosity and core porosity values also show good agreement (Fig. **F50**). Neutron porosity log values agree closely with core porosity measurements throughout. Density porosities are similar to neutron and core porosities between 150 and 750 mbsf but are ~8% lower than both below 750 mbsf. Spikes in downhole density and porosity are generally correlative with equivalent core measurements, demonstrating that fluctuations in the logs represent sedimentological variability and that there is relatively little depth mismatch between the two data sets. The failure of the core measurements to record every porosity minimum and density maximum between 273 and 465 mbsf reflects the poor core recovery over this interval.

Because there was no sonic velocity log from this site, the *P*-wave velocity data measured vertically on half cores (see **"Physical Properties,"** p. 54) have been used to produce an integrated traveltime data set. These data can be used to show a graph of increasing two-way traveltime vs. depth and also to plot the *P*-wave velocities against time for comparison with the seismic section (Fig. **F51**). The sharp increases in *P*-wave velocity between ~274 and 427 mbsf (~0.33–0.49 s) correspond to major reflectors in the seismic section. The reflector at ~0.59 s (~519 mbsf) correlates with an increase in *P*-wave velocities and also to a sharp increase in both core and log density values (see **"Log Unit 4: 520–890 mbsf,"** p. 59, and **"Discussion,"** p. 59).

**F46.** Details of the logging operations, Hole 1171D, p. 117.
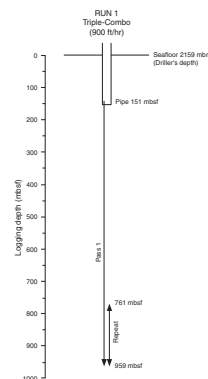
**F47.** Caliper, medium resistivity, porosity, density, and photoelectric effect values, Hole 1171D, p. 118.
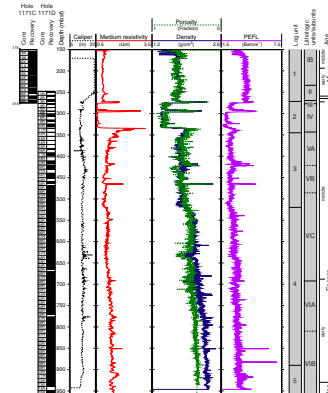
**F48.** Total gamma-ray and spectral gamma-ray values, Hole 1171D, p. 119.
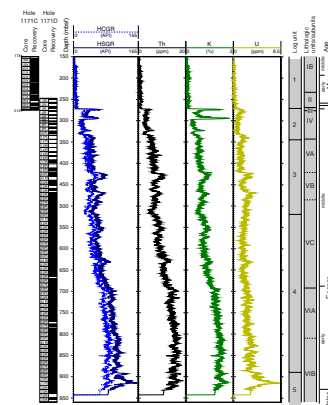
## Log Units

All of the log data show marked and often correlative downhole fluctuations (Figs. F47, F48) that are used to divide the logged interval into five units. The two log parameters that show the greatest downhole variation are density and natural gamma; a crossplot of these data (Fig. F52) gives a good visual representation of the five different logging units, which are described in more detail below.

### Log Unit 1: Base of the Pipe (151 mbsf) to 272 mbsf

The natural gamma values are low (~5 API) and show only small variations (~3–8 API) throughout this unit, suggesting there is little terrestrial material in these sediments. Photoelectric log values remain near 4 barn/e⁻, suggesting a high carbonate content, which is consistent with core measurements of ~90 wt% $CaCO_3$ over this interval (see "Organic Geochemistry," p. 44). Resistivity values are also low and fairly stable throughout this unit, consistent with the homogeneity observed in other log parameters.

### Log Unit 2: 272–345 mbsf

Density, resistivity, and photoelectric log values are generally low (~1.4 gm/cm³, ~0.6 Ωm, and ~1.1 barn/e⁻, respectively), whereas porosity values increase to >80% and natural gamma logs also increase over much of the interval. The increase in natural gamma and decrease in photoelectric values suggest greater terrestrial material and lower carbonate content throughout this unit. However, the high porosities (>80%) and low densities are typical of diatomaceous sediments (Gersonde, Hodell, Blum, et al., 1999). This interpretation is consistent with the clay-and diatom-rich sediments recovered in the core (see "Lithostratigraphy," p. 10).

Interspersed within this unit are thin layers marked by high density, resistivity, photoelectric effect, and natural gamma values but relatively low porosities, most pronounced at 273–275 mbsf and 290–296 mbsf. The spectral gamma results (Fig. F48) show that most of the natural gamma increase is caused by greater K concentrations over these intervals. In conjunction with the high photoelectric values, such high K concentrations are characteristic of glauconite-bearing sediments (Rider, 1996). Glauconite was recorded in the core over this interval (see "Lithostratigraphy," p. 10), although core recovery was very low. Indeed, the inferred glauconite-rich interval between 290 and 296 mbsf was entirely missed because of poor core recovery. Density, resistivity, and photoelectric log values increase at the base of Unit 2 (334–345 mbsf), marking the bottom of the high-porosity diatomaceous interval.

### Log Unit 3: 345–520 mbsf

Density, resistivity, neutron porosity, and photoelectric log values generally covary in this unit, although no overall downhole trend is discernible. This is particularly apparent in the density log (Fig. F49), which shows no apparent compaction trend from top to bottom. The total gamma and spectral gamma-ray logs show increased values at 423–436, 467–476, and 490 mbsf, and the resistivity, density, porosity, and photoelectric effect (PEFL) show spikes at 418 and 465 mbsf. The

**F49.** Downhole log bulk density plotted with core bulk density, p. 120.
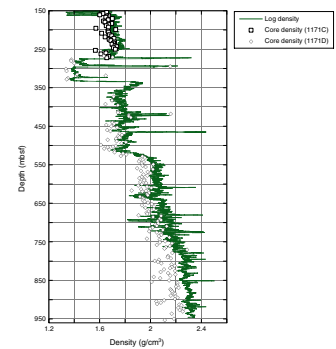


**F50.** Downhole density porosity and neutron porosity plotted with core porosity, p. 121.
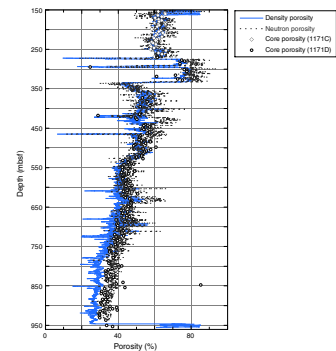


**F51.** Time/depth, P-wave velocity, and seismic data, p. 122.
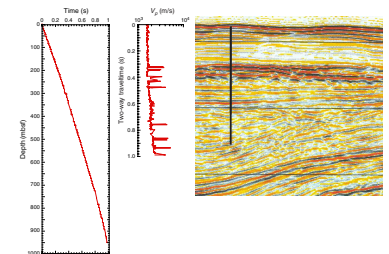


**F52.** Downhole density plotted against natural gamma, p. 123.
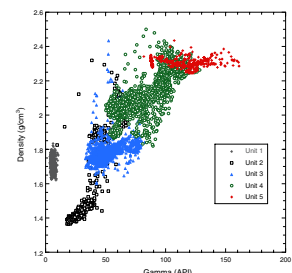
strongly fluctuating log values suggest that this unit contains variations in lithology and/or mineralogy (see "Discussion," p. 59).

## Log Unit 4: 520–890 mbsf

Densities show a sharp downhole increase at the top of log Unit 4 (from ~1.8 to ~2 g/cm³) and then continue to increase toward the base of the hole (Fig F49). Natural gamma values also show a generally linear increase down through this unit. Figure F52 shows that Units 3 and 4 have very different distributions on a crossplot of density against natural gamma. The increase in natural gamma down through log Unit 4 is mainly a result of increasing Th and K content rather than U (Fig. F48), suggesting terrestrial components increase downhole. This hypothesis is consistent with the magnetic susceptibility data from the core, which show an increase in values below 520 mbsf (see "Physical Properties," p. 54).

## Log Unit 5: 890 mbsf to Base of Hole (959 mbsf)

Log Unit 5 has been defined entirely on the presence of increased U levels, which reach their maximum value of 8.3 ppm at 915 m (Fig. F48). This peak in U is at a depth where Th values are high but relatively stable and where K values show a slight increase above already high levels. This depth also correlates with high magnetic susceptibilities in the core (see "Physical Properties," p. 54) and the highest TOC content of the sediment (see "Organic Geochemistry," p. 44). All these data imply an increase in organic matter into a sedimentary system already receiving a significant input of terrigenous material.

## Discussion

The sharp increase in densities at the top of log Unit 4 divides the underlying sediments, which show a normal compaction trend, from the overlying sequence (log Unit 3), which shows no clear density trend. At this depth (520 mbsf), Th, K, and core magnetic susceptibility also show a downward trend to increasing values, and *P*-wave velocities measured in the core show a sharp rise from ~1878 to 2056 m/s (see "Physical Properties," p. 54). There is clearly a change in sediment properties at this depth even though the other log curves and the lithostratigraphy are relatively constant across this horizon. The reason for the sudden shift in the character and value of the density log at 520 mbsf is not clear, but it may possibly relate to a hiatus in sedimentation. Magnetostratigraphic interpretations (see "Paleomagnetism," p. 40) were unable to produce a conformable reversal stratigraphy across this horizon; geochemical analyses show the presence of low TOC and high HI values at ~520 mbsf, possibly indicating a condensed section (see "Organic Geochemistry," p. 44); and dinocyst biostratigraphy suggests the presence of a ~2 to 3-m.y. hiatus between Cores 189-1171A-29R and 35R (~510–570 mbsf; see "Biostratigraphy," p. 25).

The strongly varying log parameters in log Unit 3 suggest that changes in the sedimentary environment occurred throughout this interval. Preliminary interpretation of the logs suggests that spikes in resistivity, density, and PEFL are often correlative and that they tend to be directly above increased natural gamma values (e.g., 400–500 mbsf; Fig. F53). This pattern of log variations may well be a response to alternating marine vs. terrestrial influences. Figure F53 shows the zones where

**F53.** Detailed downhole spectral gamma-ray, porosity, density, photoelectric effect, and resistivity logs, p. 124.
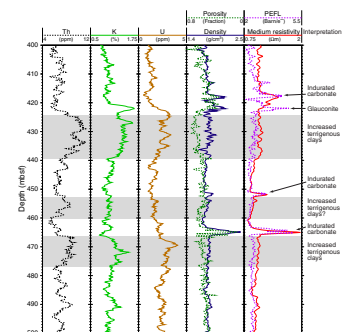
Th and K values are highest, possibly indicating an increased input of terrigenous clays. Interestingly, in the area of high Th values between ~425 and 439 mbsf, the density and porosity logs have a noticeable mismatch (Fig. F53), implying that some of the neutron porosity values may be derived from water bound in clays. The spikes in resistivity, PEFL, and density probably indicate areas of indurated carbonate. An exception to this is present at 422 mbsf, where increased PEFL values and densities, with no concomitant increase in resistivity, correlate with an increase in K. This indicates the presence of glauconite. The presence of glauconite may indicate a slightly anoxic, sediment-starved environment, whereas the indurated carbonate may be indicative of more open marine conditions.

The fluctuating sedimentary environments indicated by log Unit 3 could be caused by variations in relative sea level or climate. However, any changes in paleowater depths must be relatively small because middle neritic (~50–100 m) benthic foraminifer faunas are found throughout this interval (see "Biostratigraphy," p. 25). Confirmation that the variations in log data from log Unit 3 are a result of sea-level change will require postcruise core/log analyses and detailed comparison between the logs and seismic stratigraphy, as well as the results of further microfossil and sedimentological analysis.

On a finer scale, downhole logs appear to be strongly cyclic in many intervals. For example, the Th spectrum of the natural gamma-ray log, which showed strong cyclicity in the middle to late Eocene at Site 1170, also shows strong cyclicity in the middle Eocene at this site (Fig. F54). A prominent peak in the middle Eocene Th power spectrum is present at ~2 m as opposed to the ~4-m period found at Site 1170. A shift in the apparent periodicity between sites could be explained by a lower sedimentation rate (~50%) at Site 1171 relative to Site 1170. Preliminary magnetic and biostratigraphic results from this site (see "Paleomagnetism," p. 40, and "Biostratigraphy," p. 25) are consistent with lower sedimentation rates in general, but confirmation that the shift in periodicity is the result of sedimentation-rate differences will require further lithostratigraphic, magnetic, and biostratigraphic integration.

**F54.** Downhole spectral gamma-ray data for Th and Blackman-Tukey power spectrum of Th, p. 125.
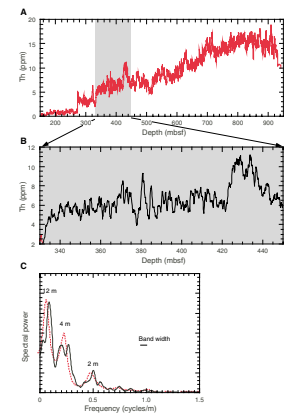
# REFERENCES

Adams, J.A.S., and Weaver, C.E., 1958. Thorium-to-uranium ratios as indicators of sedimentary processes: example of concept of geochemical facies. *AAPG Bull.,* 42:387–430.

Austin, J.A., Jr., Christie-Blick, N., Malone, M.J., et al., 1998. *Proc. ODP, Init. Repts.,* 174A: College Station, TX (Ocean Drilling Program).

Baker, P.A., 1986. Pore-water chemistry of carbonate-rich sediments, Lord Howe Rise, Southwest Pacific Ocean. *In* Kennett, J.P., von der Borch, C.C., et al., *Init. Repts. DSDP,* 90 (Pt. 2): Washington (U.S. Govt. Printing Office), 1249–1256.

Baker, P.A., Gieskes, J.M., and Elderfield, H., 1982. Diagenesis of carbonates in deep-sea sediments: evidence from $Sr^{2+}/Ca^{2+}$ ratios and interstitial dissolved $Sr^{2+}$ data. *J. Sediment. Petrol.,* 52:71–82.

Berggren, W.A., 1992. Paleogene planktonic foraminifer magnetobiostratigraphy of the Southern Kerguelen Plateau (Sites 747–749). *In* Wise, S.W., Jr., Schlich, R., et al., *Proc. ODP, Sci. Results,* 120 (Pt. 2): College Station, TX (Ocean Drilling Program), 551–568.

Berner, R.A., and Raiswell, R., 1984. C/S method for distinguishing freshwater from marine sedimentary rocks. *Geology,* 12:365–368.

Brinkhuis, H., and Biffi, U., 1993. Dinoflagellate cyst stratigraphy of the Eocene/Oligocene transition in central Italy. *Mar. Micropaleontol.,* 22:131–183.

Brinkhuis, H., Powell, A.J., and Zevenboom, D., 1992. High-resolution dinoflagellate cyst stratigraphy of the Oligocene/Miocene transition interval in north-west and central Italy. *In* Head, M.J., and Wrenn, J.H. (Eds.), *Neogene and Quaternary Dinoflagellate Cysts and Acritarchs.* Am. Assoc. Stratigr. Palynol. Found., 219–258.

Bujak, J.P., and Brinkhuis, H., 1998. Global warming and dinocyst changes across the Paleocene/Eocene boundary. *In* Aubry, M.-P., et al. (Eds.), *Late Paleocene-Early Eocene Climatic and Biotic Events in the Marine and Terrestrial Records:* New York (Columbia Univ. Press), 277–295.

Cande, S.C., Stock, J.M., Muller, R.D., and Ishihara, T., 2000. Cenozoic motion between east and west Antarctica. *Nature,* 404:145–150.

Cape Roberts Science Team, 2000. Studies from the Cape Roberts Project, Ross Sea, Antarctica: initial Report on CRP-3. *Terra Antart.,* 7.

Chamley, H., 1989. *Clay Sedimentology:* Berlin (Springer-Verlag).

Claypool, G.E., and Kaplan, I.R., 1974. The origin and distribution of methane in marine sediments. *In* Kaplan, I.R. (Ed.), *Natural Gases in Marine Sediments:* New York (Plenum), 99–139.

Clementz, D.M., 1979. Effect of oil and bitumen saturation on source-rock pyrolysis. *AAPG Bull.,* 63:2227–2232.

Crouch, E.M., and Hollis, C.J., 1996. Paleogene palynomorph and radiolarian biostratigraphy of DSDP Leg 29, Sites 280 and 281, South Tasman Rise. *Inst. Geol. Nucl. Sci., Sci. Rep.,* 96/19.

De Carlo, E.H., 1992. Geochemistry of pore water and sediments recovered from the Exmouth Plateau. *In* von Rad, U., Haq, B.U., et al., *Proc. ODP, Sci. Results,* 122: College Station, TX (Ocean Drilling Program), 295–308.

Ehrmann, W.U., 1991. Implications of sediment composition on the southern Kerguelen Plateau for paleoclimate and depositional environment. *In* Barron, J., Larsen, B., et al., *Proc. ODP, Sci. Results,* 119: College Station, TX (Ocean Drilling Program), 185–210.

Espitalié, J., Madec, M., and Tissot, B., 1977. Source rock characterization method for petroleum exploration. *Proc. Annu. Offshore Technol. Conf.,* 3:439–443.

Exon, N.F., Moore, A.M.G., and Hill, P.J., 1997. Geological framework of the South Tasman Rise, south of Tasmania, and its sedimentary basins. *Aust. J. Earth Sci.,* 44:561–577.

Fenner, J., 1984. Eocene-Oligocene planktic diatom stratigraphy in the low latitudes and the high southern latitudes. *Micropaleontology,* 30:319–342.

Fourtanier, E., 1991. Paleocene and Eocene diatom biostratigraphy and taxonomy of eastern Indian Ocean Site 752. *In* Weissel, J., Peirce, J., Taylor, E., Alt, J., et al., *Proc. ODP, Sci. Results,* 121: College Station, TX (Ocean Drilling Program), 171–188.

Gersonde, R., Hodell, D.A., Blum, P., et al., 1999. *Proc. ODP, Init. Repts,* 177 [CD-ROM]. Available from: Ocean Drilling Program, Texas A&M University, College Station, TX 77845-9547, U.S.A.

Gieskes, J.M., 1981. Deep-sea drilling interstitial water studies: implications for chemical alteration of the oceanic crust, layers I and II. *In* Warme, J.E., Douglas, R.G., and Winterer, E.L. (Eds.), *The Deep Sea Drilling Project: A Decade of Progress.* Spec. Publ.—Soc. Econ. Paleontol. Mineral., 32:149–167.

————, 1983. The chemistry of interstitial waters of deep-sea sediments: interpretation of deep-sea drilling data. *In* Riley, J.P., and Chester, R. (Eds.), *Chemical Oceanography,* 8:221–269.

Hesse, R., and Harrison, W.E., 1981. Gas hydrates (clathrates) causing pore-water freshening and oxygen isotope fractionation in deep-water sedimentary sections of terrigenous continental margins. *Earth Planet. Sci. Lett.,* 55:453–462.

Hinz, K., Willcox, J.B., Whiticar, M., Kudrass, H.-R., Exon, N.F., and Feary, D.A., 1986. The West Tasmanian Margin: an underrated petroleum province? *In* Glenie, R.C. (Ed.), *Tech. Papers at 2nd South-Eastern Australia Oil Exploration Symposium,* Melbourne, November 14–15, 1985. Pet. Expl. Soc. Aust., 395–410.

Huber, B.T., 1991. Paleogene and early Neogene planktonic foraminifer biostratigraphy of Sites 738 and 744, Kerguelen Plateau (southern Indian Ocean). *In* Barron, J., Larsen, B., et al., *Proc. ODP, Sci. Results,* 119: College Station, TX (Ocean Drilling Program), 427–449.

Hunt, J.M., 1996. *Petroleum Geochemistry and Geology* (2nd ed.): New York (W.H. Freeman).

Jenkins, D.G., 1993a. Cenozoic southern mid- and high-latitude biostratigraphy and chronostratigraphy based on planktonic foraminifera. *In* Kennett, J.P., and Warnke, D.A. (Eds.), *The Antarctic Paleoenvironment: A Perspective on Global Change.* Antarct. Res. Ser., 60:125–144.

Jenkins, D.G., 1993b. The evolution of the Cenozoic Southern high-and mid-latitude planktonic foraminiferal faunas. *In* Kennett, J.P., and Warnke, D.A. (Eds.), *The Antarctic Paleoenvironment: a Perspective of Global Change.* Antarct. Res. Ser., 60:175–194.

Kastner, M., Elderfield, H., and Martin, J.B., 1991. Fluids in convergent margins: what do we know about their composition, origin, role in diagenesis and importance for oceanic chemical fluxes? *Philos. Trans. R. Soc. London A,* 335:243–259.

Kennett, J.P., Houtz, R.E., et al., 1975. *Init. Repts. DSDP,* 29: Washington (U.S. Govt. Printing Office).

Kennett, J.P., and Srinivasan, M.S., 1983. *Neogene Planktonic Foraminifera: A Phylogenetic Atlas:* Stroudsburg, PA (Hutchinson Ross).

Loughnan, F.C., 1969. *Chemical Weathering of Siliciclastic Minerals:* New York (Elsevier).

Manheim, F.T., and Sayles, F.L., 1974. Composition and origin of interstitial waters of marine sediments, based on deep sea drill cores. *In* Goldberg, E.D. (Ed.), *The Sea* (Vol. 5): *Marine Chemistry: The Sedimentary Cycle:* New York (Wiley), 527–568.

McDuff, R.E., 1985. The chemistry of interstitial waters, Deep Sea Drilling Project Leg 86. *In* Heath, G.R., Burckle, L.H., et al., *Init. Repts. DSDP,* 86: Washington (U.S. Govt. Printing Office), 675–687.

McRae, S.G., 1972. Glauconite. *Earth-Sci. Rev.,* 8:397–440.

Miller, K.G., Wright, J.D., and Fairbanks, R.G., 1991. Unlocking the Ice House: Oligocene-Miocene oxygen isotopes, eustasy, and margin erosion. *J. Geophys. Res.,* 96:6829–6848.

Mohr, B.A.R., 1990. Eocene and Oligocene sporomorphs and dinoflagellate cysts from Leg 113 drill sites, Weddell Sea, Antarctica. *In* Barker, P.F., Kennett, J.P., et al., *Proc. ODP, Sci. Results,* 113: College Station, TX (Ocean Drilling Program), 595–612.

Mortlock, R.A., Charles, C.D., Froelich, P.N., Zibello, M.A., Saltzman, J., Hays, J.D., and Burckle, L.H., 1991. Evidence for lower productivity in the Antarctic Ocean during the last glaciation. *Nature,* 351:220–223.

Ninnemann, U.S., and Charles, C.D., 1997. Regional differences in Quaternary sub-antarctic nutrient cycling: link to intermediate and deep water ventilation. *Paleoceanography,* 12:560–567.

O'Sullivan, P.B., and Kohn, B.P., 1997. Apatite fusion track thermochronology of Tasmania. *Aust. Geol. Surv. Org. Rec.,* 1997/35:61.

Paull, C.K., Matsumoto, R., Wallace, P.J., et al., 1996. *Proc. ODP, Init. Repts.,* 164: College Station, TX (Ocean Drilling Program).

Peters, K.E., 1986. Guidelines for evaluating petroleum source rock using programmed pyrolysis. *AAPG Bull.,* 70:318–329.

Raine, J.I., Askin, R.A., Crouch, E.M., Hannah, M.J., Levy, R.H., and Wrenn, J.H., 1997. Palynomorphs. *In* Hannah, M.J., and Raine, J.I. (Eds), *Southern Ocean Late Cretaceous/Early Cenozoic Biostratigraphic Datums.* Inst. Geol. Nucl. Sci., Sci. Rep., 97:25–33.

Rider, M., 1996. *The Geological Interpretation of Well Logs* (2nd ed.): Caithness (Whittles Publishing).

Robert, C., 1987. Clay mineral associations and structural evolution of the South Atlantic: Jurassic to Eocene. *Palaeogeogr., Palaeoclimatol., Palaeoecol.,* 58:87–108.

Robert, C., and Kennett, J.P., 1992. Paleocene and Eocene kaolinite distribution in the South Atlantic and Southern Ocean: Antarctic climatic and paleoceanographic implications. *Mar. Geol.,* 103:99–110.

————, 1994. Antarctic subtropical humid episode at the Paleocene-Eocene boundary: clay mineral evidence. *Geology,* 22:211–214.

Robert, C., and Maillot, H., 1983. Paleoenvironmental significance of clay mineralogical and geochemical data, Southwest Atlantic, DSDP Legs 36 and 71. *In* Ludwig, W.J., Krasheninnikov, V.A., et al., *Init. Repts. DSDP,* 71: Washington (U.S. Govt. Printing Office), 317–343.

————, 1990. Paleoenvironments in the Weddell Sea area and Antarctic climates, as deduced from clay mineral associations and geochemical data, ODP Leg 113. *In* Barker, P.F., Kennett, J.P., et al., *Proc. ODP, Sci. Results,* 113: College Station, TX (Ocean Drilling Program), 51–70.

Robert, C., Stein, R., and Acquaviva, M., 1985. Cenozoic evolution and significance of clay associations in the New Zealand region of the South Pacific, DSDP Leg 90. *In* Kennett, J.P., von der Borch, C.C., et al., *Init. Repts. DSDP,* 90: Washington (U.S. Govt. Printing Office), 1225–1238.

Royer, J.-Y., and Rollet, N., 1997. Plate-tectonic setting of the Tasmanian region. *In* Exon, N.F., and Crawford, A.J. (Eds.), *West Tasmanian Margin and Offshore Plateaus: Geology, Tectonic and Climatic History, and Resource Potential.* Aust. J. Earth Sci., 44:543–560.

Schrag, D.P., Hampt, G., and Murray, D.W., 1996. Pore fluid constraints on the temperature and oxygen isotopic composition of the glacial ocean. *Science,* 272:1930–1932.

Stein, R., and Robert, C., 1986. Siliciclastic sediments at Sites 588, 590 and 591: Neogene and Paleogene evolution in the Southwest Pacific and Australian climate. *In* Kennett, J.P., von der Borch, C.C., et al., *Init. Repts. DSDP,* 90 (Pt. 2): Washington (U.S. Govt. Printing Office), 1437–1455.

Stott, L.D., and Kennett, J.P., 1990. Antarctic Paleogene planktonic foraminifer biostratigraphy: ODP Leg 113, Sites 689 and 690. *In* Barker, P.F., Kennett, J.P., et al., *Proc. ODP, Sci. Results,* 113: College Station, TX (Ocean Drilling Program), 549–569.

Thomas, E., Zahn, R., and Diester-Hauss, L., 1995. The Eocene-Oligocene transition at high latitudes: benthic foraminifera, sediments and stable isotopes. *Eos,* 76 Suppl.:S187.

Weaver, C.E., 1989. *Clays, Muds, and Shales:* New York (Elsevier).

Willcox, J.B., Baillie, P., Exon, N.F., Lee, C.-S., and Thomas, B., 1989. The geology of western Tasmania and its continental margin—with particular reference to petroleum potential. *Bureau Mineral Resources (Australia),* Record 1989/13:27.

Williams, G.L., Brinkhuis, H., et al., 1998. Cenozoic dinocyst events. *In* De Gracianski, et al. (Eds.), *Sequence Stratigraphy of European Basins.* Spec. Publ.—Soc. Econ. Paleontol. Mineral., 60.

Wilson, G.J., 1988. Paleocene and Eocene dinoflagellate cysts from Waipawa, Hawkes Bay, New Zealand. *N.Z. Geol. Surv. Paleontol. Bull.,* 57.

Wrenn, J.H., and Hart, G.F., 1988. Paleogene dinoflagellate cyst biostratigraphy of Seymour Island, Antarctica. *Mem.—Geol. Soc. Am.,* 169:321–447.

Zachos, J.C., Quinn, R.M., and Salamy, K., 1996. High resolution ($10^4$ yr) deep-sea foraminiferal stable isotope records of the Eocene-Oligocene climate transition. *Paleoceanography,* 11:251–266.

**Figure F1.** Postdrilling interpretation for local seismic profile AGSO 202-5, across Site 1171, showing broad ages and lithostratigraphic units. The site is in a north-south strike-slip basin on the central block of the South Tasman Rise (STR), just west of the northward continuation of the Balleny Fracture Zone (and the eastern block of the Rise). It is the only STR site that penetrated the Paleocene, and the relationships at the Paleocene/Eocene unconformity indicate that the fracture zone's last movement was in the late Paleocene. This probably represents the time of initial spreading to the south. Note the thick Eocene, the very thin Oligocene, and the thin Pliocene–Pleistocene sections at this site.
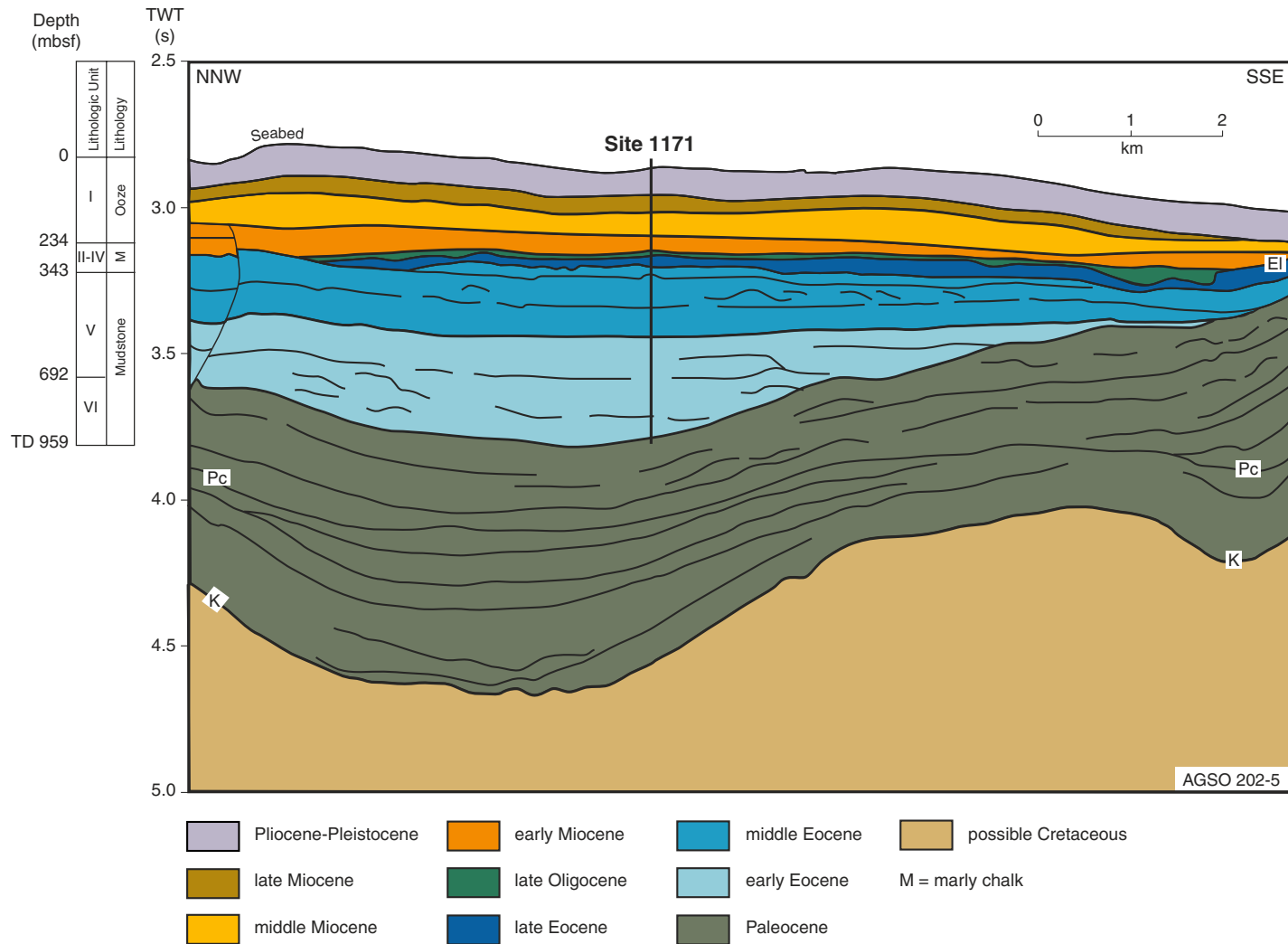
**Figure F2.** Regional cross section through time across Site 1171, southwest from the Tasman Sea oceanic crust, across two blocks of the South Tasman Rise, and southwest to the abyssal plain (formerly the Antarctic margin), based on seismic profile *Sonne* SO36-52 and other geological information. Note the pre-existing Tasman Sea crust and major continental blocks in the latest Cretaceous to Paleocene; the Eocene development of more fault blocks by fast north-south strike-slip motion between Australia and Antarctica, the departure of Antarctica by north-south spreading, and the emplacement of oceanic crust; and the Oligocene collapse of the southwestern margin. BFZ = Balleny Fracture Zone.
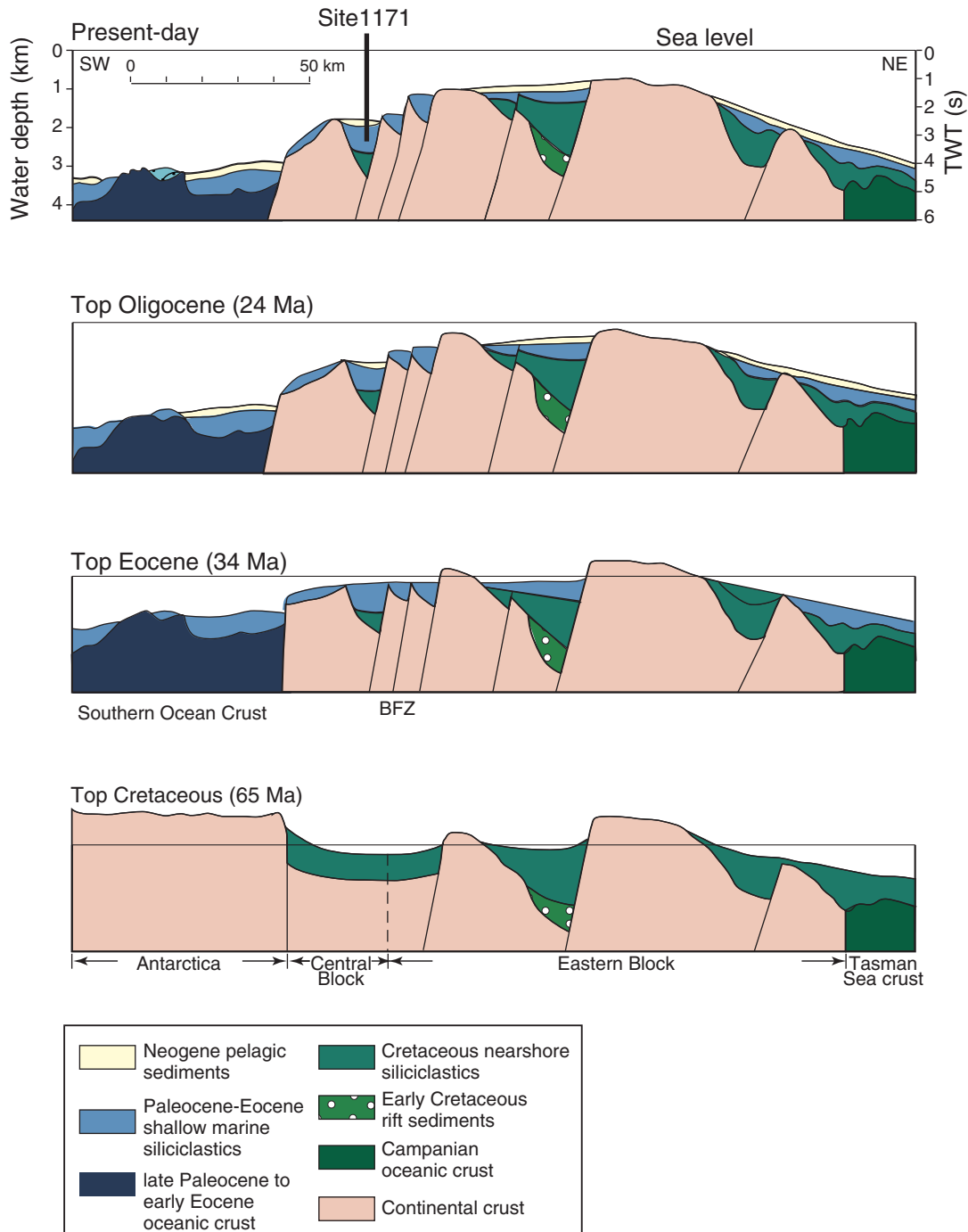
**Figure F3.** Portion of seismic profile AGSO 202-05 through Site 1171. SP = shotpoint.
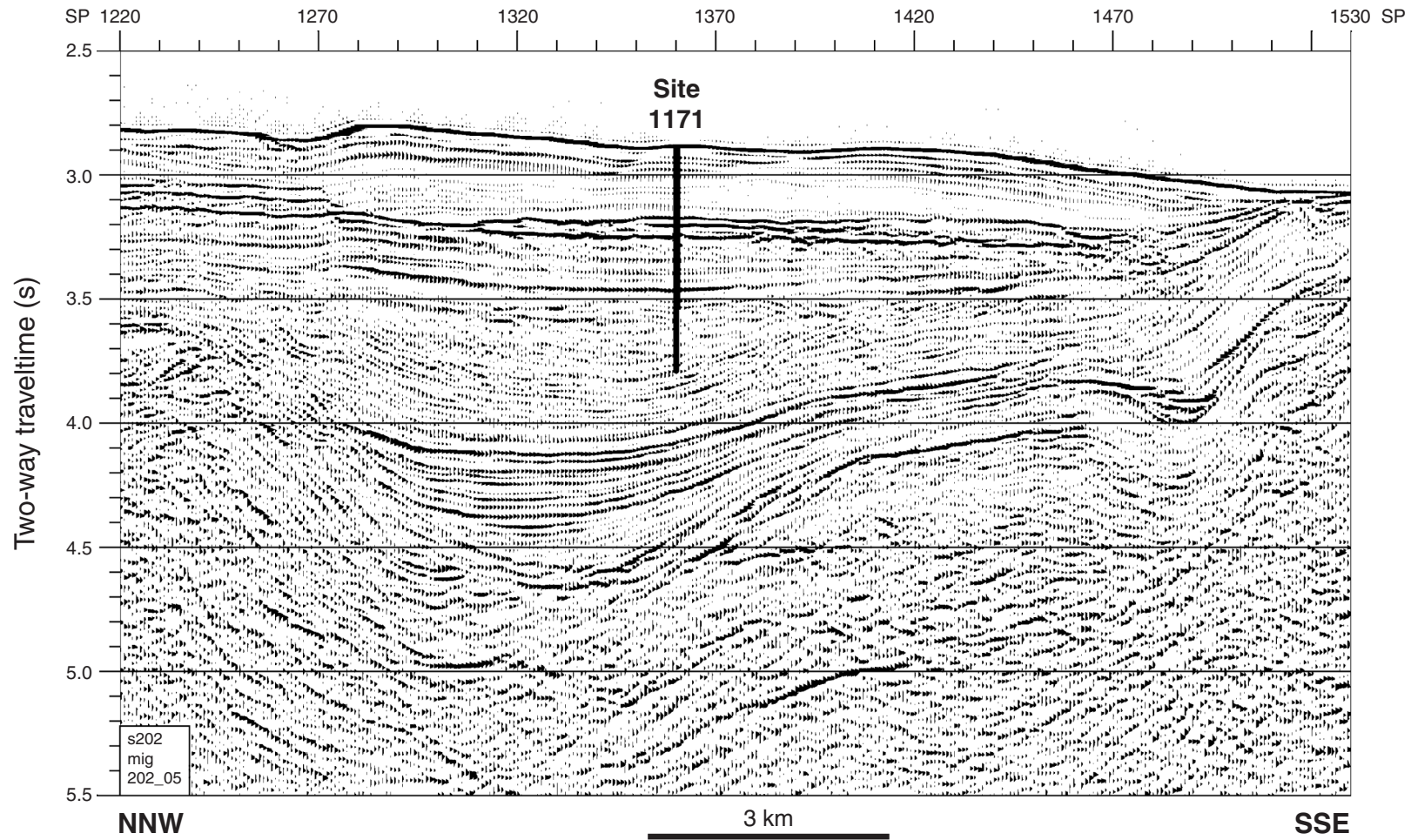
**Figure F4.** Summary of Site 1171 lithostratigraphic units, biozonation, carbonate content, and physical properties (see "Physical Properties," p. 54). TD = total depth.
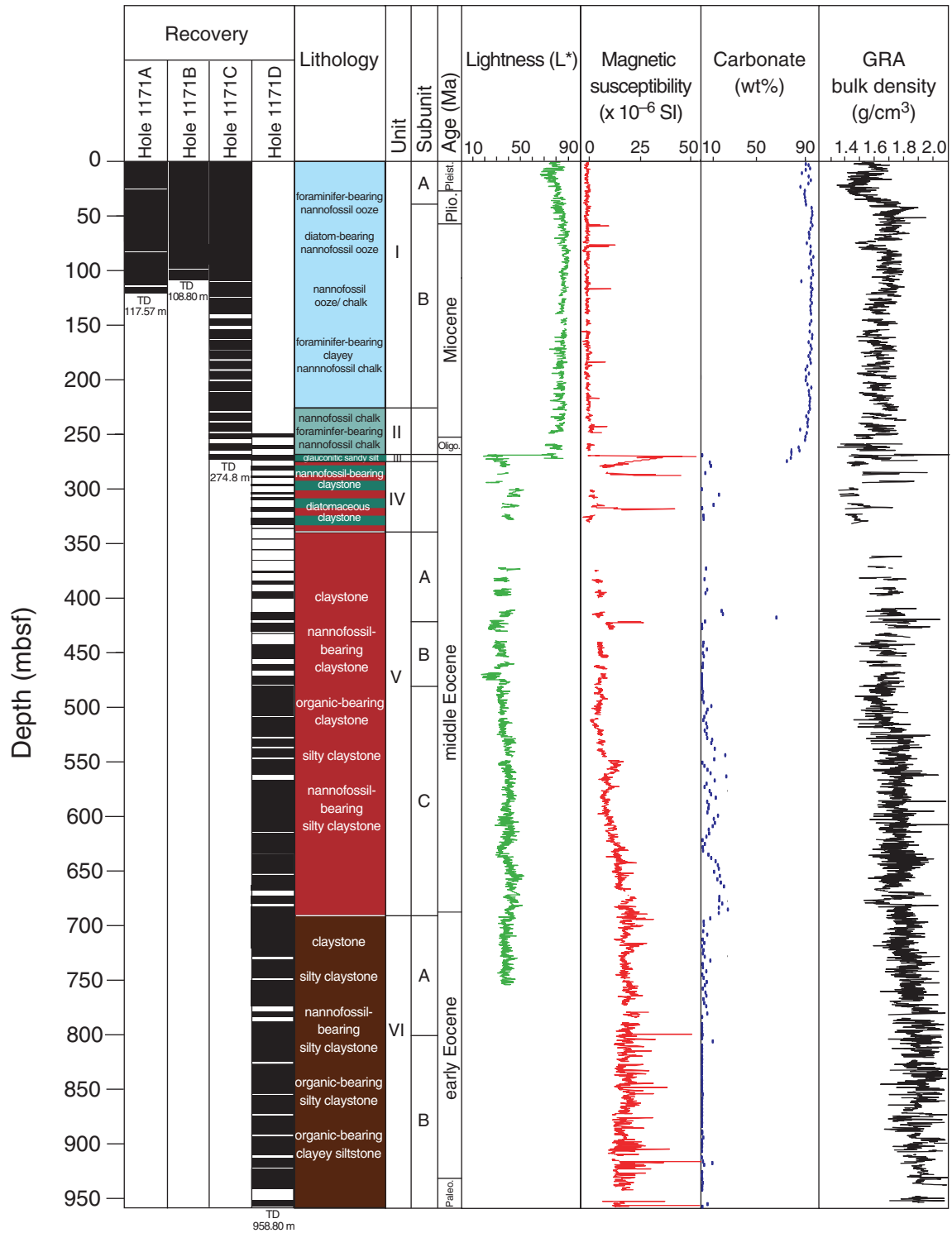
**Figure F5.** Detailed summary of Site 1171 for the 0–958.8 mbsf interval. Drilling disturbance ratings for the relatively soft sediments of Hole 1171C consist of F0 (undisturbed sediments with only minor "edge effect"), F1 (upward bowing of up to approximately one-third core width [~2.2 cm of vertical stretching] or 30° inclination of sediments), F2 (extreme upward bowing of approximately one-third to one-half core width [~2.2–3.4 cm of vertical stretching] or 30°–60° inclination of sediments), F3 (onset of minor flow-in beyond that of F2), and F4 (massive flow-in). Drilling disturbance ratings for Hole 1171D are based on the percentage of "coherent" (i.e., nondrill slurry and not highly fractured/brecciated) sediment along the core center and consist of B0 (>98%), B1 (97%–91%), B2 (90%–85%), B3 (84%–70%), and B4 (<70%) (see **"Drilling Disturbance,"** p. 6, in "Lithostratigraphy" in the "Explanatory Notes" chapter). Physical properties data should be considered suspect for F3 and B3 and not considered robust for F4 and B4 categories. TD = total depth. (**Figure shown on next page.** Continued on next five pages.)

**Figure F5 (continued). A.** Summary for the 0–200 mbsf interval.

**A**

**Figure F5 (continued). B.** Summary for the 200–400 mbsf interval.
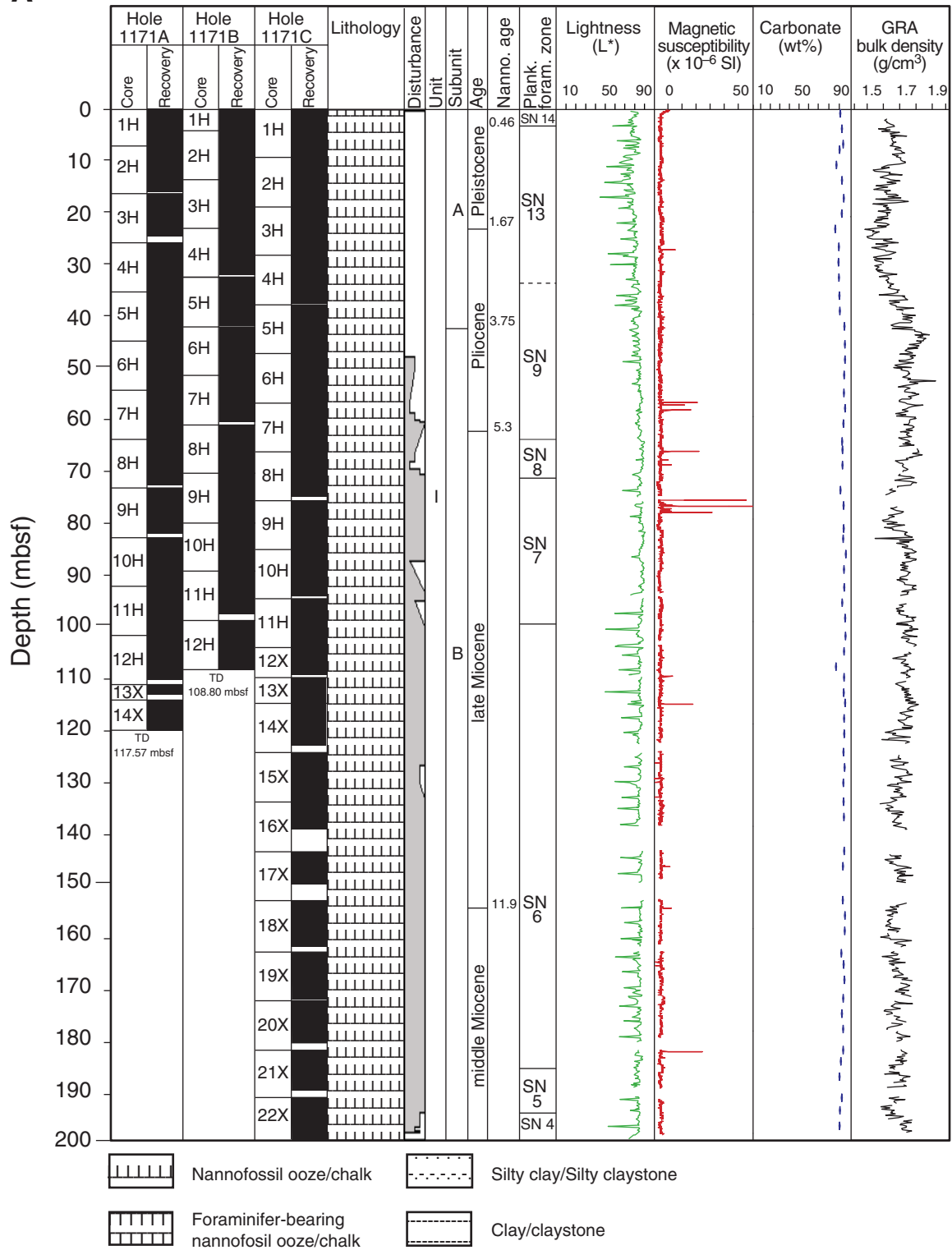
**Figure F5 (continued). C.** Summary for the 400–600 mbsf interval.
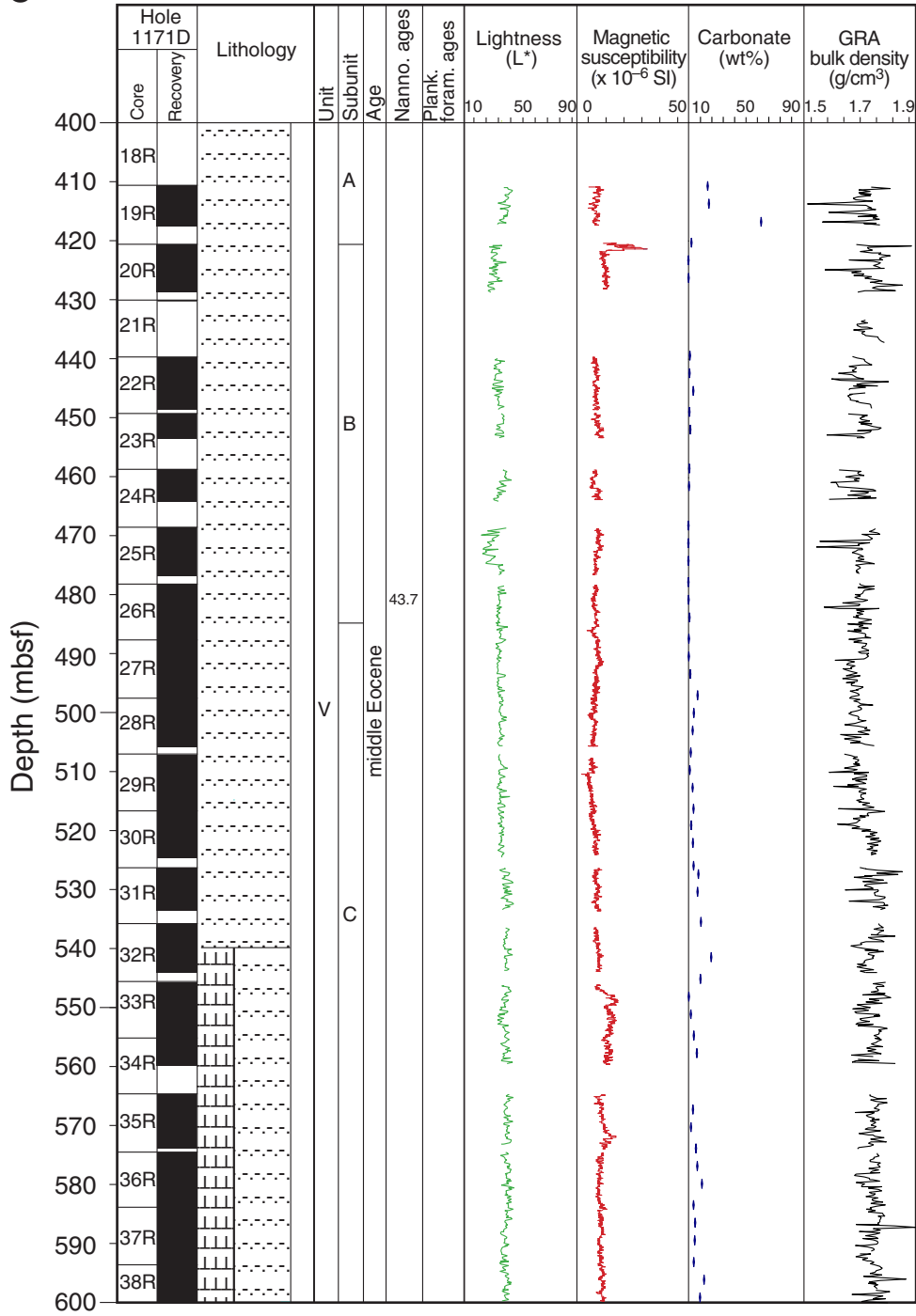
**Figure F5 (continued). D.** Summary for the 600–800 mbsf interval.
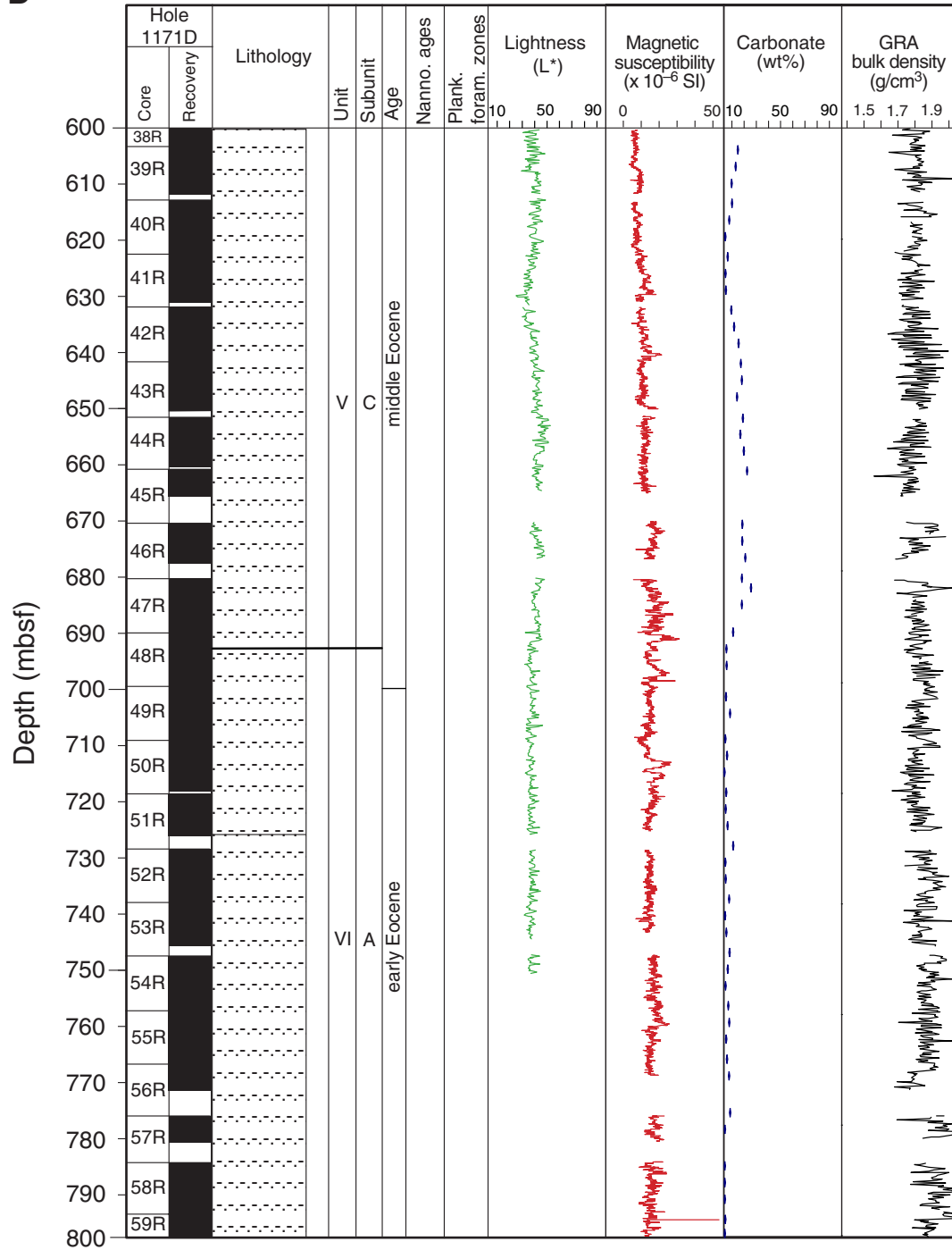
**Figure F5 (continued). E.** Summary for the 800–958.8 mbsf interval.
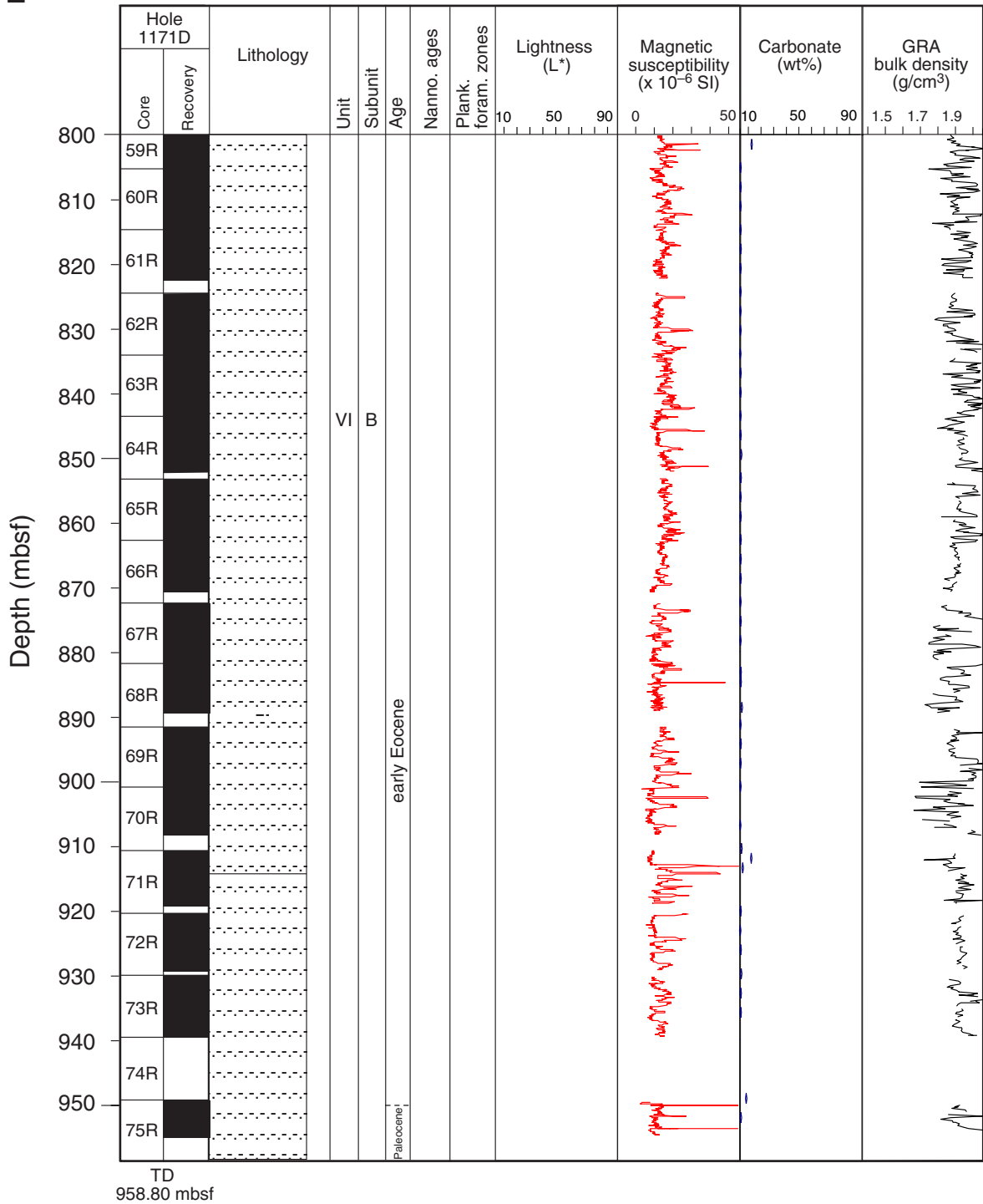
**Figure F6.** Lithologic composition of Holes 1171A, 1171B, and 1171C sediments based on smear-slide analysis.
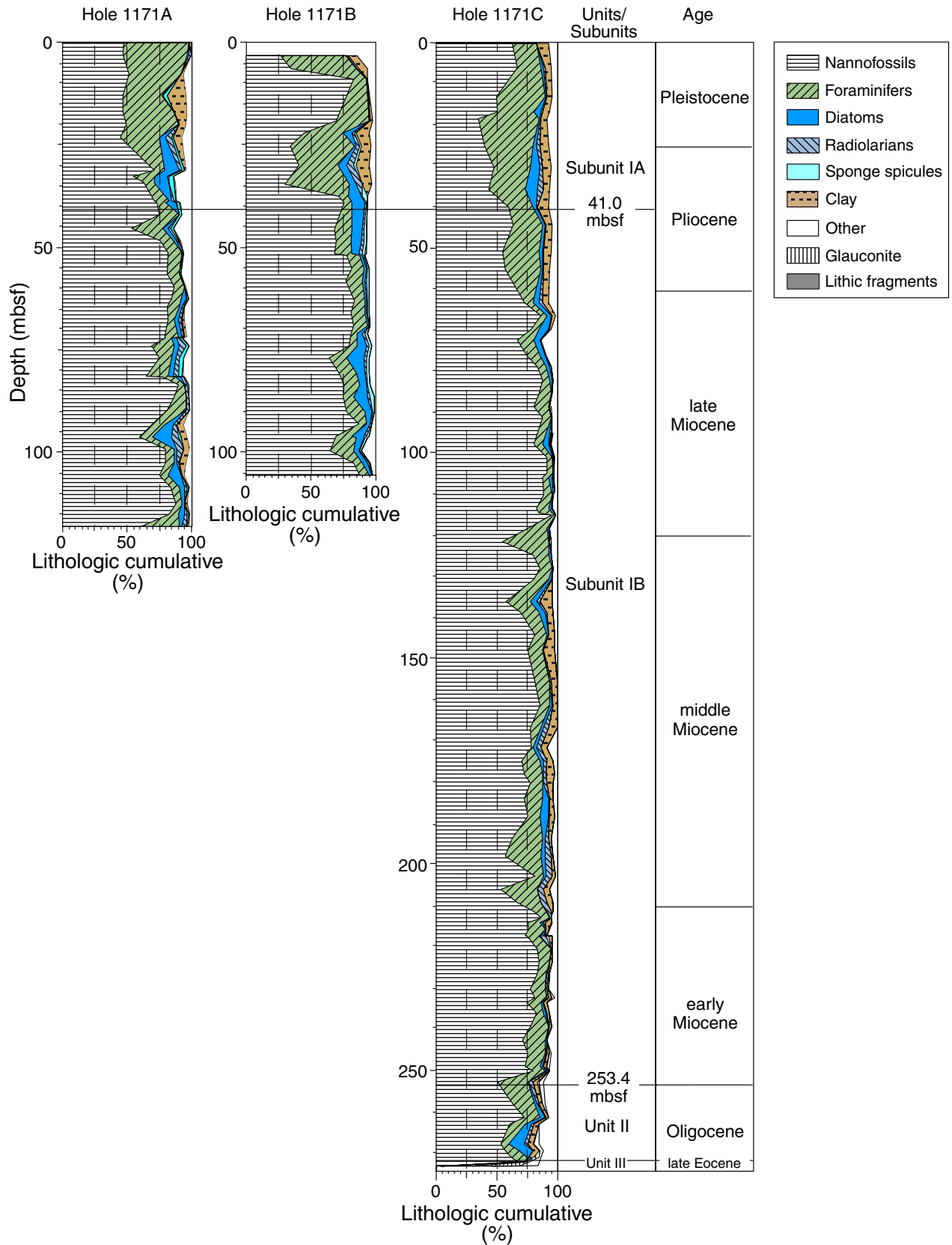
**Figure F7.** Close-up photograph of the striking lithologic contact between Units II and III at 272.8 mbsf (interval 189-1171D-3R-3, 18–32 cm). This corresponds to the Eocene–Oligocene transition and marks a significant change in the depositional environment, from pelagic carbonate-dominated deposition during the Oligocene to the predominantly siliciclastic deposition during the late Eocene.
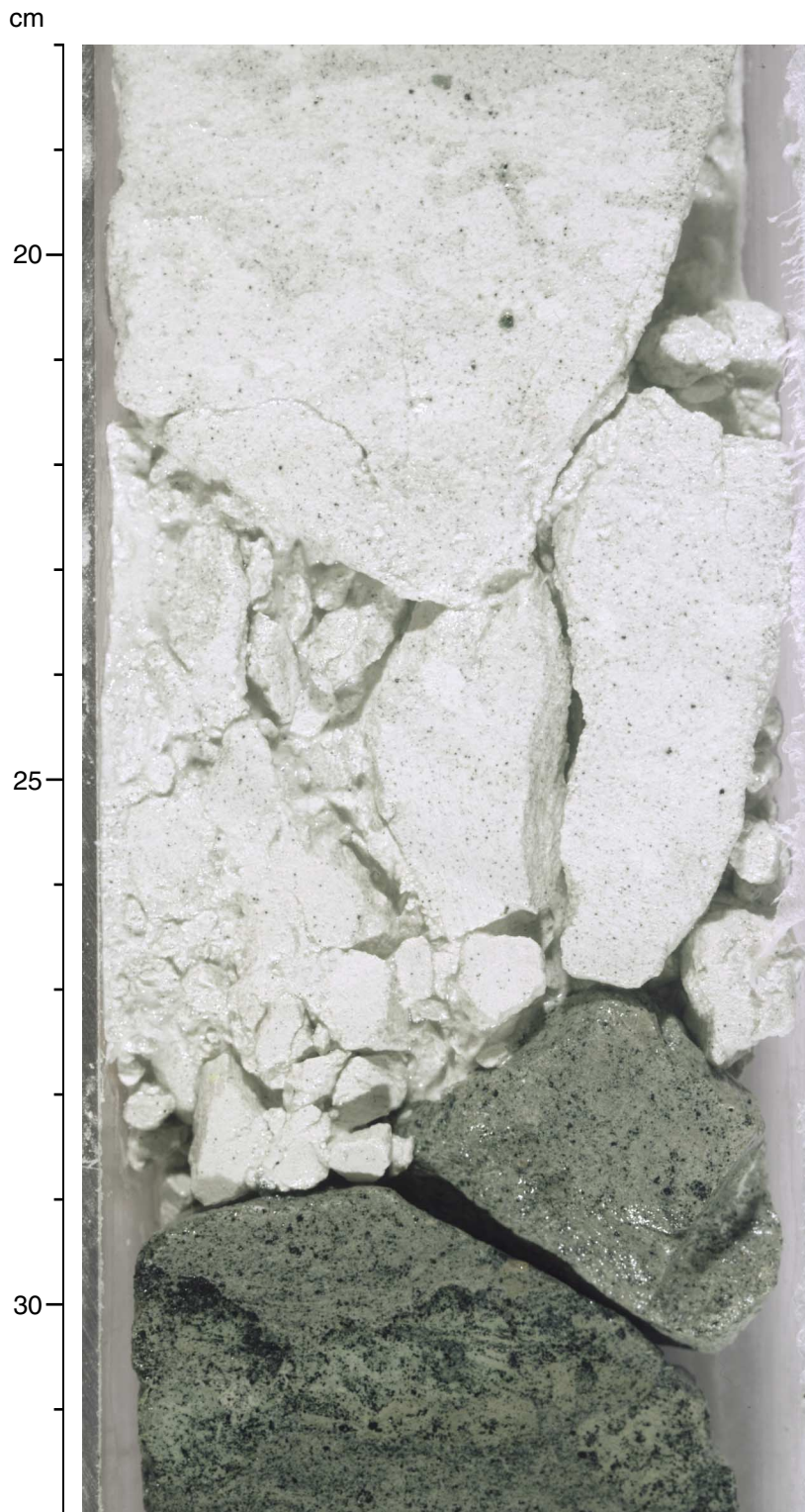
**Figure F8.** Lithologic composition of Hole 1171D sediments based on smear-slide analysis. In the lower portion of Subunit VIB, the organic matter percentage from the smear-slide data is generally overestimated, compared to measured total organic carbon (see **"Organic Geochemistry,"** p. 44). (**Figure shown on next page.**)

**Figure F8 (continued). (Caption shown on previous page.)**
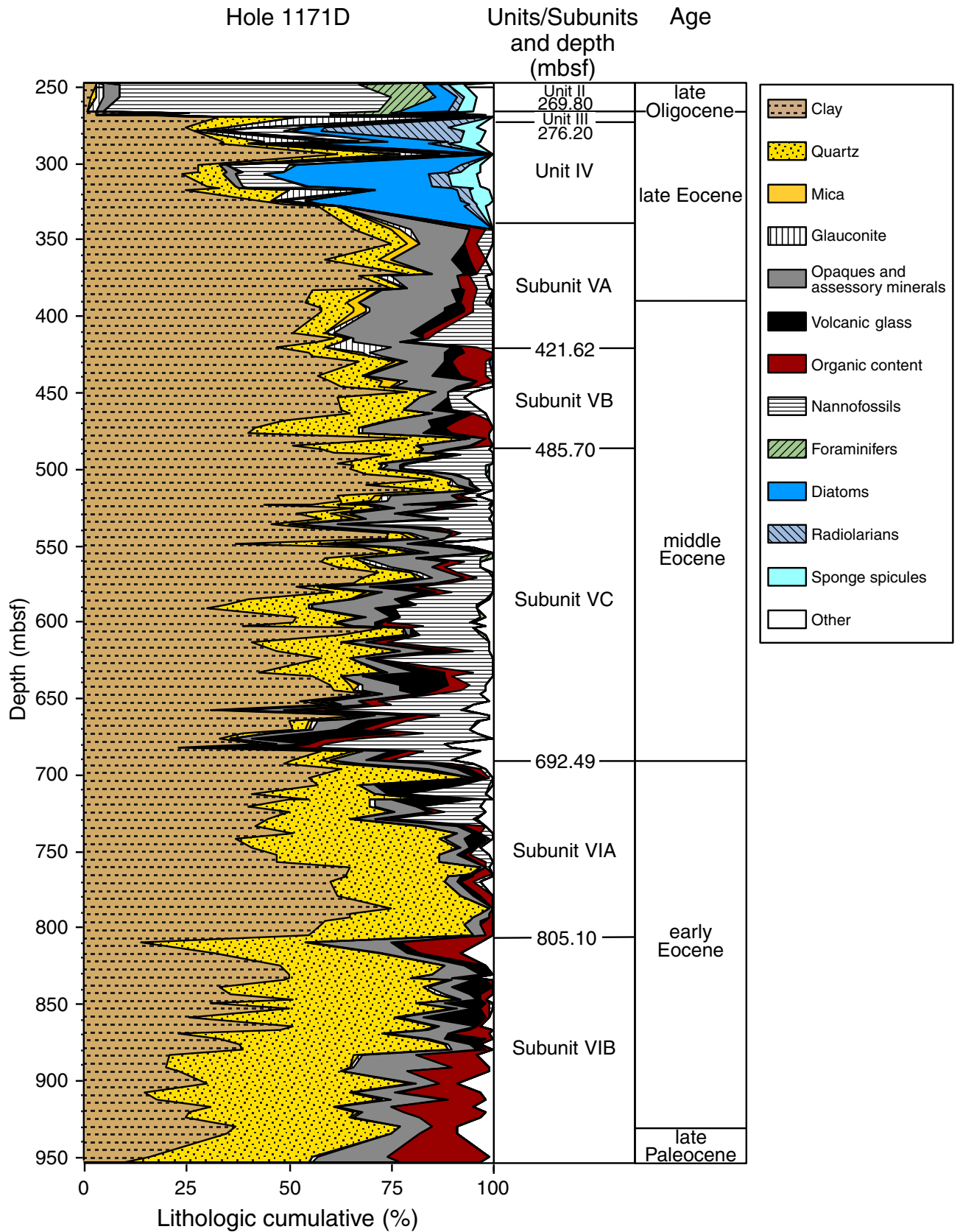
**Figure F9.** Comparison of chromaticity coordinate a* (green and red) from the photospectrometer to carbonate content (yellow shaded area) (see "Organic Geochemistry," p. 44) and nannofossil percent (gray circles) for 400–500 mbsf. The comparison shows good agreement in increasing greenness and nannofossil and carbonate percentages. This relationship suggests chromaticity coordinate a* can be used as an indicator of nannofossil abundance. These changes in abundance may be caused by oscillations in the ventilation of the depositional environment. Although smear slides tend to overestimate nannofossil abundances (compared to carbonate content), both data sets show general good agreement.
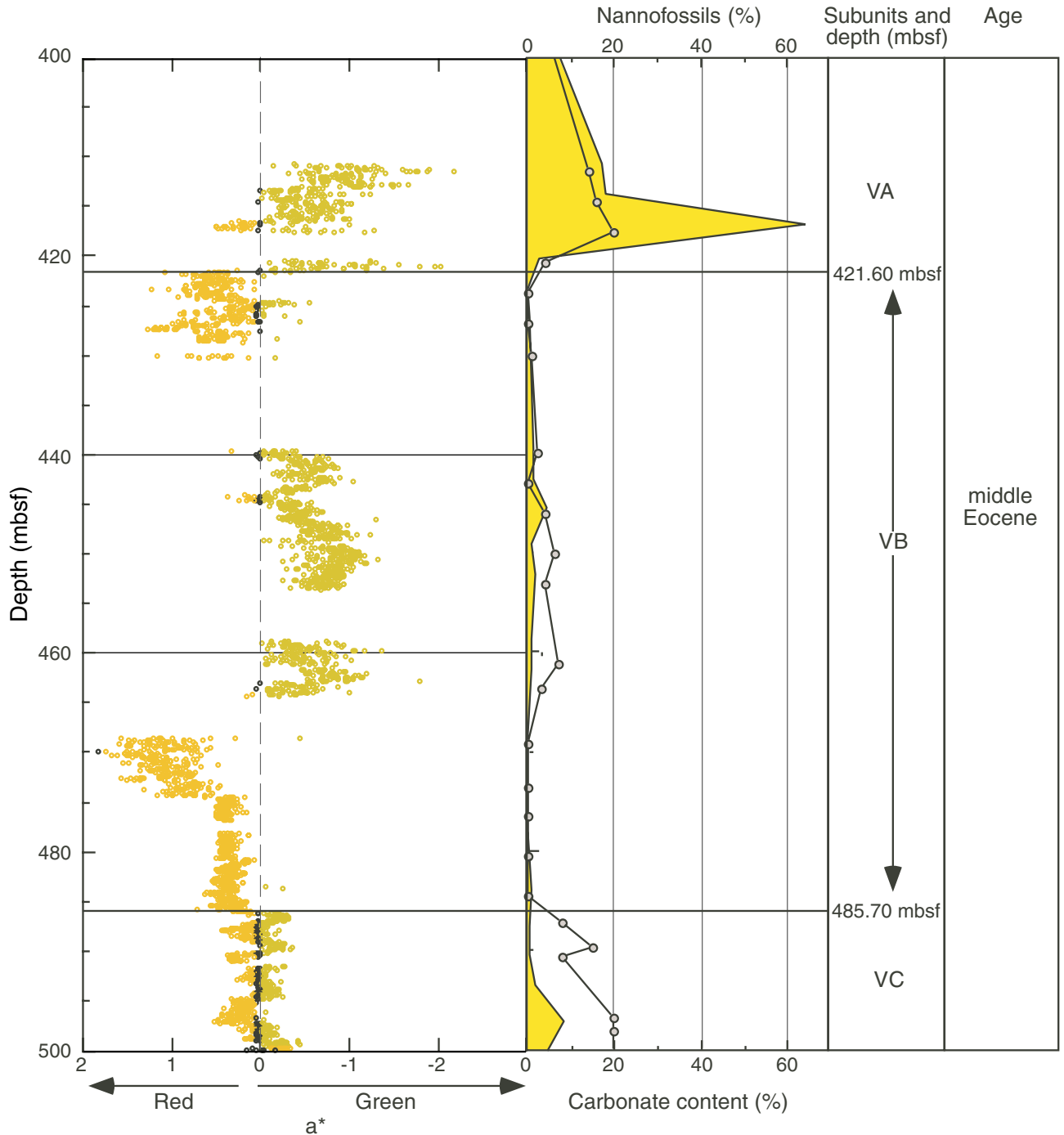
**Figure F10.** Comparison of chromaticity coordinate a* (green and red) from the photospectrometer to carbonate content (yellow shaded area) (see "Organic Geochemistry," p. 44) and the nannofossil percent (gray circles) for 450–700 mbsf. Nannofossil percentages generally increase downsection in Subunit VC. Chromaticity coordinate a* indicates an increase in green and a decrease in red downsection and may be an indicator of changes in nannofossil and perhaps organic carbon contents. The two green peaks correspond to glauconitic intervals that are above the sequence boundaries at 550 and 572 mbsf.
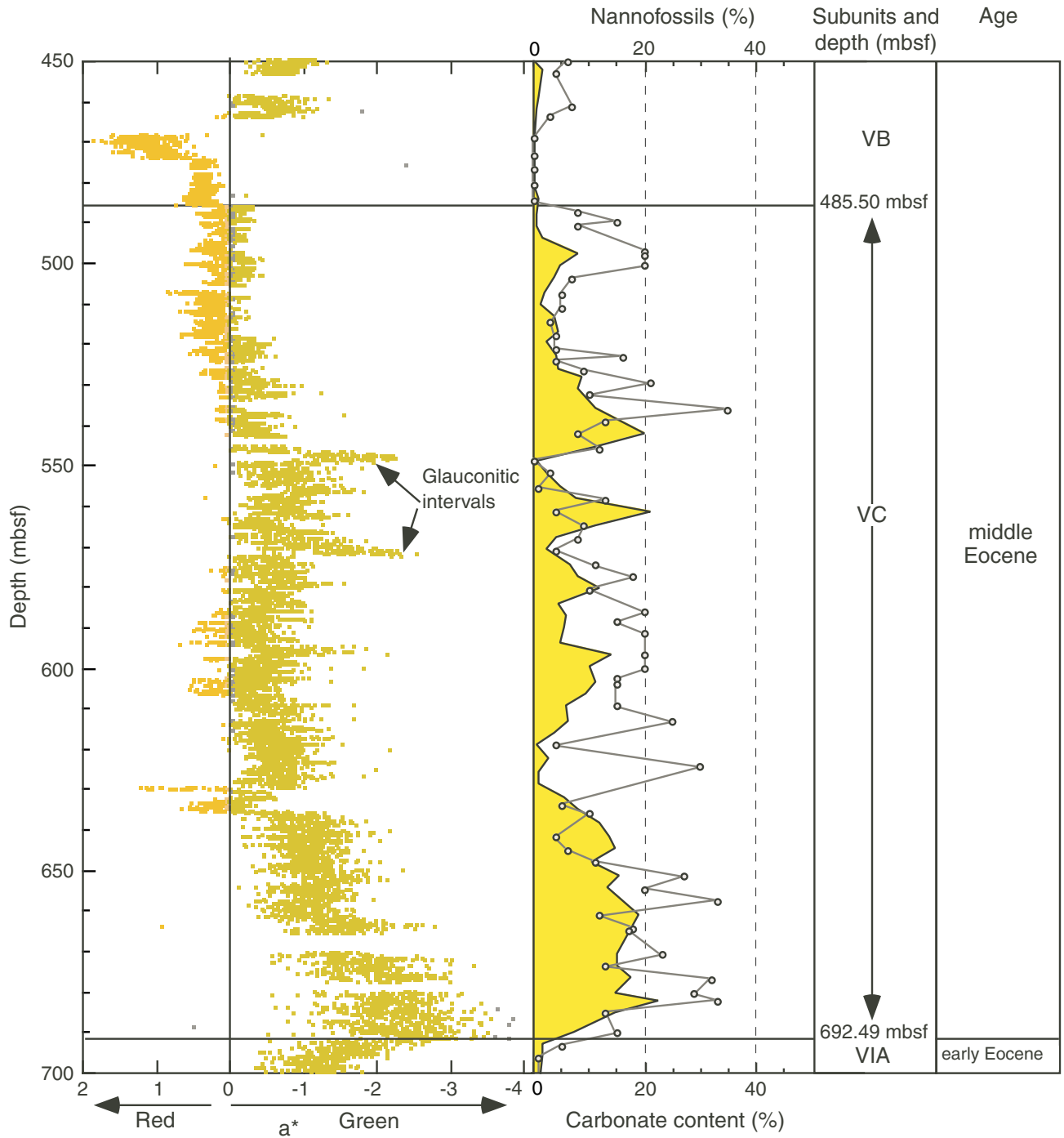
**Figure F11.** Close-up photograph of a sharp bioturbated surface at 548.90 mbsf. Glauconite-filled burrows are found below the contact (interval 189-1171D-33R-3, 5–45 cm).
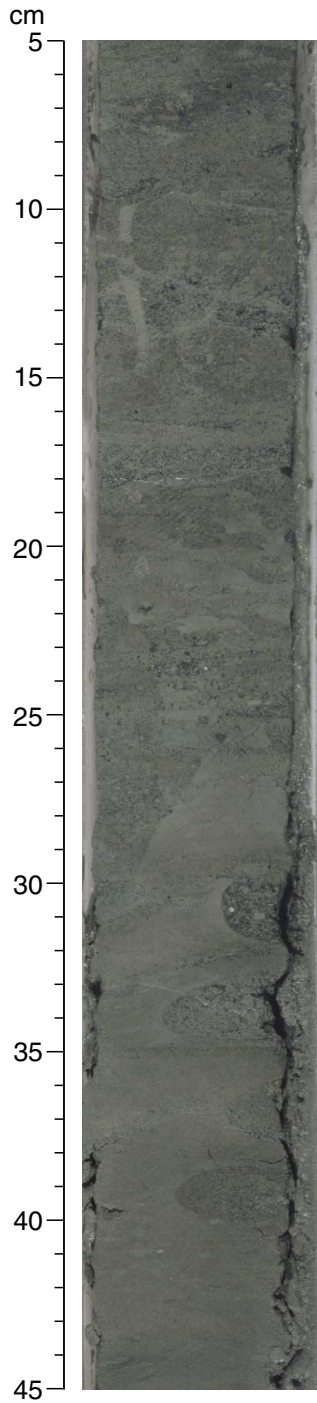
**Figure F12.** Close-up photograph of a thin (6 cm) black sediment bed containing abundant shells at 579.47 mbsf. Sediments below are generally more massive and lighter in color than those above (interval 189-1171D-36R-4, 55–75 cm).
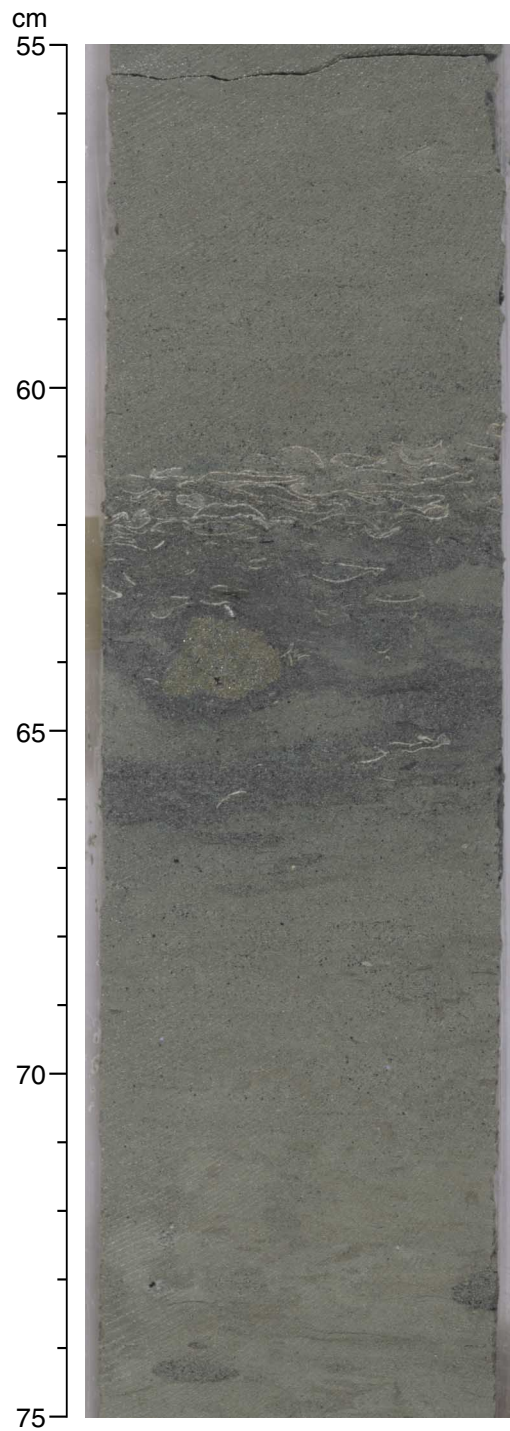
**Figure F13.** Close-up photograph of microfaults offsetting bioturbated claystone (interval 189-1171D-54R-5, 45–55 cm).
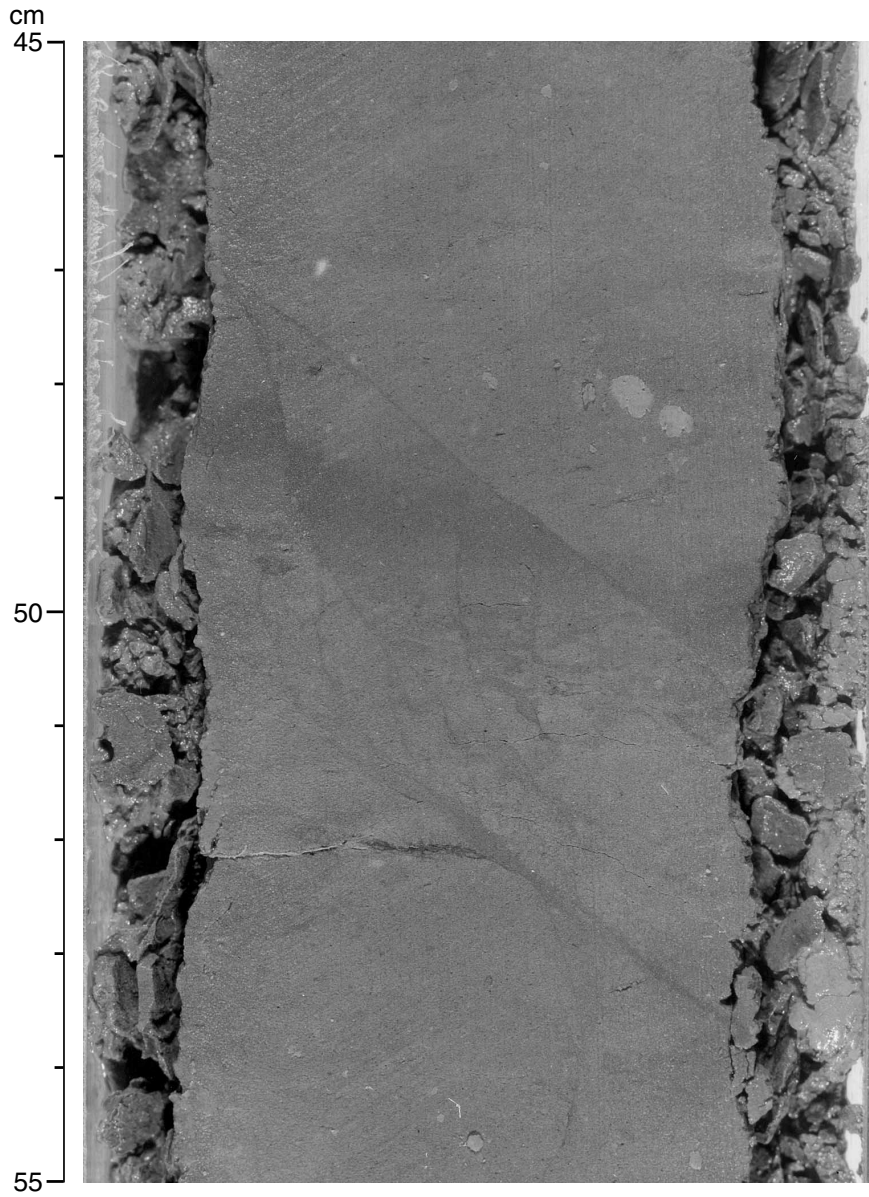
**Figure F14.** Close-up photograph of a distinct surface that separates a massive very dark grayish brown (2.5Y 3/2) clay above from a glauconitic dark grayish brown (2.5Y 4/2) clay below (interval 189-1171D-71R-2, 50–94 cm).
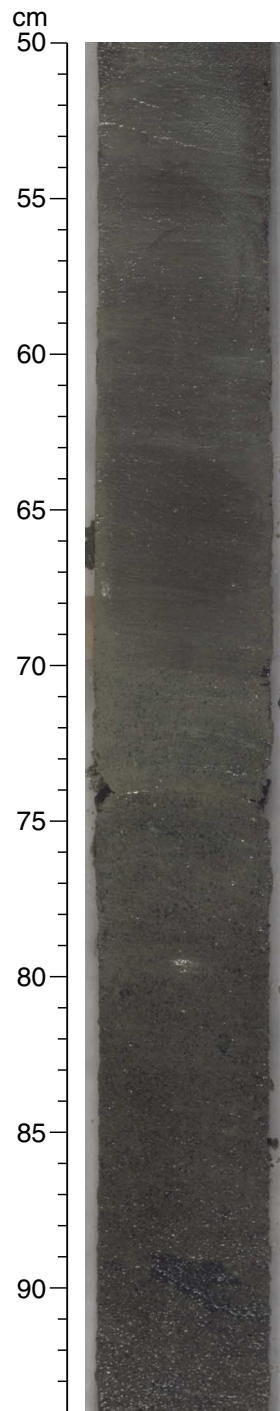
**Figure F15.** Close-up photograph of the surface of Section 189-1171D-71R-2. Glauconite decreases downward toward Section 189-1171D-71R-3, where a lighter colored extensively bioturbated layer is found (interval 189-1171D-71R-3, 40–80 cm).
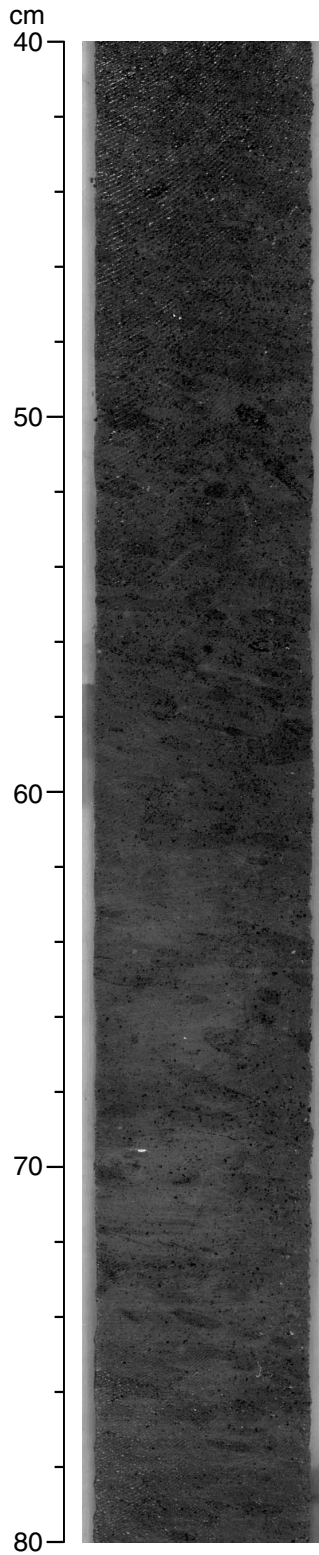
**Figure F16.** Close-up photograph of a distinct well-defined surface at the base of Subunit VA (421.62 mbsf), which is interpreted as a basal sequence boundary (interval 189-1171-20R-1, 100–130 cm).
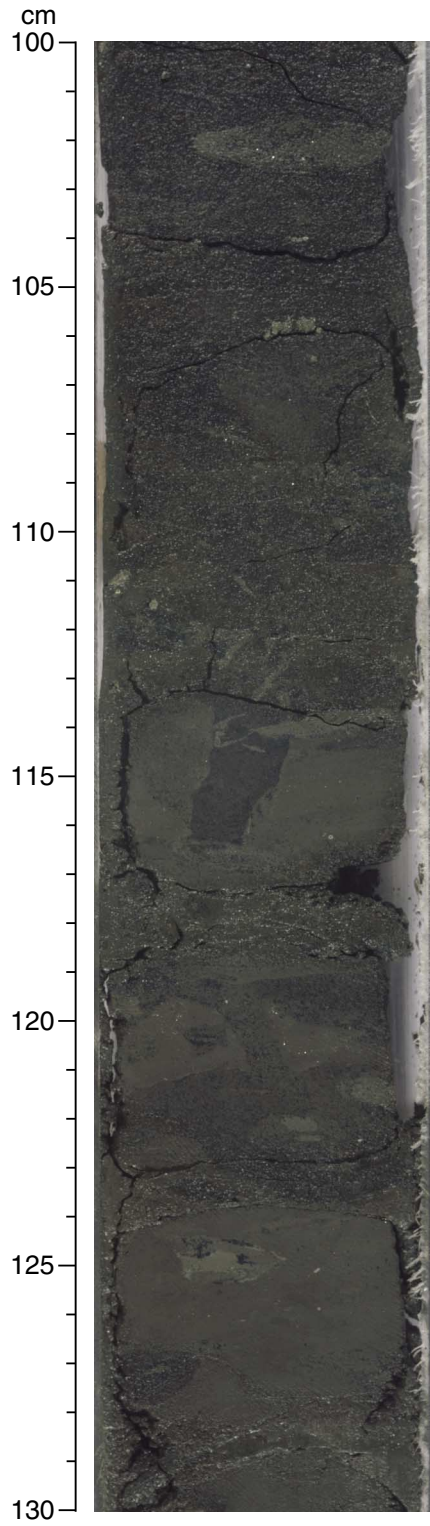
**Figure F17.** Close-up photograph of a sharp, although heavily bioturbated and irregular, surface. This surface (at 548.90 mbsf) is interpreted as a sequence boundary in Subunit VC (interval 189-1171D-33R-3, 5–45 cm).
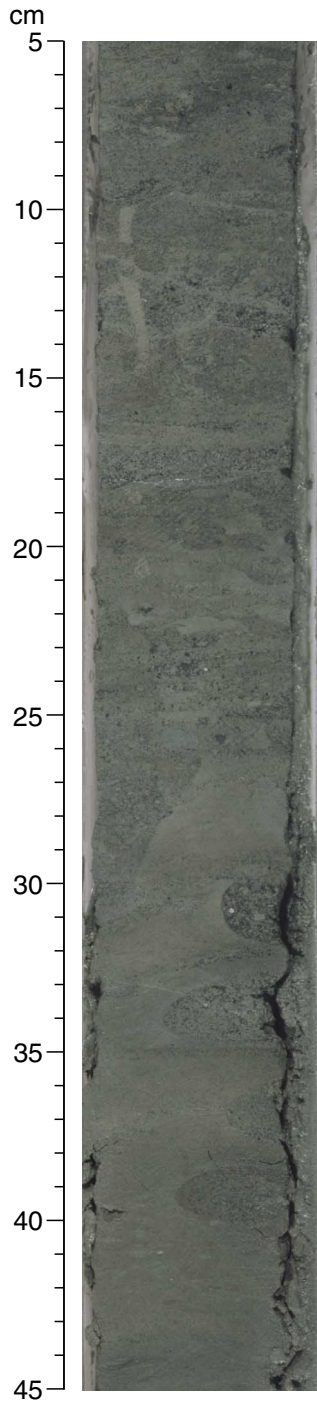
**Figure F18.** Clay mineral units of Site 1171, eastern South Tasman Rise.
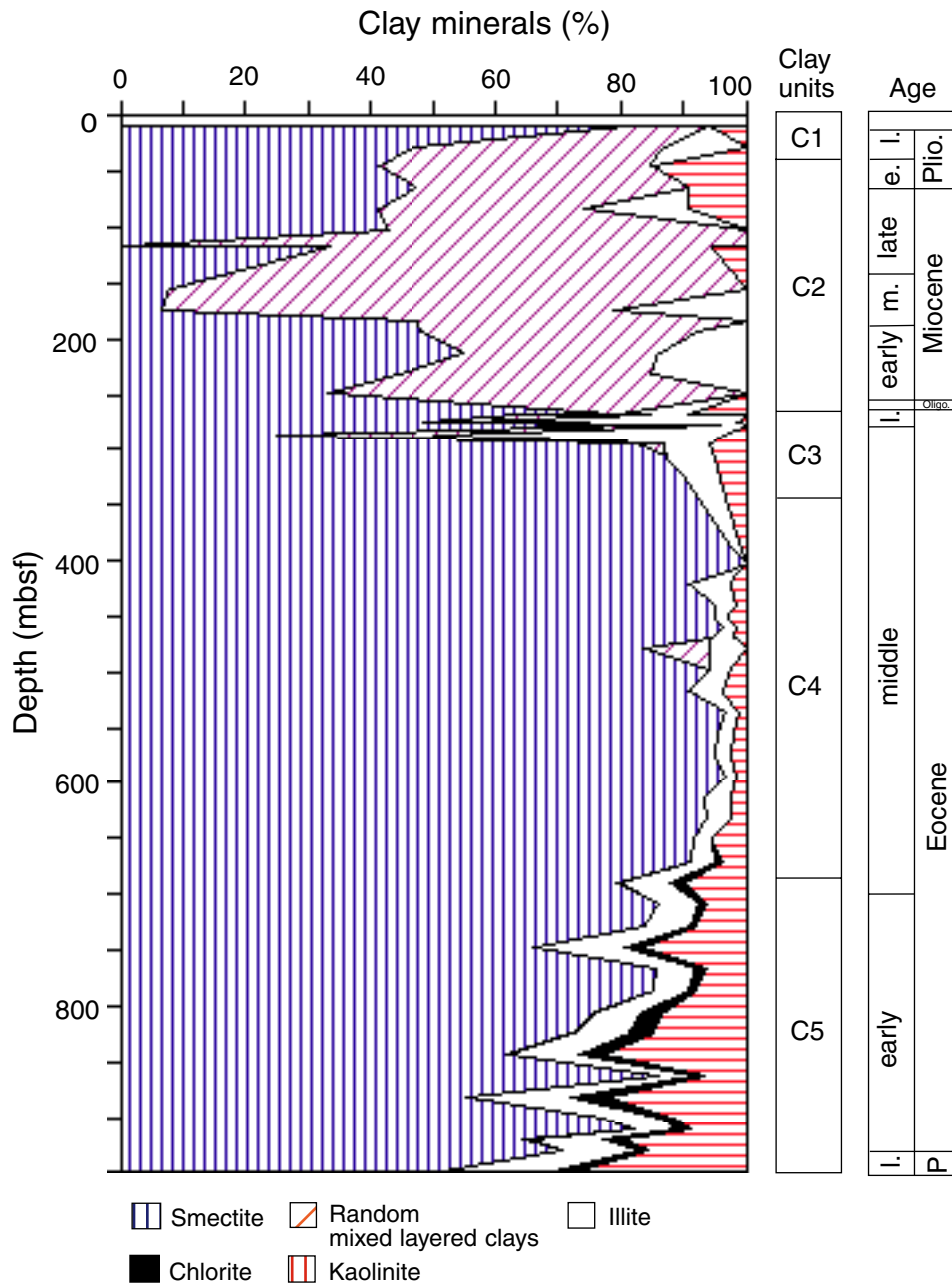
**Figure F19.** Site 1171 age-depth plot and linear sedimentation rates. The age-depth plot uses multiple microfossil and paleomagnetic datums for Site 1171. Events used are listed in Table T13, p. 154, and in "Paleomagnetism," p. 40. Below 281 mcd, there is a constant offset of +9.78 m from mbsf. For mbsf values of all datums, see Table T13, p. 154.
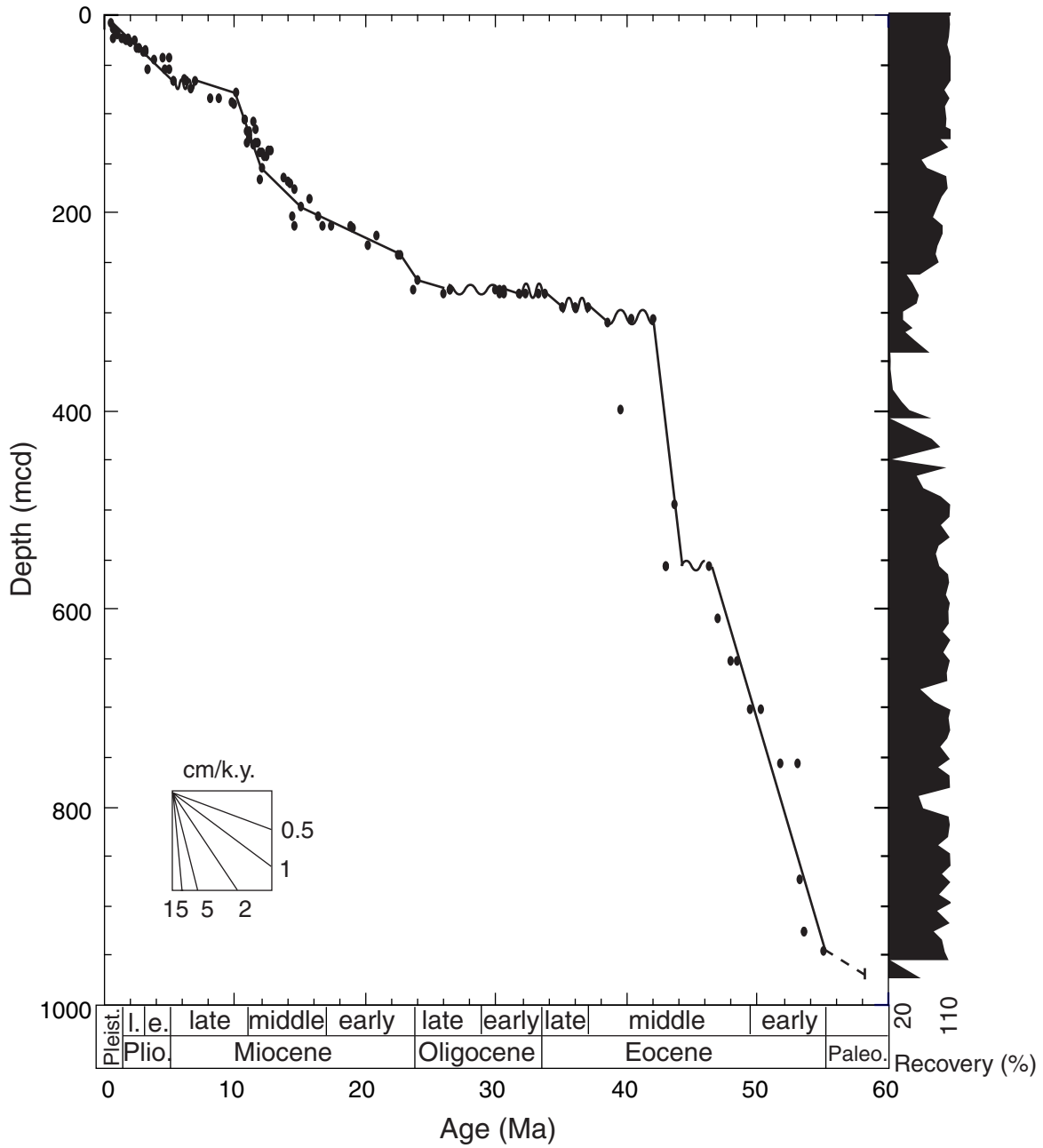
**Figure F20.** Combined biostratigraphic interpretation of the Eocene–Oligocene transition at Site 1171. The events are placed at mean depth of event occurrence. Data from Hole 1171C and 1171D have been used and listed by their mean composite depth (mcd). N = nannofossil, F = planktonic foraminifer, sm = small, R = radiolarian, D = diatom, and C = dinocyst. TD = total depth.
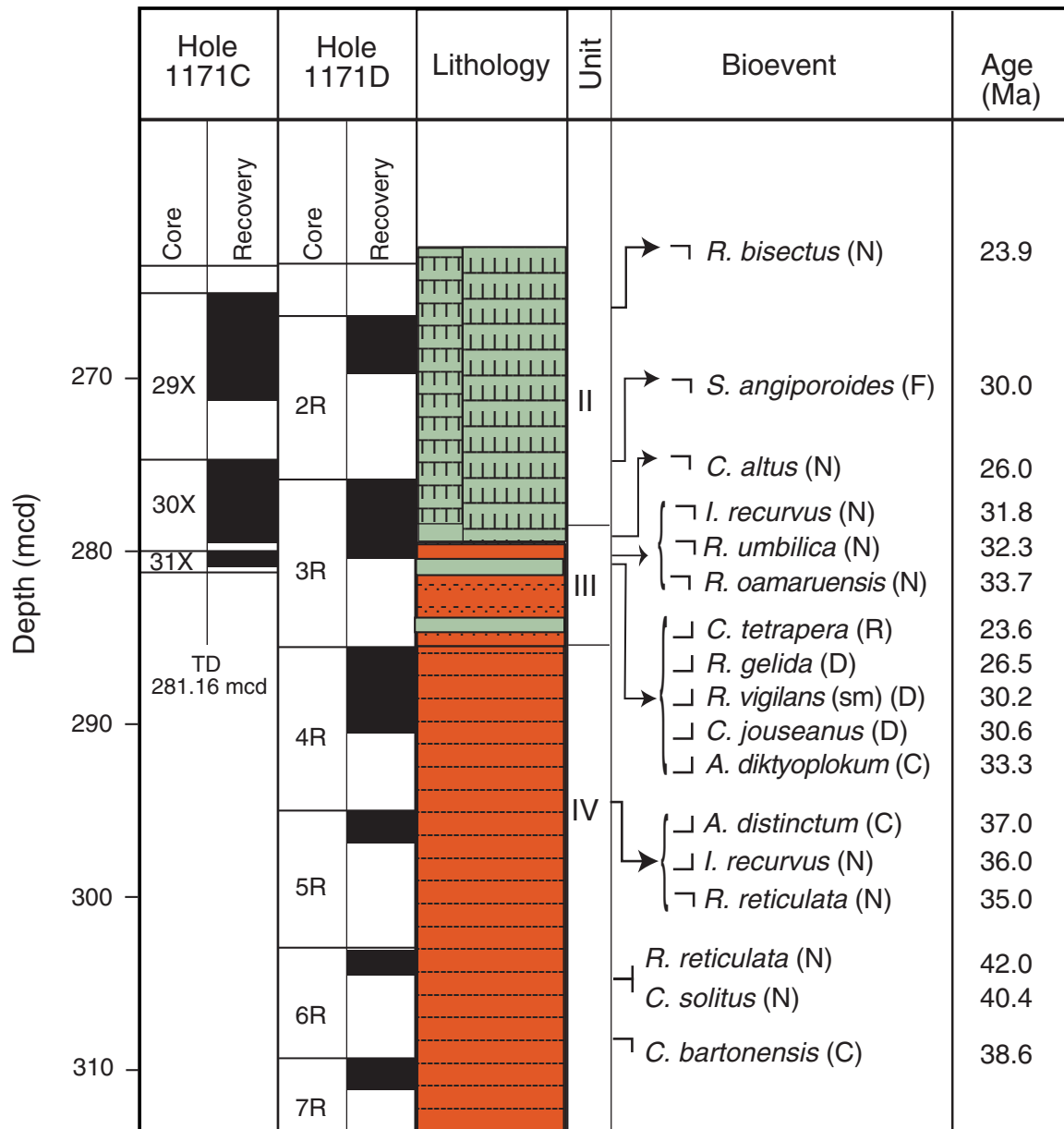
**Figure F21.** Correlations between Holes 1171A, 1171B, and 1171C based on calcareous nannofossil bio-stratigraphy.
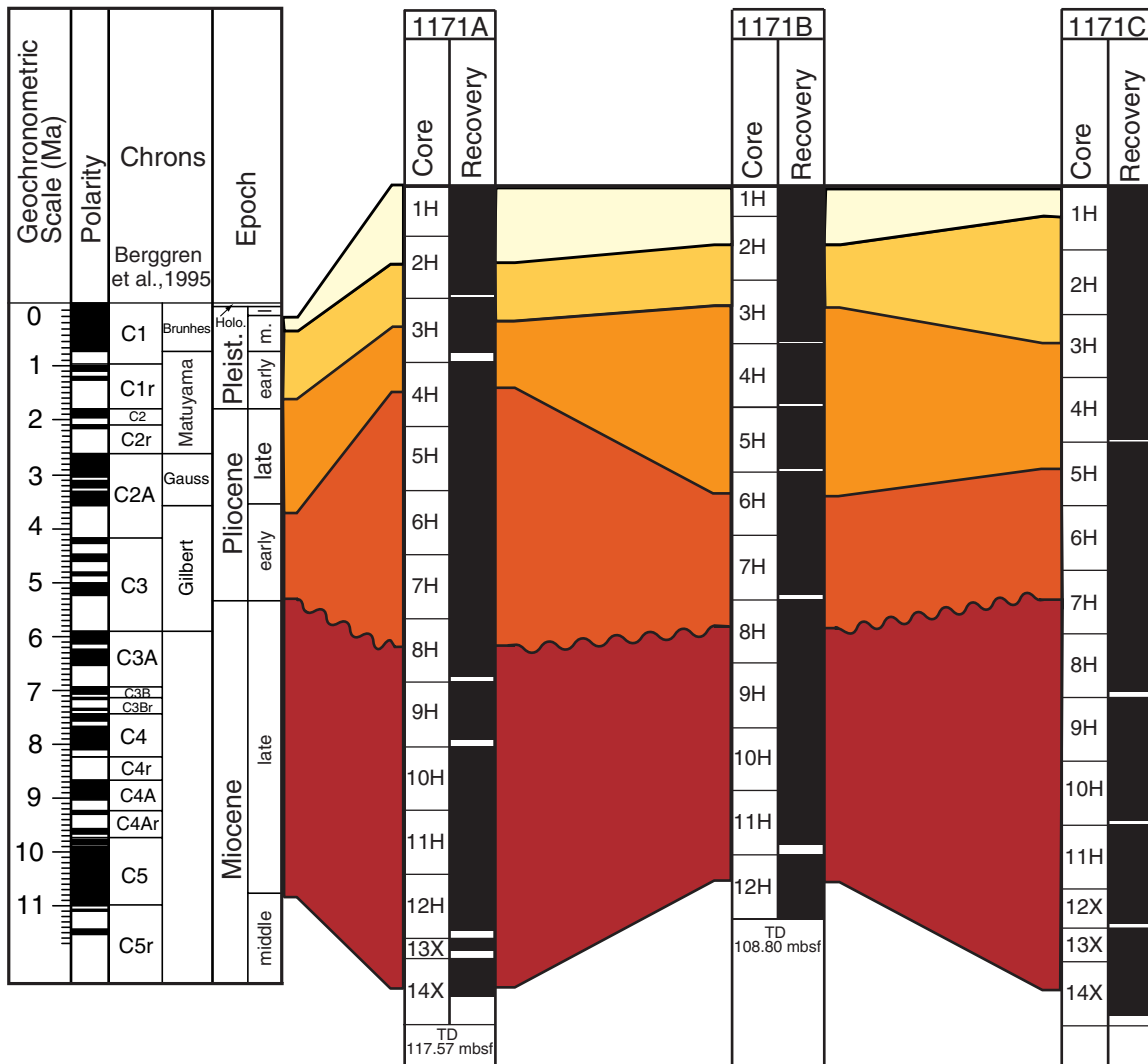
**Figure F22.** Benthic foraminiferal assemblages and inferred paleodepths.
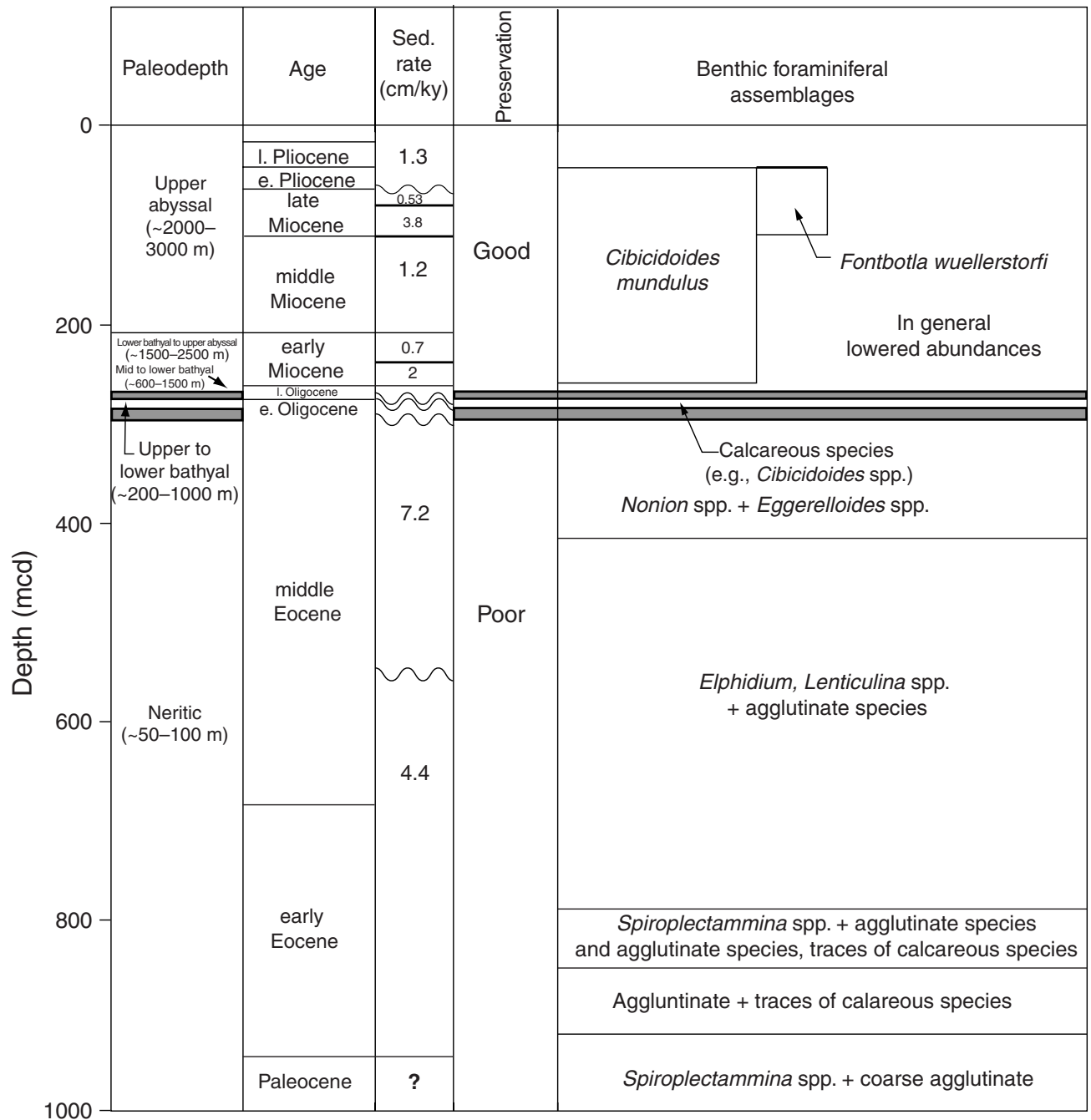
**Figure F23.** The age-depth plot and linear sedimentation rates for the composite sections for the last 12 m.y. at Site 1171. The age-depth plot uses microfossil and paleomagnetic datums through the composite sections at Site 1171. The events used are listed in Table **T13,** p. 154, and in **"Paleomagnetism,"** p. 40.
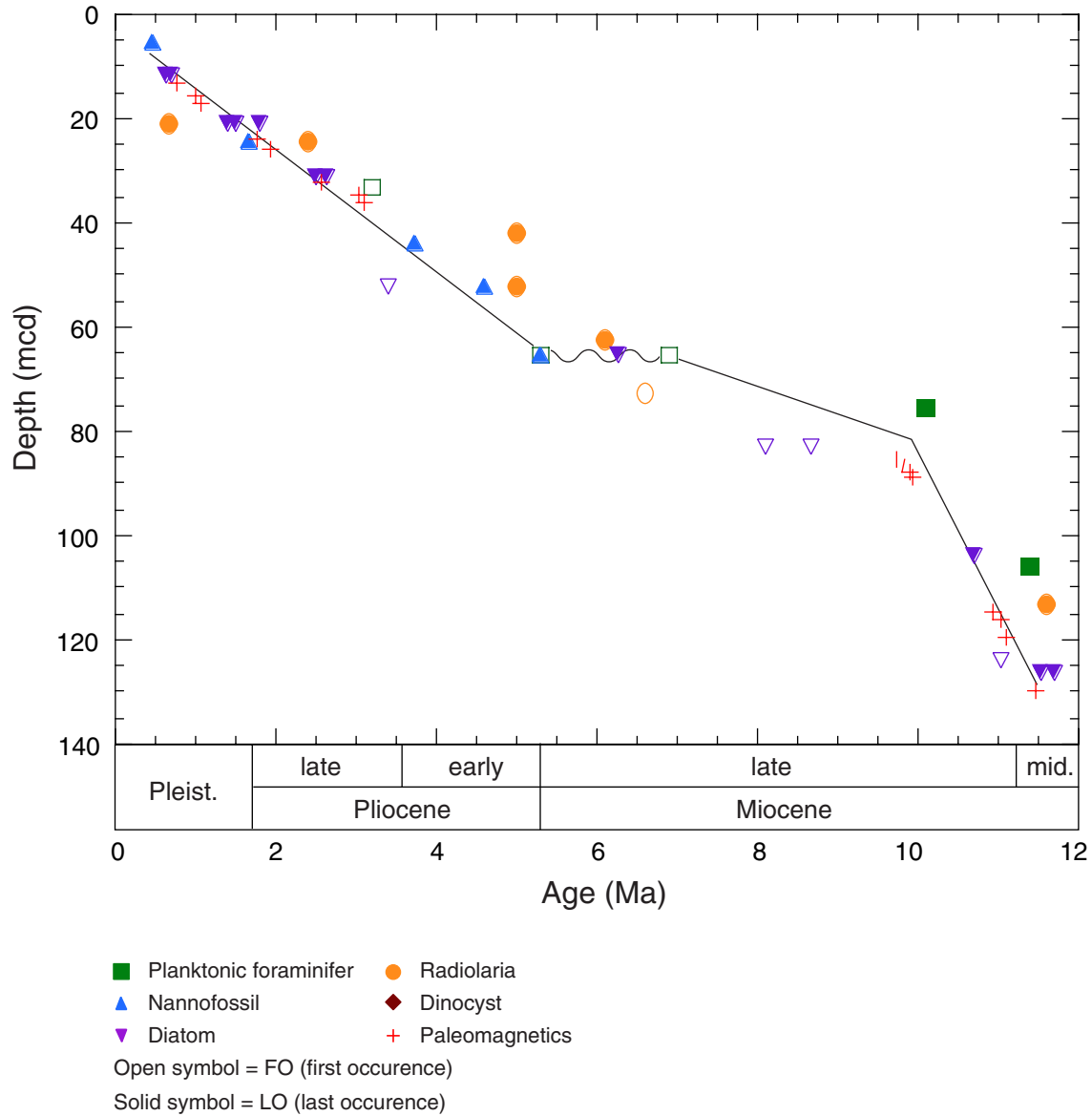
**Figure F24.** Long-core measurements from 0 to 120 mbsf for Holes 1171A, 1171B, and 1171C showing inclination, intensity, and interpreted magnetostratigraphy.

**Figure F25.** Long-core measurements from 120 to 240 mbsf for Hole 1171C showing inclination, intensity, and interpreted magnetostratigraphy.

**Figure F26.** Long-core measurements from 400 to 950 mbsf for Hole 1170D showing inclination, intensity, and interpreted magnetostratigraphy.
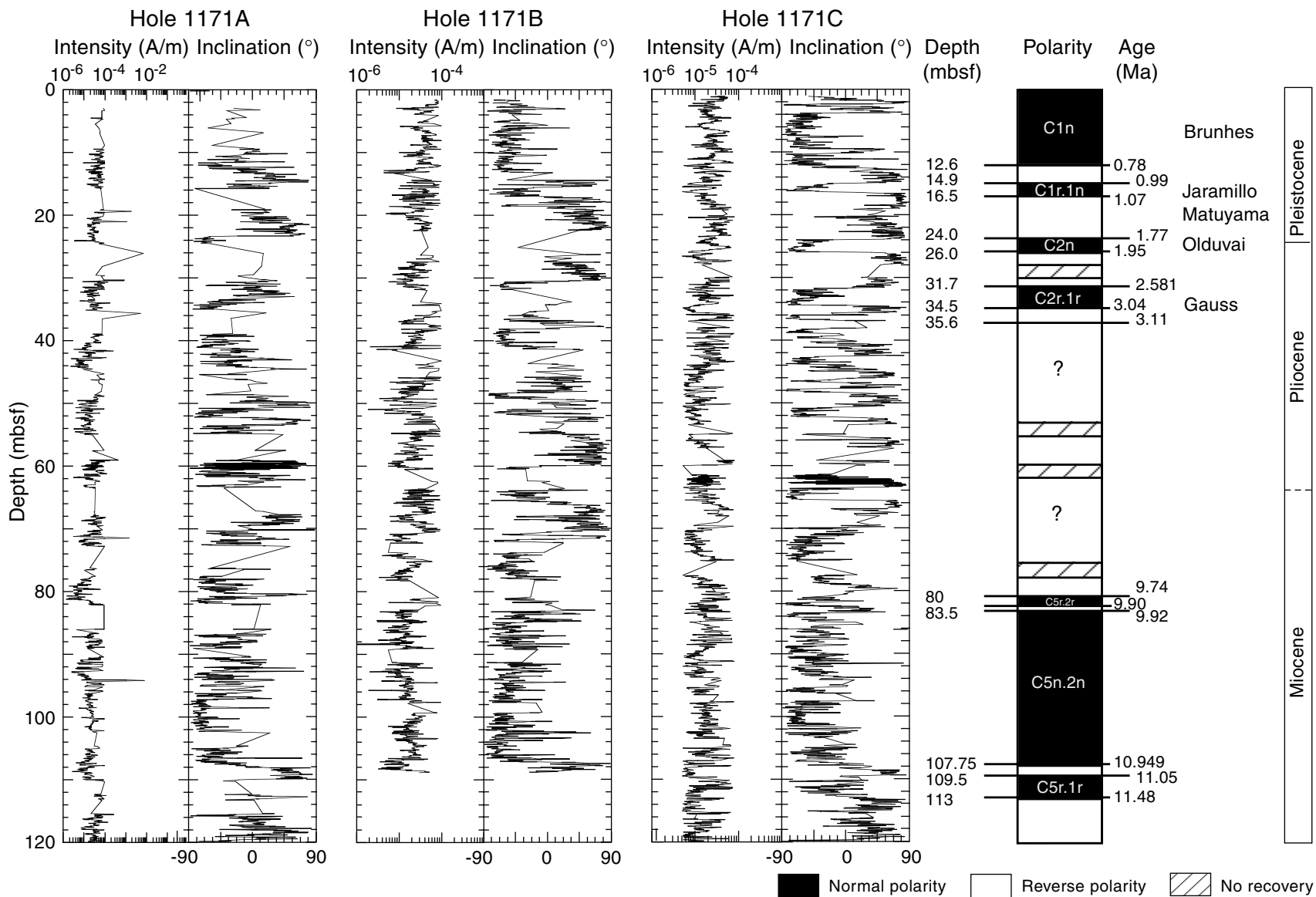
**Figure F27.** Variation of magnetic properties in Holes 1171A, 1171C, and 1171D. **A.** Variation of intensity of ARM and IRM. **B.** Variation of normalized IRM demagnetized between 0 and 20 mT and normalized IRM acquired between 200 and 500 mT.
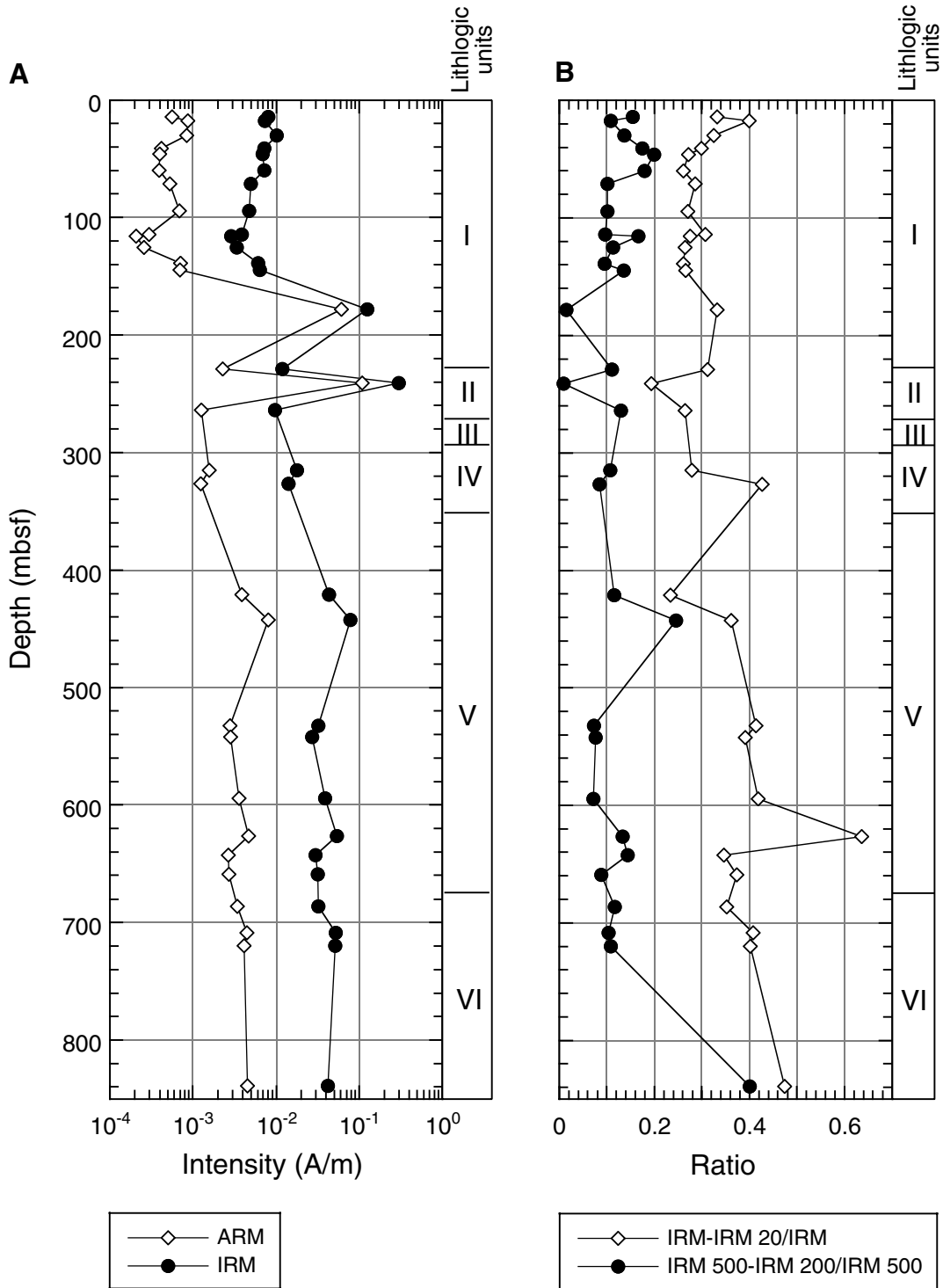
**Figure F28**. Age-depth relationship from paleomagnetic data for the Neogene for Hole 1171C.
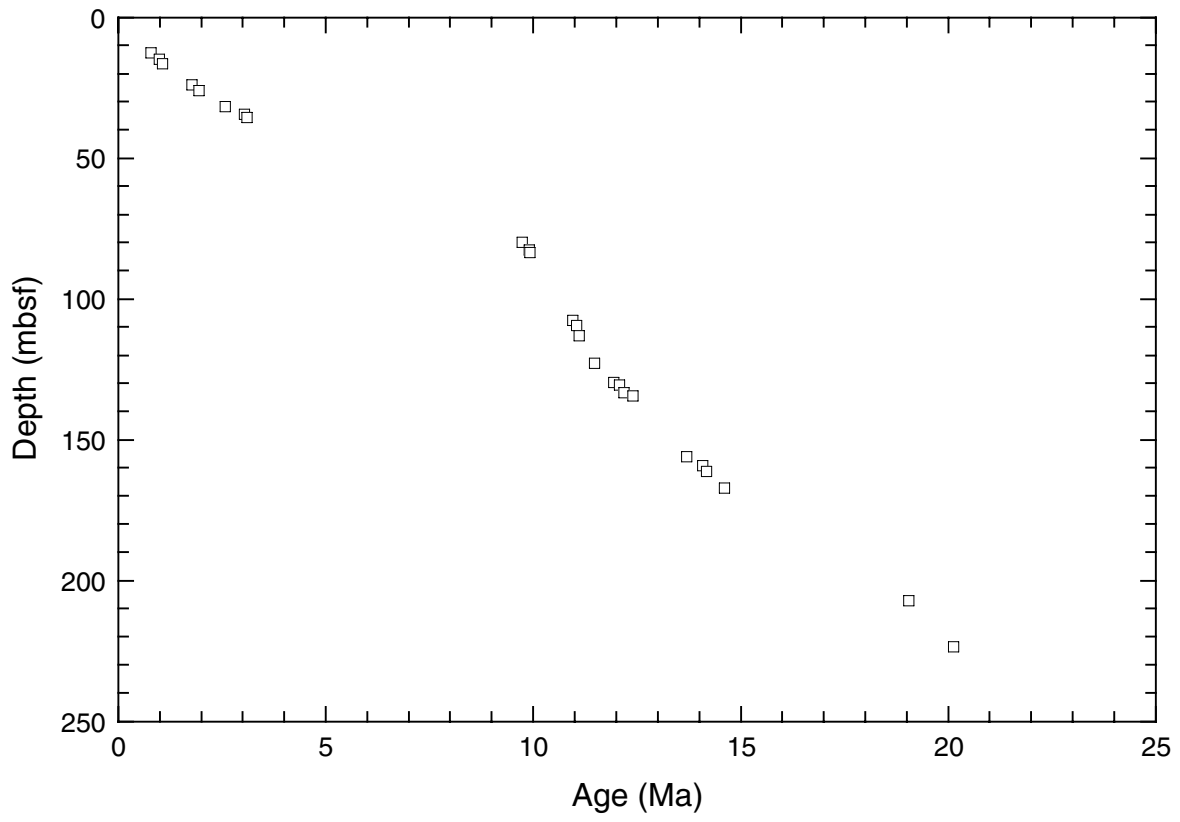
**Figure F29. A.** Smoothed (21-cm Gaussian) GRA bulk density data for the upper 118 mcd from Holes 1171A (left), 1171B (middle), and 1171C (right). Holes 1171B and 1171C are offset from Hole 1171A by constants (0.1 g/cm³ and 0.2 g/cm³, respectively). **B.** Smoothed (21- cm Gaussian) spectral reflectance (L*) data for the upper 118 mcd from Holes 1171A (left), 1171B (middle), and 1171C (right). Holes 1171B and 1171C are offset from Hole 1171A by constants (20 and 40 L* units, respectively).
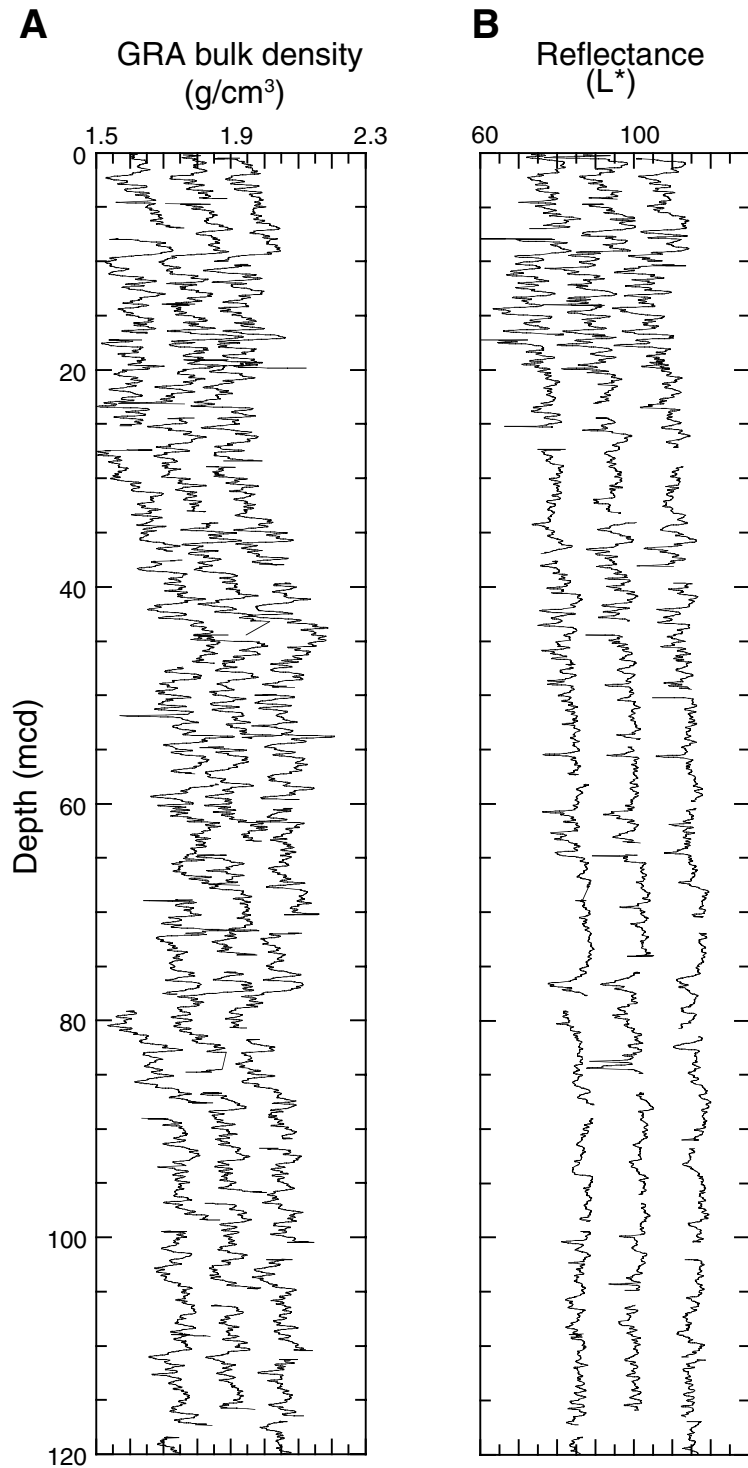
**Figure F30.** Plots of carbonate, total organic carbon (TOC) (squares = CNS analyzer data; dots = Rock-Eval pyrolysis values), total nitrogen, C/N ratios, and hydrogen index values for Site 1171. Data from Hole 1171A are presented in black, Hole 1171C data are shown in blue, and Hole 1171D data are in green. Shaded areas on the C/N ratio plot delineate typical marine and terrestrial organic matter fields. The shaded peak areas on the hydrogen index plot indicate marine organic matter. Lithostratigraphic and preliminary biostratigraphic units are on the right side of the figure.
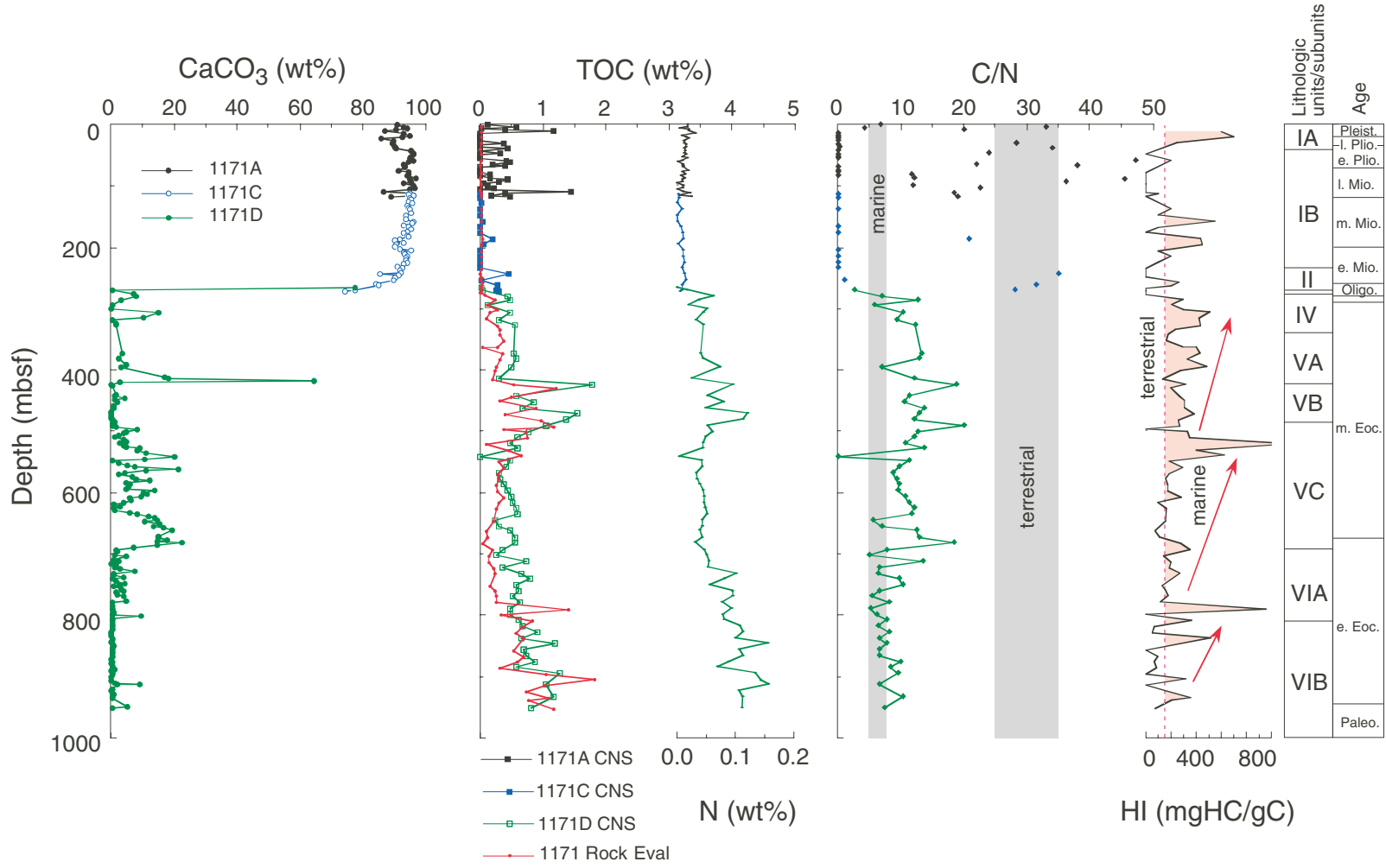
**Figure F31.** Total sulfur content (squares) compared to C/S ratios (circles) for Site 1171. Dashed lines = transitions between marine, brackish, and fresh water environments. Lithostratigraphic and preliminary biostratigraphic units are on the right side of the diagram.
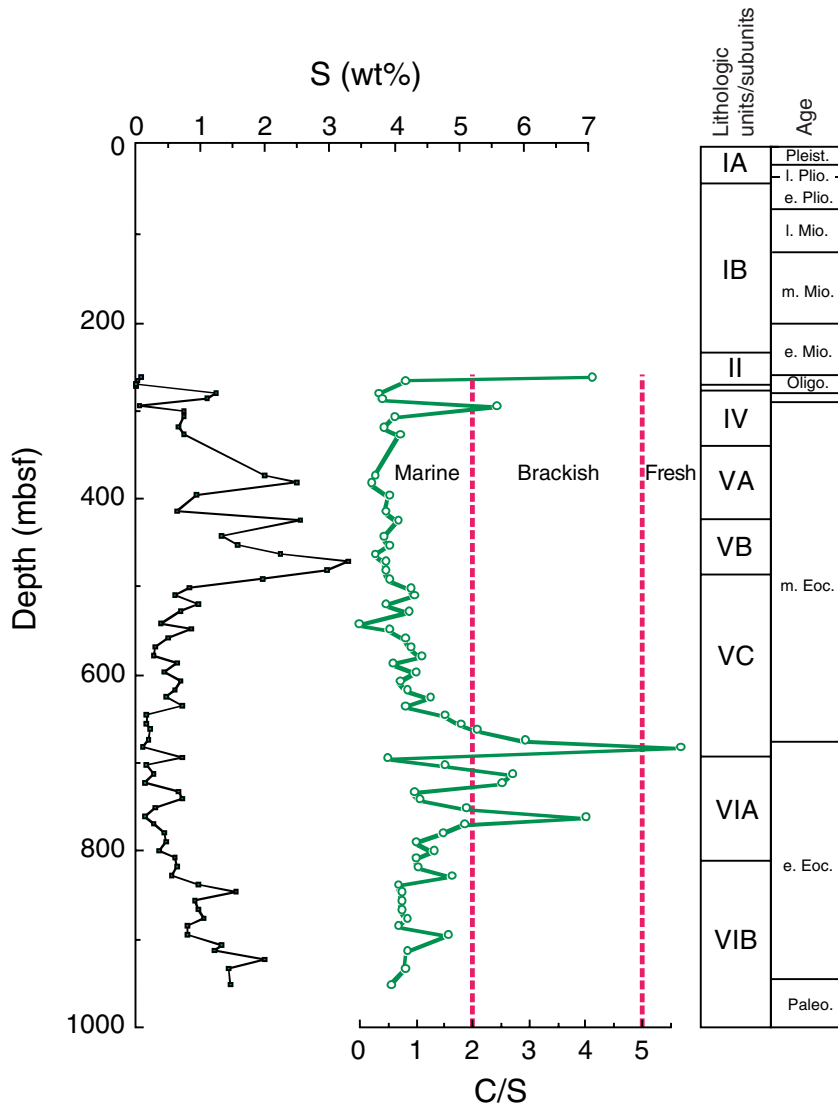
**Figure F32.** $T_{max}$ values generated from Rock-Eval pyrolysis analyses of organic matter for Site 1171. The high variability of values above ~460 mbsf is likely caused by very low TOC values in these samples. Below 460 mbsf, $T_{max}$ values are indicative of immature organic matter relative to oil generation and the presence of bitumen, although values approach the "oil window" (dashed vertical lines) at the base of the core. Lithostratigraphic and preliminary biostratigraphic units are indicated on the right side of the diagram.
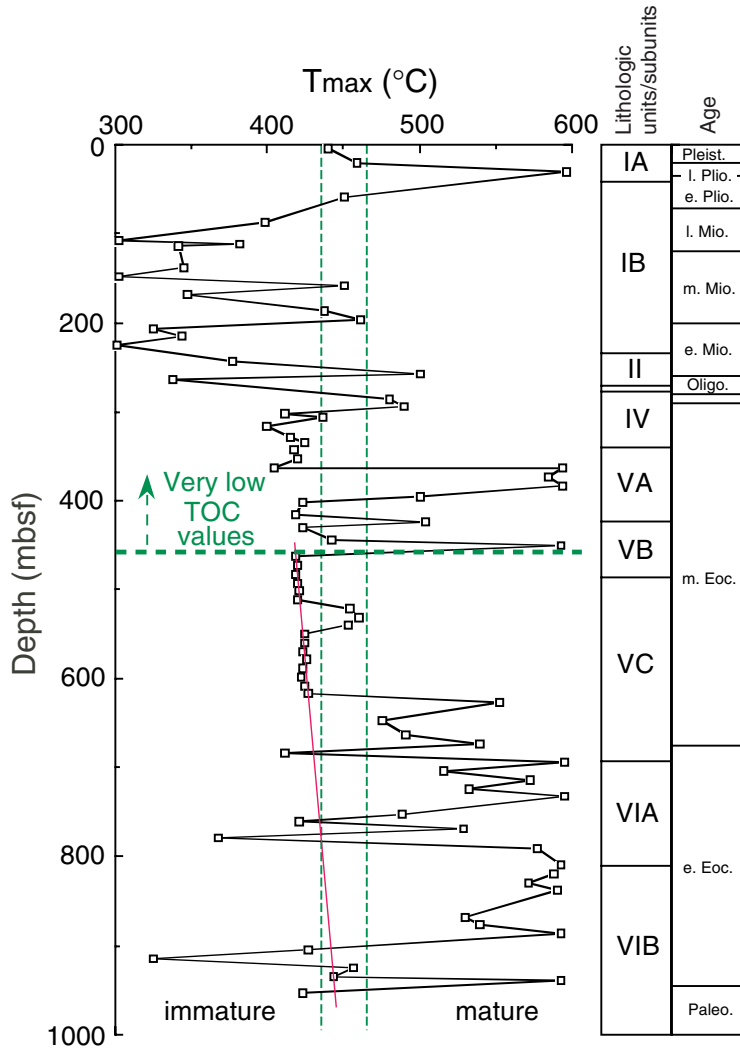
**Figure F33.** Methane ($C_1$) and dissolved sulfate ($SO_4^{2-}$) concentrations, methane vs. ethane plus propane ratio ($C_1/C_2+C_3$), and the percent wetness ($[C_2^+/C_1^+] \times 100$) from headspace gas analysis at Site 1171. Dashed lines delineate biogenic and thermogenic fields on the $C_1/C_2+C_3$ plot (Hinz et al., 1986), whereas the shaded area on the percent wetness plot marks values typical for economically viable gas reservoirs. Lithostratigraphic and preliminary biostratigraphic units are indicated on the right side of the diagram.
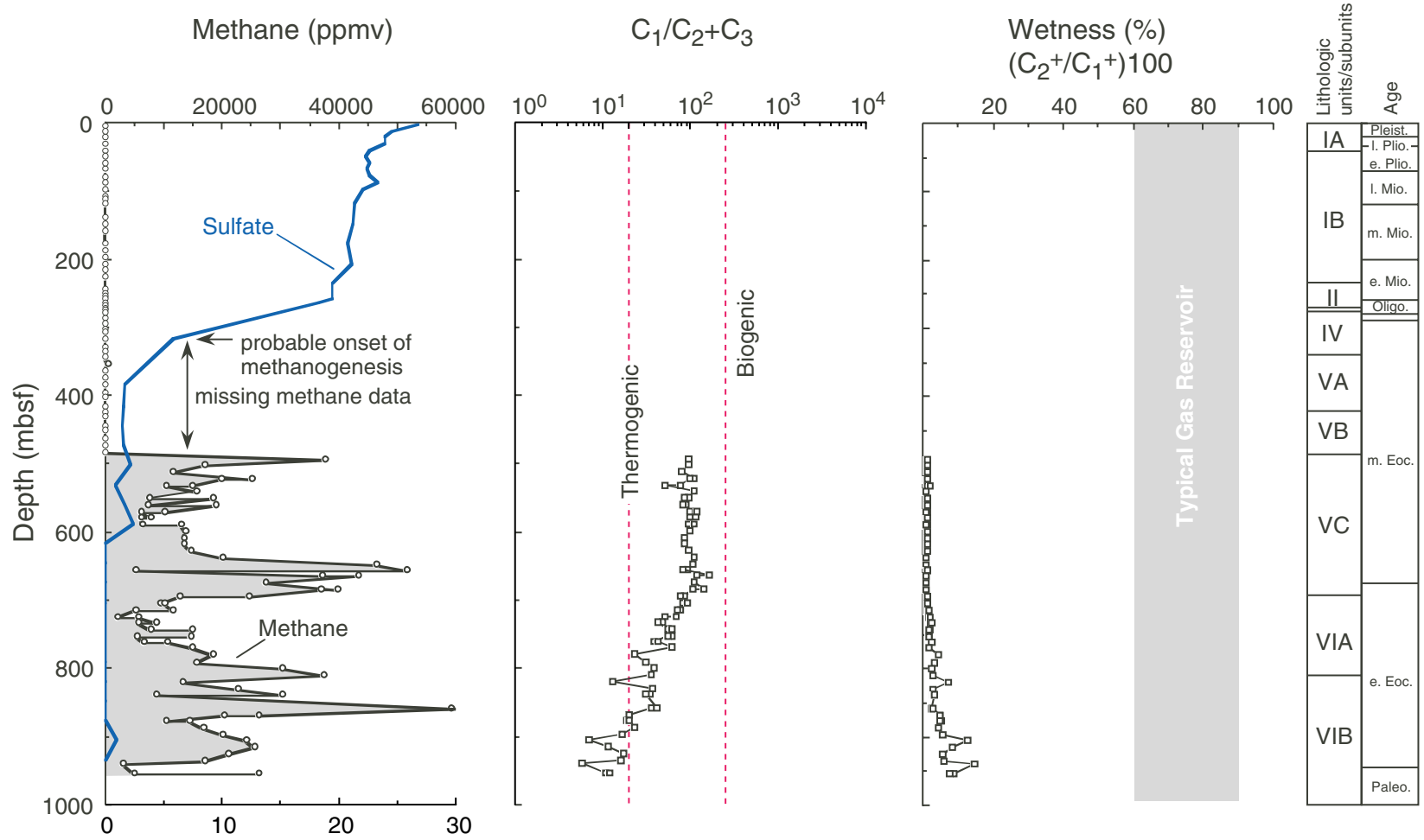
**Figure F34.** Concentration-depth profile of Cl⁻ compared to methane (see **"Volatile Hydrocarbons,"** p. 49, in "Organic Geochemistry") and Na⁺ compared to Na⁺/Cl⁻ ratios at Site 1171. Approximate locations of lithostratigraphic and biostratigraphic boundaries (see **"Lithostratigraphy,"** p. 10, and **"Biostratigraphy,"** p. 25) and standard seawater (SW) concentrations are indicated. Dashed lines mark depths of pronounced pore-water chemistry changes.
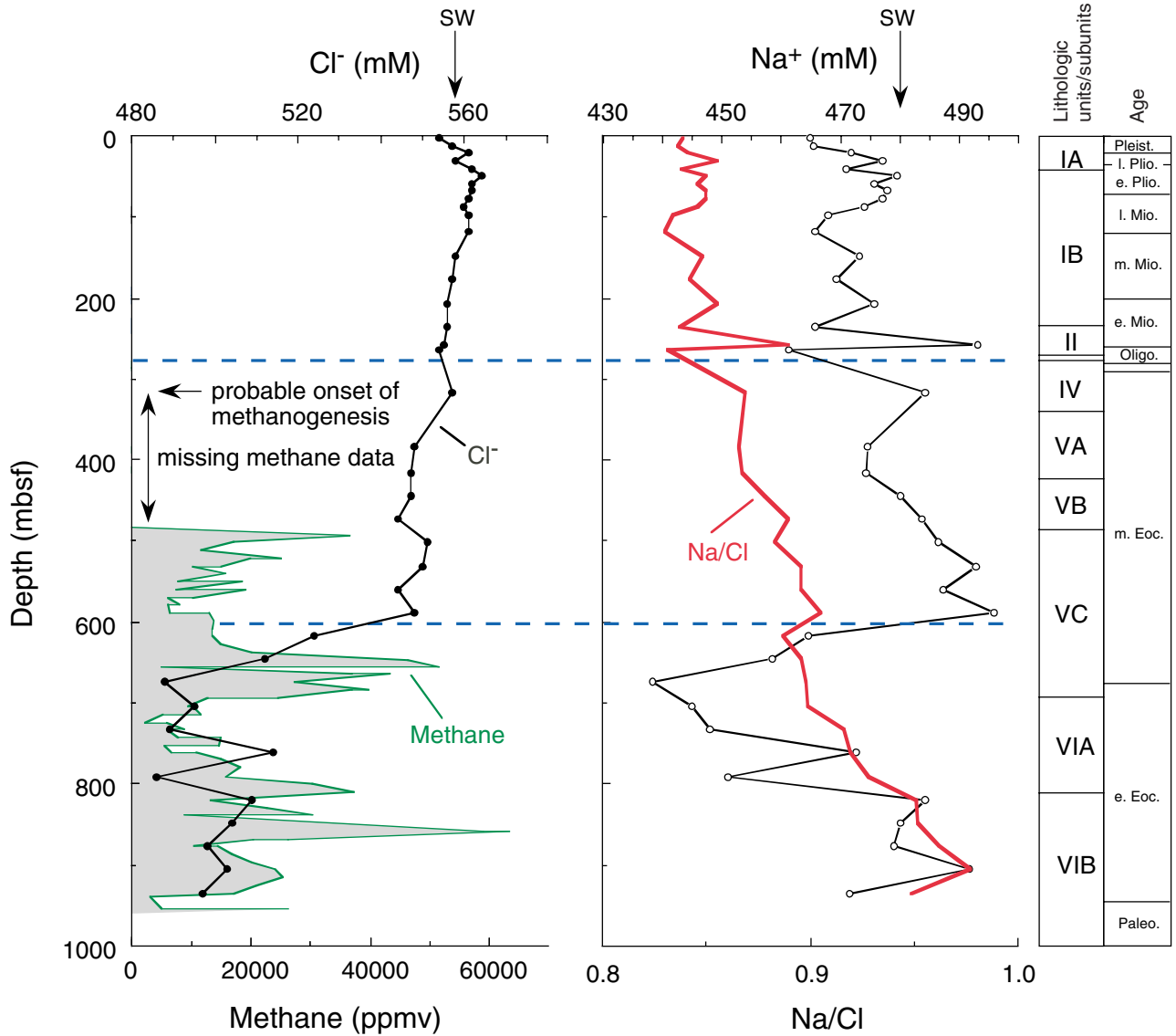
**Figure F35.** Concentration-depth profiles of SO$_4^{2-}$, pH, alkalinity, and NH$_4^+$ at Site 1171. Methane concentrations (see **"Volatile Hydrocarbons,"** p. 49, in "Organic Geochemistry") are plotted for comparison. Alkalinity and pH values were not measured in many of the lithified siliciclastics samples in which pore-water volume was limited. Approximate locations of lithostratigraphic and biostratigraphic boundaries (see **"Lithostratigraphy,"** p. 10, and **"Biostratigraphy,"** p. 25) and standard seawater (SW) concentrations are indicated. Dashed lines mark depths of pronounced pore-water chemistry changes.
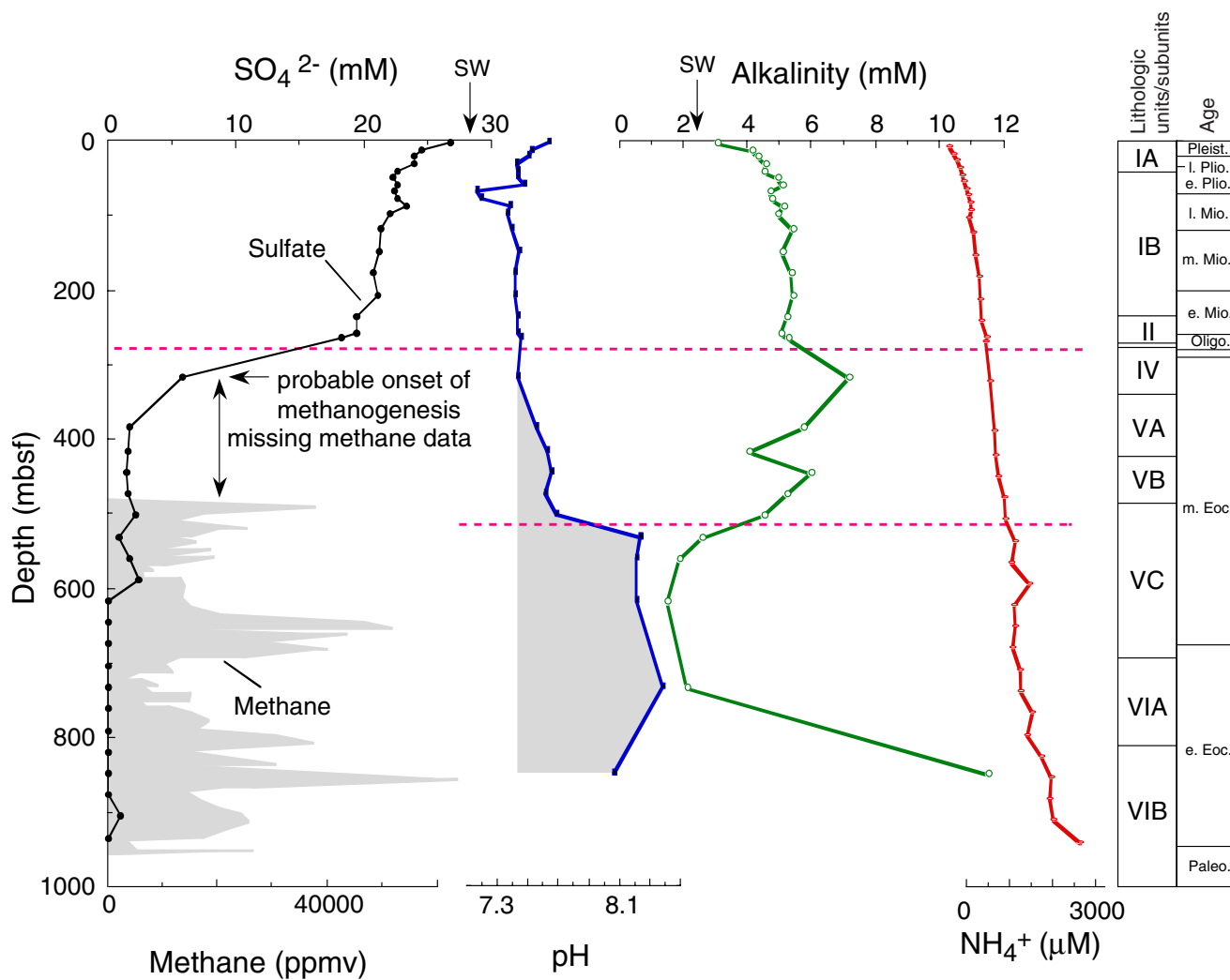
**Figure F36.** Concentration-depth profiles of $Sr^{2+}$, $Ca^{2+}$, and $Li^+$ at Site 1171 with approximate location of lithostratigraphic and biostratigraphic boundaries (see **"Lithostratigraphy,"** p. 10, and **"Biostratigraphy,"** p. 25). For comparison, $CaCO_3$ content (see **"Organic Geochemistry,"** p. 44) and $Sr^{2+}/Ca^{2+}$ and $Li^+/Ca^{2+}$ ratios are plotted. Standard seawater (SW) concentrations are indicated.
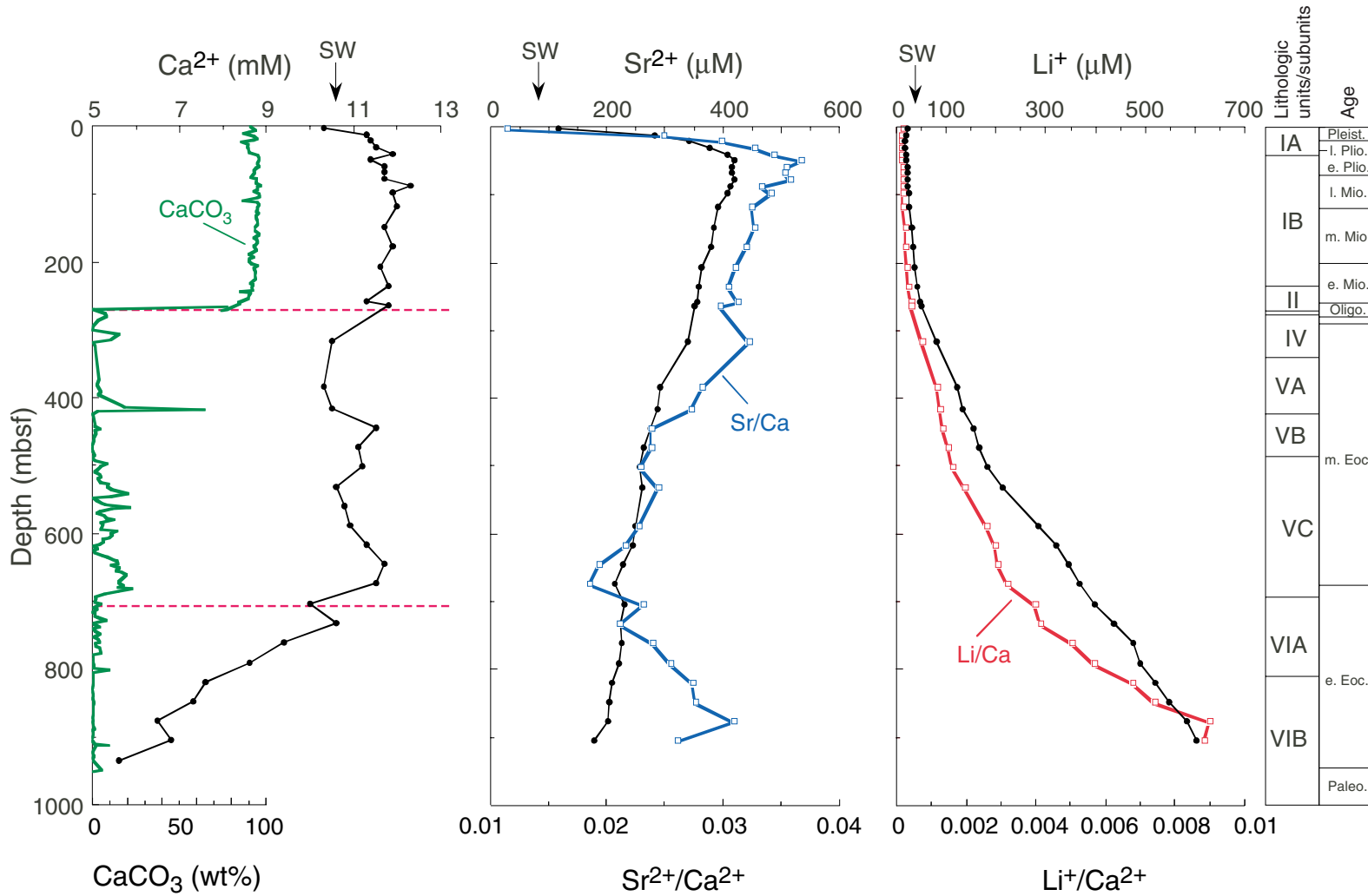
**Figure F37.** Concentration-depth profiles of $Mg^{2+}$ and $K^+$ at Site 1171. For comparison, $Mg^{2+}/Cl^-$ and $K^+/Cl^-$ ratios are plotted. The insert shows the high correlation between $Mg^{2+}$ and $K^+$. Approximate locations of lithostratigraphic and biostratigraphic boundaries (see **"Lithostratigraphy,"** p. 10, and **"Biostratigraphy,"** p. 25) and standard seawater (SW) concentrations are indicated. The dashed line marks depth of pronounced pore-water chemistry change.
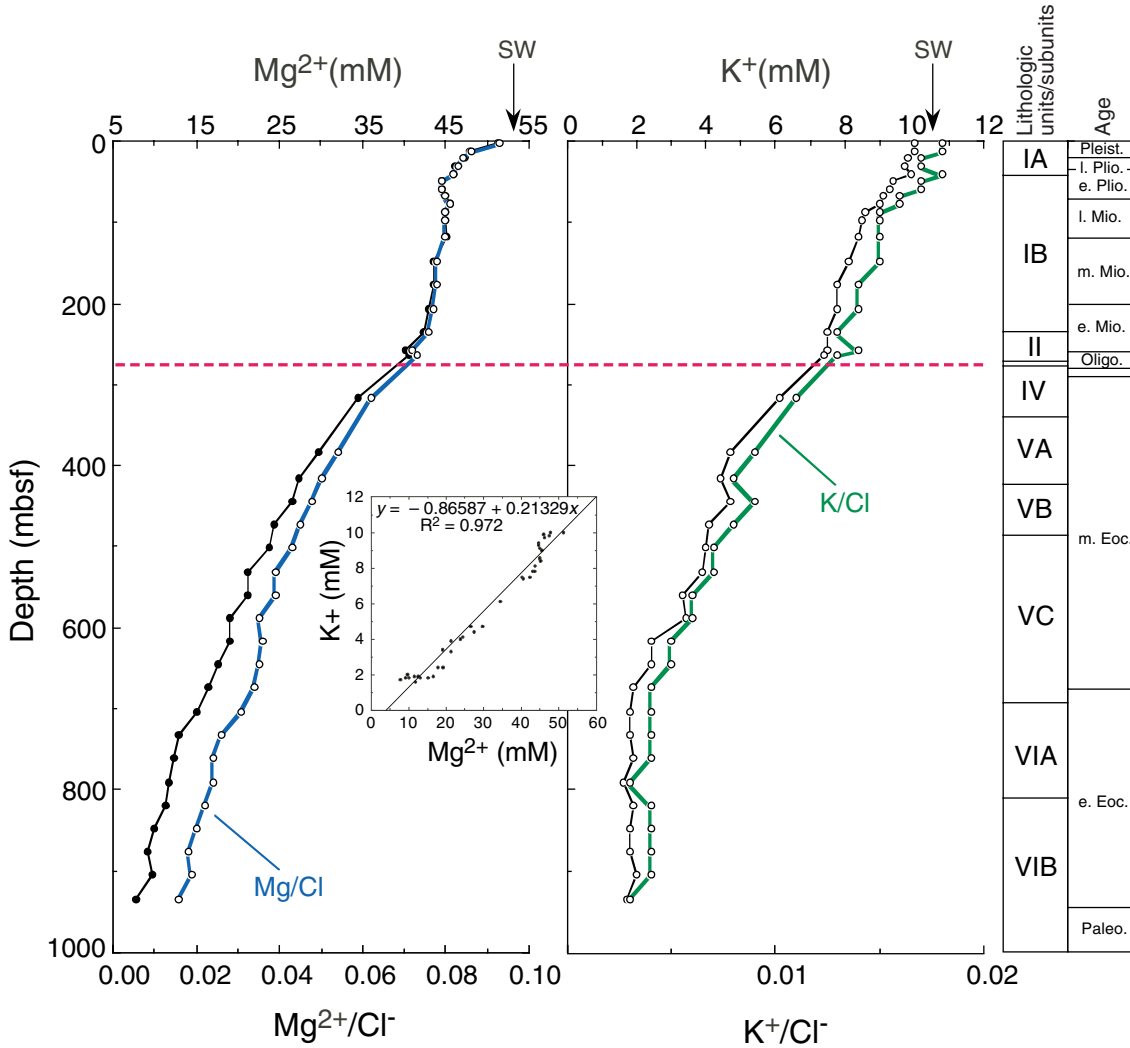
**Figure F38.** Concentration-depth profile of dissolved silica within interstitial water at Site 1171. The shaded area marks the abundances of radiolarians (barren to common; see "Biostratigraphy," p. 25), whereas black horizontal bars indicate poor preservation of radiolarians. Solid squares indicate the presence of opal-CT within the sediments. Approximate locations of lithostratigraphic and biostratigraphic boundaries (see "Lithostratigraphy," p. 10, and "Biostratigraphy," p. 25) are indicated. Dashed lines mark depths of pronounced dissolved silica changes.
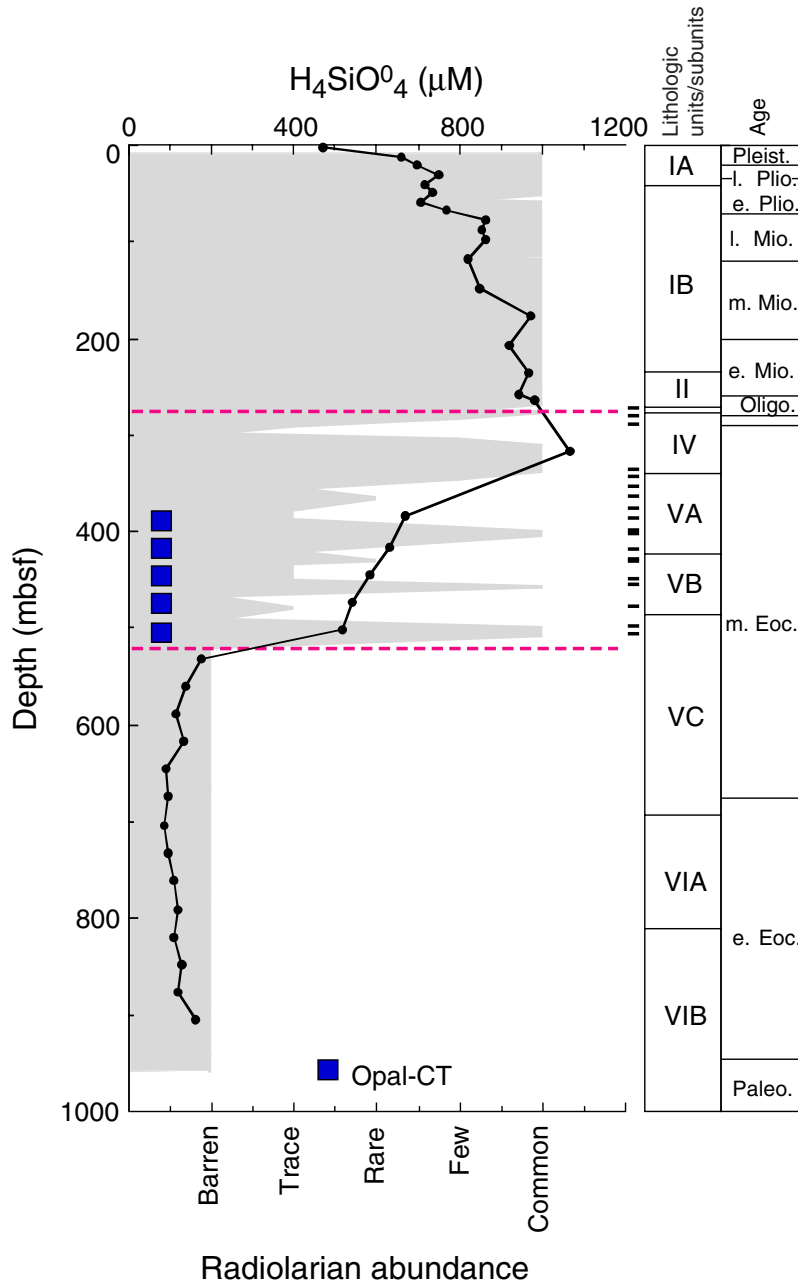
**Figure F39. A.** Magnetic susceptibility measured on whole cores by the MST vs. depth for Hole 1171A. (Continued on next page.)
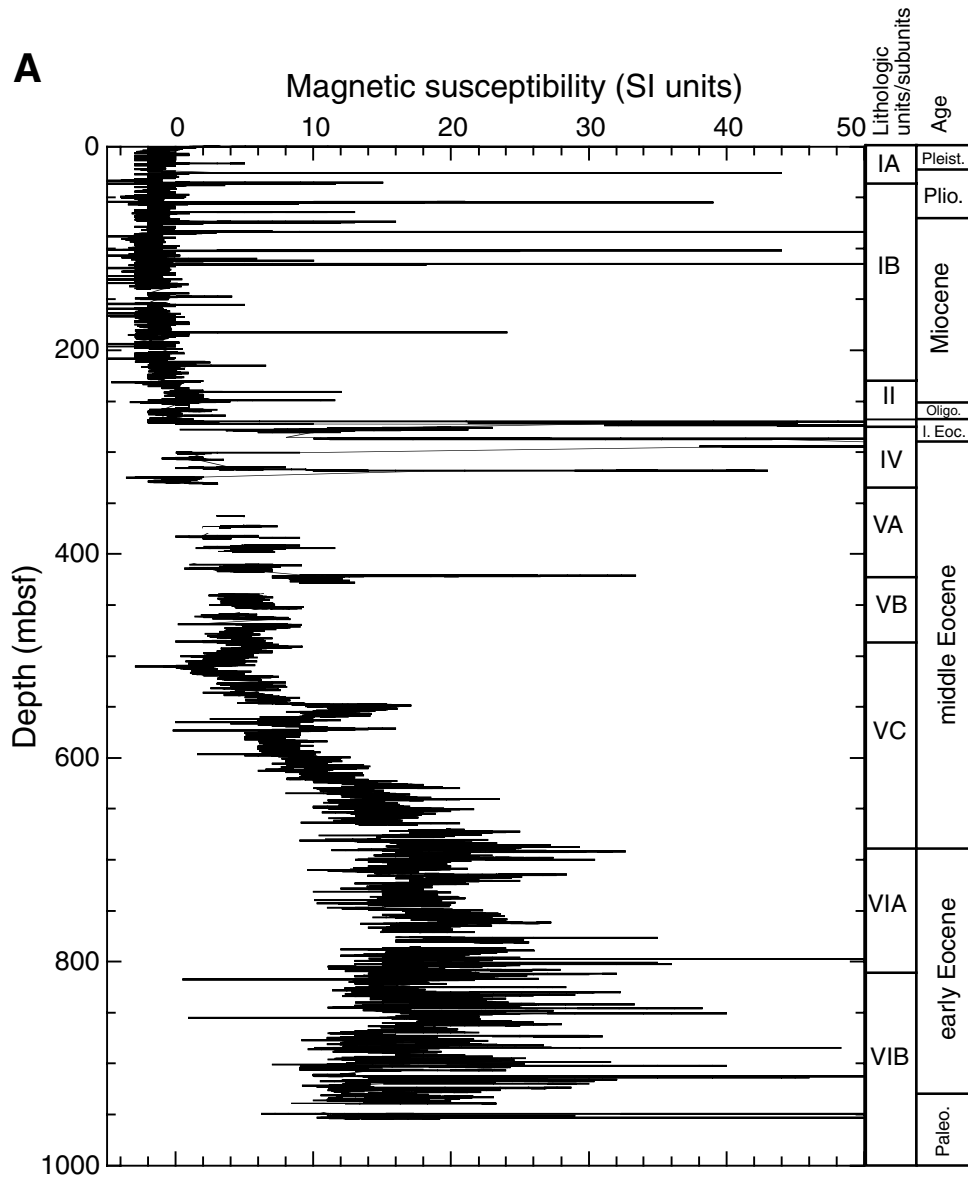
**Figure F39 (continued). B.** GRA density (crosses) and wet bulk density determined for discrete samples (solid circles) vs. depth for Hole 1171.
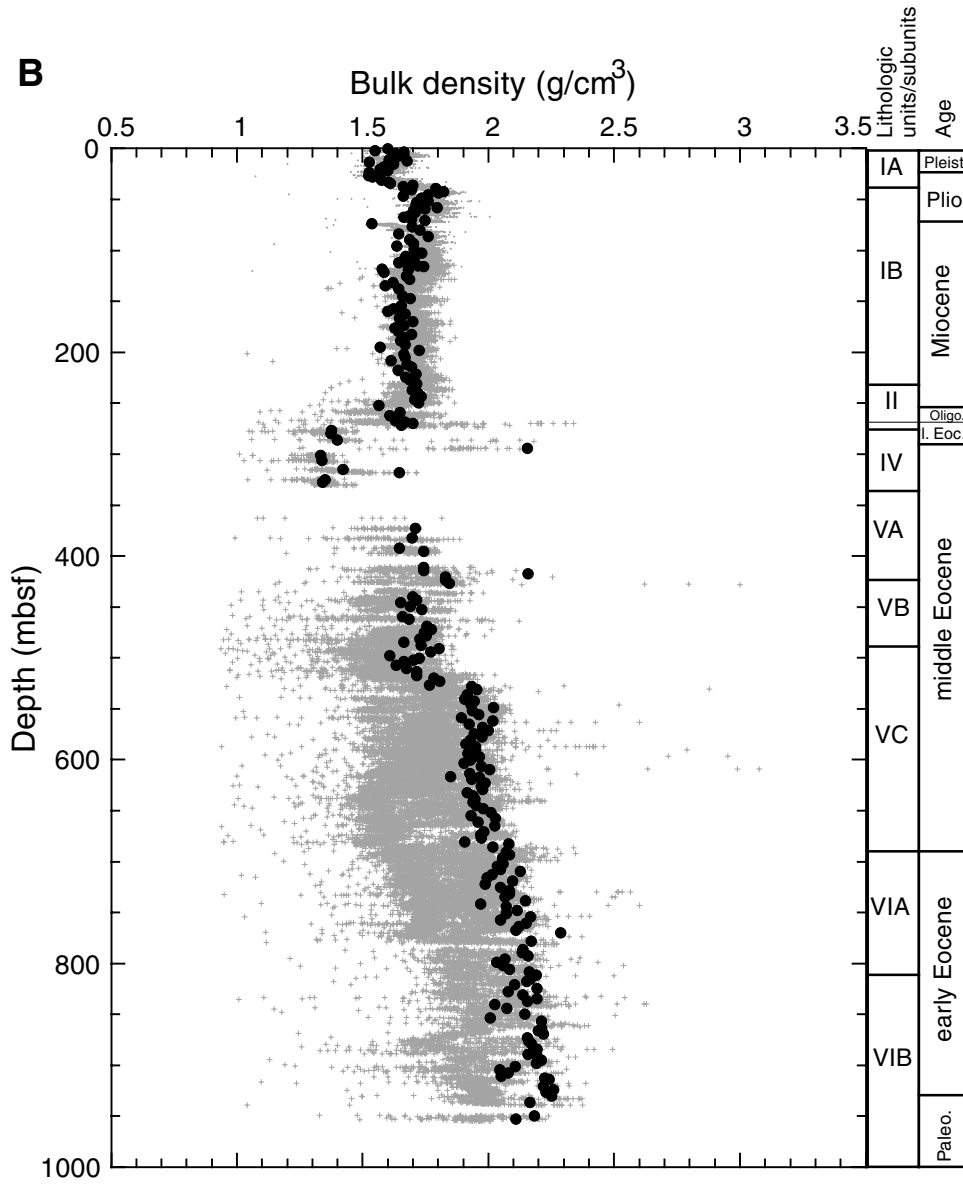
**Figure F40.** *P*-wave velocities (PWS1 along core and PWS3 across core) measured for discrete samples and *P*-wave velocities measured in whole cores (MST) vs. depth, Site 1171.
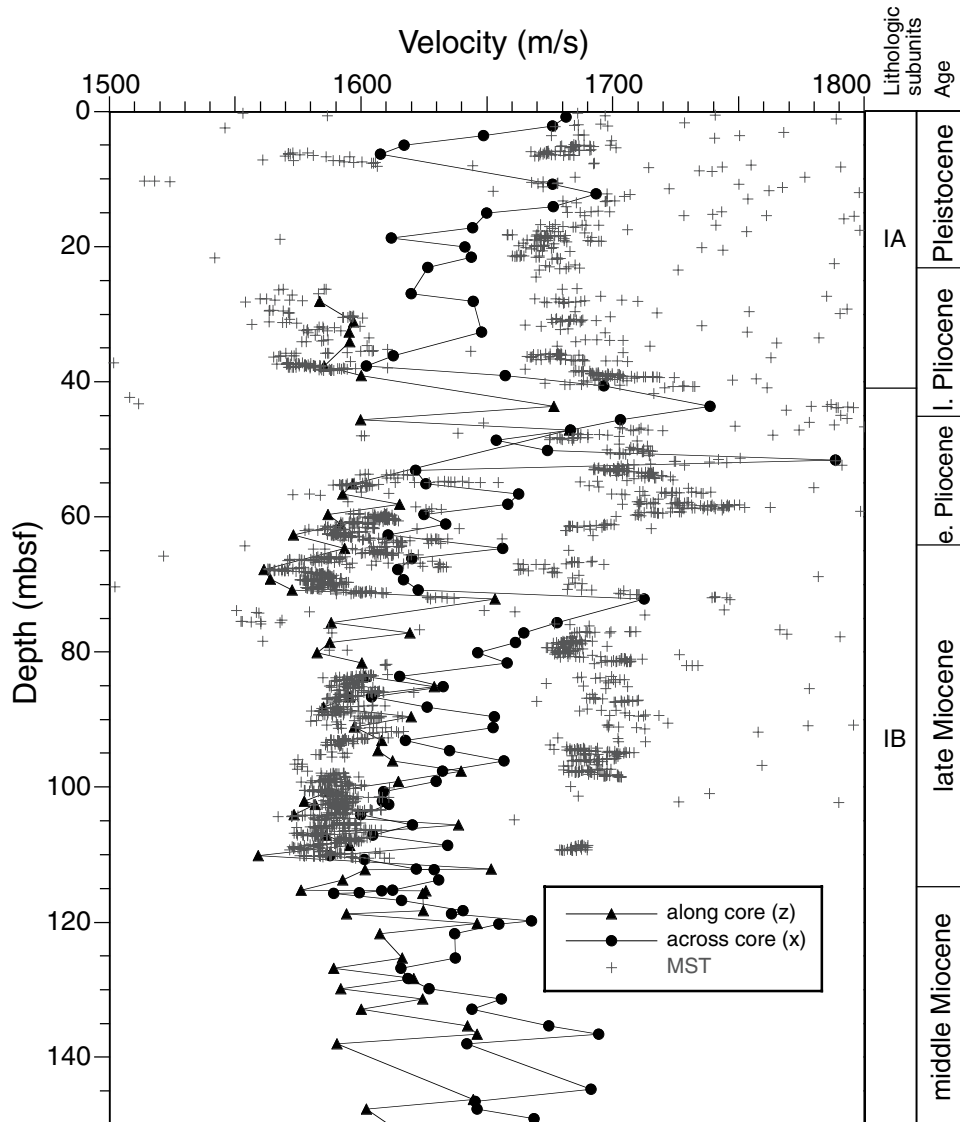
**Figure F41.** *P*-wave velocities (PWS3) measured for discrete samples vs. depth, Site 1171.
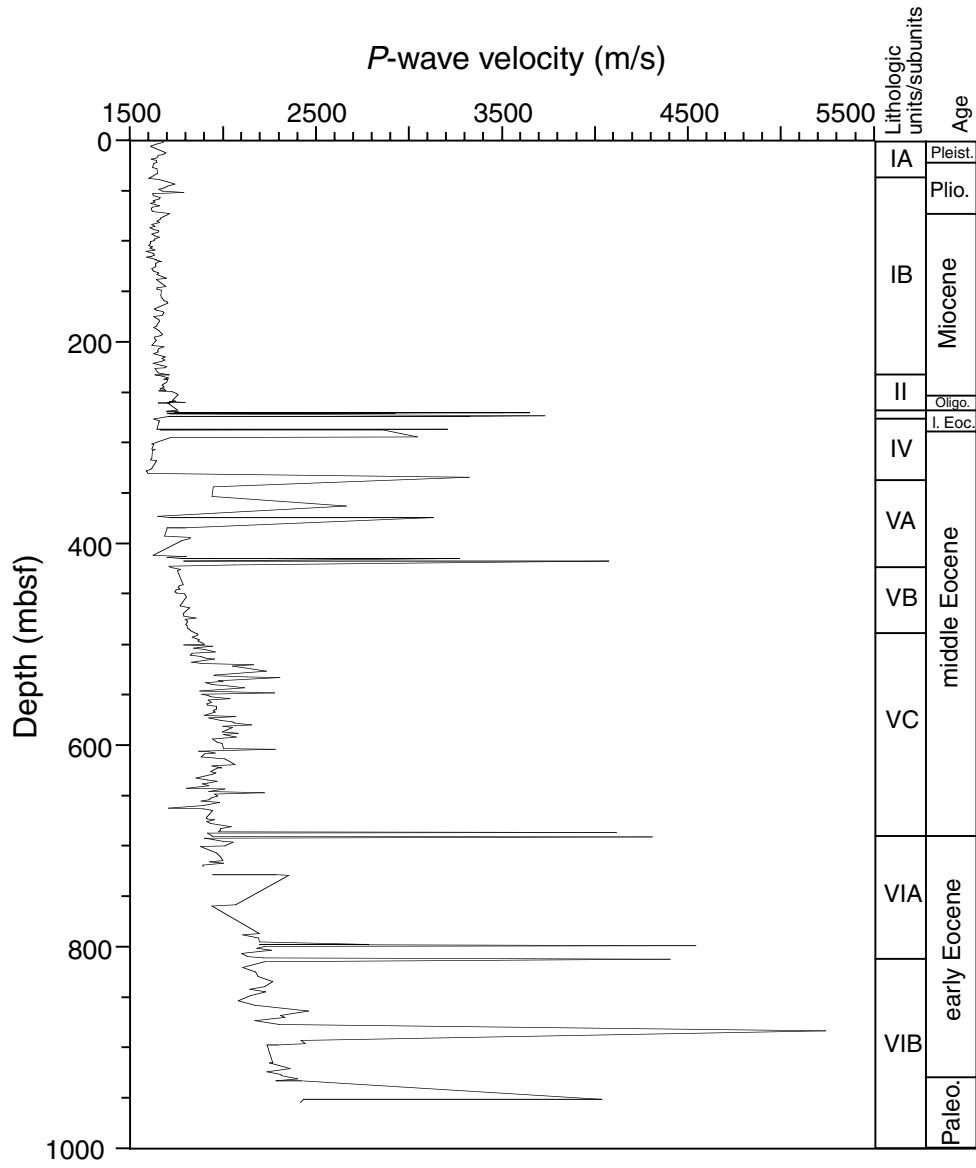
**Figure F42.** Thermal conductivity measured on whole cores vs. depth, Site 1171.
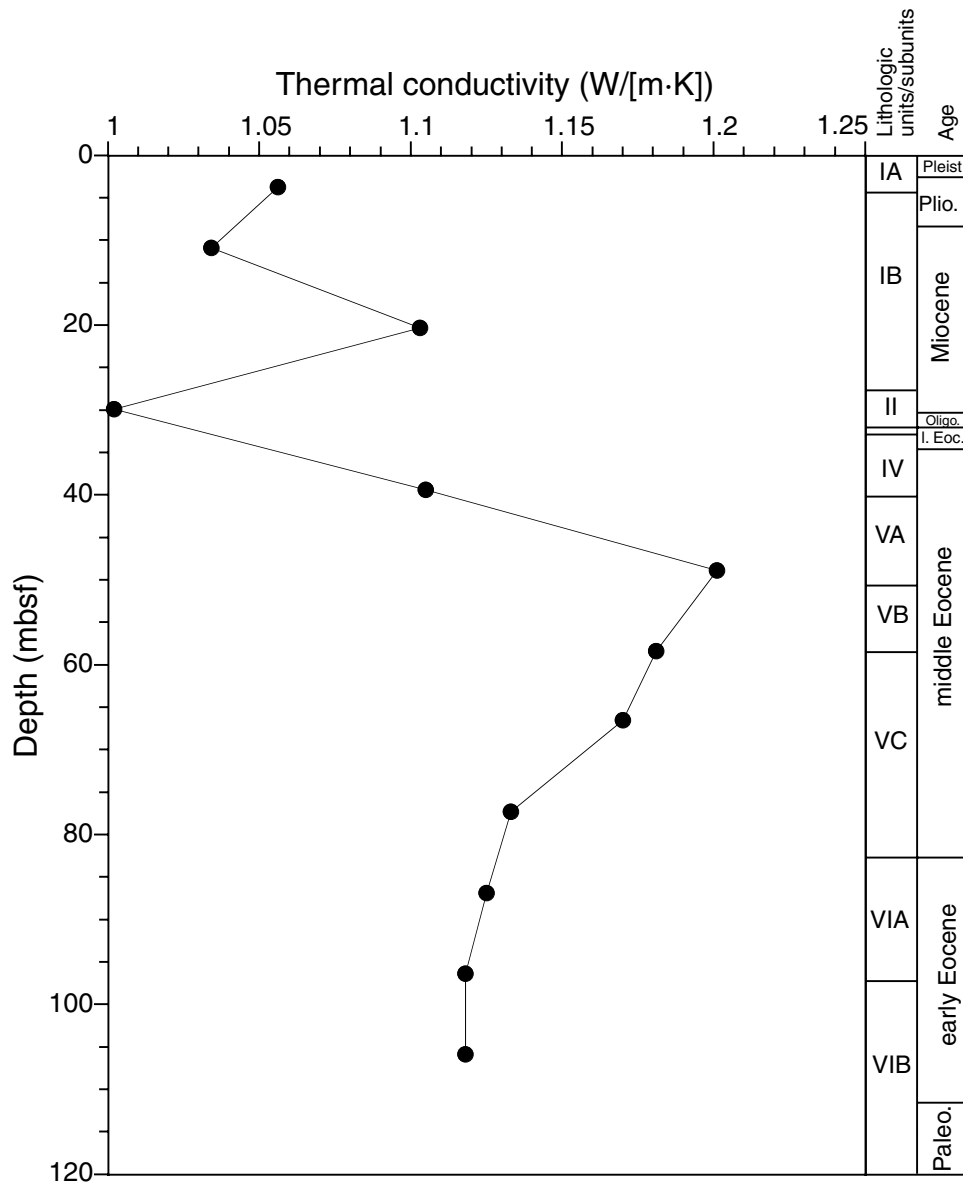
**Figure F43.** Temperature vs. depth for Site 1171.
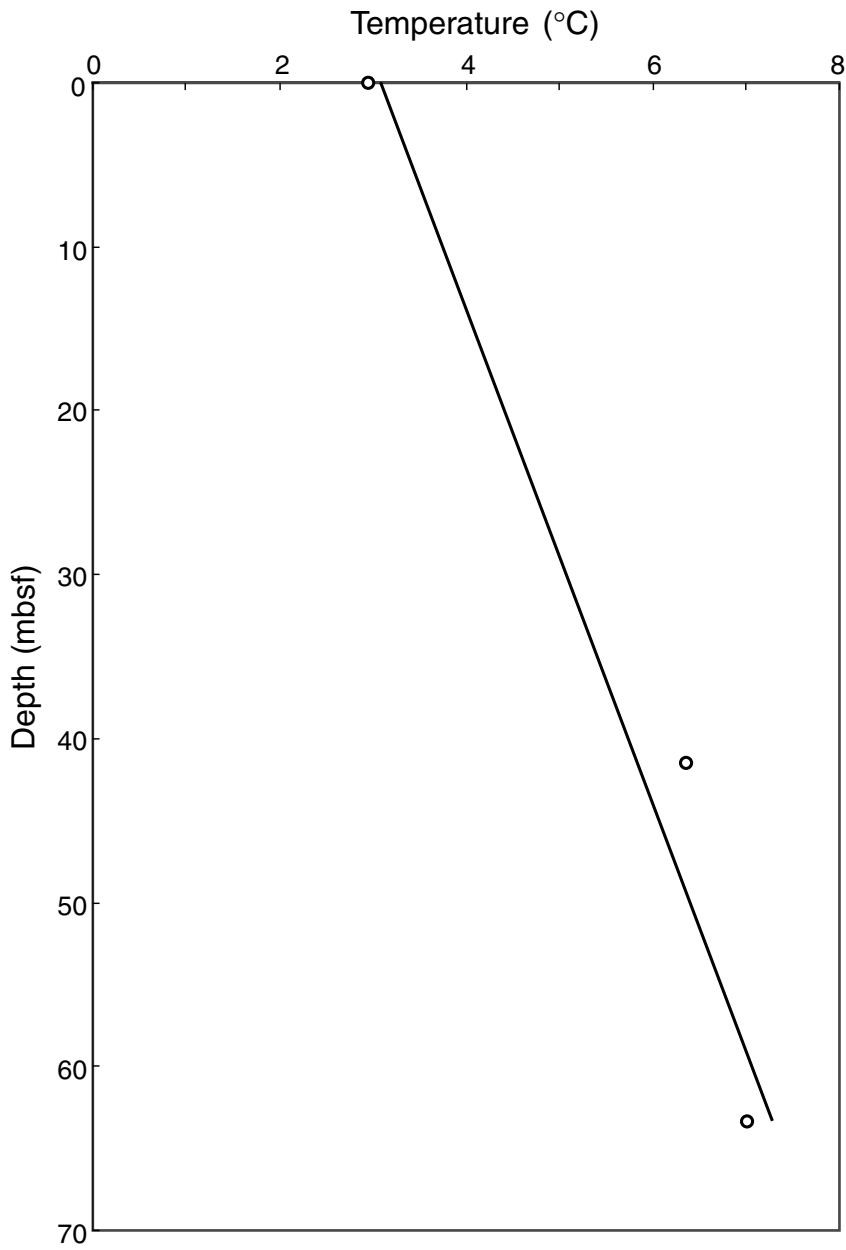


$y = 0.0662x + 3.0943$

Geothermal gradient = 62°C/km

Average thermal conductivity = 1.112 (W/[m·k])

Heat flow = 68.96 W/m$^2$

**Figure F44.** Undrained shear strength from miniature vane-shear measurements vs. depth for Hole 1171A.
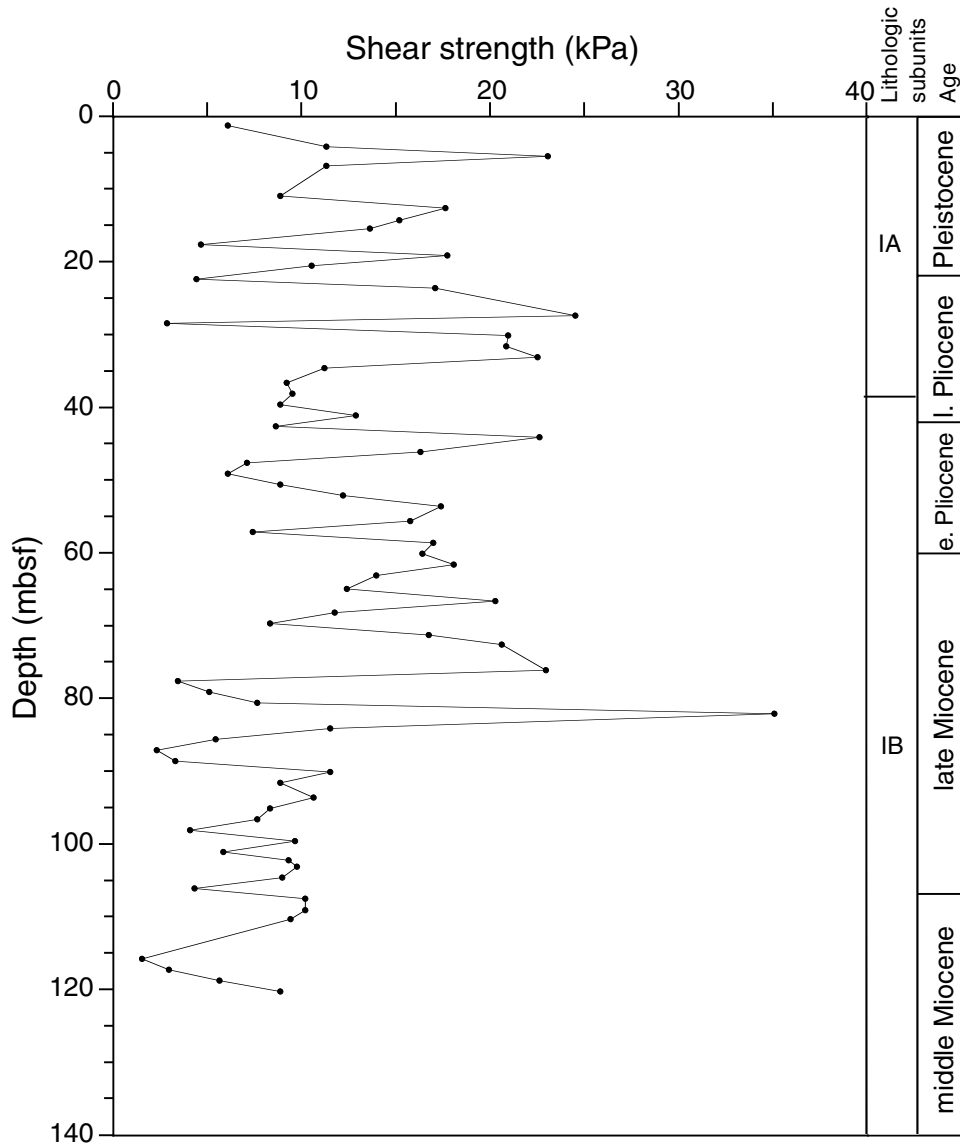
**Figure F45.** Wet bulk density, water content, and porosity measured at discrete intervals vs. depth for Site 1171.
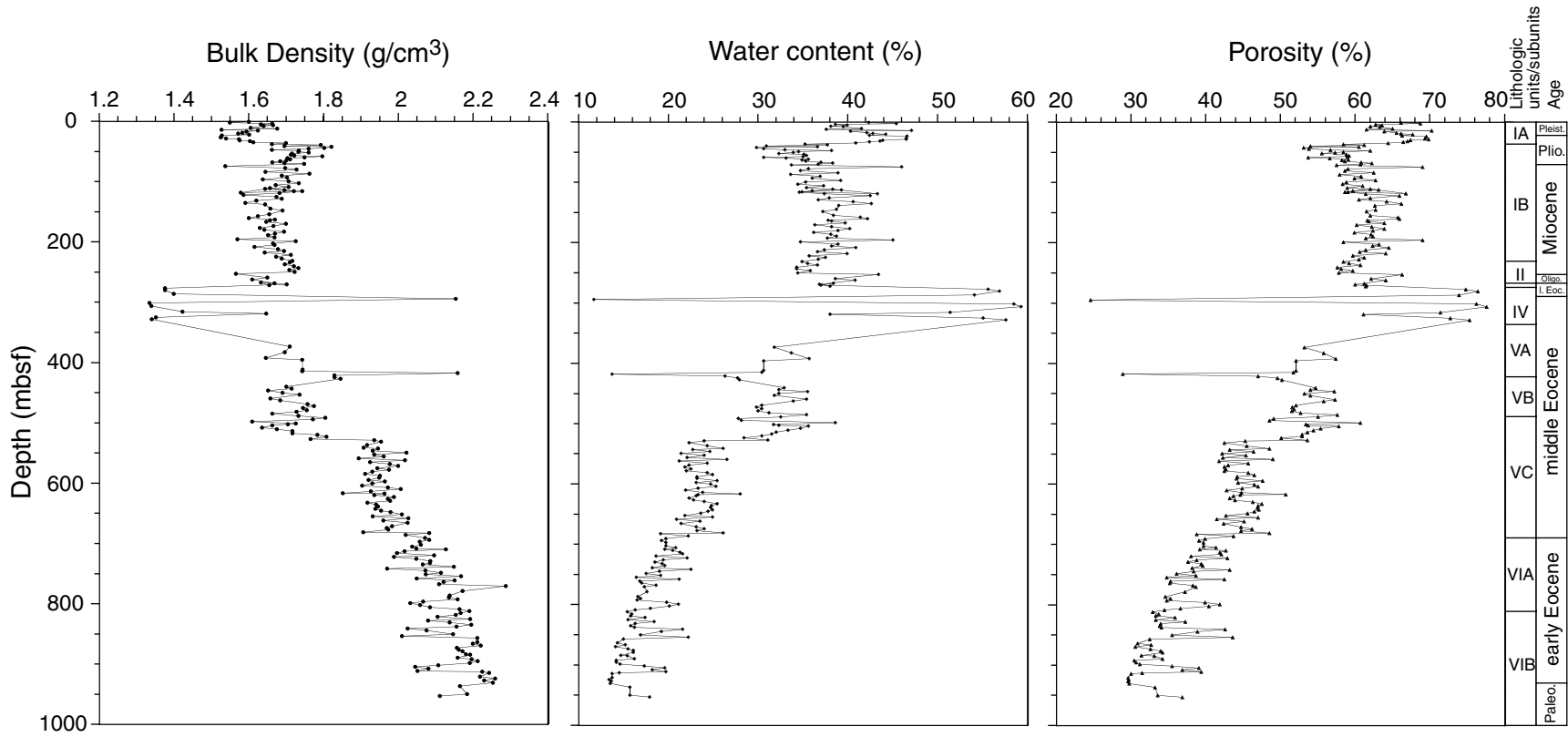
**Figure F46.** Details of the logging operations in Hole 1171D. Depths are shown in either meters below rig floor (mbrf) or meters below seafloor (mbsf).
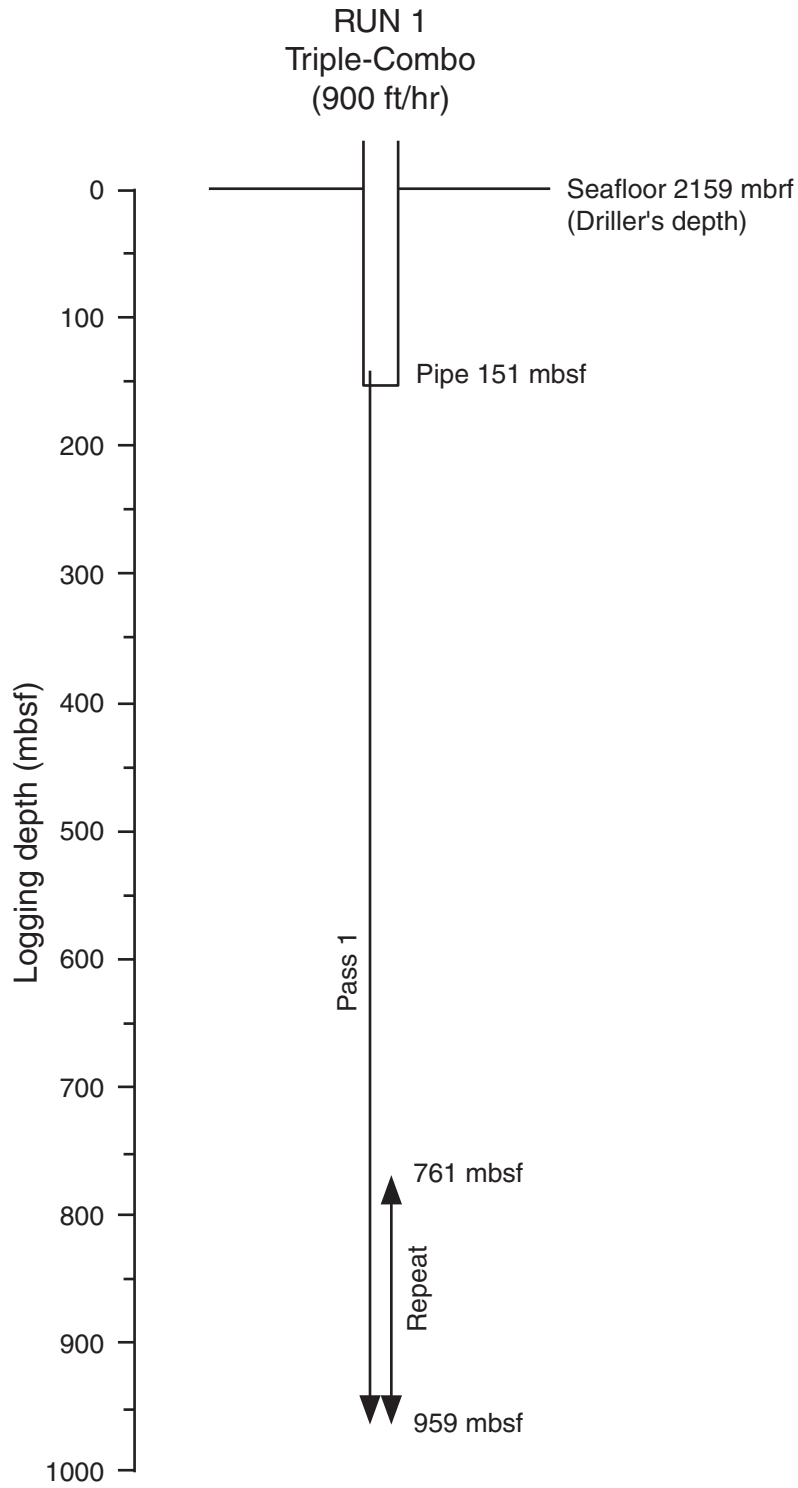
**Figure F47.** Caliper, medium resistivity, porosity, density, and photoelectric effect (PEFL) values from Hole 1171D.
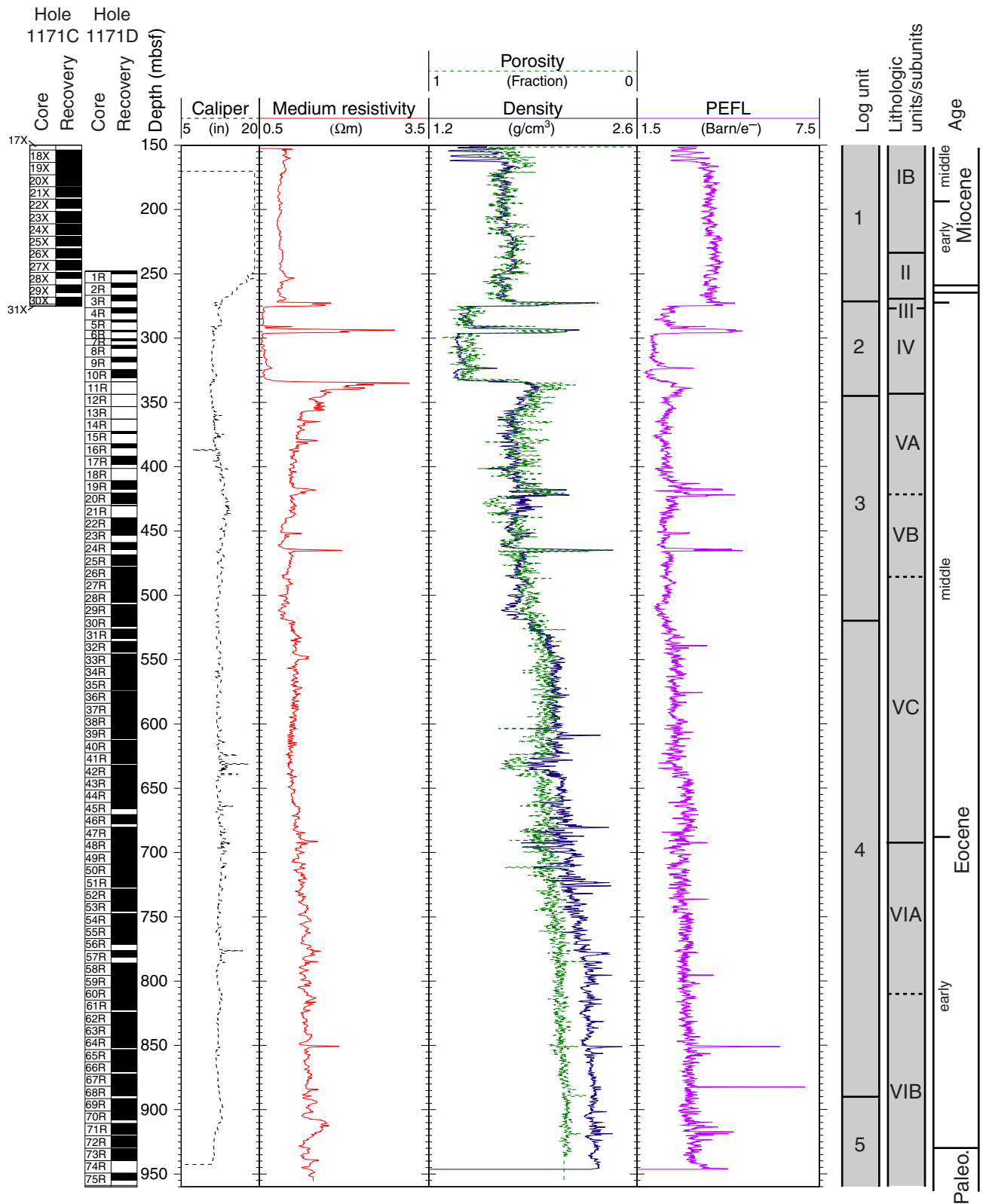
**Figure F48.** Total gamma-ray and spectral gamma-ray values from Hole 1171D. HSGR = total gamma radiation (from Th, K, and U). HCGR = gamma radiation from Th and K only.
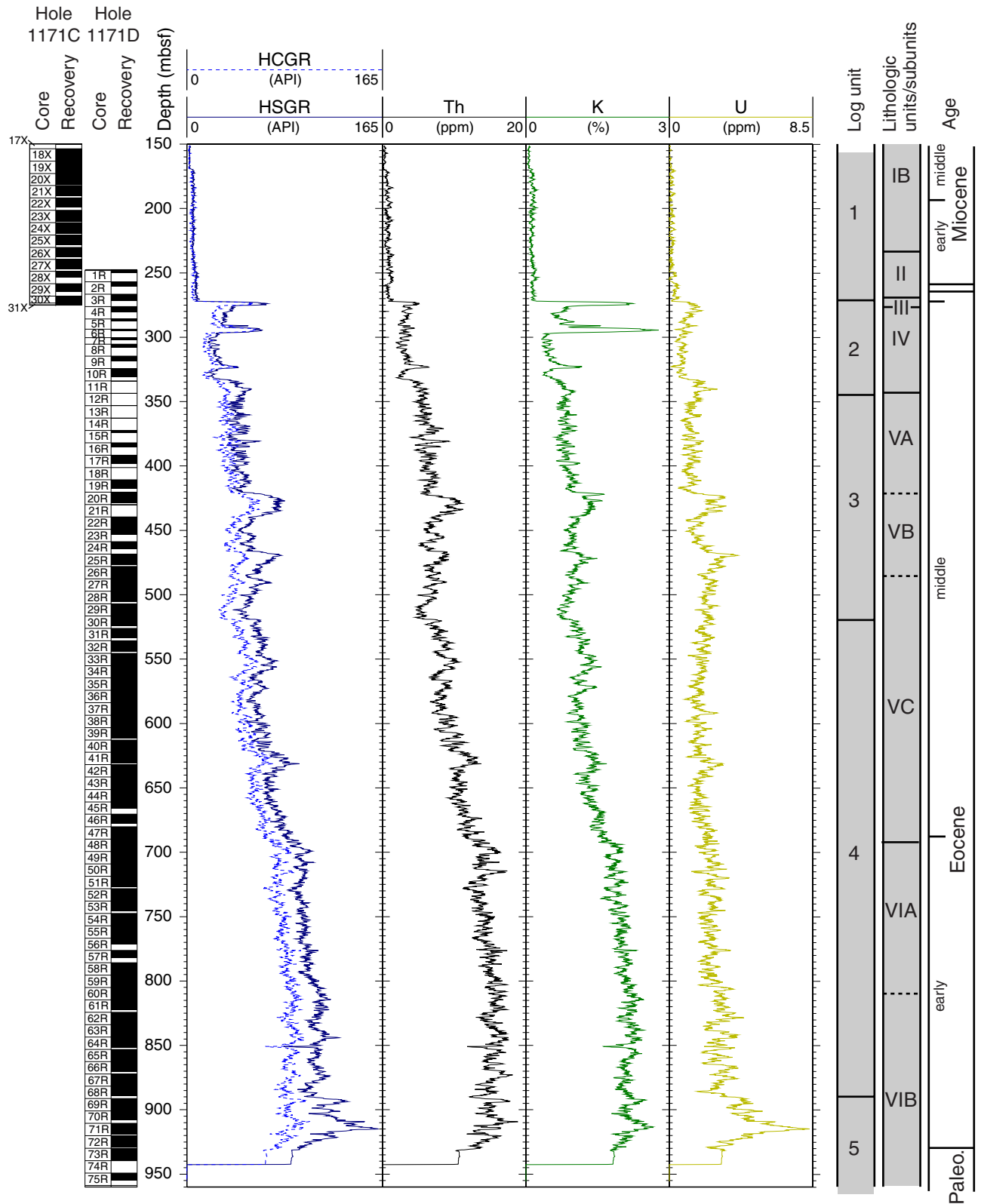
**Figure F49.** Downhole log bulk density plotted with core bulk density.
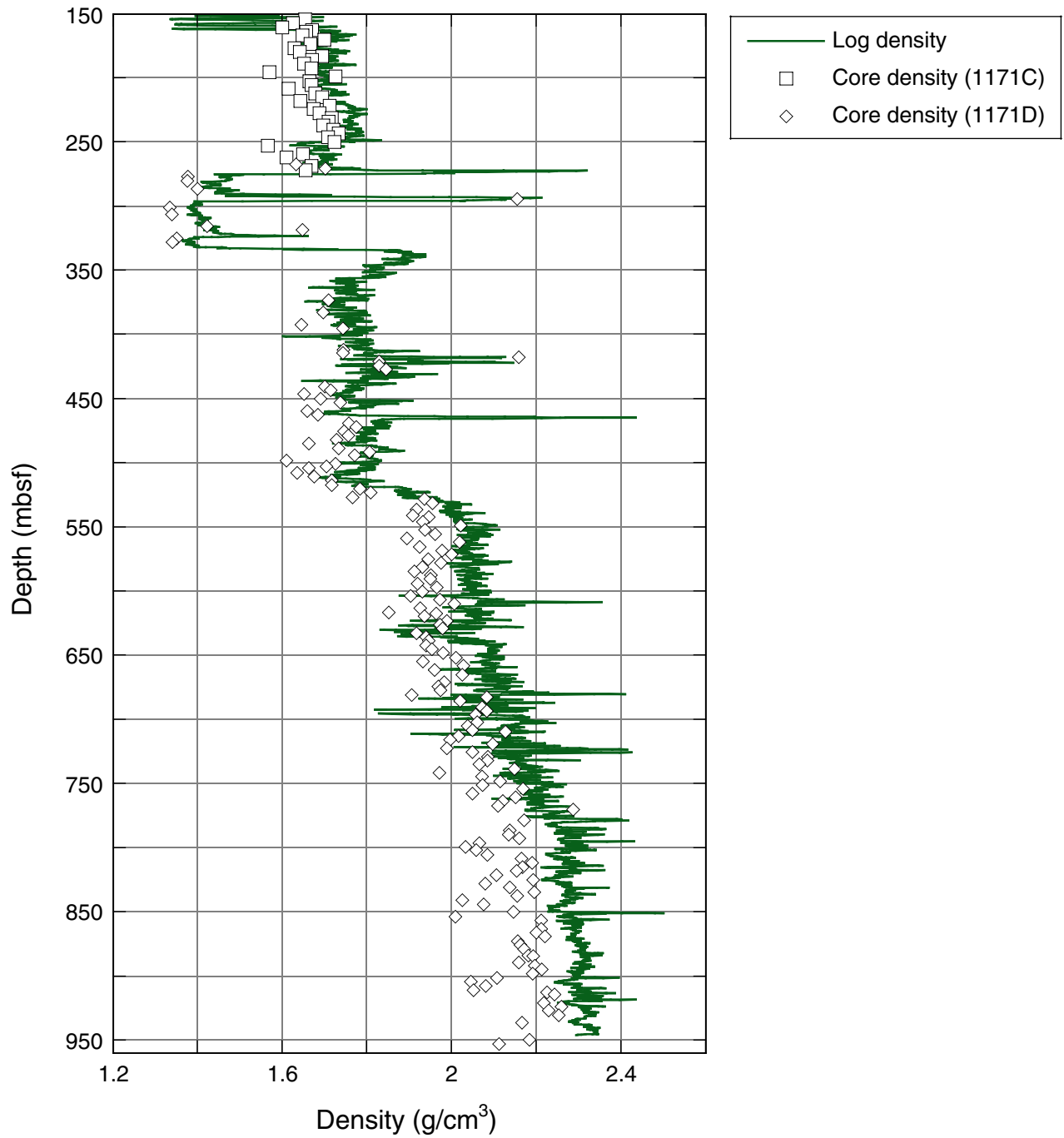
**Figure F50.** Downhole density porosity and neutron porosity plotted with core porosity.
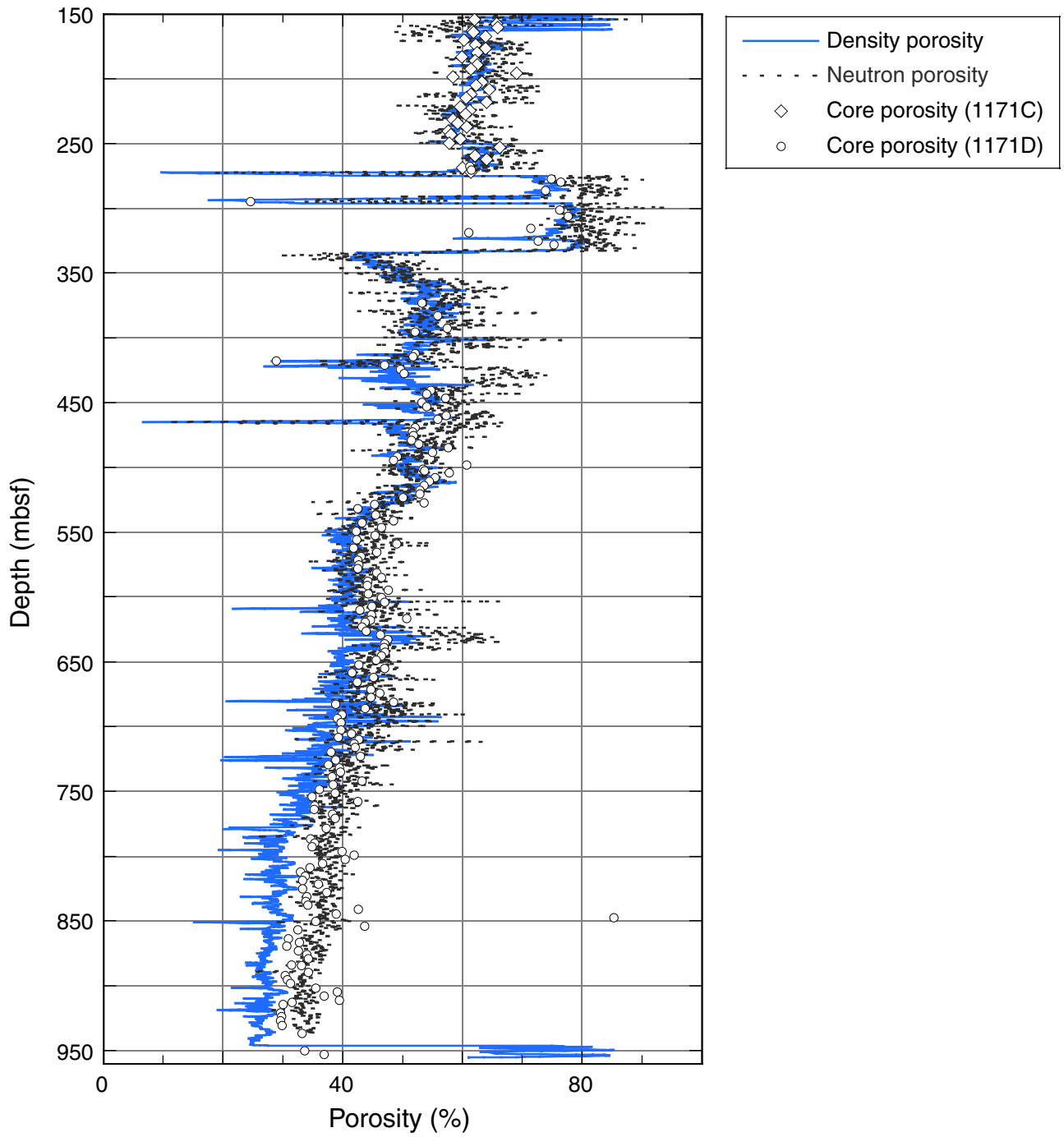
**Figure F51.** Time/depth, *P*-wave velocity ($V_p$) (measured in the core, see **"Physical Properties,"** p. 54), and seismic data from Site 1171. The time/depth relationship was calculated using the $V_p$, which are shown plotted against time. Many of the changes in $V_p$ correlate with reflectors in the seismic section.
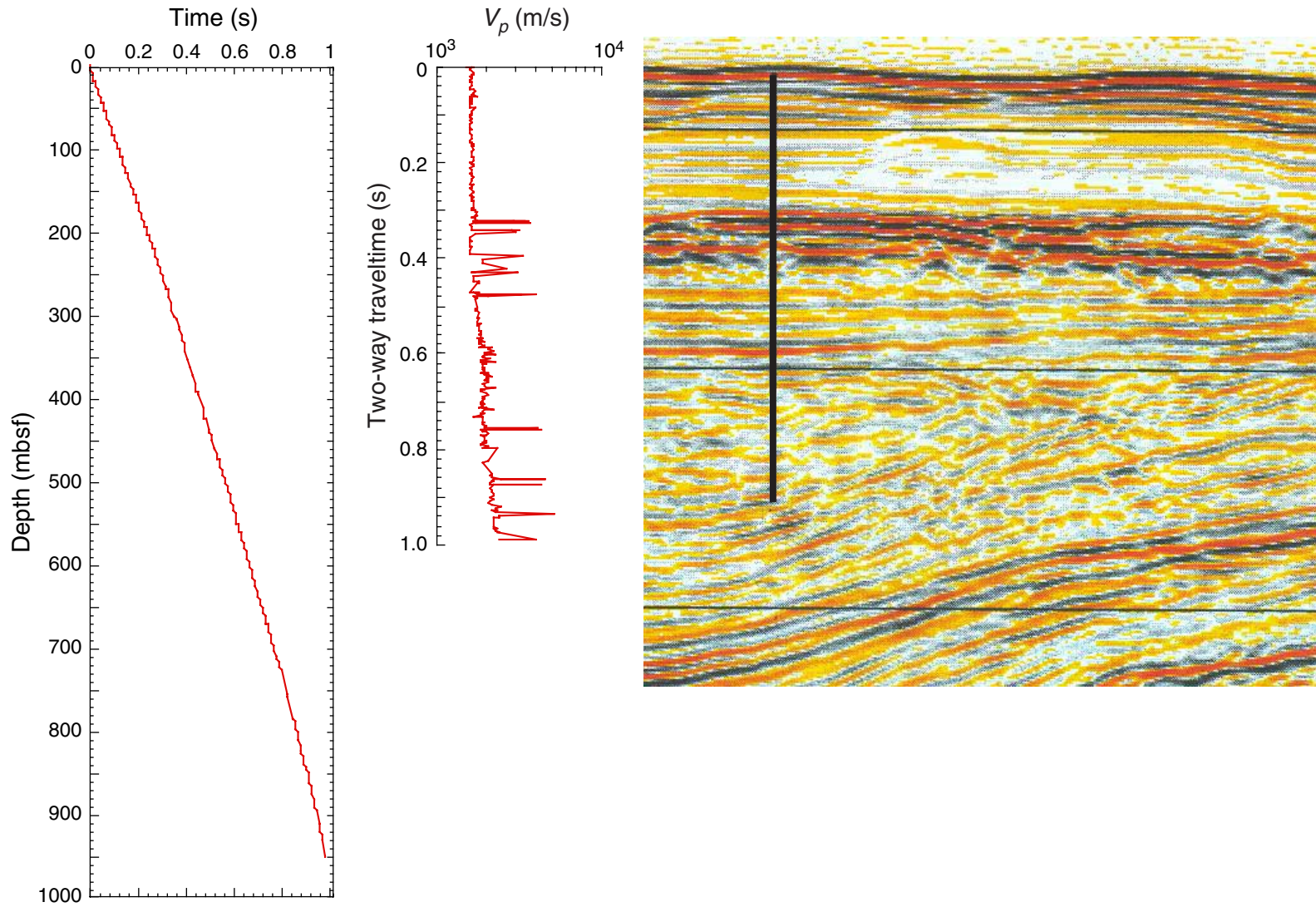
**Figure F52.** Downhole density plotted against natural gamma. The five log units (see **"Log Units,"** p. 58, in "Downhole Measurements" for details) tend to plot in different areas of the graph.
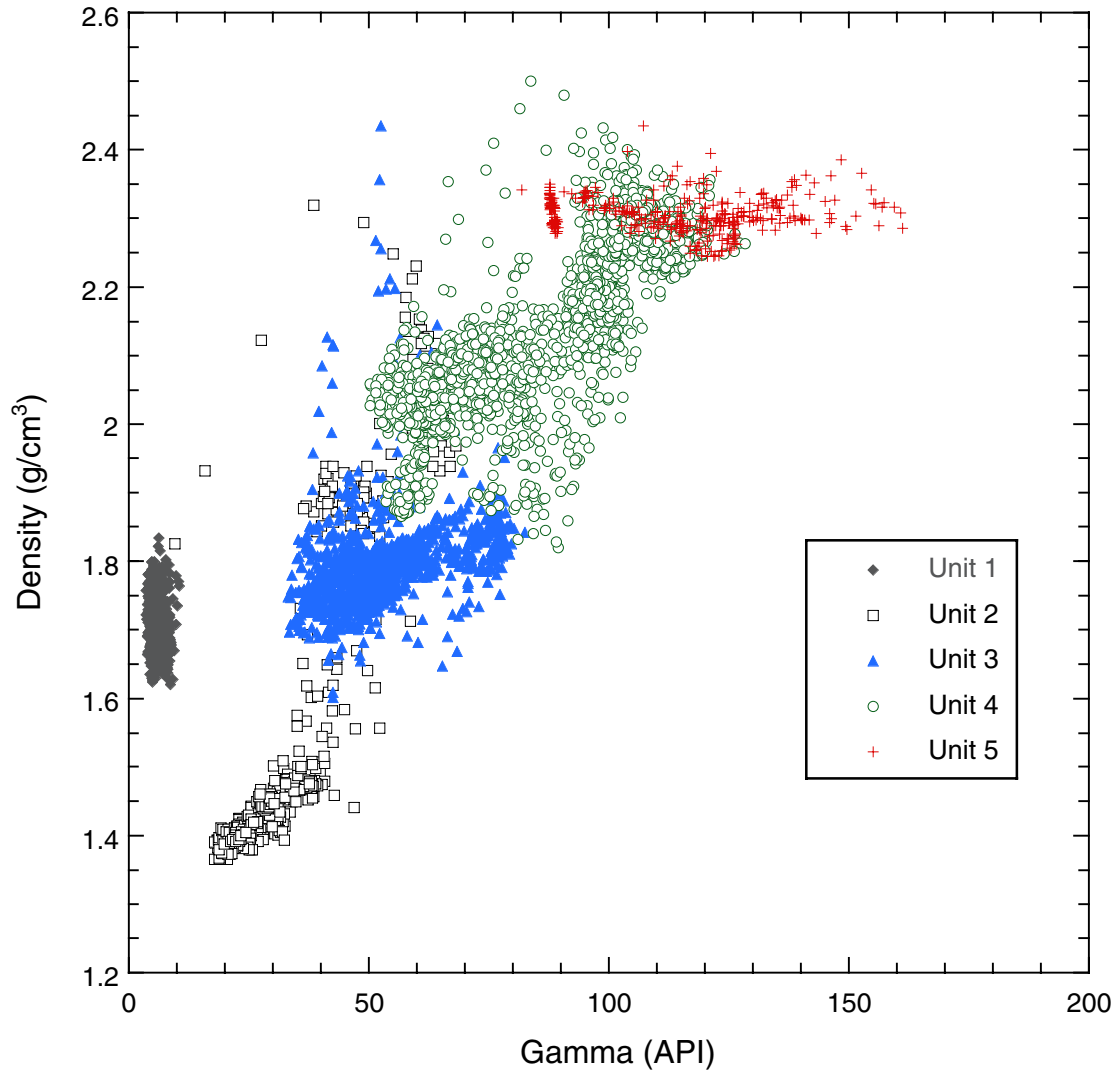
**Figure F53.** Detailed downhole spectral gamma-ray, porosity, density, photoelectric effect (PEFL), and resistivity logs between 400 and 500 mbsf showing a sequence of facies changes.
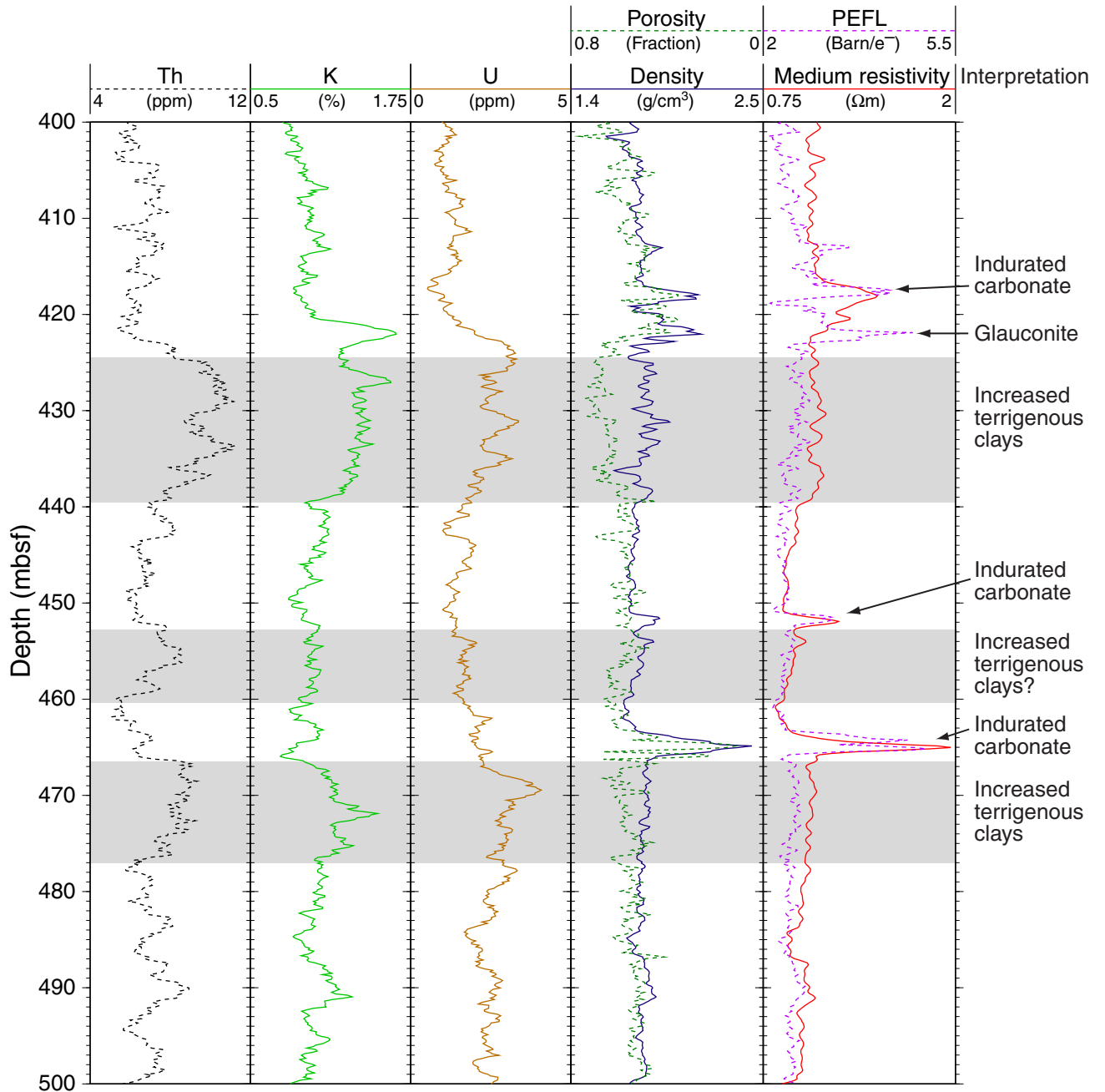
**Figure F54.** (**A, B**) Downhole spectral gamma-ray data for Th, and (**C**) preliminary power spectrum of Th between 334 and 422 mbsf using both the Blackman-Tukey (solid line) and maximum entropy (dashed line) methods. For the Blackman-Tukey method, 95% confidence is 0.49 < DP/P < 3.08.
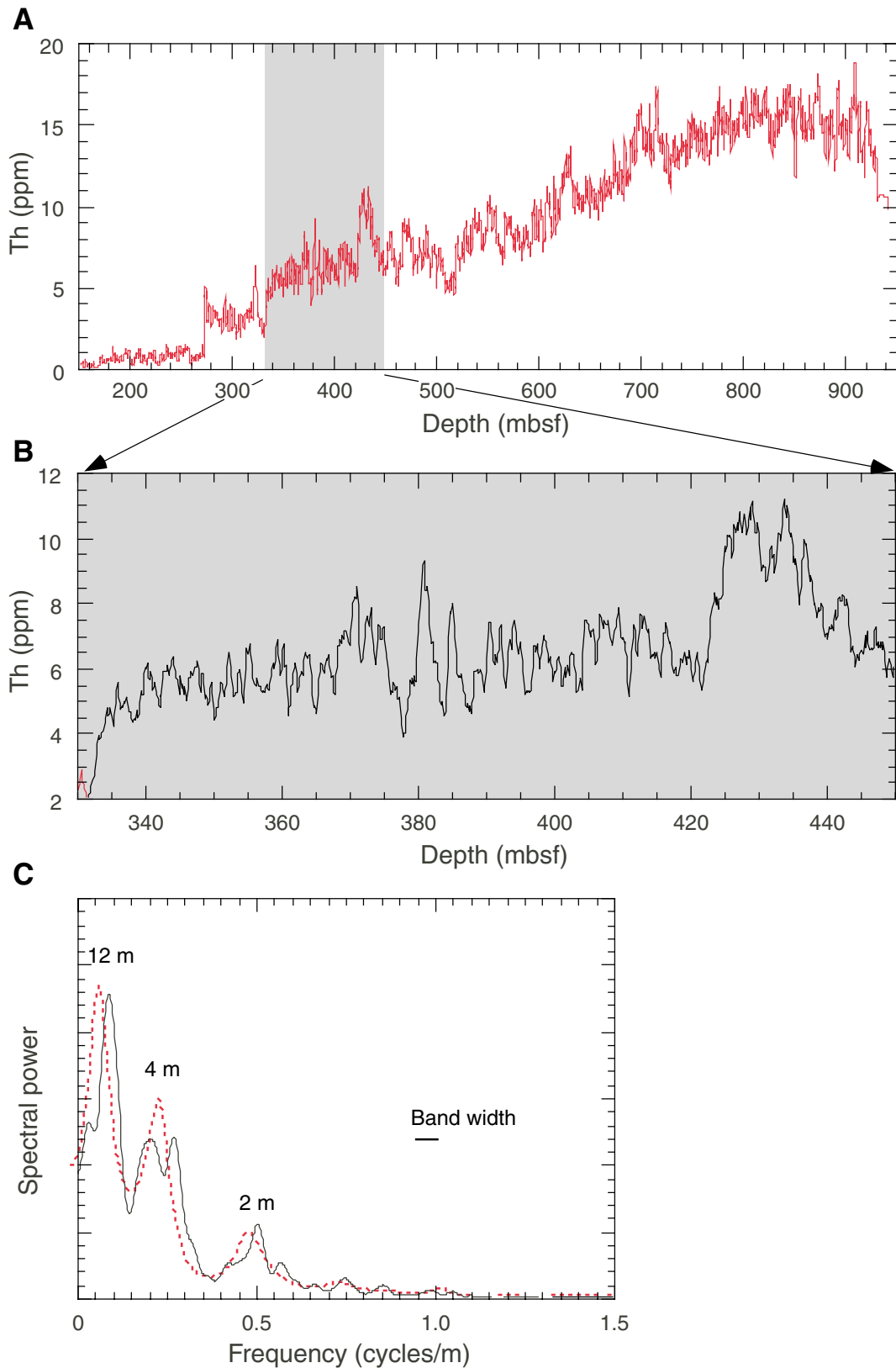
**Table T1.** Coring summary, Site 1171. (Continued on next two pages.)

**Hole 1171A**
Latitude: 48°29.9960'S
Longitude: 149°6.6901'E
Time on site: 240 hr (0645 hr, 12 April–0645 hr, 22 April 2000)
Time on hole: 21.75 hr (0645 hr, 12 April–0430, 13 April 2000)
Seafloor (drill pipe measurement from rig floor, mbrf): 2159.4
Distance between rig floor and sea level (m): 11.2
Water depth (drill pipe measurement from sea level, m): 2148.2
Total depth (from rig floor, mbrf): 2283.8
Total penetration (mbsf): 124.4
Total length of cored section (m): 124.4
Total core recovered (m): 117.52
Core recovery (%): 94.5
Total number of cores: 14

**Hole 1171B**
Latitude: 48°29.9854'S
Longitude: 149°6.6863'E
Time on hole: 11.25 hr (0430 hr, 13 April–1545 hr, 13 April 2000)
Seafloor (drill pipe measurement from rig floor, mbrf): 2159.2
Distance between rig floor and sea level (m): 11.2
Water depth (drill pipe measurement from sea level, m): 2148.0
Total depth (from rig floor, mbrf): 2268.0
Total penetration (mbsf): 108.8
Total length of cored section (m): 108.8
Total core recovered (m): 106.73
Core recovery (%): 98.1
Total number of cores: 12

**Hole 1171C**
Latitude: 48°29.9971'S
Longitude: 149°6.7051'E
Time on hole: 29.25 hr; 1 day, 5 hr, 15 min (1545 hr, 13 April–2100 hr, 14 April 2000)
Seafloor (drill pipe measurement from rig floor, mbrf): 2159.0
Distance between rig floor and sea level (m): 11.2
Water depth (drill pipe measurement from sea level, m): 2147.8
Total depth (from rig floor, mbrf): 2433.8
Total penetration (mbsf): 274.8
Total length of cored section (m): 274.8
Total core recovered (m): 245.58
Core recovery (%): 89.4
Total number of cores: 31

**Hole 1171D**
Latitude: 48°29.9975'S
Longitude: 149°6.7222'E
Time on hole: 177.75 hr; 7 days, 9 hr, 45 min (2100 hr, 14 April–0645 hr, 22 April 2000)
Seafloor (drill pipe measurement from rig floor, mbrf): 2159.0
Distance between rig floor and sea level (m): 11.2
Water depth (drill pipe measurement from sea level, m): 2147.8
Total depth (from rig floor, mbrf): 3117.8
Total penetration, mbsf: 958.8
Total length of cored section (m): 711.2
Total length of drilled intervals (m): 247.6
Total core recovered (m): 525.4
Core recovery (%): 73.9
Total number of cores: 75

| Core | Date (April 2000) | Local time | Depth (mbsf) Top | Depth (mbsf) Bottom | Length (m) Cored | Length (m) Recovered | Recovery (%) |
|---|---|---|---|---|---|---|---|
| 189-1171A- | | | | | | | |
| 1H | 12 | 1440 | 0.0 | 7.1 | 7.1 | 7.07 | 99.6 |
| 2H | 12 | 1540 | 7.1 | 16.6 | 9.5 | 9.07 | 95.5 |
| 3H | 12 | 1645 | 16.6 | 26.1 | 9.5 | 8.21 | 86.4 |
| 4H | 12 | 1740 | 26.1 | 35.6 | 9.5 | 9.73 | 102.4 |
| 5H | 12 | 1900 | 35.6 | 45.1 | 9.5 | 9.81 | 103.3 |
| 6H | 12 | 1950 | 45.1 | 54.6 | 9.5 | 10.12 | 106.5 |
| 7H | 12 | 2100 | 54.6 | 64.1 | 9.5 | 9.65 | 101.6 |
| 8H | 12 | 2145 | 64.1 | 73.6 | 9.5 | 9.00 | 94.7 |
| 9H | 12 | 2230 | 73.6 | 83.1 | 9.5 | 8.85 | 93.2 |
| 10H | 12 | 2315 | 83.1 | 92.6 | 9.5 | 9.61 | 101.2 |
| 11H | 13 | 0005 | 92.6 | 102.1 | 9.5 | 9.94 | 104.6 |
| 12H | 13 | 0115 | 102.1 | 111.6 | 9.5 | 8.57 | 90.2 |

Table T1 (continued).

| Core | Date (April 2000) | Local time | Depth (mbsf) Top | Depth (mbsf) Bottom | Length (m) Cored | Length (m) Recovered | Recovery (%) |
|------|------|------|------|------|------|------|------|
| 13X | 13 | 0225 | 111.6 | 114.8 | 3.2 | 2.11 | 65.9 |
| 14X | 13 | 0315 | 114.8 | 124.4 | 9.6 | 5.78 | 60.2 |
| | | | | Totals: | 124.4 | 117.52 | 94.5 |
| 189-1171B- | | | | | | | |
| 1H | 13 | 0600 | 0.0 | 4.3 | 4.3 | 4.26 | 99.1 |
| 2H | 13 | 0640 | 4.3 | 13.8 | 9.5 | 9.54 | 100.4 |
| 3H | 13 | 0730 | 13.8 | 23.3 | 9.5 | 9.42 | 99.2 |
| 4H | 13 | 0815 | 23.3 | 32.8 | 9.5 | 8.94 | 94.1 |
| 5H | 13 | 0910 | 32.8 | 42.3 | 9.5 | 9.28 | 97.7 |
| 6H | 13 | 0955 | 42.3 | 51.8 | 9.5 | 9.79 | 103.1 |
| 7H | 13 | 1035 | 51.8 | 61.3 | 9.5 | 8.99 | 94.6 |
| 8H | 13 | 1130 | 61.3 | 70.8 | 9.5 | 9.50 | 100.0 |
| 9H | 13 | 1220 | 70.8 | 80.3 | 9.5 | 9.48 | 99.8 |
| 10H | 13 | 1310 | 80.3 | 89.8 | 9.5 | 9.52 | 100.2 |
| 11H | 13 | 1400 | 89.8 | 99.3 | 9.5 | 8.18 | 86.1 |
| 12H | 13 | 1500 | 99.3 | 108.8 | 9.5 | 9.83 | 103.5 |
| | | | | Totals: | 108.8 | 106.73 | 98.1 |
| 189-1171C- | | | | | | | |
| 1H | 13 | 1700 | 0.0 | 9.5 | 9.5 | 9.70 | 102.1 |
| 2H | 13 | 1735 | 9.5 | 19.0 | 9.5 | 9.79 | 103.1 |
| 3H | 13 | 1845 | 19.0 | 28.5 | 9.5 | 9.61 | 101.2 |
| 4H | 13 | 1930 | 28.5 | 38.0 | 9.5 | 9.35 | 98.4 |
| 5H | 13 | 2040 | 38.0 | 47.5 | 9.5 | 9.91 | 104.3 |
| 6H | 13 | 2130 | 47.5 | 57.0 | 9.5 | 9.99 | 105.2 |
| 7H | 13 | 2220 | 57.0 | 66.5 | 9.5 | 10.18 | 107.2 |
| 8H | 13 | 2305 | 66.5 | 76.0 | 9.5 | 8.89 | 93.6 |
| 9H | 13 | 2355 | 76.0 | 85.5 | 9.5 | 9.69 | 102.0 |
| 10H | 14 | 0040 | 85.5 | 95.0 | 9.5 | 8.98 | 94.5 |
| 11H | 14 | 0130 | 95.0 | 104.5 | 9.5 | 9.20 | 96.8 |
| 12X | 14 | 0235 | 104.5 | 110.2 | 5.7 | 5.47 | 96.0 |
| 13X | 14 | 0320 | 110.2 | 115.2 | 5.0 | 5.57 | 111.4 |
| 14X | 14 | 0405 | 115.2 | 124.8 | 9.6 | 8.34 | 86.9 |
| 15X | 14 | 0435 | 124.8 | 134.5 | 9.7 | 9.70 | 100.0 |
| 16X | 14 | 0515 | 134.5 | 144.1 | 9.6 | 5.21 | 54.3 |
| 17X | 14 | 0600 | 144.1 | 153.7 | 9.6 | 6.13 | 63.9 |
| 18X | 14 | 0630 | 153.7 | 163.3 | 9.6 | 9.28 | 96.7 |
| 19X | 14 | 0705 | 163.3 | 172.9 | 9.6 | 9.51 | 99.1 |
| 20X | 14 | 0740 | 172.9 | 182.2 | 9.3 | 8.27 | 88.9 |
| 21X | 14 | 0810 | 182.2 | 191.8 | 9.6 | 7.96 | 82.9 |
| 22X | 14 | 0845 | 191.8 | 201.5 | 9.7 | 7.18 | 74.0 |
| 23X | 14 | 0920 | 201.5 | 211.1 | 9.6 | 8.67 | 90.3 |
| 24X | 14 | 0955 | 211.1 | 220.7 | 9.6 | 8.69 | 90.5 |
| 25X | 14 | 1030 | 220.7 | 230.3 | 9.6 | 7.83 | 81.6 |
| 26X | 14 | 1105 | 230.3 | 239.6 | 9.3 | 7.31 | 78.6 |
| 27X | 14 | 1200 | 239.6 | 248.9 | 9.3 | 7.78 | 83.7 |
| 28X | 14 | 1245 | 248.9 | 258.5 | 9.6 | 4.94 | 51.5 |
| 29X | 14 | 1340 | 258.5 | 268.1 | 9.6 | 6.38 | 66.5 |
| 30X | 14 | 1445 | 268.1 | 273.5 | 5.4 | 4.92 | 91.1 |
| 31X | 14 | 1620 | 273.5 | 274.8 | 1.3 | 1.15 | 88.5 |
| | | | | Totals: | 274.8 | 245.58 | 89.4 |
| 189-1171D- | | | | | | | |
| Drilled interval | | | 0.0 | 100.0 | | | |
| Drilled interval | | | 100.0 | 247.6 | | | |
| 1R | 15 | 1340 | 247.6 | 257.0 | 9.4 | 2.72 | 28.9 |
| 2R | 15 | 1440 | 257.0 | 266.6 | 9.6 | 3.73 | 38.9 |
| 3R | 15 | 1710 | 266.6 | 276.2 | 9.6 | 4.79 | 49.9 |
| 4R | 15 | 1825 | 276.2 | 285.8 | 9.6 | 4.44 | 46.3 |
| 5R | 15 | 2120 | 285.8 | 293.8 | 8.0 | 1.84 | 23.0 |
| 6R | 15 | 2310 | 293.8 | 300.4 | 6.6 | 1.51 | 22.9 |
| 7R | 16 | 0005 | 300.4 | 305.4 | 5.0 | 1.95 | 39.0 |
| 8R | 16 | 0100 | 305.4 | 314.7 | 9.3 | 2.49 | 26.8 |
| 9R | 16 | 0155 | 314.7 | 324.3 | 9.6 | 4.12 | 42.9 |
| 10R | 16 | 0240 | 324.3 | 333.9 | 9.6 | 6.53 | 68.0 |
| 11R | 16 | 0435 | 333.9 | 343.5 | 9.6 | 0.13 | 1.4 |
| 12R | 16 | 0605 | 343.5 | 353.2 | 9.7 | 0.19 | 2.0 |
| 13R | 16 | 0735 | 353.2 | 362.8 | 9.6 | 0.15 | 1.6 |
| 14R | 16 | 0855 | 362.8 | 372.4 | 9.6 | 0.53 | 5.5 |
| 15R | 16 | 1015 | 372.4 | 382.0 | 9.6 | 2.00 | 20.8 |

**Table T1 (continued).**

| Core | Date (April 2000) | Local time | Depth (mbsf) Top | Bottom | Length (m) Cored | Recovered | Recovery (%) |
|---|---|---|---|---|---|---|---|
| 16R | 16 | 1135 | 382.0 | 391.6 | 9.6 | 3.23 | 33.7 |
| 17R | 16 | 1310 | 391.6 | 401.2 | 9.6 | 6.85 | 71.4 |
| 18R | 16 | 1440 | 401.2 | 410.8 | 9.6 | 0.03 | 0.3 |
| 19R | 16 | 1805 | 410.8 | 420.4 | 9.6 | 6.88 | 71.7 |
| 20R | 16 | 1940 | 420.4 | 430.0 | 9.6 | 8.31 | 86.6 |
| 21R | 16 | 2110 | 430.0 | 439.6 | 9.6 | 0.38 | 4.0 |
| 22R | 16 | 2255 | 439.6 | 449.2 | 9.6 | 9.29 | 96.8 |
| 23R | 17 | 0030 | 449.2 | 458.8 | 9.6 | 4.43 | 46.2 |
| 24R | 17 | 0240 | 458.8 | 468.5 | 9.7 | 5.57 | 57.4 |
| 25R | 17 | 0430 | 468.5 | 478.1 | 9.6 | 8.36 | 87.1 |
| 26R | 17 | 0600 | 478.1 | 487.7 | 9.6 | 9.93 | 103.4 |
| 27R | 17 | 0750 | 487.7 | 497.3 | 9.6 | 9.80 | 102.1 |
| 28R | 17 | 0910 | 497.3 | 507.0 | 9.7 | 8.48 | 87.4 |
| 29R | 17 | 1030 | 507.0 | 516.6 | 9.6 | 9.84 | 102.5 |
| 30R | 17 | 1205 | 516.6 | 526.2 | 9.6 | 8.03 | 83.7 |
| 31R | 17 | 1330 | 526.2 | 535.8 | 9.6 | 7.58 | 79.0 |
| 32R | 17 | 1455 | 535.8 | 545.5 | 9.7 | 8.21 | 84.6 |
| 33R | 17 | 1630 | 545.5 | 555.1 | 9.6 | 9.57 | 99.7 |
| 34R | 17 | 1750 | 555.1 | 564.7 | 9.6 | 9.74 | 101.5 |
| 35R | 17 | 1915 | 564.7 | 574.3 | 9.6 | 9.21 | 95.9 |
| 36R | 17 | 2145 | 574.3 | 583.9 | 9.6 | 9.85 | 102.6 |
| 37R | 17 | 2215 | 583.9 | 593.6 | 9.7 | 9.72 | 100.2 |
| 38R | 17 | 2340 | 593.6 | 603.2 | 9.6 | 9.67 | 100.7 |
| 39R | 18 | 0055 | 603.2 | 612.8 | 9.6 | 8.70 | 90.6 |
| 40R | 18 | 0220 | 612.8 | 622.4 | 9.6 | 9.95 | 103.7 |
| 41R | 18 | 0340 | 622.4 | 632.0 | 9.6 | 8.79 | 91.6 |
| 42R | 18 | 0455 | 632.0 | 641.6 | 9.6 | 9.86 | 102.7 |
| 43R | 18 | 0610 | 641.6 | 651.3 | 9.7 | 9.46 | 97.5 |
| 44R | 18 | 0725 | 651.3 | 660.9 | 9.6 | 9.46 | 98.5 |
| 45R | 18 | 0835 | 660.9 | 670.5 | 9.6 | 5.01 | 52.2 |
| 46R | 18 | 1000 | 670.5 | 680.2 | 9.7 | 7.34 | 75.7 |
| 47R | 18 | 1130 | 680.2 | 689.9 | 9.7 | 10.09 | 104.0 |
| 48R | 18 | 1300 | 689.9 | 699.5 | 9.6 | 9.65 | 100.5 |
| 49R | 18 | 1425 | 699.5 | 709.1 | 9.6 | 9.92 | 103.3 |
| 50R | 18 | 1545 | 709.1 | 718.7 | 9.6 | 9.43 | 98.2 |
| 51R | 18 | 1705 | 718.7 | 728.3 | 9.6 | 8.30 | 86.5 |
| 52R | 18 | 1840 | 728.3 | 737.9 | 9.6 | 9.86 | 102.7 |
| 53R | 18 | 2005 | 737.9 | 747.5 | 9.6 | 7.95 | 82.8 |
| 54R | 18 | 2130 | 747.5 | 757.1 | 9.6 | 9.81 | 102.2 |
| 55R | 18 | 2300 | 757.1 | 766.7 | 9.6 | 9.90 | 103.1 |
| 56R | 19 | 0035 | 766.7 | 776.3 | 9.6 | 4.75 | 49.5 |
| 57R | 19 | 0215 | 776.3 | 785.9 | 9.6 | 5.48 | 57.1 |
| 58R | 19 | 0350 | 785.9 | 795.5 | 9.6 | 9.64 | 100.4 |
| 59R | 19 | 0530 | 795.5 | 805.1 | 9.6 | 9.87 | 102.8 |
| 60R | 19 | 0700 | 805.1 | 814.7 | 9.6 | 9.55 | 99.5 |
| 61R | 19 | 0840 | 814.7 | 824.3 | 9.6 | 7.95 | 82.8 |
| 62R | 19 | 1025 | 824.3 | 833.9 | 9.6 | 9.90 | 103.1 |
| 63R | 19 | 1210 | 833.9 | 843.5 | 9.6 | 9.96 | 103.8 |
| 64R | 19 | 1350 | 843.5 | 853.1 | 9.6 | 8.56 | 89.2 |
| 65R | 19 | 1540 | 853.1 | 862.7 | 9.6 | 9.95 | 103.7 |
| 66R | 19 | 1715 | 862.7 | 872.3 | 9.6 | 8.09 | 84.3 |
| 67R | 19 | 1920 | 872.3 | 881.7 | 9.4 | 9.97 | 106.1 |
| 68R | 19 | 2150 | 881.7 | 891.3 | 9.6 | 7.77 | 80.9 |
| 69R | 19 | 2320 | 891.3 | 900.9 | 9.6 | 9.84 | 102.5 |
| 70R | 20 | 0145 | 900.9 | 910.5 | 9.6 | 7.22 | 75.2 |
| 71R | 20 | 0345 | 910.5 | 920.2 | 9.7 | 8.67 | 89.4 |
| 72R | 20 | 0545 | 920.2 | 929.9 | 9.7 | 9.14 | 94.2 |
| 73R | 20 | 0740 | 929.9 | 939.5 | 9.6 | 9.66 | 100.6 |
| 74R | 20 | 0945 | 939.5 | 949.2 | 9.7 | 0.08 | 0.8 |
| 75R | 20 | 1205 | 949.2 | 958.8 | 9.6 | 5.79 | 60.3 |
| | | | Coring totals: | | 711.2 | 525.40 | 73.9 |
| | | | Drilled totals: | | 247.6 | | |
| | | | Totals: | | 958.8 | | |

**Table T2.** Lithostratigraphic summary, Site 1171.

| Lithostratigraphic unit and subunit | Series | Core intervals | Lithology | Depth (mbsf) | Comments |
|---|---|---|---|---|---|
| IA | Holocene to lower Pliocene | 1171A-1H to 5H; 1171B-1H to 5H; 1171C-1H to 5H | Foraminifer-bearing nannofossil ooze to diatom-bearing nannofossil ooze and nannofossil ooze | 0-41.0 | Contains a high foraminiferal content (up to 50%). |
| IB | lower Pliocene to lowermost Miocene | 1171A-6H to 14X; 1171B-6H to 12H; 1171C-6H to 25X | Foraminifer-bearing nannofossil chalk to diatom-bearing nannofossil chalk and foraminifer-bearing clay nannofossil chalk | 41.0-124.4 41.0-108.8 41.0-233.7 | Rare to occasional detrital silt-size glauconite caused by bottom current action. |
| II | Oligocene | 1171C-28X to 30X; 1171D-2R to 3R | Foraminifer-bearing nannofossil chalk to foraminiferal nannofossil chalk | 253.4-272.8 257.0-269.8 | Downsection increase in glauconite, clay, accessory minerals, quartz, radiolarians, bioclasts, sponge spicules, and volcanic glass and a decrease in biogenic carbonates. Dramatic lithologic contact at base. |
| III | uppermost Eocene | 1171C-30X to 31X 1171D-3R | Glauconitic sandy silt to clayey glauconitic siltstone | 272.8-274.8 269.8-276.2 | Thin, highly bioturbated glauconitic unit below major lithologic transition. |
| IV | upper Eocene | 1171D-4R to 11R | Diatom-bearing claystone, diatom and nannofossil-bearing claystone, diatomaceous claystone | 276.2-343.5 | Alternating lithified and unlithified strata, limited recovery. |
| VA | upper to middle Eocene | 1171D-11R to 20R | Claystone, nannofossil-bearing claystone | 343.50-421.50 | Alternating darker and lighter strata at the decimeter to meter scale. Lighter colored intervals contain higher nannofossil and lower organic material percentages than darker intervals. There is a prominent surface at the base of this subunit. |
| VB | middle Eocene | 1171D-20R to 26R | Claystone to occasional organic-bearing claystone | 421.50-485.70 | Higher organic and lower nannofossil percentages in the upper and lower intervals with slightly elevated nannofossil contents and lower organic matter content within the middle section. |
| VC | middle Eocene | 1171D-26R to 48R | Claystone, silty claystone, to nannofossil claystone | 485.70-692.49 | Overall increase in lightness and nannofossil percentages from the unit above. High-frequency oscillations in the lighter and darker strata at the decimeter to meter scale for most of this subunit. |
| VIA | lower Eocene | 1171D-48R to 59R | Claystone, silty claystone, nannofossil-bearing silty claystone | 692.49-805.1 | An overall decrease in nannofossil abundance (to <1%) is accompanied by a rise in quartz silt from the unit above. |
| VIB | lower Eocene to upper Paleocene | 1171D-59R to 75R | Organic matter-bearing silty claystone, silty claystone, organic matter-bearing clayey siltstone | 805.1-958.8 | Quartz, organic debris, and opaque minerals increase downsection. Bioturbation diminishes downsection with laminations occurring in the last two cores. No obvious lithologic change across the Paleocene and Eocene boundary. |

**Table T3.** Identification and abundances of nannofossils, Site 1171. (**See table notes.** Continued on next seven pages.)

| Core, section, interval (cm) | Depth (mbsf) | Preservation | Group abundance | Amaurolithus delicatus | Amaurolithus tricorniculatus | Calcidiscus leptoporus | Calcidiscus macintyrei | Calcidiscus premacintyrei | Chiasmolithus altus | Chiasmolithus consuetus | Chiasmolithus expansus | Chiasmolithus medius | Chiasmolithus nitidus | Chiasmolithus solitus | Chiasmolithus spp. | Coccolithus miopelagicus | Coccolithus pelagicus | Cyclicargolithus abisectus | Cyclicargolithus floridanus | Dictyococcites bisectus | Discoaster asymmetricus | Discoaster deflandrei | Discoaster distinctus | Discoaster intercalaris | Discoaster kuepperi | Discoaster kugleri | Discoaster lodoensis | Discoaster spp. | Discoaster surculus | Discoaster tamalis | Discoaster variabilis | Ellipsolithus lajollaensis | Ericsonia formosa | Gephyrocapsa >4.5 μm | Gephyrocapsa spp. (small) | Helicosphaera intermedia | Helicosphaera kamptneri | Helicosphaera spp. | Neococcolithes dubius | Pontosphaera spp. | Princius bisulcus | Pseudoemiliania lacunosa | Reticulofenestra dictyoda | Reticulofenestra gelida | Reticulofenestra minuta | Reticulofenestra oamaruensis | Reticulofenestra perplexa | Reticulofenestra psuedoumbilica |
|---|---|---|---|---|---|---|---|---|---|---|---|---|---|---|---|---|---|---|---|---|---|---|---|---|---|---|---|---|---|---|---|---|---|---|---|---|---|---|---|---|---|---|---|---|---|---|---|---|
| **189-1171A-** | | | | | | | | | | | | | | | | | | | | | | | | | | | | | | | | | | A | A | | | | | | | | | | | | | |
| 1H-CC, 8-13 | 7.02 | G | A | | | | | | | | | | | | | | | | | | | | | | | | | | | | | | | A | A | | | | | | | | | | | | | |
| 2H-CC, 18-25 | 16.10 | G | A | | | A | | | | | | | | | | | A | | | | | | | | | | | | | | | | | A | A | | | | | | | | | | | | | |
| 3H-CC, 17-22 | 24.76 | G | A | | | | C | | | | | | | | | | A | | | | | | | | | | | | | | | | | | | | | | | | | | F | | | | | |
| 4H-CC, 20-25 | 35.78 | G | A | | | | C | C | | | | | | | | | C | | | | | | | | | | | | | | | | | | | | | | | | | | | F | | | | |
| 5H-CC, 18-23 | 45.36 | G | A | | | | | C | | | | | | | | | | | | | | | | | | | | | | | | | | | | | | | | | | | | F | | | | |
| 6H-CC, 17-22 | 55.17 | G | A | R | | | A | C | | | | | | | | | | | | | R | | | | | | | | | R | | | | | | | | | | | | | | | C | | | | |
| 7H-CC, 25-30 | 64.20 | G | A | | | | | | | | | | | | | | C | | | | | | | | | | | | | R | | | | | | | | | | | | | | | A | | V | | |
| 8H-CC, 14-19 | 73.05 | G | A | | | | | C | | | | | | | | | | | | | | | | | | | | | | | | | | | | | | | | | | | | A | | | | |
| 9H-CC, 19-24 | 82.40 | G | A | | | | | C | | | | | | | | | | | | | | | | | | | | | | | | | | | | | | | | | | | | A | | | | |
| 10H-CC, 14-19 | 92.66 | G | A | | | | C | C | | | | | | | | | | | | | | | | | | | | | | | | | | | | | | | | | | | | A | | | | |
| 11H-CC, 13-18 | 102.49 | M | A | | | | A | A | | | | | | | | | A | | | | | | | | | | | | | F | | | | | | | | | | | | | | | A | | | | C |
| 12H-CC, 5-10 | 110.62 | M | A | | | | C | C | | | | | | | | | A | | | | | | | | | | | | | | | | | | | | | | R | | | | | | V | | | | F |
| 13X-CC, 20-25 | 113.66 | M | A | | | | C | F | | | | | | | | | F | | | | | | | | | | | | | | | | | | | | | | | | | | | | V | | | C | |
| 14X-CC, 15-20 | 120.53 | M | A | | | | C | F | | | | | | | A | | C | | | | | | | | | | | | | | | | | | | | | | | | | | | | A | | | | |
| **189-1171B-** | | | | | | | | | | | | | | | | | | | | | | | | | | | | | | | | | | | | | | | | | | | | | | | |
| 1H-CC, 9-14 | 4.21 | G | A | | | | | | | | | | | | | | C | | | | | | | | | | | | | | | | | | | A | | | | | | | | | | | | | |
| 2H-CC, 15-20 | 13.79 | G | A | | | C | | | | | | | | | | | A | | | | | | | | | | | | | | | | | | | | | F | | | | F | F | | | | | |
| 3H-CC, 14-19 | 23.17 | G | A | | | C | C | | | | | | | | | | C | | | | | | | | | | | | | | | | | | | | | | | | | | | | | | | | |
| 4H-CC, 13-18 | 32.19 | G | A | | | C | C | | | | | | | | | | C | | | | | | | | | | | | | | | | | | | | | | | | | | | | A | | | | |
| 5H-CC, 4-9 | 42.03 | M | A | | | C | | | | | | | | | | | C | | | | | | | | | | | | | | | | | | | | | | | | | | | | V | | | | |
| 6H-CC, 13-18 | 52.04 | M | A | R | R | A | | | | | | | | | | | F | | | | | | | | | | | | | | | | | | | | | | | | | | | F | A | | | |
| 7H-CC, 15-20 | 60.74 | M | A | | | C | | | | | | | | | | | C | | | | | | | | | | | | F | F | R | | | | | | | | | | | | | A | | | | C |
| 8H-CC, 14-19 | 70.75 | G | A | | | | | | | | | | | | | | | | | | | | | | | | | | | F | R | | | | | | | | | | | | | | A | | | | |
| 9H-CC, 8-13 | 80.23 | G | A | | | | | | | | | | | | | | | | | | | | | | | | | | | | | R | | | | | | | | | | | | | A | | | | |
| 10H-CC, 14-19 | 89.77 | G | A | | | | | | | | | | | | | | | | | | | | | | | | | | | | | | | | | | | | | | | | | A | | | | |
| 11H-CC, 13-18 | 97.93 | M | A | | | | | | | | | | | | | | | | | | | | | | | | | | | | | | | | | | | | | | | | | A | | | | |
| 12H-CC, 11-18 | 109.06 | M | A | | | | | | | | | | | | | | | | | | | | | | | | | | | | | | | | | | | | | | | | | A | | A | | |
| **189-1171C-** | | | | | | | | | | | | | | | | | | | | | | | | | | | | | | | | | | | | | | | | | | | | | | | |
| 1H-CC, 6-11 | 9.65 | G | A | | | | | | | | | | | | | | | | | | | | | | | | | | | | | | | C | | | | | | | | C | | | | | | |
| 2H-CC, 8-13 | 19.24 | G | A | | | C | | | | | | | | | | | | | | | | | | | | | | | | | | | | A | | | | | | | | | | | | | | |
| 3H-CC, 17-22 | 28.56 | G | A | | | C | F | | | | | | | | | | | | | | | | | | | | | | | | | | | | | | | | | | | | | | | | | |
| 4H-CC, 14-19 | 37.80 | G | A | | | C | R | | | | | | | | | | | | | | | | | | | | | | | | | | | | | | | | | | | | | C | | | | |
| 5H-CC, 17-22 | 47.86 | G | A | | | C | C | | | | | | | | | | | | | | | | | | | | | | | | | | | | | | | | | | | | | A | | | | |
| 6H-CC, 18-22 | 57.45 | G | A | | | C | C | | | | | | | | | | | | | | | | | | | | | | | | | | | | | | | | | | | | | A | | | | |
| 7H-CC, 23-28 | 67.13 | G | A | | | C | C | | | | | | | | | | | | | | | | | | | | | | | | | | | | | | | | | | | | | A | | | | |
| 8H-CC, 0-6 | 75.33 | G | A | | | C | C | | | | | | | | | | | | | | | | | | | | | | | | | | | | | | | | | | | | | A | | | | |
| 9H-CC, 12-17 | 85.64 | M | A | | | C | F | | | | | | | | | | | | | | | | | | | | | | R | | | | | | | | | | | | | | | A | | | C | |
| 10H-CC, 14-22 | 94.40 | M | A | | | | F | | | | | | | | | | C | | | | | | | | | | | | R | | | | | | | | | | | | | | | A | | | | C |

# Table T3 (continued).

| Core, section, interval (cm) | Depth (mbsf) | Preservation | Group abundance | Reticulofenestra reticulata | Reticulofenestra samodurovii | Reticulofenestra spp. | Reticulofenestra umbilicus | Sphenolithus moriformis | Sphenolithus primus | Sphenolithus radians | Sphenolithus spiniger | Sphenolithus spp. | Toweius callosus | Toweius pertusus | Transversopontis pulcher | Transversopontis pulcheroides | Transversopontis rectipons | Triquetrorhabdulus rugosus | Zygrhablithus bijugatus |
|---|---|---|---|---|---|---|---|---|---|---|---|---|---|---|---|---|---|---|---|
| **189-1171A-** | | | | | | | | | | | | | | | | | | | |
| 1H-CC, 8-13 | 7.02 | G | A | | | | | | | | | | | | | | | | |
| 2H-CC, 18-25 | 16.10 | G | A | | | | | | | | | | | | | | | | |
| 3H-CC, 17-22 | 24.76 | G | A | | | | | | | | | | | | | | | | |
| 4H-CC, 20-25 | 35.78 | G | A | | | | | | | | | | | | | | | | |
| 5H-CC, 18-23 | 45.36 | G | A | | | | | | | | | | | | | | | | |
| 6H-CC, 17-22 | 55.17 | G | A | | | | | | | | | | | | | | | | |
| 7H-CC, 25-30 | 64.20 | G | A | | | | | | | | | | | | | | | | |
| 8H-CC, 14-19 | 73.05 | G | A | | | | | | | | | | | | | | | F | |
| 9H-CC, 19-24 | 82.40 | G | A | | | | | | | | | | | | | | | | |
| 10H-CC, 14-19 | 92.66 | G | A | | | | | | | | | | | | | | | | |
| 11H-CC, 13-18 | 102.49 | M | A | | | | | | F | | | | | | | | | | |
| 12H-CC, 5-10 | 110.62 | M | A | | | | | | | | | | | | | | | | |
| 13X-CC, 20-25 | 113.66 | M | A | | | | | | | | | | | | | | | | |
| 14X-CC, 15-20 | 120.53 | M | A | | | | | | | | | | | | | | | | |
| **189-1171B-** | | | | | | | | | | | | | | | | | | | |
| 1H-CC, 9-14 | 4.21 | G | A | | | | | | | | | | | | | | | | |
| 2H-CC, 15-20 | 13.79 | G | A | | | | F | | | | | | | | | | | | |
| 3H-CC, 14-19 | 23.17 | G | A | | | | | | | | | | | | | | | | |
| 4H-CC, 13-18 | 32.19 | G | A | | | | | | | | | | | | | | | | |
| 5H-CC, 4-9 | 42.03 | M | A | | | | | | | | | | | | | | | | |
| 6H-CC, 13-18 | 52.04 | M | A | | | | | | | | | | | | | | | | |
| 7H-CC, 15-20 | 60.74 | M | A | | | | | | | | | | | | | | | | |
| 8H-CC, 14-19 | 70.75 | G | A | | | | | | | | | | | | | | | R | |
| 9H-CC, 8-13 | 80.23 | G | A | | | | | | | | | | | | | | | | |
| 10H-CC, 14-19 | 89.77 | G | A | | | | | | | | | | | | | | | | |
| 11H-CC, 13-18 | 97.93 | M | A | | | | | | | | | | | | | | | R | |
| 12H-CC, 11-18 | 109.06 | M | A | | | | | | | | | | | | | | | | |
| **189-1171C-** | | | | | | | | | | | | | | | | | | | |
| 1H-CC, 6-11 | 9.65 | G | A | | | | | | | | | | | | | | | | |
| 2H-CC, 8-13 | 19.24 | G | A | | | | | | | | | | | | | | | | |
| 3H-CC, 17-22 | 28.56 | G | A | | | | | | | | | | | | | | | | |
| 4H-CC, 14-19 | 37.80 | G | A | | | | | | | | | | | | | | | | |
| 5H-CC, 17-22 | 47.86 | G | A | | | | | | | | | | | | | | | | |
| 6H-CC, 18-22 | 57.45 | G | A | | | | | | | | | | | | | | | | |
| 7H-CC, 23-28 | 67.13 | G | A | | | | | | | | | | | | | | | R | |
| 8H-CC, 0-6 | 75.33 | G | A | | | | | | | | | | | | | | | | |
| 9H-CC, 12-17 | 85.64 | M | A | | | | | | | | | | | | | | | | |
| 10H-CC, 14-22 | 94.40 | M | A | | | | | | F | | | | | | | | | | |

# Table T3 (continued).

| Core, section, interval (cm) | Depth (mbsf) | Preservation | Group abundance | Amaurolithus delicatus | Amaurolithus tricorniculatus | Calcidiscus leptoporus | Calcidiscus macintyrei | Calcidiscus premacintyrei | Chiasmolithus altus | Chiasmolithus consuetus | Chiasmolithus expansus | Chiasmolithus medius | Chiasmolithus nitidus | Chiasmolithus solitus | Chiasmolithus spp. | Coccolithus miopelagicus | Coccolithus pelagicus | Cyclicargolithus abisectus | Cyclicargolithus floridanus | Dictyococcites bisectus | Discoaster asymmetricus | Discoaster deflandrei | Discoaster distinctus | Discoaster intercalaris | Discoaster kuepperi | Discoaster kugleri | Discoaster lodoensis | Discoaster spp. | Discoaster surculus | Discoaster tamalis | Discoaster variabilis | Ellipsolithus lajollaensis | Ericsonia formosa | Gephyrocapsa > 4.5 | Gephyrocapsa spp. (small) | Helicosphaera intermedia | Helicosphaera kamptneri | Helicosphaera spp. | Neococcolithes dubius | Pontosphaera spp. | Princius bisulcus | Pseudoemiliania lacunosa | Reticulofenestra dictyoda | Reticulofenestra gelida | Reticulofenestra minuta | Reticulofenestra oamaruensis | Reticulofenestra perplexa | Reticulofenestra psuedoumbilica |
|---|---|---|---|---|---|---|---|---|---|---|---|---|---|---|---|---|---|---|---|---|---|---|---|---|---|---|---|---|---|---|---|---|---|---|---|---|---|---|---|---|---|---|---|---|---|---|---|---|
| 11H-CC, 0-8 | 104.12 | M | A | | | C | R | | | | | | | | | F | | | | | | | | | | | | | | | | | | | | | | | | | | | | | A | | | | |
| 12X-CC, 11-16 | 109.92 | M | A | | | C | C | | | | | | | | | | C | | | | | | | | | | | | | | | | | | | | | | | | | | | | A | | | | F |
| 13X-CC, 13-18 | 115.72 | M | A | | | A | A | | | | | | | | | | C | | | | | | | | | | | | | | | | | | | | | | | | | | | | A | | | F | C |
| 14X-CC, 13-18 | 123.49 | M | A | | | C | | | | | | | | | | C | | | | | | | | | | | | | | | | | | | | | | | | | | | | | A | | | | |
| 15X-CC, 13-18 | 134.45 | M | A | | | C | C | | | | | | | | | | A | | | | | | | | | | | | | | | | | | | | | | | | | | | | A | | | | C |
| 16X-CC, 17-22 | 139.66 | M | A | | | C | F | | | | | | | | | C | | | | | | | | | | | | | | | | | | | | R | | | | | | | | | A | | | | F |
| 17X-CC, 11-16 | 150.18 | M | A | | | | C | | | | | | | | | | A | | | | | | | | | | | | | | | | | | | | | | | | | | | | C | | | | |
| 18X-CC, 16-21 | 162.93 | M | A | | | | | F | | | | | | | | | A | | A | | | | | | | | | | | | | | | | | | | | | | | | | | | | | | |
| 19X-CC, 12-17 | 172.76 | M | A | | | F | | F | | | | | | | | C | F | | V | | | | | | | | F | | | | | | | | | | | | | | | | | | | | | | |
| 20X-CC, 16-23 | 181.10 | M | A | | | C | | C | | | | | | | | | A | | A | | | | | | | | | | | | | | | | | F | | | | | | | | | | | | | |
| 21X-CC, 18-23 | 190.11 | M | A | | | F | | F | | | | | | | | F | A | | A | | | | | | | | | | | | | | | | | | | | | | | | | | | | | | |
| 22X-CC, 16-21 | 198.93 | M | A | | | F | F | F | | | | | | | | A | A | R | C | | | R | | | | F | | | | | | | | | | | | | | | | | | | | | | |
| 23X-CC, 18-23 | 210.12 | M | A | | | F | | F | | | | | | | | A | A | | F | | | | | | | | | | | | | | | | | | | | | | | | | | | | | | |
| 24X-CC, 23-28 | 219.74 | M | A | | | R | | | | | | | | | | | A | | V | | | | | | | F | | | | | | | | | | | | | | | F | | | | | | | |
| 25X-CC, 19-24 | 228.48 | M | A | | | R | | | | | | | | | | A | C | F | F | | | F | | | | | | C | | | | | | | | | | | | | | | | | | | | |
| 26X-CC, 14-19 | 237.56 | M | A | | | | | | | | | | | | | C | A | A | F | | | F | | | | | | | | | | | | | | R | | | | | | | | | | | | | |
| 27X-CC, 36-41 | 247.33 | M | A | | | | | | | | | | | | | | | | A | | | | | | | | | | | | | | | | | | | | | | | | | | | | | | |
| 28X-CC, 29-34 | 253.79 | M | A | | | | | | | | | | | | | | | | A | | | | | | | | | | | | | | | | | | | | | | | | | | | | | | |
| 29X-CC, 35-40 | 264.83 | M | A | | | | | | | | | | | | | | | | A | | | | | | | | | | | | | | | | | | | | | | | | | | | | | | |
| 30X-CC, 13-18 | 272.87 | M | A | | | | | | C | | | | | | | | | | C | | | | | | | | | | | | | | | | | | | | | | | | | | | | | | |
| 31X-CC, 28-33 | 274.43 | P | R | | | | | | R | | | | | | | | | | R | | | | | | | | | | | | | | | | | | | | | | | | | | | | | | |
| **189-1171D-** | | | | | | | | | | | | | | | | | | | | | | | | | | | | | | | | | | | | | | | | | | | | | | | |
| 1R-CC, 15-20 | 250.27 | M | A | | | | | | | | | | | | | | | A | C | | | | | | | | | | | | | | | | | | | | | | | | | | | | | |
| 2R-CC, 17-22 | 260.68 | M | A | | | | | | | | | | | | | | | C | C | | | | | | | | | | | | | | | | | | | | | | | | | | | | | |
| 3R-CC, 14-19 | 271.34 | G | C | | | | | | F | | | | | | | | | | F | | | | | | | | | | | | | | | | | | | | | | | | | | | | F | |
| 4R-CC, 15-20 | 280.59 | G | A | | | | | | F | | | | | | | | | | C | | | | | | | | | | | | | | | | | | | | | | | | | | | | F | |
| 5R-CC, 15-20 | 287.53 | P | F | | | | | | C | | | | | | | | | | F | | | | | | | | | | | | | | | | | | | | | | | | | | | | | |
| 6R-CC, 7-12 | 295.26 | P | R | | | | | | C | | | | | C | | | | | R | | | | | | | | | | | | | | | | | | | | | | | | | | | | | |
| 7R-CC, 15-20 | 302.30 | M | C | | | | | | C | C | | | | A | | | R | R | | | | | | | | | | | | | | | | | | | | | R | | | | | | | | |
| 8R-CC, 0-5 | 307.84 | M | C | | | | | | | F | | | | C | | | R | | | | | | | | | | | | | | | | | | | | | | R | | | | | | | | |
| 9R-CC, 12-17 | 318.77 | M | F | | | | | | | R | | | | | | | | | | | | | | | | | | | | | | | | | | | | | | | | | | | | | | |
| 10R-CC, 12-17 | 330.78 | P | R | | | | | | | | | | | | | | | | | | | | | | | | | | | | | | | | | | | | | | | | | | | | | R | |
| 11R-CC, 12-13 | 334.02 | P | F | | | | | | | R | | | | | | | | | | | | | | | | | | | | | | | | | | | | | | | | | | | | | | R | |
| 12R-CC, 11-13 | 343.61 | M | C | | | | | | | F | | | | F | | | | | | | | | | | | | | | | | | | | | | | | | | | | | | | | | | |
| 13R-CC, 8-11 | 353.28 | M | C | | | | | | | F | | | | C | F | | | | | | | | | | | | | | | | | | | | | | | | | | | | | | | | | |
| 14R-CC, 16-21 | 363.28 | P | C | | | | | | | R | | | | F | | | | | | | | | | | | | | | | | | | | | | | | | | | C | | | | | | | |
| 15R-CC, 20-25 | 374.35 | M | F | | | | | | | F | | | | C | F | | | | | | | | | | | | | | | | | | | | | | | | | | | | | | | | | |
| 16R-CC, 18-23 | 385.18 | P | C | | | | | | | F | | | | C | C | | | | | | | | | | | | | | | | | | | | | | | | | | R | | | | | | | |
| 17R-CC, 24-29 | 398.40 | M | C | | | | | | | F | | | | C | | | | | | | | | | | | | | | | | | | | | | | | | | | | | | | | | | |
| 18R-CC, 0-3 | 401.20 | M | C | | | | | | | F | | | | C | | | | | | | | | | | | | | | | | | | | | | | | | | | | | | | | | | |

# Table T3 (continued).

| Core, section, interval (cm) | Depth (mbsf) | Preservation | Group abundance | *Reticulofenestra reticulata* | *Reticulofenestra samodurovii* | *Reticulofenestra spp.* | *Reticulofenestra umbilicus* | *Sphenolithus moriformis* | *Sphenolithus primus* | *Sphenolithus radians* | *Sphenolithus spiniger* | *Sphenolithus spp.* | *Toweius callosus* | *Toweius pertusus* | *Transversopontis pulcher* | *Transversopontis pulcheroides* | *Transversopontis rectipons* | *Triquetrorhabdulus rugosus* | *Zygrhablithus bijugatus* |
|---|---|---|---|---|---|---|---|---|---|---|---|---|---|---|---|---|---|---|---|
| 11H-CC, 0-8 | 104.12 | M | A | | | | | R | | | | | | | | | | | |
| 12X-CC, 11-16 | 109.92 | M | A | | | | | R | | | | | | | | | | | |
| 13X-CC, 13-18 | 115.72 | M | A | | | | | F | | | | | | | | | | | |
| 14X-CC, 13-18 | 123.49 | M | A | | | | | C | | | | | | | | | | | |
| 15X-CC, 13-18 | 134.45 | M | A | | | | | F | | | | | | | | | | | |
| 16X-CC, 17-22 | 139.66 | M | A | | | | | F | | | | | | | | | | | |
| 17X-CC, 11-16 | 150.18 | M | A | | | | | F | | | | | | | | | | | |
| 18X-CC, 16-21 | 162.93 | M | A | | | | | | | | | | | | | | | | |
| 19X-CC, 12-17 | 172.76 | M | A | | | | | | | | | | | | | | | | |
| 20X-CC, 16-23 | 181.10 | M | A | | | | C | | | | | | | | | | | | |
| 21X-CC, 18-23 | 190.11 | M | A | | | | | F | | | | | | | | | | | |
| 22X-CC, 16-21 | 198.93 | M | A | | | | | | | | | | | | | | | | |
| 23X-CC, 18-23 | 210.12 | M | A | | | | | F | | | | | | | | | | | |
| 24X-CC, 23-28 | 219.74 | M | A | | | | | F | | | | | | | | | | | |
| 25X-CC, 19-24 | 228.48 | M | A | | | | | F | | | | | | | | | | | |
| 26X-CC, 14-19 | 237.56 | M | A | | | | | F | | | | | | | | | | | |
| 27X-CC, 36-41 | 247.33 | M | A | | | | | | | | | | | | | | | | |
| 28X-CC, 29-34 | 253.79 | M | A | | | | | | | | | | | | | | | | |
| 29X-CC, 35-40 | 264.83 | M | A | | | | | | | | | | | | | | | | |
| 30X-CC, 13-18 | 272.87 | M | A | | | | | | | | | | | | | | | | |
| 31X-CC, 28-33 | 274.43 | P | R | | | | | | | | | | | | | | | | |
| 189-1171D- | | | | | | | | | | | | | | | | | | | |
| 1R-CC, 15-20 | 250.27 | M | A | | | | | | | | | | | | | | | | |
| 2R-CC, 17-22 | 260.68 | M | A | | | | | | | | | | | | | | | | |
| 3R-CC, 14-19 | 271.34 | G | C | | | | | R | | | | | | | | | | | |
| 4R-CC, 15-20 | 280.59 | G | A | | | | | C | | | | | | | | | | | |
| 5R-CC, 15-20 | 287.53 | P | F | F | | | | F | | | | | | | | | | | |
| 6R-CC, 7-12 | 295.26 | P | R | R | | | | C | | | | | | | | | | | |
| 7R-CC, 15-20 | 302.30 | M | C | | | | | F | | | | | | | | | | | |
| 8R-CC, 0-5 | 307.84 | M | C | | | C | | C | | | | | | | | | | | |
| 9R-CC, 12-17 | 318.77 | M | F | | | F | | C | | | | | | | | | | | |
| 10R-CC, 12-17 | 330.78 | P | R | | | | | C | | | | | | | | | | | |
| 11R-CC, 12-13 | 334.02 | P | F | | | | R | C | | | | | | | | | | | |
| 12R-CC, 11-13 | 343.61 | M | C | | | C | F | C | | | | | | | | | | | |
| 13R-CC, 8-11 | 353.28 | M | C | | | C | | F | | | | | | | | | | R | |
| 14R-CC, 16-21 | 363.28 | P | C | | | C | | F | | | | | | | | | | R | |
| 15R-CC, 20-25 | 374.35 | M | F | | | F | | F | | | | | | | | | | | |
| 16R-CC, 18-23 | 385.18 | P | C | F | | | | R | | | | | | | | | | | |
| 17R-CC, 24-29 | 398.40 | M | C | | | | | F | | | | | | | | | | | |
| 18R-CC, 0-3 | 401.20 | M | C | | | | | F | | | | | | | | | | | |

## Table T3 (continued).

| Core, section, interval (cm) | Depth (mbsf) | Preservation | Group abundance | Amaurolithus delicatus | Amaurolithus tricorniculatus | Calcidiscus leptoporus | Calcidiscus macintyrei | Calcidiscus premacintyrei | Chiasmolithus altus | Chiasmolithus consuetus | Chiasmolithus expansus | Chiasmolithus medius | Chiasmolithus nitidus | Chiasmolithus solitus | Chiasmolithus spp. | Coccolithus miopelagicus | Coccolithus pelagicus | Cyclicargolithus abisectus | Cyclicargolithus floridanus | Dictyococcites bisectus | Discoaster asymmetricus | Discoaster deflandrei | Discoaster distinctus | Discoaster intercalaris | Discoaster kuepperi | Discoaster kugleri | Discoaster lodoensis | Discoaster spp. | Discoaster surculus | Discoaster tamalis | Discoaster variabilis | Ellipsolithus lajollaensis | Ericsonia formosa | Gephyrocapsa > 4.5 | Gephyrocapsa spp. (small) | Helicosphaera intermedia | Helicosphaera kamptneri | Helicosphaera spp. | Neococcolithes dubius | Pontosphaera spp. | Princius bisulcus | Pseudoemiliania lacunosa | Reticulofenestra dictyoda | Reticulofenestra gelida | Reticulofenestra minuta | Reticulofenestra oamaruensis | Reticulofenestra perplexa | Reticulofenestra psuedoumbilica |
|---|---|---|---|---|---|---|---|---|---|---|---|---|---|---|---|---|---|---|---|---|---|---|---|---|---|---|---|---|---|---|---|---|---|---|---|---|---|---|---|---|---|---|---|---|---|---|---|---|
| 19R-CC, 0-5 | 417.63 | P | C | | | | | | | | F | | | C | | | | | | | | | | | | | | | | | | | | | | | | | | | | | | | | | | | |
| 20R-CC, 6-12 | 428.65 | M | R | | | | | | | | F | | | C | | | | | | | | | | | | | | | | | | | | | | | | | | | | | | | | | | | |
| 21R-CC, 32-38 | 430.32 | | B | | | | | | | | F | | | C | | | | | | | | | | | | | | | | | | | | | | | | | | | | | | | | | | | |
| 22R-CC, 12-17 | 448.84 | M | A | | | | | | | | F | | | C | | | | | | | | | | | | | | | | | | | | | | | | | | | | | | | | | | | |
| 23R-CC, 10-16 | 453.57 | P | F | | | | | | | | R | | | C | | C | | | | | | | | | | | | | | | | | | | | | | | | | | | | | | | | | |
| 24R-CC, 29-34 | 464.32 | | B | | | | | | | | | | | C | | | | | | | | | | | | | | | | | | | | | | | | | | | | | | | | | | | |
| 25R-CC, 0-5 | 476.81 | | B | | | | | | | | | | | C | | | | | | | | | | | | | | | | | | | | | | | | | | | | | | | | | | | |
| 26R-CC, 15-20 | 487.98 | M | F | | | | | | | | F | | | C | F | | | | | | | | | | | | | | | | | | | | | | | | | | R | | | | | | | | | |
| 27R-CC, 7-12 | 497.45 | M | A | | | | | | | | F | | | A | | | | | | | | | | | | | | | | | | | | | | | | | | F | | | | | | | | | |
| 28R-CC, 5-10 | 505.73 | P | C | | | | | | | | | | | C | | | | | | | | | | | | | | | | | | | | | | | | | | F | | | | | | | | | |
| 29R-CC, 13-18 | 516.79 | M | A | | | | | | | | C | | | A | | | | | | | | | | | | | | | | | | | | | | | | | | F | | | | | | | | | |
| 30R-CC, 12-17 | 524.58 | M | A | | | | | | | | | | | C | | | | | | | | | | | | | | | | | | | | | | | | | | | | | | | | | | | |
| 31R-CC, 28-33 | 533.73 | M | A | | | | | | | | F | | | C | | | | | | | | | | | | | | | | | | | | | | | | | | | | | | | | | | | |
| 32R-CC, 0-5 | 543.96 | M | A | | | | | | | | | | | C | | | | | | | | | | | | | | | | | | | | | | | | | | | | | | | | | | | |
| 33R-CC, 0-5 | 555.02 | M | A | | | | | | | | | | | C | | | | | | | | | | | | | | | | | | | | | | | | | | | | | | | | | | | |
| 34R-CC, 0-5 | 564.79 | M | A | | | | | | | | F | | | C | | | | | | | | | | | | | | | | | | | | | | | | | | | | | | | | | | | |
| 35R-CC, 7-12 | 573.86 | M | A | | | | | | | | | | | C | | | | | | | | | | | | | | | | | | | | | | | | | | | | | | | | | | | |
| 36R-CC, 13-18 | 584.10 | M | A | | | | | | | | F | | | C | | | | | | | | | | | | | | | | | | | | | | | | | | | | | | | | | | | |
| 37R-CC, 17-23 | 593.56 | M | A | | | | | | | | | | | C | | | | | | | | | | | | | | | | | | | | | | | | | | | | | | | | | | | |
| 38R-CC, 0-5 | 603.22 | M | A | | | | | | | C | | | | A | | | | C | | | | | | | | | | | | | | | | | | | | | F | | | | | | | F | | | |
| 39R-CC, 0-5 | 611.85 | M | A | | | | | | | F | | C | | A | | C | | | | | | | | | | | | | R | | | C | | | | | F | | | F | | | | | | F | | | |
| 40R-CC, 19-24 | 622.70 | M | A | | | | | | | C | R | | | A | | | | | | | R | | | | R | | | | | | | C | | | | | C | | | | | | | | | R | |
| 41R-CC, 12-17 | 631.14 | M | C | | | | | | F | F | | | | C | | | | F | | | | | | | | | | | | | | | | | | | | | | | | | | | | | F | |
| 42R-CC, 13-18 | 641.81 | M | C | | | | | | F | | | | C | | | | F | | | | | | | | | | | | | | | | | | | | | | | | | | | | | F | |
| 43R-CC, 9-14 | 651.01 | M | A | | | | | | | | C | | C | | | | | | | | | | | | | | | | | | | | | | | | | | | | | | | | | F | |
| 44R-CC, 17-22 | 660.71 | M | A | | | | | | F | | | | A | | | | F | | | | | | | | | | | | | | | | | | | | | | F | F | | | | | | F | |
| 45R-CC, 16-21 | 665.86 | M | A | | | | | | | | | | C | F | | | C | | | | | | | | | F | | | | | | | | | C | | | | F | F | | | | | | | |
| 46R-CC, 0-5 | 677.79 | M | A | | | | | | | | | | C | F | | | C | | | | | | | | | R | | | | | | | | | C | | | | C | | | | | | | F | |
| 47R-CC, 17-22 | 690.24 | M | A | | | | | | | | | | C | | | | | | | | | | | | | F | | | | | | | | | | | | | | | F | | | | | | | |
| 48R-CC, 0-5 | 699.50 | P | R | | | | | | | | | | | | | | | | | | | | | | | | | | | | | | | | | | | | | | | | | | | | | |
| 49R-CC, 0-7 | 709.35 | P | R | | | | | | | | | | | | | | | | | | | | | | | | | | | | | | | | | | | | | | | | | | | | | |
| 50R-CC, 23-28 | 718.48 | M | R | | | | | | | | | | | | | | | | | | | | | | | | | | | | | | | | | | | | | | | | | | | | | |
| 51R-CC, 0-6 | 726.94 | M | F | | | | | | | | | | | | | | | | | | | | | | R | | | | | | | | | | | | | | | | | | | | | | |
| 52R-CC, 8-13 | 738.11 | M | R | | | | | | | | | | | | | | | | | | | | | | | | | | | | | | | | | | | | | | | | | | | | | |
| 53R-CC, 16-21 | 745.80 | M | R | | | | | | | | | | | | | | | | | | | | | | F | | | | | | | | | | | | | | | | | | | | | | |
| 54R-CC, 9-14 | 757.26 | M | C | | | | | | | | | | | | | | | | | | | | | | | | | | | | | | | | | | | | | | | | | | | | | |
| 55R-CC, 11-16 | 766.95 | M | R | | | | | | | | | | | | | | | | | | | | | | | | | | | | | | | | | | | | | | | | | | | | | |
| 56R-CC, 17-22 | 771.40 | P | R | | | | | | | | | | | | | | | | | | | | | | R | | | | | | | | | | | | | | | | | | | | | | |
| 57R-CC, 16-21 | 781.73 | P | R | | | | | | | | | | R | R | | F | | | | | | | | | | | | | | | | | | | | | | | | | | | | | | | |
| 58R-CC, 11-16 | 795.49 | | B | | | | | | | | | | | | | | | | | | | | | | | | | | | | | | | | | | | | | | | | | | | | | |

# Table T3 (continued).

| Core, section, interval (cm) | Depth (mbsf) | Preservation | Group abundance | *Reticulofenestra reticulata* | *Reticulofenestra samodurovii* | *Reticulofenestra spp.* | *Reticulofenestra umbilicus* | *Sphenolithus moriformis* | *Sphenolithus primus* | *Sphenolithus radians* | *Sphenolithus spiniger* | *Sphenolithus spp.* | *Toweius callosus* | *Toweius pertusus* | *Transversopontis pulcher* | *Transversopontis pulcheroides* | *Transversopontis rectipons* | *Triquetrorhabdulus rugosus* | *Zygrhablithus bijugatus* |
|---|---|---|---|---|---|---|---|---|---|---|---|---|---|---|---|---|---|---|---|
| 19R-CC, 0-5 | 417.63 | P | C | | | | | | | | | | | | | | | | |
| 20R-CC, 6-12 | 428.65 | M | R | | | | | | | | | | | | | | | | |
| 21R-CC, 32-38 | 430.32 | | B | | | | | | | | | | | | | | | | |
| 22R-CC, 12-17 | 448.84 | M | A | | | | | R | | | | | | | | | | | |
| 23R-CC, 10-16 | 453.57 | P | F | | F | C | R | | | | | | | | | R | R | | |
| 24R-CC, 29-34 | 464.32 | | B | | | | | | | | | | | | | | | | |
| 25R-CC, 0-5 | 476.81 | | B | | | | | | | | | | | | | | | | |
| 26R-CC, 15-20 | 487.98 | M | F | | | | | F | R | | | | | | | | | | |
| 27R-CC, 7-12 | 497.45 | M | A | F | | | | | | | | | | | | | | | |
| 28R-CC, 5-10 | 505.73 | P | C | F | | C | | | | | | | | | | | | | |
| 29R-CC, 13-18 | 516.79 | M | A | F | | | | | | | | | | | | | | | |
| 30R-CC, 12-17 | 524.58 | M | A | | | | | | | | | | | | | | | | |
| 31R-CC, 28-33 | 533.73 | M | A | | | | | | | | | | | | | | | | |
| 32R-CC, 0-5 | 543.96 | M | A | | | | | | | | | | | | | | | | |
| 33R-CC, 0-5 | 555.02 | M | A | | | | | | | | | | | | | | | | |
| 34R-CC, 0-5 | 564.79 | M | A | | | | | | | | | | | | | | | | |
| 35R-CC, 7-12 | 573.86 | M | A | | | | | | | | | | | | | | | | |
| 36R-CC, 13-18 | 584.10 | M | A | | | | | | | | | | | | | | | | |
| 37R-CC, 17-23 | 593.56 | M | A | | | | | | | | | | | | | | | | |
| 38R-CC, 0-5 | 603.22 | M | A | | | C | | | | | | | | | | | | | |
| 39R-CC, 0-5 | 611.85 | M | A | | F | C | | | | | | | | | | | | R | |
| 40R-CC, 19-24 | 622.70 | M | A | | | | | | | | | | | | C | C | | | |
| 41R-CC, 12-17 | 631.14 | M | C | | | F | | | | | | | | | | | | | |
| 42R-CC, 13-18 | 641.81 | M | C | | | F | | | | | | | | | | | | | |
| 43R-CC, 9-14 | 651.01 | M | A | | | C | | | | | | | | | F | F | | | |
| 44R-CC, 17-22 | 660.71 | M | A | | | | | | | | | | | F | F | F | F | | C |
| 45R-CC, 16-21 | 665.86 | M | A | | | | | F | | R | | | | | C | | | | A |
| 46R-CC, 0-5 | 677.79 | M | A | | | | | F | | | R | | | | | C | F | | A |
| 47R-CC, 17-22 | 690.24 | M | A | | | | | F | R | | | | | | | | | | F |
| 48R-CC, 0-5 | 699.50 | P | R | | | R | | | | | | | | | | | | | |
| 49R-CC, 0-7 | 709.35 | P | R | | | R | | | | | | | | | | | | | |
| 50R-CC, 23-28 | 718.48 | M | R | | | R | | | | | | | | | | | | | |
| 51R-CC, 0-6 | 726.94 | M | F | | | R | | | | | | | | | | | | | |
| 52R-CC, 8-13 | 738.11 | M | R | | | R | | | | | | | | | | | | | |
| 53R-CC, 16-21 | 745.80 | M | R | | | R | | | | | | | | | | | | | |
| 54R-CC, 9-14 | 757.26 | M | C | | | R | | | | | | | | R | | | | | |
| 55R-CC, 11-16 | 766.95 | M | C | | | R | | | | | | | | R | | | | | |
| 56R-CC, 17-22 | 771.40 | P | R | | | R | | | | R | | | | | | | R | | |
| 57R-CC, 16-21 | 781.73 | P | R | | | | | | R | | | | | | | | | | |
| 58R-CC, 11-16 | 795.49 | | B | | | | | | | | | | | | | | | | |

**Table T3 (continued).**

| Core, section, interval (cm) | Depth (mbsf) | Preservation | Group abundance | Amaurolithus delicatus | Amaurolithus tricorniculatus | Calcidiscus leptoporus | Calcidiscus macintyrei | Calcidiscus premacintyrei | Chiasmolithus altus | Chiasmolithus consuetus | Chiasmolithus expansus | Chiasmolithus medius | Chiasmolithus nitidus | Chiasmolithus solitus | Chiasmolithus spp. | Coccolithus miopelagicus | Coccolithus pelagicus | Cyclicargolithus abisectus | Cyclicargolithus floridanus | Dictyococcites bisectus | Discoaster asymmetricus | Discoaster deflandrei | Discoaster distinctus | Discoaster intercalaris | Discoaster kuepperi | Discoaster kugleri | Discoaster lodoensis | Discoaster spp. | Discoaster surculus | Discoaster tamalis | Discoaster variabilis | Ellipsolithus lajollaensis | Ericsonia formosa | Gephyrocapsa > 4.5 | Gephyrocapsa spp. (small) | Helicosphaera intermedia | Helicosphaera kamptneri | Helicosphaera spp. | Neococcolithes dubius | Pontosphaera spp. | Prinsius bisulcus | Pseudoemiliania lacunosa | Reticulofenestra dictyoda | Reticulofenestra gelida | Reticulofenestra minuta | Reticulofenestra oamaruensis | Reticulofenestra perplexa | Reticulofenestra psuedoumbilica |
|---|---|---|---|---|---|---|---|---|---|---|---|---|---|---|---|---|---|---|---|---|---|---|---|---|---|---|---|---|---|---|---|---|---|---|---|---|---|---|---|---|---|---|---|---|---|---|---|
| 59R-CC, 10-15 | 805.32 | | B | | | | | | | | | | | | | | | | | | | | | | | | | | | | | | | | | | | | | | | | | | | | | |
| 60R-CC, 10-15 | 814.60 | | B | | | | | | | | | | | | | | | | | | | | | | | | | | | | | | | | | | | | | | | | | | | | | |
| 61R-CC, 6-11 | 822.60 | | B | | | | | | | | | | | | | | | | | | | | | | | | | | | | | | | | | | | | | | | | | | | | | |
| 62R-CC, 9-14 | 834.15 | | B | | | | | | | | | | | | | | | | | | | | | | | | | | | | | | | | | | | | | | | | | | | | | |
| 63R-CC, 15-20 | 843.81 | | B | | | | | | | | | | | | | | | | | | | | | | | | | | | | | | | | | | | | | | | | | | | | | |
| 64R-CC, 9-14 | 852.01 | P | R | | | | | | | | | | | | | | R | | | | | | | | | | | | | | | | | | | | | | | R | | | | | | | |
| 65R-CC, 20-25 | 863.00 | P | R | | | | | | | | | | | | | | R | | | | | | | | | | | | | | | | | | | | | | | | | | | | | | | |
| 66R-CC, 0-8 | 870.71 | P | R | | | | | | | | | | | | | | | | | | | | | | | | | | | | | | | | | | | | | | | | | | | | | |
| 67R-CC, 21-26 | 882.22 | P | R | | | | | | | | | | | | | | | | | | | | | | | | | | | | | | | | | | | | | | R | | | | | | | |
| 68R-CC, 0-5 | 889.42 | | B | | | | | | | | | | | | | | | | | | | | | | | | | | | | | | | | | | | | | | | | | | | | | |
| 69R-CC, 27-33 | 901.08 | | B | | | | | | | | | | | | | | | | | | | | | | | | | | | | | | | | | | | | | | | | | | | | | |
| 70R-CC, 17-22 | 908.07 | | B | | | | | | | | | | | | | | | | | | | | | | | | | | | | | | | | | | | | | | | | | | | | | |
| 71R-CC, 34-39 | 919.12 | | B | | | | | | | | | | | | | | | | | | | | | | | | | | | | | | | | | | | | | | | | | | | | | |
| 72R-CC, 0-5 | 929.29 | | B | | | | | | | | | | | | | | | | | | | | | | | | | | | | | | | | | | | | | | | | | | | | | |
| 73R-CC, 0-5 | 939.51 | | B | | | | | | | | | | | | | | | | | | | | | | | | | | | | | | | | | | | | | | | | | | | | | |
| 74R-CC, 0-8 | 939.50 | | B | | | | | | | | | | | | | | | | | | | | | | | | | | | | | | | | | | | | | | | | | | | | | |
| 75R-CC, 23-28 | 954.94 | | B | | | | | | | | | | | | | | | | | | | | | | | | | | | | | | | | | | | | | | | | | | | | | |

Notes: Preservation: G = good, M = moderate, P = poor. Abundance: A = abundant, C = common, F = few, R = rare B = barren.

# Table T3 (continued).

| Core, section, interval (cm) | Depth (mbsf) | Preservation | Group abundance | Reticulofenestra reticulata | Reticulofenestra samodurovii | Reticulofenestra spp. | Reticulofenestra umbilicus | Sphenolithus moriformis | Sphenolithus primus | Sphenolithus radians | Sphenolithus spiniger | Sphenolithus spp. | Toweius callosus | Toweius pertusus | Transversopontis pulcher | Transversopontis pulcheroides | Transversopontis rectipons | Triquetrorhabdulus rugosus | Zygrhablithus bijugatus |
|---|---|---|---|---|---|---|---|---|---|---|---|---|---|---|---|---|---|---|---|
| 59R-CC, 10-15 | 805.32 | | B | | | | | | | | | | | | | | | | |
| 60R-CC, 10-15 | 814.60 | | B | | | | | | | | | | | | | | | | |
| 61R-CC, 6-11 | 822.60 | | B | | | | | | | | | | | | | | | | |
| 62R-CC, 9-14 | 834.15 | | B | | | | | | | | | | | | | | | | |
| 63R-CC, 15-20 | 843.81 | | B | | | | | | | | | | | | | | | | |
| 64R-CC, 9-14 | 852.01 | P | R | | | | | | | | | | | | | | | | |
| 65R-CC, 20-25 | 863.00 | P | R | | | | | | | | | | | R | | | | | |
| 66R-CC, 0-8 | 870.71 | P | R | | | | | | | | | | | | | | | | |
| 67R-CC, 21-26 | 882.22 | P | R | | | | | | | | | | R | | | | | | |
| 68R-CC, 0-5 | 889.42 | | B | | | | | | | | | | | | | | | | |
| 69R-CC, 27-33 | 901.08 | | B | | | | | | | | | | | | | | | | |
| 70R-CC, 17-22 | 908.07 | | B | | | | | | | | | | | | | | | | |
| 71R-CC, 34-39 | 919.12 | | B | | | | | | | | | | | | | | | | |
| 72R-CC, 0-5 | 929.29 | | B | | | | | | | | | | | | | | | | |
| 73R-CC, 0-5 | 939.51 | | B | | | | | | | | | | | | | | | | |
| 74R-CC, 0-8 | 939.50 | | B | | | | | | | | | | | | | | | | |
| 75R-CC, 23-28 | 954.94 | | B | | | | | | | | | | | | | | | | |

**Table T4.** Calcareous nannofossil datum levels, Site 1171.

| Hole | Datum | Age (Ma) | Interval (cm) | | Depth (mbsf) | | Mean (m) | Error bar (m) |
|------|-------|----------|-----|--------|-----|--------|----------|---------------|
| | | | Top | Bottom | Top | Bottom | | |
| 1171A | | | | | | | | |
| | LO *Pseudoemiliania lacunosa* | 0.46 | 1H-CC | 2H-CC | 7.02 | 16.10 | 11.56 | 4.54 |
| | LO *Calcidiscus macintyrei* | 1.67 | 2H-CC | 3H-CC | 16.10 | 24.76 | 20.43 | 4.33 |
| | LO *Reticulofenestra pseudoumbilica* | 3.75 | 3H-CC | 4H-CC | 24.76 | 35.78 | 30.27 | 5.51 |
| | LO *Amaurolithus delicatus* | 4.60 | 5H-CC | 6H-CC | 45.36 | 55.17 | 50.27 | 4.91 |
| | LO *Triquetrorhabdulus rugosus* | 5.23 | 7H-CC | 8H-CC | 64.20 | 73.05 | 68.63 | 4.43 |
| 1171B | | | | | | | | |
| | LO *Pseudoemiliania lacunosa* | 0.46 | 1H-CC | 2H-CC | 4.21 | 13.79 | 9.00 | 4.79 |
| | LO *Calcidiscus macintyrei* | 1.67 | 2H-CC | 3H-CC | 13.79 | 23.17 | 18.48 | 4.69 |
| | LO *Reticulofenestra pseudoumbilica* | 3.75 | 5H-CC | 6H-CC | 42.03 | 52.04 | 47.04 | 5.01 |
| | LO *Amaurolithus delicatus* | 4.60 | 5H-CC | 6H-CC | 42.03 | 52.04 | 47.04 | 5.01 |
| 1171C | | | | | | | | |
| | LO *Pseudoemiliania lacunosa* | 0.46 | Top of core | 1H-CC | 0.00 | 9.65 | 4.83 | 4.83 |
| | LO *Calcidiscus macintyrei* | 1.67 | 2H-CC | 3H-CC | 19.24 | 28.53 | 23.89 | 4.65 |
| | LO *Reticulofenestra pseudoumbilica* | 3.75 | 4H-CC | 5H-CC | 37.80 | 47.86 | 42.83 | 5.03 |
| | LO *Triquetrorhabdulus rugosus* | 5.30 | 6H-CC | 7H-CC | 57.45 | 67.13 | 62.29 | 4.84 |
| | LO *Cyclicargolithus floridanus* | 11.90 | 17X-CC | 18X-CC | 150.18 | 162.93 | 156.56 | 6.38 |
| | FO *Calcidiscus premacintyrei* | 17.40 | 22X-CC | 23X-CC | 198.93 | 210.12 | 204.53 | 5.60 |
| | LO *Reticulofenestra bisecta* | 23.90 | 28X-CC | 29X-CC | 253.79 | 264.83 | 259.31 | 5.52 |
| | LO *Chiasmolithus altus* | 26.10 | 29X-CC | 30X-CC | 264.83 | 272.87 | 268.85 | 4.02 |
| 1171D | | | | | | | | |
| | LO *Chiasmolithus altus* | 26.10 | 1R-CC | 2R-CC | 250.27 | 260.90 | 255.59 | 0.10 |
| | LO *Reticulofenestra umbilica* | 31.20 | 3R-3, 20 | 3R-CC | 269.78 | 271.34 | 270.56 | 5.30 |
| | LO *Isthmolithus recurvus* | 32.80 | 3R-3, 20 | 3R-CC | 269.78 | 271.34 | 270.56 | 4.60 |
| | LO *Reticulofenestra oamaruensis* | 33.70 | 3R-3, 20 | 3R-CC | 269.78 | 271.34 | 270.56 | 5.30 |
| | FO *Isthmolithus recurvus* | 36.00 | 4R-CC | 5R-CC | 280.59 | 287.73 | 284.16 | 3.50 |
| | LO *Chiasmolithus solitus* | 40.40 | 5R-CC | 7R-1, 25 | 287.53 | 300.65 | 294.09 | 6.60 |
| | FO *Reticulofenestra reticulata* | 42.00 | 5R-CC | 7R-1, 25 | 287.53 | 300.65 | 294.09 | 6.60 |
| | FO *Reticulofenestra umbilica* | 43.70 | 26R-CC | 27R-CC | 487.98 | 497.57 | 492.78 | 5.60 |

Notes: The mean depth of each datum is assigned at the midpoint between two samples. LO = last occurrence, FO = first occurrence.

**Table T5.** Range chart of planktonic foraminifers, Site 1171. (**See table note.** Continued on next three pages.)

| Hole, core, section, interval (cm) | Depth (mbsf) | Catapsydrax dissimilis | Catapsydrax unicavus | Chiloguembelina cubensis | Dentoglobigerina altispira | Dentoglobigerina globularis | Dentoglobigerina praedehiscens | Globigerina bulloides | Globigerina eamsi | Globigerina falconensis | Globigerina officinalis | Globigerina praebulloides | Globigerina quinqueloba | Globigerinella aequilateralis | Globigerinella calida | Globigerinella obesa | Globigerinita glutinata | Globigerinita praestainforthi | Globigerinita uvula | Globoquadrina dehiscens | Globorotalia cibaoensis | Globorotalia conica | Globorotalia conomiozea | Globorotalia crassacarina | Globorotalia crassaconica | Globorotalia crassaformis (sin) | Globorotalia crassula | Globorotalia hirsuta | Globorotalia incognita | Globorotalia inflata (sin) | Globorotalia juanai | Globorotalia limbata | Globorotalia miotumida | Globorotalia miozea | Globorotalia panda | Globorotalia paralenuagensis | Zone/ Subzone | Age |
|---|---|---|---|---|---|---|---|---|---|---|---|---|---|---|---|---|---|---|---|---|---|---|---|---|---|---|---|---|---|---|---|---|---|---|---|---|---|---|
| **189-** | | | | | | | | | | | | | | | | | | | | | | | | | | | | | | | | | | | | | | |
| 1171B-01H-CC | 4.21 | | | | | | | X | | X | | X | | | | X | X | | | | | | | X | X | X | X | | | X | | | | | | | SN14 | Pleistocene |
| 1171A-01H-CC | 7.02 | | | | | | | X | | X | | X | X | | | X | | | | | | | | X | | X | X | | | X | | | | | | | | |
| 1171C-01H-CC | 9.65 | | | | | | | X | | X | | X | X | | | X | X | | | | | | | X | X | X | X | | | X | | | | | | | | |
| 1171B-02H-CC | 13.79 | | | | | | | X | | | | X | X | X | | X | | | | | | | | | X | X | X | | | X | | | | | | | | |
| 1171A-02H-CC | 16.10 | | | | | | | X | | X | | X | X | | | X | | | | | | | | X | X | X | X | | | X | | | | | | | | |
| 1171C-02H-CC | 19.24 | | | | | | | X | | X | | X | | | | X | X | | | | | | | X | X | X | X | | | X | | | | | | | SN13 | |
| 1171B-03H-CC | 23.17 | | | | | | | X | | X | | X | X | | X | X | X | | | | | | | X | X | X | X | | | | | | | | | | | late |
| 1171A-03H-CC | 24.76 | | | | | | | X | | X | | X | ? | | | X | X | | | | | | | X | X | X | X | | | X | | | | | | | | |
| 1171C-03H-CC | 28.56 | | | | | | | X | | X | | X | | | | X | X | | | | | | | X | X | X | X | | | X | | | | | | | | |
| 1171B-04H-CC | 32.19 | | | | | | | X | | X | | X | | | | X | X | | | | | | | | | X | | | | | | | | | | | | |
| 1171A-04H-CC | 35.78 | | | | | | | X | | X | | X | | | | X | | | | | | | | | | X | X | | | | | | | | | | | early | Pliocene |
| 1171C-04H-CC | 37.80 | | | | | | | X | | X | | X | | | | X | X | | | | | | | | | X | X | | | | | | | | | | | |
| 1171B-05H-CC | 42.03 | | | | | | | X | | X | | X | | | | X | X | | | | | | | | | X | | | | | | | | | | | | |
| 1171A-05H-CC | 45.36 | | | | | | | X | | X | | X | | | | X | | | | | | | | | | X | X | | | | | | | | | | | |
| 1171C-05H-CC | 47.86 | | | | | | | X | | X | | X | | | | X | | X | | | | | | | | X | X | | | | | | | | | | SN12b | |
| 1171B-06H-CC | 52.04 | | | | | | | X | | X | | X | | | | X | X | X | | | | | | | | X | X | | | | | | | | | | | |
| 1171A-06H-CC | 55.17 | | | | | | | X | | X | | X | | | | X | | X | | | | | | | | X | | | | | | | | | | | | |
| 1171C-06H-CC | 57.45 | | | | | | | X | | X | | X | | | | X | X | X | X | | | | | | | X | X | | | | X | | | | | | | |
| 1171B-07H-05, 23-25 | 58.03 | | | | | | | X | | X | | | | | | X | X | X | | | ? | | | | | | | | | | | | | | | | | |
| 1171B-07H-05, 41-43 | 58.21 | | | | | | | X | | | | X | | | | X | X | X | | | ? | | | | | | | | | | | | | | | | | |
| 1171B-07H-CC | 60.74 | | | | | | | X | | | | X | | | | X | | | X | | ? | | | | | | | | | | | X | X | | | | SN9 | |
| 1171A-07H-CC | 64.20 | | | | | | | X | | | | X | | | | X | | | | | ? | | | | | | | | | | | X | ? | X | | | | |
| 1171C-07H-CC | 67.13 | | | | | | | X | | | | X | | | | X | X | | X | | X | | | | X | X | | | | X | | X | X | X | | | | |
| 1171B-08H-CC | 70.75 | | | | | | | X | | | | X | | | | X | X | | | | | | | | | | | | | | | X | X | X | | | | late |
| 1171A-08H-CC | 73.05 | | | | | | | X | | | | X | | | | X | | | | | | | | | | | | | | | X | X | X | X | | | | |
| 1171C-08H-CC | 75.33 | | | | | | | X | | | | | | X | | X | X | | | X | | | | | | | | | | | | X | X | X | | | | |
| 1171B-09H-CC | 80.23 | | | | | | | X | | | | X | | | | X | | | | | | | | | | | | | | | | X | X | X | | | | |
| 1171A-09H-CC | 82.40 | | | | | | | X | | X | | X | | | | X | X | | | | | | | | | | X | X | X | | | X | X | X | | | SN8 | |
| 1171C-09H-CC | 85.64 | | | | | | | X | | | | X | | | X | X | X | X | | | | | | | | | X | | | | | X | X | X | | | | |
| 1171B-10H-CC | 89.77 | | | | | | | X | | | | X | | | | X | X | | | | | | | | | | | | | | | X | X | X | | | | |
| 1171A-10H-CC | 92.66 | | | | | | | X | X | X | | X | | | | X | X | | | | | | | | | | X | X | X | | X | ? | | | | | | |
| 1171C-10H-CC | 94.40 | | | | | | | X | | | | X | | | X | X | X | | | | | | | | | | X | | | | X | X | X | | | | |
| 1171B-11H-CC | 97.93 | | | | | | | X | | | | X | | | | X | X | | | | | | | | | | X | | | | X | X | X | | | | middle | Miocene |
| 1171A-11H-CC | 102.49 | | | | | | | X | | | | X | | X | X | X | X | X | | | | | | | | | X | | | | X | | X | | | | | |
| 1171C-11H-CC | 104.12 | | | | | | | X | | | | X | | X | | X | X | | | | | | | | | | | | | | X | X | X | | | | |
| 1171B-12H-CC | 109.06 | | | | | | | X | | | | X | | | | X | X | | | | | | | | | | | | | | X | X | | | | SN7 | |
| 1171C-12X-CC | 109.92 | | | | | | | X | | | | X | | | | X | X | | | | | X | | | | | | | | X | | X | X | | | | |
| 1171A-12H-CC | 110.62 | | | | | | | X | | | | X | | | | X | X | | | | | | | | | | | | | | X | | X | X | X | | | |
| 1171A-13X-CC | 113.66 | | | | | | | X | | | | X | | | | X | X | | | | | | | | | | | | | | X | | X | X | X | | | |

# Table T5 (continued).

| Core, section, interval (cm) | Depth (mbsf) | Globorotalia peripheroacuta | Globorotalia peripheroronda | Globorotalia praemenardii | Globorotalia praescitula | Globorotalia puncticulata | Globorotalia puncticuloides | Globorotalia scitula | Globorotalia sphericomiozea | Globorotalia tosaensis | Globorotalia triangula | Globorotalia truncatulinoides | Globorotalia zealandica | Globorotaloides suteri | Globorotaloides variabilis | Globoturborotalita apertura | Globoturborotalita connecta | Globoturborotalita decoraperta | Globoturborotalita nepenthes | Turborotalia euapertura | Globoturborotalita woodi | Neogloboquadrina dutertrei | Neogloboquadrina pachydermas | Orbulina suturalis | Orbulina universa | Paragloborotalia continuosa | Paragloborotalia mayeri | Paragloborotalia nana | Paragloborotalia nympha | Paragloborotalia semivera | Praeorbulina curva | Pulleniatina obliquiloculata | Subbotina angiporoides | Tenuitella clemenciae | Tenuitella gemma | Tenuitella munda | Tenuitellinata angustiumbilicata | Zone/ Subzone | Age |
|---|---|---|---|---|---|---|---|---|---|---|---|---|---|---|---|---|---|---|---|---|---|---|---|---|---|---|---|---|---|---|---|---|---|---|---|---|---|---|---|
| 189- | | | | | | | | | | | | | | | | | | | | | | | | | | | | | | | | | | | | | | | |
| 1171B-01H-CC | 4.21 | | | | | | X | X | | | X | X | | | | | | | | | | X | X | | X | | | | | | | | | | | | | | Pleistocene |
| 1171A-01H-CC | 7.02 | | | | | | | X | | | X | X | | | | | | | | | | X | X | | X | | | | | | | | | | | | | | |
| 1171C-01H-CC | 9.65 | | | | | | | X | | | X | | | | | | | | | | | | X | | | | | | | | | | | | | | | SN14 | |
| 1171B-02H-CC | 13.79 | | | | | X | X | X | | | | | | | | | | | | | | | X | | X | | | | | | | X | | | | | | | |
| 1171A-02H-CC | 16.10 | | | | | | | X | | X | | | | | | | | | | | | | X | | X | | | | | | | | | | | | | | Pleistocene |
| 1171C-02H-CC | 19.24 | | | | | | | X | | | | | | | | | | | | | | | X | | | | | | | | | | | | | | | | |
| 1171B-03H-CC | 23.17 | | | | | X | X | X | | | X | | | | | | | | | | | X | X | | X | | | | | | | | | | | | | SN13 | |
| 1171A-03H-CC | 24.76 | | | | | | | X | | | | | | | | | | | | | | X | X | | X | | | | | | | | | | | | | | late |
| 1171C-03H-CC | 28.56 | | | | | | | X | | | X | | | | | | | | | | | | X | | | | | | | | | | | | | | | | |
| 1171B-04H-CC | 32.19 | | | | | X | X | X | | | | | | | | | | | | | | X | X | | | | | | | | | | | | | | | | |
| 1171A-04H-CC | 35.78 | | | | | X | X | X | | | | | | | | | | | | | | | X | | | | | | | | | | | | | | | | |
| 1171C-04H-CC | 37.80 | | | | | X | X | X | | | | | | | | | | | | | | | X | | | | | | | | | | | | | | | | Pliocene |
| 1171B-05H-CC | 42.03 | | | | | X | X | X | | | | | | | | | | | | | | | | | X | | | | | | | | | | | | | | |
| 1171A-05H-CC | 45.36 | | | | | X | X | X | ? | | | | | | | | | | | | | X | X | | | | | | | | | | | | | | | | |
| 1171C-05H-CC | 47.86 | | | | | X | X | X | | | | | | | | | | | | | | X | X | | | | | | | | | | | | | | | SN12b | early |
| 1171B-06H-CC | 52.04 | | | | | X | X | | ? | | | | | | | | | | | | | X | X | | | | | | | | | | | | | | | | |
| 1171A-06H-CC | 55.17 | | | | | X | X | | ? | | | | | | | | | | | | | X | X | | | | | | | | | | | | | | | | |
| 1171C-06H-CC | 57.45 | | | | | X | X | X | | | | | | | | | | | | | | X | X | | X | | | | | | | | | | | | | | |
| 1171B-07H-05, 23-25 | 58.03 | | | | | X | X | | X | | | | | | | X | | | | | | | X | | | | | | | | | | | | | | | | |
| 1171B-07H-05, 41-43 | 58.21 | | | | | X | X | | X | | | | | | | X | | X | | | | | X | | | | | | | | | | | | | | | | |
| 1171B-07H-CC | 60.74 | | | | | | | | | | | | | | | X | | X | | | X | | X | | | | | | | | | | | | | | | | |
| 1171A-07H-CC | 64.20 | | | | | | | | | | | | | | | X | | | | | | X | X | | | X | | | | | | | | | | | | SN9 | |
| 1171C-07H-CC | 67.13 | | | | | | | X | | | | | | | | | | | | | X | X | X | | | | | | | | | | | | | | | | late |
| 1171B-08H-CC | 70.75 | | | | | | | | | | | | | | | X | | X | | | | X | X | | | | | | | | | | | | | | | | |
| 1171A-08H-CC | 73.05 | | | | | | | | | | | | | | | X | | X | ? | | X | X | X | | | | | X | X | | | | | | | | | | |
| 1171C-08H-CC | 75.33 | | | X | | | | | | | | | | | | | | X | | | X | X | X | | | | | | | X | | | X | | | | | | |
| 1171B-09H-CC | 80.23 | | | | | | | | | | | | | | | X | | X | | | X | | X | | | | | | X | X | | | | | | | | SN8 | |
| 1171A-09H-CC | 82.40 | | | | | | | | | | | | | | | | | X | | | X | X | X | | | | | | | X | | | | | | | | | |
| 1171C-09H-CC | 85.64 | | | | | | | | | | | | | | | | | X | | | X | X | X | | | | | | | X | X | | | | | | | | |
| 1171B-10H-CC | 89.77 | | | | | | | | | | | | | | | | | X | | | X | | X | | | | | | X | X | | | | | | | | | Miocene |
| 1171A-10H-CC | 92.66 | | | | | | | | | | | | | | | X | | X | | | X | | X | | | | | | | X | | | | | | | | | |
| 1171C-10H-CC | 94.40 | X | | | | | | | | | | | | | | X | | X | | | X | | X | X | X | | | | | X | | | | | | | | | |
| 1171B-11H-CC | 97.93 | | | | | | | | | | | | | | | | | X | | | X | | X | X | X | X | | | | | | | | | | | | | middle |
| 1171A-11H-CC | 102.49 | | | | | | | | | | | | | | | X | | X | | | X | | X | X | X | | | | | | | | | | | | | | |
| 1171C-11H-CC | 104.12 | | | | | | | | | | | | | | | | | X | | | X | | X | X | X | | X | X | | | | | | | | | | SN7 | |
| 1171B-12H-CC | 109.06 | | | | X | | | | | | | | | | | | | X | | | X | | X | | | | | X | X | | | | | | | | | | |
| 1171C-12X-CC | 109.92 | X | | | | | | | | | | | | | | | | X | | | X | | X | | | X | X | X | | | | | | | | | | | |
| 1171A-12H-CC | 110.62 | X | | | | | | | | | | | | | | | | X | | | X | | X | | | X | X | X | | | | | | | | | | | |
| 1171A-13X-CC | 113.66 | X | | | | | | | | | | | | | | X | | X | | | X | | X | X | X | | | X | X | | | | | | | | | | |

# Table T5 (continued).

| Core, section, interval (cm) | Depth (mbsf) | *Catapsydrax dissimilis* | *Catapsydrax unicavus* | *Chiloguembelina cubensis* | *Dentoglobigerina altispira* | *Dentoglobigerina globularis* | *Dentoglobigerina praedehiscens* | *Globigerina bulloides* | *Globigerina eamsi* | *Globigerina falconensis* | *Globigerina officinalis* | *Globigerina praebulloides* | *Globigerina quinqueloba* | *Globigerinella aequilateralis* | *Globigerinella calida* | *Globigerinella obesa* | *Globigerinita glutinata* | *Globigerinita praestainforthi* | *Globigerinita uvula* | *Globoquadrina dehiscens* | *Globorotalia cibaoensis* | *Globorotalia conica* | *Globorotalia conomiozea* | *Globorotalia crassacarina* | *Globorotalia crassaconica* | *Globorotalia crassaformis* (sin) | *Globorotalia crassula* | *Globorotalia hirsuta* | *Globorotalia incognita* | *Globorotalia inflata* (sin) | *Globorotalia juanai* | *Globorotalia limbata* | *Globorotalia miotumida* | *Globorotalia miozea* | *Globorotalia panda* | *Globorotalia paralenuagensis* | Zone/ Subzone | Age |
|---|---|---|---|---|---|---|---|---|---|---|---|---|---|---|---|---|---|---|---|---|---|---|---|---|---|---|---|---|---|---|---|---|---|---|---|---|---|---|
| 189- | | | | | | | | | | | | | | | | | | | | | | | | | | | | | | | | | | | | | | |
| 1171C-13X-CC | 115.72 | | | | | | | X | | | | X | | | | | X | X | | | | | | | | | | | | | | | | | X | | | |
| 1171A-14X-CC | 120.58 | | | | | | | X | | | | X | | | | | X | X | | | | | | | | | | | | | X | | X | X | X | | | |
| 1171C-14X-CC | 123.49 | | | | | | | X | | | | X | | | | | X | X | | | | | | | | | | | | | | | | | X | | SN7 | |
| 1171C-15X-CC | 134.45 | | | | | | | X | | | | X | X | | | | X | X | | | | | | | | | | | | | | | | X | X | | | |
| 1171C-16X-CC | 139.66 | | | | | | | X | | X | | X | X | | | X | X | X | | | | ? | | | | | | | | | | | | X | X | | | middle |
| 1171C-17X-CC | 150.18 | | | | | | | X | | | | X | X | | | | X | X | | | | X | | | X | | | | | | | | | | X | | SN6 | |
| 1171C-18X-CC | 162.93 | | | | | | | X | | | | X | X | | | | X | | | | | X | | | | | | | | | | | X | X | X | | | Miocene |
| 1171C-19X-CC | 172.76 | | | | | | | X | | | | X | X | | | | X | X | | | | X | | | | | | | | | | | | X | X | | | |
| 1171C-20X-CC | 181.10 | | | | | | | X | | | | X | X | | | | X | | | | | X | | | | | | | | | | | | | X | | | |
| 1171C-21X-CC | 190.11 | | | | | | | X | | | | X | X | | | | X | | | | | X | | | | | | | | | | | | | X | | SN5 | |
| 1171C-22X-CC | 198.93 | | | | | | | X | | | | X | | | | | X | | X | | | X | | | | | | | | | | | | | X | | SN4 | |
| 1171C-23X-CC | 210.12 | X | | X | | | | X | | | | X | X | | | | X | | | | | | | | | | | | X | | | | | | | | SN3 | early |
| 1171C-24X-CC | 219.74 | X | | | | | | X | | | | X | | | | | X | | | | | X | X | | | | | | | | | | | | | | SN2 | |
| 1171C-25X-CC | 228.48 | X | | | | | | X | | X | | X | X | | | | X | | X | | | | | | | | | | ? | | | | | | | | | |
| 1171C-26X-CC | 237.56 | X | X | | | | | X | | | | X | | | | | X | | | | | | | | | | | | X | | | | | | | | SN1 | |
| 1171C-27X-CC | 247.33 | X | X | | | | | X | | | | X | X | | | | X | | X | X | | | | | | | | | | | | | | | | | | |
| 1171D-01R-CC | 250.27 | X | X | ? | | | | X | | | X | X | | | | | X | | | | | | | | | | | | | | | | | | | | SP14b | late |
| 1171C-28X-CC | 253.79 | X | X | | X | | | X | | | | X | X | | | | X | | | | | | | | | | | | | | | | | | | | | |
| 1171D-02R-CC | 260.68 | X | X | | | | X | | X | | X | X | | | | | X | | | | | | | | | | | | | | | | | | | | | |
| 1171C-29X-CC | 264.83 | X | X | X | | | | | | | | X | | | | | X | | | | | | | | | | | | | | | | | | | | AP13 | Oligocene |
| 1171C-30X-01, 7-9 | 268.17 | | X | X | | | | | | | X | X | | | | | X | | | | | | | | | | | | | | | | | | | | ND | early |
| 1171C-30X-01, 141-143 | 271.34 | X | X | | | | | | | | | X | | | | | X | | | | | | | | | | | | | | | | | | | | AP13 | |
| 1171D-03R-CC | 271.34 | | | | | | | | | | | | | | | | | | | | | | | | | | | | | | | | | | | | ND | |
| 1171C-30X-CC | 272.87 | X | X | | | | | | | | | X | | | | | | | | | | | | | | | | | | | | | | | | | AP13 | |

Note: X = present, ? = questionable identification, ND = not determined.

**Table T5 (continued).**

| Core, section, interval (cm) | Depth (mbsf) | *Globorotalia peripheroacuta* | *Globorotalia peripheroronda* | *Globorotalia praemenardii* | *Globorotalia praescitula* | *Globorotalia puncticulata* | *Globorotalia puncticuloides* | *Globorotalia scitula* | *Globorotalia sphericomiozea* | *Globorotalia tosaensis* | *Globorotalia triangula* | *Globorotalia truncatulinoides* | *Globorotalia zealandica* | *Globorotaloides suteri* | *Globorotaloides variabilis* | *Globoturborotalita apertura* | *Globoturborotalita connecta* | *Globoturborotalita decoraperta* | *Globoturborotalita nepenthes* | *Turborotalia euapertura* | *Globoturborotalita woodi* | *Neogloboquadrina dutertrei* | *Neogloboquadrina pachyderma* | *Orbulina suturalis* | *Orbulina universa* | *Paragloborotalia continuosa* | *Paragloborotalia mayeri* | *Paragloborotalia nana* | *Paragloborotalia nympha* | *Paragloborotalia semivera* | *Praeorbulina curva* | *Pulleniatina obliquiloculata* | *Subbotina angiporoides* | *Tenuitella clemenciae* | *Tenuitella gemma* | *Tenuitella munda* | *Tenuitellinata angustiumbilicata* | Zone/Subzone | Age |
|---|---|---|---|---|---|---|---|---|---|---|---|---|---|---|---|---|---|---|---|---|---|---|---|---|---|---|---|---|---|---|---|---|---|---|---|---|---|---|---|
| 189- | | | | | | | | | | | | | | | | | | | | | | | | | | | | | | | | | | | | | | | |
| 1171C-13X-CC | 115.72 | X | | | | | | X | | | | | | | | | | X | | | X | X | X | X | | X | X | | | | | | | | | | | | middle Miocene |
| 1171A-14X-CC | 120.58 | | | | | | | | | | | | | | | | | | | | | | X | X | | X | X | | | | | | | | | | X | | middle Miocene |
| 1171C-14X-CC | 123.49 | | | | | | | | | | | | | | | | | | | | | | X | X | | X | X | | | | | | | | | | X | SN7 | middle Miocene |
| 1171C-15X-CC | 134.45 | X | | | | | | X | | | | | | | | | | X | | | X | X | X | X | | | | | | | | | | | | | | | middle Miocene |
| 1171C-16X-CC | 139.66 | X | | | | | | X | | | | | | | | | | X | | | X | X | X | X | | | X | | | | | | | X | | | X | | middle Miocene |
| 1171C-17X-CC | 150.18 | X | | | | | | X | | | | | | | | | | | | | X | X | X | | | | | | | | | | | X | | | X | | middle Miocene |
| 1171C-18X-CC | 162.93 | | | X | ? | | | X | | | | | | | | | X | | | | X | | | | | | | | | | | | | X | | | | SN6 | middle Miocene |
| 1171C-19X-CC | 172.76 | | | X | | | | X | | | | | | | | | X | | | | X | X | | | | | | | | | | | | X | | | X | SN6 | middle Miocene |
| 1171C-20X-CC | 181.10 | | | X | X | | | | | | | | | | | | X | | | | X | | | | | | | X | | | | | | | | | | | middle Miocene |
| 1171C-21X-CC | 190.11 | | | X | X | | | | | | | | X | | | | X | | | | X | | | | | | | | X | | | | | | | | | SN5 | early Miocene |
| 1171C-22X-CC | 198.93 | X | | X | X | | | | | | | | | | | | X | | | | X | | | | | | | | | X | | | | | | | X | SN4 | early Miocene |
| 1171C-23X-CC | 210.12 | | | | | | | | | | | | | | | | X | | | ? | X | | | | | | | | | | | | | | | | | SN3 | early Miocene |
| 1171C-24X-CC | 219.74 | | | | | | | | | | | | | | | | | | | ? | X | | | | | X | | | | | | | | | | | | SN2 | early Miocene |
| 1171C-25X-CC | 228.48 | | | | | | | | | | | | | X | | | | | | X | X | | | | | X | | | | X | | | | | | | X | SN2 | early Miocene |
| 1171C-26X-CC | 237.56 | | | | | | | | | | | | | | | | | | | | X | | | | | X | | | | | | | | | | | | SN1 | early Miocene |
| 1171C-27X-CC | 247.33 | | | | | | | | | | | | | | | | | | | X | | | | | | X | | | | | | | | | | | | | early Miocene |
| 1171D-01R-CC | 250.27 | | | | | | | | | | | | X | | | | | | | X | X | | | | | | | | | | | | | | X | X | X | SP14b | late Oligocene |
| 1171C-28X-CC | 253.79 | | | | | | | | | | | | X | X | | | | | | | X | | | | | | | | | | | | | | X | X | | | late Oligocene |
| 1171D-02R-CC | 260.68 | | | | | | | | | | | | X | | | | | | | | X | | | | | | | | | | | | | | X | X | X | | late Oligocene |
| 1171C-29X-CC | 264.83 | | | | | | | | | | | | X | | | | | | | | | | | | | | | | | | | | | X | | X | X | AP13 | early Oligocene |
| 1171C-30X-01, 7-9 | 268.17 | | | | | | | | | | | | | | | | | | | | | | | | | | | | | | | | X | | | X | X | ND | early Oligocene |
| 1171C-30X-01, 141-143 | 271.34 | | | | | | | | | | | | X | | | | | | | | | | | | | | | | | | | | X | | X | X | X | AP13 | early Oligocene |
| 1171D-03R-CC | 271.34 | | | | | | | | | | | | | | | | | | | | | | | | | | | | | | | | | | | | | ND | early Oligocene |
| 1171C-30X-CC | 272.87 | | | | | | | | | | | | | | | | | | | | | | | | | | | | | | | | X | | | X | X | AP13 | early Oligocene |

**Table T6.** Core depths of selected planktonic foraminiferal datums, Site 1171.

| Bioevent | Age (Ma) | Interval Top | Interval Bottom | Depth (mbsf) Top | Depth (mbsf) Bottom | Mean (mbsf) | Error bar (m) |
|---|---|---|---|---|---|---|---|
| **Hole 1171A** | | | | | | | |
| FO *Globorotalia truncatulinoides* | 1.96 | 1H-CC | 2H-CC | 7.02 | 16.10 | 11.56 | 4.54 |
| FO *Globorotalia inflata* | 3.20 | 3H-CC | 4H-CC | 24.76 | 35.78 | 30.27 | 5.51 |
| LO *Paragloborotalia continuosa* | 8.00 | 6H-CC | 7H-CC | 55.17 | 64.20 | 59.69 | 4.52 |
| LO *Paragloborotalia nympha* | 10.10 | 7H-CC | 8H-CC | 64.20 | 73.05 | 68.63 | 4.43 |
| LO *Paragloborotalia mayeri* | 11.40 | 10H-CC | 11H-CC | 92.66 | 102.49 | 97.58 | 4.92 |
| **Hole 1171B** | | | | | | | |
| FO *Globorotalia truncatulinoides* | 1.96 | 1H-CC | 2H-CC | 4.21 | 13.79 | 9.00 | 4.79 |
| FO *Globorotalia inflata* | 3.20 | 2H-CC | 3H-CC | 13.79 | 23.17 | 18.48 | 4.69 |
| LO *Paragloborotalia continuosa* | 8.00 | 6H-CC | 7H-CC | 52.04 | 60.74 | 56.39 | 4.35 |
| LO *Paragloborotalia nympha* | 10.10 | 8H-CC | 9H-CC | 70.75 | 80.23 | 75.49 | 4.74 |
| LO *Paragloborotalia mayeri* | 11.40 | 10H-CC | 11H-CC | 89.77 | 97.93 | 93.85 | 4.08 |
| **Hole 1171C** | | | | | | | |
| FO *Globorotalia truncatulinoides* | 1.96 | Top of core | 1H-CC | 0 | 9.65 | 4.83 | 4.83 |
| FO *Globorotalia inflata* | 3.20 | 3H-CC | 4H-CC | 28.56 | 37.80 | 33.18 | 4.62 |
| LO *Paragloborotalia continuosa* | 8.00 | 6H-CC | 7H-CC | 57.45 | 67.13 | 62.29 | 4.84 |
| LO *Paragloborotalia nympha* | 10.10 | 7H-CC | 8H-CC | 67.13 | 75.33 | 71.23 | 4.10 |
| LO *Paragloborotalia mayeri* | 11.40 | 10H-CC | 11H-CC | 94.40 | 104.12 | 99.26 | 4.86 |
| FO *Paragloborotalia mayeri* | 12.10 | 16X-CC | 17X-CC | 139.66 | 150.18 | 144.92 | 5.26 |
| FO *Orbulina suturalis* | 15.10 | 20X-CC | 21X-CC | 181.10 | 190.11 | 185.61 | 4.51 |
| FO *Praeorbulina curva* | 16.30 | 21X-CC | 22X-CC | 190.11 | 198.93 | 194.52 | 4.41 |
| FO *Globigerinoides trilobus* | 18.80 | 22X-CC | 23X-CC | 198.93 | 210.12 | 204.53 | 5.60 |
| FO *Globoturborotalita connecta* | 20.90 | 23X-CC | 24X-CC | 210.12 | 219.74 | 214.93 | 4.81 |
| FO *Globoturborotalita woodi* | 22.60 | 25X-CC | 26X-CC | 228.48 | 237.56 | 233.02 | 4.54 |
| FO *Globoquadrina dehiscens* | 23.20 | 27X-CC | 28X-CC | 247.33 | 253.79 | 250.56 | 3.23 |
| LO *Chiloguembelina cubensis* | 28.50 | 28X-CC | 29X-CC | 247.33 | 253.79 | 250.56 | 3.23 |
| LO *Subbotina angiporoides* | 30.00 | 29X-CC | 30X-CC | 264.83 | 268.17 | 266.50 | 1.67 |

Note: FO = first occurrence, LO = last occurrence.

**Table T7.** Core depths of selected radiolarian datums, Site 1171.

| Datum | | Age (Ma) | Interval Top | Interval Bottom | Depth (mbsf) Top | Depth (mbsf) Bottom | Mean (mbsf) | Error bar (m) |
|---|---|---|---|---|---|---|---|---|
| **Hole 1171A** | | | | | | | | |
| LO | *Antarctissa* sp. G | 0.68 | 2H-CC | 3H-CC | 16.10 | 24.76 | 20.43 | 8.66 |
| LO | *Pseudocubus vema* | 2.4 | 3H-CC | 4H-CC | 24.76 | 35.78 | 30.27 | 11.02 |
| FO | *Pseudocubus vema* | 4.5 | 4H-CC | 5H-CC | 35.78 | 45.36 | 40.57 | 9.58 |
| LCO | *Stichocorys peregrina* | 5 | 4H-CC | 5H-CC | 35.78 | 45.36 | 40.57 | 9.58 |
| LO | *Lychnocanoma grande* | 5 | 5H-CC | 6H-CC | 45.36 | 55.17 | 50.27 | 9.81 |
| LO | *Stichocorys delomontensis* | 5.18-6.90 | 6H-CC | 7H-CC | 55.17 | 64.20 | 59.69 | 9.03 |
| LO | *Amphymenium challengerae* | 6.1 | 6H-CC | 7H-CC | 55.17 | 64.20 | 59.69 | 9.03 |
| FO | *Amphymenium challengerae* | 6.6 | 7H-CC | 8H-CC | 64.20 | 73.05 | 68.63 | 8.85 |
| LAO | *Stichocorys peregrina* | | 7H-CC | 8H-CC | 64.20 | 73.05 | 68.63 | 8.85 |
| FAO | *Stichocorys peregrina* | 7.1? | 9H-CC | 10H-CC | 82.40 | 92.66 | 87.53 | 10.26 |
| LAO | *Cyrtocapsella japonica* | | 11H-CC | 12H-CC | 102.49 | 110.62 | 106.56 | 8.13 |
| **Hole 1171B** | | | | | | | | |
| LO | *Pseudocubus vema* | 2.4 | 3H-CC | 4H-CC | 23.17 | 32.19 | 27.68 | 9.02 |
| FO | *Pseudocubus vema* | 4.5 | 4H-CC | 5H-CC | 32.19 | 42.03 | 37.11 | 9.84 |
| LCO | *Stichocorys peregrina* | 5 | 5H-CC | 6H-CC | 42.03 | 52.04 | 47.04 | 10.01 |
| LO | *Lychnocanoma grande* | 5 | 6H-CC | 7H-CC | 52.04 | 60.74 | 56.39 | 8.70 |
| LO | *Stichocorys delomontensis* | 5.18-6.90 | 6H-CC | 7H-CC | 52.04 | 60.74 | 56.39 | 8.70 |
| LAO | *Stichocorys peregrina* | | 7H-CC | 8H-CC | 60.74 | 70.75 | 65.75 | 10.01 |
| FAO | *Stichocorys peregrina* | 7.1? | 9H-CC | 10H-CC | 80.23 | 89.77 | 85.00 | 9.54 |
| LAO | *Cyrtocapsella japonica* | 11.6 | 11H-CC | 12H-CC | 97.93 | 109.06 | 103.50 | 11.13 |
| **Hole 1171C** | | | | | | | | |
| LO | *Pseudocubus vema* | 2.4 | 2H-CC | 3H-CC | 19.24 | 28.56 | 23.90 | 9.32 |
| FO | *Pseudocubus vema* | 4.5 | 3H-CC | 4H-CC | 28.56 | 37.80 | 33.18 | 9.24 |
| LO | *Lychnocanoma grande* | 5 | 3H-CC | 4H-CC | 28.56 | 37.80 | 33.18 | 9.24 |
| LCO | *Stichocorys peregrina* | 5 | 5H-CC | 6H-CC | 47.86 | 57.45 | 52.66 | 9.59 |
| LO | *Stichocorys delomontensis* | 5.18-6.90 | 6H-CC | 7H-CC | 57.45 | 67.13 | 62.29 | 9.68 |
| LAO | *Stichocorys peregrina* | | 6H-CC | 7H-CC | 57.45 | 67.13 | 62.29 | 9.68 |
| FAO | *Stichocorys peregrina* | 7.1? | 8H-CC | 9H-CC | 75.33 | 85.64 | 80.49 | 10.31 |
| LAO | *Cyrtocapsella japonica* | 11.6 | 11H-CC | 12X-CC | 104.12 | 109.92 | 107.02 | 5.80 |
| LAO | *Cyrtocapsella tetrapera* | 12.5 | 14X-CC | 15X-CC | 123.49 | 134.45 | 128.97 | 10.96 |
| LO | *Lychnocanoma conica* | 13.5 | 17X-CC | 18X-CC | 150.18 | 162.93 | 156.56 | 12.75 |
| FO | *Lychnocanoma nipponica* | 15.7 | 19X-CC | 20X-CC | 172.76 | 181.10 | 176.93 | 8.34 |
| LO | *Cenosphaera coronata* | 16.7 | 22X-CC | 23X-CC | 198.93 | 210.12 | 204.53 | 11.19 |
| FO | *Eucyrtidium cienkowskii* gr. | 16.7 | 22X-CC | 23X-CC | 198.93 | 210.12 | 204.53 | 11.19 |
| FO | *Cyrtocapsella tetrapera* | 23.6 | 25X-CC | 26X-CC | 228.48 | 237.56 | 233.02 | 9.08 |
| FO | *Cenosphaera coronataformis* | 24.4 | 27X-CC | 28X-CC | 247.33 | 253.79 | 250.56 | 6.46 |
| **Hole 1171D** | | | | | | | | |
| FO | *Cyrtocapsella tetrapera* | 23.6 | 2R-CC | 3R-CC | 260.68 | 271.34 | 266.01 | 10.66 |
| FO | *Lychnocanoma conica* | 32.6-33.1 | 2R-CC | 3R-CC | 260.68 | 271.34 | 266.01 | 10.66 |

Note: LO = last occurrence, FO = first occurrence, LCO = last consistent occurrence, LAO = last abundant occurrence, FAO = first abundant occurrence.

**Table T8.** Relative abundance of selected diatom taxa, sponge spicules, and silicoflagellates, Holes 1171A, 1171B, and 1171C. (**See table notes.** Continued on next three pages.)

| Core, section, interval (cm) | Depth (mbsf) | Preservation | Group abundance | Actinocyclus dimorphus | Actinocyclus fryxellae | Actinocyclus ingens | Actinocyclus ingens var. nodus | Actinocyclus ingens var. ovalis | Actinocyclus karstenii | Actinoptychus senarius | Arachnodiscus oamaruensis | Asteromphalus kennettii | Asteromphalus parvulus | Azpeitia nodulifer | Azpeitia cf. nodulifer | Azpeitia tabularis group | Chaetoceros resting spores | Coscinodiscus lewisianus | Coscinodiscus marginatus | Coscinodiscus rhombicus | Coscinodiscus lewisianus | Dactyliosolen antarcticus | Denticulopsis dimorpha | Denticulopsis hustedtii | Denticulopsis maccollumii | Denticulopsis praedimorpha | Eucampia antarctica | Fragilariopsis barronii | Fragilariopsis doliolus | Fragilariopsis kerguelensis | Fragilariopsis reinholdii | Fragilariopsis spp. | Fragilariopsis weaveri | Hemiaulus spp. | Hemidiscus cf. cuneiformis | Hemidiscus karstenii | Lizitzinia ornata | Nitzschia denticuloides | Paralia sulcata var. crenulata | Proboscia barboi | Pyxilla fragments | Rhizosolenia styliformis | Rocella gelida |
|---|---|---|---|---|---|---|---|---|---|---|---|---|---|---|---|---|---|---|---|---|---|---|---|---|---|---|---|---|---|---|---|---|---|---|---|---|---|---|---|---|---|---|---|
| **189-1171A-** | | | | | | | | | | | | | | | | | | | | | | | | | | | | | | | | | | | | | | | | | | | | |
| 1H-CC, 8-13 | 7.02 | M | C | | | | | | | | | | | | | C | | | | | | | | | | | | F | | A | | | | | | | | | | W | | | | |
| 2H-CC, 18-25 | 16.10 | G | A | F | | C | | | | | | | R | | | | | | R | | | | | | | | | | R | A | D | F | F | | | | | | | W | | | R | |
| 3H-CC, 17-22 | 24.76 | G | A | | | C | | | | | | | | | | | | | | | | | | | | | | C | | F | R | | | | | | | | | D | | | | |
| 4H-CC, 20-25 | 35.78 | G | A | | | C | R | | | | | | | | | | | | R | | | | | | | | | | | R | | C | C | | C | R | C | | | C | | | | |
| 5H-CC, 18-23 | 45.36 | P | F | | | C | W | | | | | | | | | C | W | | R | W | F | | | | | | | | | R | | | | | R | C | | | | W | R | W | | |
| 6H-CC, 17-22 | 55.17 | P | C | | W | C | | W | | | | W | | R | | | | | R | | R | W | | | | | | | | C | R | | C | | | | | | | W | C | | R | |
| 7H-CC, 25-30 | 64.20 | M | C | | | C | | R | R | | | W | | | | | | | | | W | | | | | | | | | | | | | | | | | | | W | R | | W | |
| 8H-CC, 14-19 | 73.05 | G | A | | | R | D | F | | | | | | | | | | | F | | | | | C | | | | | | C | | | | | | | | | | W | R | | | |
| 9H-CC, 19-24 | 82.40 | G | C | | | R | R | | | | | | R | | | | | | C | F | | | | C | C | F | | | | | | | | F | R | | | | | W | R | | | |
| 10H-CC, 14-19 | 92.66 | G | A | | | F | D | | | | | | | | | | | | F | | | C | | | | | | | | | | | | | | | | | | R | R | | | |
| 11H-CC, 13-18 | 102.49 | MG | A | | | F | D | | | | | | | | | R | | | R | | | C | A | C | R | | | | | | | | | | | | | | | R | | | | |
| 12H-CC, 5-10 | 110.62 | G | A | | | R | C | | | | | | | | | | | | R | | | A | A | | | | | | | | | | | | | | | | | R | R | | | |
| 13X-CC, 20-25 | 113.66 | MG | A | | | F | C | | | | | | | | | | | | R | | | A | A | | | | | | | | | | | | | | | | | W | | | F | |
| 14X-CC, 15-20 | 120.53 | MP | A | | | | C | | | | | | | R | | | | | | | | A | | | | | | | | | | | | | | | | | | R | | | | |
| **189-1171B-** | | | | | | | | | | | | | | | | | | | | | | | | | | | | | | | | | | | | | | | | | | | | |
| 1H-CC, 9-14 | 4.21 | M | C | | | | | | | | | | | | | | | | | | | | | W | F | | | | | C | W | | | | | | C | | | | | | W | |
| 7H-5, 23-24 | 58.03 | P | F | | | F | | | | | | | | | | | | | F | | | | | | | | | | | | F | | | | | | | | | | F | W | | |
| 8H-6, 41-42 | 72.57 | P | F | | | F | | | | | | | | | | | | | F | | | | | | | | | | | | F | | | | | | | | | | F | W | | |
| **189-1171C-** | | | | | | | | | | | | | | | | | | | | | | | | | | | | | | | | | | | | | | | | | | | | |
| 6H-CC, 18-22 | 57.45 | M | F | | | | | | | | | | | | | | | | R | | | | | | | | | | | | R | | | | | R | | R | | C | R | | | |
| 7H-CC, 23-28 | 67.13 | G | A | | | C | | C | | | | | | | | | | | R | | | | | | | | | | | | F | | | | | C | | | | C | R | | | |
| 12X-CC, 11-16 | 109.92 | M | C | | | C | | | | | | | | | | | | | R | | | A | A | F | | | | | | | | | | | | | | | | | | | | |
| 13X-CC, 13-18 | 115.72 | G | C | | | C | | | | | | | | | | R | | | | | | A | C | | | | | | | | | | | | | | | | | | | | R |
| 14X-CC, 13-18 | 123.49 | G | A | | | C | | | | | | | | A | | | | | | | | A | C | | | | | | | R | | | | | | | | | C | R | | | |
| 15X-CC, 13-18 | 134.45 | G | A | | | D | C | | | | | | | A | R | | | | | | | | C | | | | | | | | F | | | | | | | | | C | C | | | |
| 16X-CC, 17-22 | 139.66 | M | C | | | C | R | | | | | | | | | | | C | R | | | | R | | | | | | | | | | | | | | | | | | F | | | |
| 17X-CC, 11-16 | 150.18 | MG | F | | | C | C | | | | | | | | | | | C | R | | | | C | | | | | | | | | | | | R | | | | | | | | | |
| 18X-CC, 16-21 | 162.93 | G | A | | | R | C | | | | | | | R | | | | | C | | | | C | | | | | | | | | | | | | | | | | | | | | |
| 19X-CC, 12-17 | 172.76 | MP | C | | | | D | | | | | | | | | | | | | | | | | | | | | | | | | | | | | | | | | | | | | |
| 20X-CC, 16-23 | 181.10 | M | A | | | | | | | | | | | | | | | R | R | | | | | | | W | | | | | | | | | | | | | | W | | | | |
| 21X-CC, 18-23 | 190.11 | G | A | | | C | C | | | | | | | | | C | | R | R | | | | | | | C | | | | | | | | R | | | | | W | | | | |
| 22X-CC, 16-21 | 198.93 | M | C | | | | | | | | | | | ?W | | | | ?W | | | | | | | | | | | | | | | | | | | | | | ?W | ?W | | W | |
| 23X-CC, 18-23 | 210.12 | G | A | | | | | | ?W | | | | | ?W | | | | | | C | C | | | | | | | | | | | | | | | | W | | | ?W | | | | |
| 24X-CC, 23-28 | 219.74 | G | A | | | | | | | W | | | | ?W | | | | | | | | | | | | | | | | | | | | | ?W | | | | | ?W | ?W | | | |
| 25X-CC, 19-24 | 228.48 | M | A | | | | | | | | | | | | | | | R | F | | | | | | | | | | | | | | | | | | | | | | | ?W | | | |

# Table T8 (continued).

| Core, section, interval (cm) | Depth (mbsf) | Preservation | Group abundance | *Rocella gelida* var. *schraderi* | *Rocella vigilans* | *Rodella praenitida* | *Rossiella* spp. | *Stephanopyxis grunowii* | *Stephanopyxis turris* | *Synedra jouseana* | *Thalassionema nitzschioides* | *Thalassionema nitzschioides* var. *parva* | *Thalassiosira complicata* | *Thalassiosira eccentrica* | *Thalassiosira elliptipora* | *Thalassiosira fasciculata* | *Thalassiosira gracilis* | *Thalassiosira insigna* | *Thalassiosira inura* | *Thalassiosira kolbei* | *Thalassiosira lentiginosa* | *Thalassiosira leptopus* | *Thalassiosira oestrupii* | *Thalassiosira oliverana* | *Thalassiosira striata* | *Thalassiosira symmetrica* | *Thalassiosira tetraoestrupii* var. *reimeri* | *Thalassiosira trifulta* | *Thalassiothrix antarctica* | *Triceratium* spp. | *Xanthiopyxis* spp. | Silicoflagellate tests | Sponge spicules |
|---|---|---|---|---|---|---|---|---|---|---|---|---|---|---|---|---|---|---|---|---|---|---|---|---|---|---|---|---|---|---|---|---|---|
| **189-1171A-** | | | | | | | | | | | | | | | | | | | | | | | | | | | | | | | | | |
| 1H-CC, 8-13 | 7.02 | M | C | | | | | | R | | C | | | | | | | | | | A | R | F | | | | | | D | | | F | C |
| 2H-CC, 18-25 | 16.10 | G | A | | | | | | | | | | | F | R | F | R | R | | | C | F | C | C | F | | R | | C | | | F | C |
| 3H-CC, 17-22 | 24.76 | G | A | | | | | | | | C | | | | | | R | R | | | C | F | C | C | C | | F | | C | | | F | C |
| 4H-CC, 20-25 | 35.78 | G | A | | | | | | | | | | C | F | C | | | | F | C | | | | C | | | | | D | | | C | C |
| 5H-CC, 18-23 | 45.36 | P | F | | W | | | | W | | | | | F | R | | | | | | | | | R | R | | | | F | | W | F | F |
| 6H-CC, 17-22 | 55.17 | P | C | | W | W | | | W | | C | R | | | | | R | R | | | | | | | | | | | C | | | F | F |
| 7H-CC, 25-30 | 64.20 | M | C | | W | | | | | | | | | | | | R | R | | | | | | | | | | | C | | | F | F |
| 8H-CC, 14-19 | 73.05 | G | A | | | W | | | | | | | | | | | | | | | | | | | | | | | C | | W | F | F |
| 9H-CC, 19-24 | 82.40 | G | C | | | | | | | | | R | | | | | | | | | | | | | | | | | C | | | C | F |
| 10H-CC, 14-19 | 92.66 | G | A | | | | | | | | | | | | | | | | | | | | | | | | | | C | | | F | R |
| 11H-CC, 13-18 | 102.49 | MG | A | | | | | | | | | | | | | | | | | | | | | | | | | | C | | | | F |
| 12H-CC, 5-10 | 110.62 | G | A | | | | | | | | | | | | | | | | | | | | | | | | | | C | | | | F |
| 13X-CC, 20-25 | 113.66 | MG | A | | | | | | W | | | | | | | | | | | | | | | | | | | | C | | | | F |
| 14X-CC, 15-20 | 120.53 | MP | A | | | | | | | | | | | | | | | | | | | | | | | | | | C | | | | |
| **189-1171B-** | | | | | | | | | | | | | | | | | | | | | | | | | | | | | | | | | |
| 1H-CC, 9-14 | 4.21 | M | C | | | | | | | R | | | | | | | | | | | C | | | | | | | | | | | F | |
| 7H-5, 23-24 | 58.03 | P | F | | | | | | W | | | | | | | | | | | | | | | | | | | | F | | | | |
| 8H-6, 41-42 | 72.57 | P | F | | | | | | W | | | | | | | | | | | | | | | | | | | | F | | | | |
| **189-1171C-** | | | | | | | | | | | | | | | | | | | | | | | | | | | | | | | | | |
| 6H-CC, 18-22 | 57.45 | M | F | | | | | | | R | | | | | | | | | | | | | | | | | | | C | | | | |
| 7H-CC, 23-28 | 67.13 | G | A | | | | | | | C | | | | | | | | | | | | | | | | | | | | | F | | |
| 12X-CC, 11-16 | 109.92 | M | C | | | | | | | | | | | | | | | | | | | | | | | | | | C | | | | F |
| 13X-CC, 13-18 | 115.72 | G | C | | | | | | | | | | | | | | | | | | | | | | | | | | C | | | | |
| 14X-CC, 13-18 | 123.49 | G | A | | | | | | | | | | | | | | | | | | | | | | | | | | C | | F | | |
| 15X-CC, 13-18 | 134.45 | G | A | | | | | | W | | | | | | | | | | | | | | | | | | | | C | | F | | |
| 16X-CC, 17-22 | 139.66 | M | C | | | | | | R | | | | | | | | | | | | | | | | | | | | C | | F | | C |
| 17X-CC, 11-16 | 150.18 | MG | F | | | W | | | W | | | | | | | | | | | | | | | | | | | | C | | | | F |
| 18X-CC, 16-21 | 162.93 | G | A | | | | | | | | | | | | | | | | | | | | | | | | | | C | | F | | F |
| 19X-CC, 12-17 | 172.76 | MP | C | | | | | | | | | | C | | | | | | | | | | | | | | | | C | | F | | |
| 20X-CC, 16-23 | 181.10 | M | A | | | | | | W | | | | | | | | | | | | | | | | | | | | | | F | | |
| 21X-CC, 18-23 | 190.11 | G | A | | | | | | | | | | | | | | | | | | | | | | | | | | C | | F | | |
| 22X-CC, 16-21 | 198.93 | M | C | W | | | ?W | ?W | | | | | | | | | | | | | | | | | | | | | | | W? | | C |
| 23X-CC, 18-23 | 210.12 | G | A | W | | | ?W | ?W | C | | | | | | | | | | | | | | | | | | | | | | | | C |
| 24X-CC, 23-28 | 219.74 | G | A | | | W | ?W | ?W | C | | | | | | | | | | | | | | | | | | | | | | | ?W | C |
| 25X-CC, 19-24 | 228.48 | M | A | | | | | ?W | C | | | | | | | | | | | | | | | | | | | | | | | ?W | C |

**Table T8 (continued).**

| Core, section, interval (cm) | Depth (mbsf) | Preservation | Group abundance | Actinocyclus dimorphus | Actinocyclus fryxellae | Actinocyclus ingens | Actinocyclus ingens var. nodus | Actinocyclus ingens var. ovalis | Actinocyclus karstenii | Actinoptychus senarius | Arachnodiscus oamaruensis | Asteromphalus kennettii | Asteromphalus parvulus | Azpeitia nodulifer | Azpeitia cf. nodulifer | Azpeitia tabularis group | Chaetoceros resting spores | Coscinodiscus lewisianus | Coscinodiscus marginatus | Coscinodiscus rhombicus | Coscinodiscus lewisianus | Dactyliosolen antarcticus | Denticulopsis dimorpha | Denticulopsis hustedtii | Denticulopsis maccollumii | Denticulopsis praedimorpha | Eucampia antarctica | Fragilariopsis barronii | Fragilariopsis doliolus | Fragilariopsis kerguelensis | Fragilariopsis reinholdii | Fragilariopsis spp. | Fragilariopsis weaveri | Hemiaulus spp. | Hemidiscus cf. cuneiformis | Hemidiscus karstenii | Lizitzinia ornata | Nitzschia denticuloides | Paralia sulcata var. crenulata | Proboscia barboi | Pyxilla fragments | Rhizosolenia styliformis | Rocella gelida |
|---|---|---|---|---|---|---|---|---|---|---|---|---|---|---|---|---|---|---|---|---|---|---|---|---|---|---|---|---|---|---|---|---|---|---|---|---|---|---|---|---|---|---|---|
| 26X-CC, 14-19 | 237.56 | G | A | | | | | | | | | | | | | | ?W | | R | | | | | | | | | | | | | | | | | | | | ?W | ?W | | | W |
| 27X-CC, 36-41 | 247.33 | G | A | | | | | | | | | | | | | | | | | R | | | | | | | | | | | | | | | | | | | | ?W | | | W |
| 28X-CC, 29-34 | 253.79 | G | A | | | | | | | | | | | | | | | | | | | | | | | | | | | | | | | | | | | | | | | | |
| 29X-CC, 35-40 | 264.83 | M | A | | | | | | | | | | | | | | | | C | R | | | | | | | | | | | | | | | | | | | | | | F | |
| 30X-CC, 13-18 | 272.87 | G | A | | | | | | | | | | | | | | C | | | | | | | | | | | | | | | | | | | | | | F | | | | |
| 31X-CC, 28-33 | 274.43 | G | R | | | | | | | | | | | | | | | | | | | | | | | | | | | | | | | | | | | | | | | | |

Notes: Preservation: G = good, M = moderate, MG = moderate-good, MP = moderate-poor, P = poor. Abundance: D = dominant, A = abundant, C = common, F = few, R = rare, T = trace, B = barren, W = reworked, ?W = questionably reworked.

**Table T8 (continued).**

| Core, section, interval (cm) | Depth (mbsf) | Preservation | Group abundance | Rocella gelida var. schraderi | Rocella vigilans | Rodella praenitida | Rossiella spp. | Stephanopyxis grunowii | Stephanopyxis turris | Synedra jouseana | Thalassionema nitzschioides | Thalassionema nitzschioides var. parva | Thalassiosira complicata | Thalassiosira eccentrica | Thalassiosira elliptipora | Thalassiosira fasciculata | Thalassiosira gracilis | Thalassiosira insigna | Thalassiosira inura | Thalassiosira kolbei | Thalassiosira lentiginosa | Thalassiosira leptopus | Thalassiosira oestrupii | Thalassiosira oliverana | Thalassiosira striata | Thalassiosira symmetrica | Thalassiosira tetraoestrupii var. reimeri | Thalassiosira trifulta | Thalassiothrix antarctica | Triceratium spp. | Xanthiopyxis spp. | Silicoflagellate tests | Sponge spicules |
|---|---|---|---|---|---|---|---|---|---|---|---|---|---|---|---|---|---|---|---|---|---|---|---|---|---|---|---|---|---|---|---|---|---|---|
| 26X-CC, 14-19 | 237.56 | G | A | W | | | | | | C | | | | | | | | | | | | | | | | | | | | | ?W | | | C |
| 27X-CC, 36-41 | 247.33 | G | A | W | | | ?W | ?W | ?W | R | | | | | | | | | | | | | | | | | | | | | ?W | F | C | A |
| 28X-CC, 29-34 | 253.79 | G | A | F | | | | | | | | | | | | | | | | | | | | | | | | | | | | | F | A |
| 29X-CC, 35-40 | 264.83 | M | A | A | R | | | | R | C | | | | | | | | | | | | | | | | | | | | | | F | A | F |
| 30X-CC, 13-18 | 272.87 | G | A | C | | | R | A | R | C | | | | | | | | | | | | | | | | | | | | R | C | C | A | C |
| 31X-CC, 28-33 | 274.43 | G | R | | | | | | | R | | | | | | | | | | | | | | | | | | | | | | | | C |

**Table T9.** Relative abundance of selected diatom taxa, sponge spicules, and silicoflagellates, Hole 1171D.

| Core, section interval (cm) | Depth (mbsf) | Preservation | Group abundance | *Actinoptychus senarius* | *Actinoptychus* spp. | *Arachnodiscus oamaruensis* | *Asteromphalus* spp. | *Chaetoceros* resting spores | *Cocconeis* spp. | *Coscinodiscus oculus-iridis* | *Coscinodiscus rhombicus* | *Coscinodiscus* spp. | *Hemiaulus* spp. | *Paralia sulcata* var. *crenulata* | *Podosira* spp. | *Pyxilla* fragments | *Rocella gelida* | *Rocella gelida* var. *schraderi* | *Rocella vigilans* | *Rossiella* spp. | *Sceptroneis* spp. | *Stephanopyxis grunowii* | *Stephanopyxis turris* | *Synedra jouseana* | *Triceratium morlandii* | *Triceratium pulvinar* | *Triceratium* spp. | *Xanthiopyxis* spp. | Silicoflagellate tests | Sponge spicules |
|---|---|---|---|---|---|---|---|---|---|---|---|---|---|---|---|---|---|---|---|---|---|---|---|---|---|---|---|---|---|---|
| 189-1171D- | | | | | | | | | | | | | | | | | | | | | | | | | | | | | | |
| 1R-CC, 15-20 | 250.27 | G | A | | | R | | | | R | | D | | | | | A | A | C | C | | C | C | A | | C | | | | A |
| 2R-CC, 17-22 | 260.68 | G | A | | | | A | | | | R | C | | R | | | A | A | F | R | | | | A | | | | | A | A |
| 3R-CC, 14-19 | 271.34 | M | C | C | | R | | C | | F | | C | C | C | A | C | | | | | F | C | C | | | R | F | A | F | A |
| 4R-CC, 15-20 | 280.59 | P | C | | | R | | | | | | R | | A | A | | | | | | | A | A | | R | R | | C | F | A |
| 5R-CC, 15-20 | 287.53 | P | R | | | | | | | R | | R | | | | | R | R | | | | R | R | | | | | | | T |
| 6R-CC, 7-12 | 295.26 | P | F | | | | | | | | | | R | | | F | | | | | | F | F | | | | | | T | F |
| 7R-CC, 15-20 | 302.30 | P | C | R | | | | R | R | C | | | | R | | A | | | | | | C | D | | | | R | A | R | |
| 8R-CC, 0-5 | 307.84 | P | C | C | | | | | | F | | | | A | | A | | | | | R | R | R | | | | | R | | F |
| 9R-CC, 12-17 | 318.77 | P | C | R | | | | A | | | | | C | | | A | | | | | | C | C | | | | | R | | F |
| 10R-CC, 12-17 | 330.78 | P | C | | | | | C | | | R | R | C | C | | A | | | | | | C | C | | | | R | | | C |
| 11R-CC, 12-13 | 334.02 | P | C | | | F | | | | | | R | | F | | R | | | | | | C | F | | | | | | F | |
| 12R-CC, 11-13 | 343.61 | P | T | | | | | | | | | | | | | | | | | | | | | | | | | | | | |
| 13R-CC, 8-11 | 353.28 | P | T | | | | | | | | | | | | | | | | | | | | | | | | | | | | |
| 14R-CC, 16-21 | 363.28 | MP | F | | | R | | | | | | F | | | | | | | | | | | | | | | | | | |
| 15R-CC, 20-25 | 374.35 | MP | F | | | | | | | R | | R | R | | | R | | | | | | | | | | | | | | |
| 16R-CC, 18-23 | 385.18 | M | T | | | | | | | | | R | | | | | | | | | | R | | | | | | | | |
| 17R-CC, 24-29 | 398.40 | M | F | | | | | | | | | | R | | | R | | | | | | F | | | | | | | | |
| 18R-CC, 0-3 | 401.20 | MP | R | | | | | | | | | | | | | | | | | | | R | | | | | | | | |
| 19R-CC, 0-5 | 417.63 | P | T | | | | | | | | | R | | | | | | | | | | | | | | | | | | T |
| 20R-CC, 6-12 | 428.65 | M | T | | | | | | | | | R | | | | | | | | | | | | | | | | | | |
| 21R-CC, 32-38 | 430.32 | M | R | | | | | | | | | R | | | | | | | | | | R | | | | | | | | |
| 22R-CC, 12-17 | 448.84 | P | T | | | | | | | | | | | | | R | | | | | | | | | | | | | | |
| 23R-CC, 10-16 | 453.57 | | B | | | | | | | | | | | | | | | | | | | | | | | | | | | |
| 24R-CC, 29-34 | 464.32 | P | T | | | | | | | | | R | | | | | | | | | | R | | | | | | | | T |
| 25R-CC, 0-5 | 476.81 | P | T | | | | | | | | | T | | | | | | | | | | R | | | | | | | | T |
| 26R-CC, 15-20 | 487.98 | P | T | | | | | | | | | | | | | | | | | | | | R | | | | | | | T |
| 27R-CC, 7-12 | 497.45 | | B | | | | | | | | | | | | | | | | | | | | | | | | | | | |
| 28R-CC, 5-10 | 505.73 | | B | | | | | | | | | | | | | | | | | | | | | | | | | | | |
| 29R-CC, 13-18 | 516.79 | P | T | | | | | | | | | | | | | | | | | | | | | | | | | | | |
| 30R-CC, 12-17 | 524.58 | P | T | | | | | | | | | | | | | | | | | | | | | | | | | | | |
| 31R-CC, 28-33 | 533.73 | P | T | | | | | | | | | | | | | | | | | | | R | | | | | | | | |
| 32R-CC, 0-5 | 543.96 | P | T | | | | | | | | | T | | | | | | | | | | T | | | | | | | | |
| 33R-CC, 0-5 | 555.02 | P | F | | | | | | | | | F | | | | | | | | | | R | | | | | | | | |
| 34R-CC, 0-5 | 564.79 | | T | | | | | | | | | R | | | | | | | | | | | | | | | | | | |
| 35R-CC, 7-12 | 573.86 | | B | | | | | | | | | R | | | | | | | | | | | | | | | | | | |
| 36R-CC, 13-18 | 584.10 | P | T | | | | | | | | | | | | | | | | | | | | | | | | | | | T |

Notes: Preservation: G = good, M = moderate, MP = moderate-poor, P = poor. Abundance: D = dominant, A = abundant, C = common, F = few, R = rare, T = trace, B = barren.

**Table T10.** Diatom bioevents identified, Holes 1171A, 1171C, and 1171D.

| Hole | Bioevents | Age (Ma) | Sample Top | Sample Bottom | Depth (mbsf) Top | Depth (mbsf) Bottom | Mean (mbsf) | Error bar (m) |
|---|---|---|---|---|---|---|---|---|
| 1171A | LO *Actinocyclus ingens* | 0.64 | 1H-CC | 2H-CC | 7.02 | 16.10 | 11.56 | 4.54 |
| 1171A | LO *Fragilariopsis reinholdii* | 0.65 | 1H-CC | 2H-CC | 7.02 | 16.10 | 11.56 | 4.54 |
| 1171A | LO *Thalassiosira fasciculata* | 0.70 | 1H-CC | 2H-CC | 7.02 | 16.10 | 11.56 | 4.54 |
| 1171A | LO *Fragilariopsis barronii* | 1.40 | 2H-CC | 3H-CC | 16.10 | 24.76 | 20.43 | 4.33 |
| 1171A | LO *Thalassiosira tetraoestrupii* var. *reimeri* | 1.50 | 2H-CC | 3H-CC | 16.10 | 24.76 | 20.43 | 4.33 |
| 1171A | LO *Proboscia barboi* | 1.80 | 2H-CC | 3H-CC | 16.10 | 24.76 | 20.43 | 4.33 |
| 1171A | LO *Thalassiosira complicata* | 2.50 | 3H-CC | 4H-CC | 24.76 | 35.78 | 30.27 | 5.51 |
| 1171A | LO *Thalassiosira inura* | 2.50 | 3H-CC | 4H-CC | 24.76 | 35.78 | 30.27 | 5.51 |
| 1171A | LO *Thalassiosira insigna* | 2.63 | 3H-CC | 4H-CC | 24.76 | 35.78 | 30.27 | 5.51 |
| 1171A | LO *Fragilariopsis weaveri* | 2.65 | 3H-CC | 4H-CC | 24.76 | 35.78 | 30.27 | 5.51 |
| 1171A | FO *Fragilariopsis weaveri* | 3.40 | 6H-CC | 7H-CC | 55.17 | 64.20 | 59.69 | 4.52 |
| 1171C | LO *Actinocyclus ingens* var. *ovalis* | 6.27 | 6H-CC | 7H-CC | 57.45 | 67.13 | 62.29 | 4.84 |
| 1171A | FO *Fragilariopsis reinholdii* | 8.10 | 8H-CC | 9H-CC | 73.05 | 82.40 | 77.73 | 4.68 |
| 1171A | FO *Actinocyclus ingens* var. *ovalis* | 8.68 | 8H-CC | 9H-CC | 73.05 | 82.40 | 77.73 | 4.68 |
| 1171A | LO *Denticulopsis dimorpha* | 10.70 | 10H-CC | 11H-CC | 92.66 | 102.49 | 97.58 | 4.91 |
| 1171A | FO *Actinocyclus fryxellae* | 11.05 | 13H-CC | 14H-CC | 113.66 | 120.53 | 117.10 | 3.44 |
| 1171C | LO *Denticulopsis praedimorpha* | 11.53 | 13X-CC | 14X-CC | 115.72 | 123.49 | 119.61 | 3.88 |
| 1171C | LO *Nitzschia denticuloides* | 11.70 | 13X-CC | 14X-CC | 115.72 | 123.49 | 119.61 | 3.88 |
| 1171C | LO *Proboscia barboi* | 12.50 | 14X-CC | 15X-CC | 123.49 | 134.45 | 128.97 | 5.48 |
| 1171C | LO *Actinocyclus ingens* var. *nodus* | 12.71 | 14X-CC | 15X-CC | 123.49 | 134.45 | 128.97 | 5.48 |
| 1171C | FO *Actinocyclus ingens* var. *nodus* | 14.38 | 21X-CC | 22X-CC | 190.11 | 198.93 | 194.52 | 4.41 |
| 1171C | LO *Cavitatus (Synedra) jouseanus* | 14.61 | 22X-CC | 23X-CC | 198.93 | 210.12 | 204.53 | 5.60 |
| 1171C | LO *Rocella gelida* | 22.46 | 25X-CC | 26X-CC | 228.48 | 237.56 | 233.02 | 4.54 |
| 1171D | FO *Rocella gelida* | 26.50 | 2R-CC | 3R-CC | 260.68 | 271.34 | 266.01 | 5.33 |
| 1171C | FO *Rocella gelida* | 26.50 | 29X-CC | 30X-CC | 264.83 | 272.87 | 268.85 | 4.02 |
| 1171D | FO *Rocella vigilans* (small) | 30.24 | 2R-CC | 3R-CC | 260.68 | 271.34 | 266.01 | 5.33 |
| 1171C | FO *Rocella vigilans* (small) | 30.24 | 30X-CC | 31X-CC | 272.87 | 274.43 | 273.65 | 0.78 |
| 1171D | FO *Cavitatus (Synedra) jouseanus* | 30.62 | 2R-CC | 3R-CC | 260.68 | 271.34 | 266.01 | 5.33 |
| 1171C | FO *Cavitatus (Synedra) jouseanus* | 30.62 | 30X-CC | 31X-CC | 272.87 | 274.43 | 273.65 | 0.78 |

Note: LO = last occurrence, FO = first occurrence.

**Table T11.** Distribution of organic-walled dinoflagellate cysts (dinocysts; number of specimens) and percentages of other palynomorph groups in selected samples, 1171D. (Continued on next page.)

| Core, section, interval (cm) | Depth (mbsf) | Preservation | Group abundance | N (palynomorphs) | Dinocysts (%) | Sporomorphs (%) | Foraminifer linings (%) | Acritarchs (%) | N (dinocysts) | Achilleodinium biformoides | Achomosphaera alcicornu | Achomosphaera ramulifera | Alisocysta circumtabulata | Alterbidinium distinctum | Alterbidinium spp. | Apectodinium homomorphum | Arachnodinium antarcticum | Areoligera spp. | Areosphaeridium diktyoplokum | Batiacasphaera compta | Cassidium fragile | Cerebrocysta bartonensis | Cerodinium spp. | Charlesdowniea coleothrypta | Charlesdowniea edwardsii | Cordosphaeridium fibrospinosum | Corrudinium sp. (G&F '83) | Cribroperidinium spp. | Dapsilidinium pseudocolligerum | Deflandrea phosphoritica group | Dracodinium waipawaense | Elytrocysta spp. | Enneadocysta harrisii | Enneadocysta partridgei | Enneadocysta pectiniformis | Fibrocysta axialis | Glaphyrocysta retiintexta | Hafniasphaera septata | Hystrichokolpoma spinosum | Hystrichosphaeridium truswelliae | Hystrichosphaeridium tubiferum |
|---|---|---|---|---|---|---|---|---|---|---|---|---|---|---|---|---|---|---|---|---|---|---|---|---|---|---|---|---|---|---|---|---|---|---|---|---|---|---|---|---|---|
| 189-1171D- | | | | | | | | | | | | | | | | | | | | | | | | | | | | | | | | | | | | | | | | | |
| 1R-CC, 15-20 | 250.27 | | B | 0 | | | | | | | | | | | | | | | | | | | | | | | | | | | | | | | | | | | | | |
| 2R-CC, 17-22 | 260.68 | | B | 0 | | | | | | | | | | | | | | | | | | | | | | | | | | | | | | | | | | | | | |
| 3R-CC, 14-19 | 271.34 | G | A | 163 | 82.2 | 5.5 | 5.5 | 6.7 | 204 | | | | | 17 | 4 | | | | 1 | | | | | | | | 3 | | | 23 | 10 | | | 18 | 2 | | | | | 1 | |
| 4R-CC, 15-20 | 280.59 | G | A | 170 | 82.9 | 4.7 | 6.5 | 5.9 | 204 | | | | | 17 | 7 | | | | | | | | | | | | 6 | | | 53 | 6 | | | 8 | 3 | | | | | | 1 |
| 5R-CC, 15-20 | 287.53 | G | A | 147 | 88.4 | 4.8 | 4.1 | 2.7 | 133 | | | | | 5 | 1 | | | | | | | | | | | | 1 | | | 36 | 12 | | | 9 | 2 | | | | | | |
| 6R-CC, 7-12 | 295.26 | G | A | 88 | 92.0 | 1.1 | 4.5 | 2.3 | 126 | | | | | | | | | | | 1 | | | | | | | 1 | | | 45 | 1 | | | 5 | 1 | 1 | | | | | |
| 7R-CC, 15-20 | 302.30 | G | A | 216 | 97.7 | 0.9 | 0.9 | 0.5 | 228 | 1 | 1 | | | | 6 | 1 | | | 1 | | 1 | | | | | | | | | 112 | | | | 8 | | | | | | 1 | 1 |
| 8R-CC, 0-5 | 307.84 | G | A | 222 | 96.8 | 0.5 | 0.5 | 2.3 | 227 | | | | | | 10 | 1 | | | 1 | | 1 | | | | | | | | 1 | 107 | | | | 2 | 2 | | | | | 1 | 1 |
| 10R-CC, 12-17 | 330.78 | G | A | 263 | 97.0 | 0.8 | 1.9 | 0.4 | 260 | 4 | | | | | 1 | 1 | | | | | 1 | | 1 | | | | | | | 22 | | | | 1 | | | | | | 20 | 10 |
| 11R-CC, 12-13 | 334.02 | G | A | 181 | 96.7 | 0.0 | 2.8 | 0.6 | 219 | 1 | | | | | 5 | | | | | | 1 | | | | | | | | | 30 | | | | 1 | | | | | | 5 | 15 |
| 13R-CC, 8-11 | 353.28 | G | A | 159 | 92.5 | 0.6 | 2.5 | 4.4 | 163 | | | | | | | | | | | | 1 | 1 | | | | | | | | 81 | | | | 2 | | | | | | | |
| 15R-CC, 20-25 | 374.35 | G | A | 163 | 93.9 | 0.6 | 4.9 | 0.6 | 163 | | | | | | 1 | 1 | 1 | | | | | | | | | | | | | 91 | 1 | | | 1 | | | | | | 3 | 5 |
| 17R-CC, 24-29 | 398.40 | G | A | 183 | 92.3 | 1.1 | 3.8 | 2.7 | 140 | | | | | | | 2 | 1 | | | | 1 | | | | | | | | | 81 | | | | 30 | | | | | | 1 | 4 |
| 19R-CC, 0-5 | 417.63 | G | A | 178 | 97.8 | 0.0 | 1.7 | 0.6 | 249 | | | | | | | 1 | | | | | 1 | | | | | | | | | 70 | | | | 170 | | | | | | | |
| 21R-CC, 32-38 | 430.32 | G | A | 156 | 96.2 | 0.6 | 2.6 | 0.6 | 179 | | | | | | | 1 | | | | | 1 | | | | | 1 | | | | 110 | | | | 50 | | | | | | | |
| 23R-CC, 10-16 | 453.57 | G | A | 143 | 93.0 | 0.0 | 2.8 | 4.2 | 139 | | | | | | 15 | 1 | | | | | 1 | | | | | 3 | | | | 70 | | | | 20 | | | | | | | 7 |
| 25R-CC, 0-5 | 476.81 | G | A | 162 | 96.3 | 0.0 | 3.1 | 0.6 | 204 | | | | | | 3 | | | | | | 1 | | | | | | | | | 127 | 2 | | | 1 | | | | | | | 1 |
| 27R-CC, 7-12 | 497.45 | G | A | 222 | 95.9 | 2.3 | 1.4 | 0.5 | 234 | | | | | | 18 | 2 | | | 1 | | | | 3 | | | | | | | 90 | | | 1 | 45 | | | | | | | 16 |
| 29R-CC, 13-18 | 516.79 | G | A | 175 | 90.3 | 5.7 | 3.4 | 0.6 | 172 | | | | | | 3 | | | | 45 | 4 | | 1 | | | | | | | | 18 | | | 5 | 50 | | | | | | | 1 |
| 35R-CC, 7-12 | 573.86 | G | A | 211 | 100.0 | 0.0 | 0.0 | 0.0 | 211 | | | | | | 1 | 1 | | | | | | | | | | | | | | 200 | | | | 1 | | | | | | 1 | 1 |
| 40R-CC, 19-24 | 622.70 | G | A | 138 | 90.6 | 4.3 | 2.9 | 2.2 | 211 | | | | 1 | | | | | | | | | | | | | 1 | | 1 | | 170 | | | | | | 1 | | | 1 | | 8 |
| 44R-CC, 17-22 | 660.71 | G | A | 169 | 97.6 | 1.2 | 0.6 | 0.6 | 169 | | | | | | | | | | | | | | | | | | 1 | 1 | | 125 | | | 9 | | | | | | | 1 | 1 |
| 50R-CC, 23-28 | 718.48 | M | F | 0 | | | | | 14 | | | | | | 1 | | 1 | | | | | | | | | 1 | | | | 1 | | | | 1 | | | | | | 1 | 1 |
| 56R-CC, 17-22 | 771.40 | M | F | 0 | | | | | 15 | | | | | | 1 | | | | | | | | | | | 1 | | | | 1 | 1 | | 1 | 1 | 1 | | | | | 1 | 1 |
| 60R-CC, 10-15 | 814.60 | M | F | 0 | | | | | 14 | | | | | | 1 | | | | | | | | | | | 1 | | | | 1 | | | 1 | | | 1 | | | | 1 | 1 |
| 70R-CC, 17-22 | 908.07 | M | C | 137 | 94.9 | 1.5 | 2.2 | 1.5 | 128 | | | 1 | | | 4 | | 3 | | | | | | 4 | | | 3 | 20 | 2 | | 40 | 2 | | | | 2 | 1 | | | 4 | | 3 |
| 71R-CC, 34-39 | 919.12 | M | C | 131 | 71.8 | 19.1 | 7.6 | 1.5 | 88 | | | | | | 2 | | 1 | | | 1 | | | 10 | | | 1 | | 5 | | 12 | 6 | | | | | 2 | | | 1 | | 19 |
| 72R-CC, 0-5 | 929.29 | P | C | 93 | 75.3 | 16.1 | 5.4 | 3.2 | 56 | | | | | | 3 | | | | | | 1 | | 6 | | | 1 | | 1 | | 6 | | | | | | | 2 | 2 | | | 2 |
| 73R-CC, 0-5 | 939.51 | P | F | 0 | | | | | 12 | | | | | | 1 | 1 | | | | | 1 | | 1 | | | | | 1 | | 1 | | | | | | | | | 1 | | 1 |
| 74R-CC, 0-8 | 949.50 | P | C | 124 | 64.5 | 28.2 | 3.2 | 4.0 | 126 | | | | | | 12 | | 1 | | | | 2 | | 13 | | | 1 | | 1 | | 6 | 1 | | | | | | | 1 | 1 | 1 | 7 |
| 75R-CC, 23-28 | 954.94 | M | C | 94 | 53.2 | 37.2 | 5.3 | 4.3 | 82 | | | | | | 13 | | | | | | | 1 | 2 | | | 1 | | 8 | | 1 | 2 | | | | | | | | | 3 | 8 |

Notes: Preservation: G = good, M = moderate, P = poor. Group abundance refers to abundance of dinocysts: A = abundant, C = common, F = few, R = rare, T = trace, B = barren. B&B '93 = Brinkhuis and Biff, 1993; C&H '96 = Crouch and Hollis, 1996; G&F '83 = Goodman and Ford, 1983.

# Table T11 (continued).

| Core, section, interval (cm) | Depth (mbsf) | Hystrichostrogylon spp. | Impagidinium dispertitum | Impagidinium sp. (B&B '93) | Impagidinium sp. a (C&H '96) | Impagidinium spp. (pars) | Impagidinium victorianum | Lejeunecysta spp. | Membranophoridium perforatum | Octodinium askiniae | Operculodinium centrocarpum | Operculodinium sp. A | Operculodinium sp. B | Palaeocystodinium spp. | Pentadinium goniferum | Phthanoperidinium spp. | Pyxidinopsis sp. | Pyxidinopsis waipawaensis | Rhombodinium rhomboideum | Samlandia chlamydophora | Samlandia septata | Selenopemphix nephroides | Spinidinium densispinatum | Spinidinium macmurdoense | Spiniferites ramosus | Stoveracysta ornata | Systematophora placacantha | Tectatodinium spp. | Thalassiphora pelagica | Turbiosphaera filosa | Vozzhennikovia spp. | Wetzeliella articulata |
|---|---|---|---|---|---|---|---|---|---|---|---|---|---|---|---|---|---|---|---|---|---|---|---|---|---|---|---|---|---|---|---|---|
| 189-1171D- | | | | | | | | | | | | | | | | | | | | | | | | | | | | | | | | |
| 1R-CC, 15-20 | 250.27 | | | | | | | | | | | | | | | | | | | | | | | | | | | | | | | |
| 2R-CC, 17-22 | 260.68 | | | | | | | | | | | | | | | | | | | | | | | | | | | | | | | |
| 3R-CC, 14-19 | 271.34 | | | 1 | | 1 | 4 | 18 | | 10 | 2 | 14 | | | | 7 | | | | | | 6 | 2 | 4 | 2 | | | 1 | 2 | 6 | 45 | |
| 4R-CC, 15-20 | 280.59 | | | 1 | 2 | | 4 | 10 | | 12 | | 21 | | | 1 | 3 | | | | 1 | | 5 | 2 | 2 | 2 | | | 8 | 1 | 5 | 23 | |
| 5R-CC, 15-20 | 287.53 | | | 1 | | | 2 | 4 | | | 1 | 17 | | | | 13 | | | | | | 4 | | 6 | 8 | 1 | | 1 | | 3 | 6 | |
| 6R-CC, 7-12 | 295.26 | | | | 1 | 1 | 1 | | | | | 15 | | | | 30 | 1 | | | | | 2 | | | | | 1 | 1 | 2 | 12 | 4 | |
| 7R-CC, 15-20 | 302.3 | | | 1 | | | | | | | | 2 | | | | 43 | 1 | | | | | 1 | | 6 | 4 | | | | 1 | | 36 | |
| 8R-CC, 0-5 | 307.84 | | | 1 | | | | 1 | | 1 | | 3 | 1 | | | 47 | | | | 1 | | | | 5 | 1 | | | | | 4 | 35 | |
| 10R-CC, 12-17 | 330.78 | | | 5 | | | 5 | | | 1 | | 1 | | | | | | | | | | | | 2 | 45 | | | | | | 140 | |
| 11R-CC, 12-13 | 334.02 | | | 4 | | | 3 | 2 | | 3 | | 1 | | | | 1 | | | | | | 2 | | 3 | 25 | | | | | | 117 | |
| 13R-CC, 8-11 | 353.28 | 1 | | 3 | | | 1 | 1 | | 2 | | 4 | | | 1 | | | | | | | | | 1 | 3 | | | | | 38 | 23 | |
| 15R-CC, 20-25 | 374.35 | | | | | 1 | | 3 | | 5 | | 1 | | | | | | | | | | | | | 10 | | | | | 27 | 12 | |
| 17R-CC, 24-29 | 398.4 | 1 | | | | | 1 | 1 | | 1 | | 2 | | | | | | | | | | 1 | | | | | | 1 | 1 | 1 | 10 | |
| 19R-CC, 0-5 | 417.63 | | | | | | | 1 | | | | 3 | | | | | | | | | | | | 1 | 1 | | | | | | 1 | |
| 21R-CC, 32-38 | 430.32 | | | | 1 | | | 1 | | | | 4 | | | | | | | | | | | | | 4 | | | | | 1 | 5 | |
| 23R-CC, 10-16 | 453.57 | | | 1 | 1 | | | 1 | | | | 1 | 1 | | | 1 | | | | 1 | | 1 | | 1 | 11 | | | | 1 | | 1 | |
| 25R-CC, 0-5 | 476.81 | | | | | | | 3 | | 1 | | 7 | 14 | | | 30 | | | | | | 1 | | 1 | 1 | | | | | | 11 | |
| 27R-CC, 7-12 | 497.45 | | | | | | | 1 | | 1 | | 3 | 1 | | | 8 | | | | | | 1 | | 5 | 3 | | | | | | 35 | |
| 29R-CC, 13-18 | 516.79 | | | | | | | 1 | | | | 5 | 22 | | | 1 | | | | | | | | 1 | 12 | | | | | | 3 | |
| 35R-CC, 7-12 | 573.86 | | | | | | | 1 | 1 | | | | | | | 1 | | 1 | | | | | | | 1 | | | | | | 1 | |
| 40R-CC, 19-24 | 622.7 | 1 | | | | | | 1 | 1 | | | | | | | | | | 3 | | | | | | 20 | | 1 | | | | 1 | |
| 44R-CC, 17-22 | 660.71 | | | | | | | 1 | | | 2 | | | | | | | | 1 | | | | | | 6 | | 20 | | | | 1 | |
| 50R-CC, 23-28 | 718.48 | 1 | | | | | | | 1 | 1 | 1 | 1 | 1 | | | | | | | | | | | | 1 | | | | | | | |
| 56R-CC, 17-22 | 771.4 | | | | | | | 1 | | | 1 | 1 | | 1 | | 1 | | | | 1 | | | | | 1 | | | | | | | 1 |
| 60R-CC, 10-15 | 814.6 | | | | | | | | | | 1 | 1 | | 1 | | 1 | 1 | | | | | | | | 1 | | | | | | 1 | 1 |
| 70R-CC, 17-22 | 908.07 | | | | | | | | | | 5 | | 19 | | | | | | | | 1 | | | 1 | 6 | | 1 | | | | 6 | |
| 71R-CC, 34-39 | 919.12 | | | | | | | | | | | 3 | 8 | 2 | | | | | | | | | 1 | 1 | 10 | | | | | | 3 | |
| 72R-CC, 0-5 | 929.29 | | | | | | | 1 | | | 7 | 1 | 7 | 5 | | | 1 | | | 1 | | | | | 8 | | | | 1 | | | |
| 73R-CC, 0-5 | 939.51 | | | | | | | | | | 1 | | 1 | | | | | | | | | | | | 1 | | | | 1 | | | |
| 74R-CC, 0-8 | 939.5 | | | | | | | | | | 8 | | 29 | | | | 2 | | | | | | 5 | | 32 | | 1 | | | | 2 | |
| 75R-CC, 23-28 | 954.94 | | | | | | | | | | 8 | | 10 | | | | 1 | | | | | | 2 | | 18 | | 1 | | | | 2 | |

**Table T12.** Selected dinocyst events, Hole 1171D.

| Bioevent | Age (Ma) | Interval | | Depth (mbsf) | | Mean (mbsf) | Error bar (m) | Source |
|---|---|---|---|---|---|---|---|---|
| | | Top | Bottom | Top | Bottom | | | |
| LO *Areosphaeridium diktyoplokum* | 33.3 | 1171C-30X-CC | 1171C-31X-CC | 272.87 | 274.43 | 273.65 | 0.78 | Williams et al., 1998 |
| LO *Areosphaeridium diktyoplokum* | 33.3 | 1171D-2R-CC | 1171D-3R-CC | 260.68 | 271.34 | 266.01 | 5.33 | Williams et al., 1998 |
| FCO *Alterbidinium distinctum* | 37 | 1171D-4R-CC | 1171D-5R-CC | 280.59 | 287.53 | 284.06 | 3.47 | Raine et al., 1997 |
| LO *Cerebrocysta bartonensis* | 38.6 | 1171D-6R-CC | 1171D-7R-CC | 295.26 | 302.30 | 298.78 | 3.52 | Williams et al., 1998 |
| LAO *Enneadocysta partridgei* | 39.5 | 1171D-15R-CC | 1171D-17R-CC | 374.35 | 398.40 | 386.37 | 12.03 | Raine et al., 1997 |
| FO *Cerebrocysta bartonensis* | 43 | 1171D-29R-CC | 1171D-35R-CC | 516.79 | 573.86 | 545.33 | 28.54 | Powell, 1992 |
| FAO *Enneadocysta partridgei* | 43 | 1171D-29R-CC | 1171D-35R-CC | 516.79 | 573.86 | 545.33 | 28.54 | Raine et al., 1997 |
| LO *Membranophoridium perforatum* | 46.3 | 1171D-29R-CC | 1171D-35R-CC | 516.79 | 573.86 | 545.33 | 28.54 | Wilson, 1988 |
| LO *Hystrichokolpoma spinosa* | 47 | 1171D-35R-CC | 1171D-40R-CC | 573.86 | 622.70 | 598.28 | 24.42 | Wilson, 1988 |
| LO *Charlesdowniea edwardsii* | 48 | 1171D-40R-CC | 1171D-44R-CC | 622.70 | 660.71 | 641.71 | 19.01 | Wilson, 1988 |
| LO *Charlesdowniea coleothrypta* | 48.5 | 1171D-40R-CC | 1171D-44R-CC | 622.70 | 660.71 | 641.71 | 19.01 | Wilson, 1988 |
| FO *Pyxidinopsis waipawaense* | 49.5 | 1171D-44R-CC | 1171D-50R-CC | 660.71 | 718.48 | 689.60 | 28.89 | Wilson, 1988 |
| FO *Charlesdowniea coleothrypta* | 50.3 | 1171D-44R-CC | 1171D-50R-CC | 660.71 | 718.48 | 689.60 | 28.89 | Wilson, 1988 |
| FO *Charlesdowniea edwardsii* | 50.3 | 1171D-44R-CC | 1171D-50R-CC | 660.71 | 718.48 | 689.60 | 28.89 | Wilson, 1988 |
| FO *Areosphaeridium diktyoplokum* | 51.73 | 1171D-50R-CC | 1171D-56R-CC | 718.48 | 771.40 | 744.94 | 26.46 | Williams et al., 1998 |
| FO *Membranophoridium perforatum* | 53 | 1171D-50R-CC | 1171D-56R-CC | 718.48 | 771.40 | 744.94 | 26.46 | Wilson, 1988 |
| LO *Dracodinium waipawaense* | 53.2 | 1171D-60R-CC | 1171D-70R-CC | 814.60 | 908.07 | 861.34 | 46.74 | Wilson, 1988 |
| FO *Dracodinium waipawaense* | 53.5 | 1171D-70R-CC | 1171D-71R-CC | 908.07 | 920.20 | 914.14 | 6.07 | Wilson, 1988 |
| FO *Hystrichokolpoma spinosa* | 53.5 | 1171D-70R-CC | 1171D-71R-CC | 908.07 | 920.20 | 914.14 | 6.07 | Wilson, 1988 |
| FO *Deflandrea phosphoriticacpx* | 55 | 1171D-72R-CC | 1171D-73R-CC | 920.20 | 939.51 | 929.86 | 9.66 | Wilson, 1988 |
| FO *Apectodinium homomorphum* | ~56 | 1171D-73R-CC | 1171D-75R-CC | 939.51 | 954.94 | 947.23 | 7.72 | Williams et al., 1998 |
| LO *Cassidium fragile* | ~56 | 1171D-72R-CC | 1171D-73R-CC | 929.29 | 939.51 | 934.40 | 5.11 | Wilson, 1988 |
| LO *Spinidinium densispinatum* | ~58 | 1171D-73R-CC | 1171D-75R-CC | 939.51 | 954.94 | 947.23 | 7.72 | Wilson, 1988 |

Note: LO = last occurrence, FCO = first consistent occurrence, FO = first occurrence, FOA = first abundant occurrence.

**Table T13.** Biostratigraphic events identified, Site 1171. (**See table notes.** Continued on next page.)

| Group | Hole | Bioevent | Age (Ma) | Interval (cm) Top | Bottom | Depth (mbsf) Top | Bottom | Mean (mbsf) | +/− | Top (mcd) | Bottom (mcd) | Mean (mcd) | +/− |
|---|---|---|---|---|---|---|---|---|---|---|---|---|---|
| D | 1171A | LO *Fragilariopsis reinholdii* | 0.7 | 1H-CC | 2H-CC | 7.02 | 16.10 | 11.56 | 4.54 | 7.02 | 16.84 | 11.93 | 4.91 |
| R | 1171A | LO *Antarctissa* sp. *G* | 0.7 | 2H-CC | 3H-CC | 16.10 | 24.76 | 20.43 | 4.33 | 16.84 | 25.32 | 21.08 | 4.24 |
| D | 1171A | LO *Thalassiosira fasciculata* | 0.7 | 1H-CC | 2H-CC | 7.02 | 16.10 | 11.56 | 4.54 | 7.02 | 16.84 | 11.93 | 4.91 |
| D | 1171A | LO *Fragilariopsis barronii* | 1.4 | 2H-CC | 3H-CC | 16.10 | 24.76 | 20.43 | 4.33 | 16.84 | 25.32 | 21.08 | 4.24 |
| D | 1171A | LO *Thalassiosira tetraoestrupii* var. *reimeri* | 1.5 | 2H-CC | 3H-CC | 16.10 | 24.76 | 20.43 | 4.33 | 16.84 | 25.32 | 21.08 | 4.24 |
| D | 1171A | LO *Proboscia barboi* | 1.8 | 2H-CC | 3H-CC | 16.10 | 24.76 | 20.43 | 4.33 | 16.84 | 25.32 | 21.08 | 4.24 |
| D | 1171A | LO *Thalassiosira complicata* | 2.5 | 3H-CC | 4H-CC | 24.76 | 35.78 | 30.27 | 5.51 | 25.32 | 36.96 | 31.14 | 5.82 |
| D | 1171A | LO *Thalassiosira inura* | 2.5 | 3H-CC | 4H-CC | 24.76 | 35.78 | 30.27 | 5.51 | 25.32 | 36.96 | 31.14 | 5.82 |
| D | 1171A | LO *Thalassiosira insigna* | 2.6 | 3H-CC | 4H-CC | 24.76 | 35.78 | 30.27 | 5.51 | 25.32 | 36.96 | 31.14 | 5.82 |
| D | 1171A | LO *Fragilariopsis weaveri* | 2.7 | 3H-CC | 4H-CC | 24.76 | 35.78 | 30.27 | 5.51 | 25.32 | 36.96 | 31.14 | 5.82 |
| D | 1171A | FO *Fragilariopsis weaveri* | 3.4 | 6H-CC | 7H-CC | 55.17 | 64.20 | 59.69 | 4.52 | 47.26 | 57.43 | 52.35 | 5.09 |
| R | 1171A | FO *Pseudocubus vema* | 4.5 | 4H-CC | 5H-CC | 35.78 | 45.36 | 40.57 | 4.79 | 36.96 | 47.26 | 42.11 | 5.15 |
| N | 1171A | LO *Amaurolithus delicatus* | 4.6 | 5H-CC | 6H-CC | 45.36 | 55.17 | 50.27 | 4.91 | 47.26 | 57.43 | 52.35 | 5.09 |
| R | 1171A | LCO *Stichocorys peregrina* | 5.0 | 4H-CC | 5H-CC | 35.78 | 45.36 | 40.57 | 4.79 | 36.96 | 47.26 | 42.11 | 5.15 |
| R | 1171A | LO *Lychnocanoma grande* | 5.0 | 5H-CC | 6H-CC | 45.36 | 55.17 | 50.27 | 4.91 | 47.26 | 57.43 | 52.35 | 5.09 |
| R | 1171A | LO *Amphymenium challengerae* | 6.1 | 6H-CC | 7H-CC | 55.17 | 64.20 | 59.69 | 4.52 | 57.43 | 67.76 | 62.60 | 5.17 |
| R | 1171A | FO *Amphymenium challengerae* | 6.6 | 7H-CC | 8H-CC | 64.20 | 73.05 | 68.63 | 4.43 | 67.76 | 77.75 | 72.76 | 5.00 |
| D | 1171A | FO *Fragilariopsis reinholdii* | 8.1 | 8H-CC | 9H-CC | 73.05 | 82.40 | 77.73 | 4.68 | 77.75 | 87.84 | 82.80 | 5.05 |
| D | 1171A | FO *Actinocyclus ingens* var. *ovalis* | 8.7 | 8H-CC | 9H-CC | 73.05 | 82.40 | 77.73 | 4.68 | 77.75 | 87.84 | 82.80 | 5.05 |
| D | 1171A | LO *Denticulopsis dimorpha* | 10.7 | 10H-CC | 11H-CC | 92.66 | 102.49 | 97.58 | 4.92 | 98.54 | 109.25 | 103.90 | 5.35 |
| D | 1171A | FO *Actinocyclus fryxellae* | 11.1 | 13X-CC | 14X-CC | 113.66 | 120.53 | 117.10 | 3.44 | 120.40 | 127.27 | 123.84 | 3.43 |
| R | 1171A | LAO *Cyrtocapsella japonica* | 11.6 | 11H-CC | 12H-CC | 102.49 | 110.62 | 106.56 | 4.07 | 109.25 | 117.36 | 113.31 | 4.05 |
| N | 1171C | LO *Pseudoemiliania lacunosa* | 0.5 | 1H-0 | 1H-CC | 0.00 | 9.65 | 4.83 | 4.83 | 0.44 | 10.096 | 5.27 | 4.83 |
| N | 1171C | LO *Calcidiscus macintyrei* | 1.7 | 2H-CC | 3H-CC | 19.24 | 28.53 | 23.89 | 4.65 | 19.98 | 28.58 | 24.28 | 4.30 |
| R | 1171C | LO *Pseudocubus vema* | 2.4 | 2H-CC | 3H-CC | 19.24 | 28.56 | 23.90 | 4.66 | 19.98 | 28.58 | 24.28 | 4.30 |
| P | 1171C | FO *Globorotalia inflata* | 3.2 | 3H-CC | 4H-CC | 28.56 | 37.80 | 33.18 | 4.62 | 28.58 | 38.14 | 33.36 | 4.78 |
| N | 1171C | LO *Reticulofenestra pseudoumbilica* | 3.8 | 4H-CC | 5H-CC | 37.80 | 47.86 | 42.83 | 5.03 | 38.14 | 49.46 | 43.80 | 5.66 |
| N | 1171C | LO *Triquetrorhabdulus rugosus* | 5.3 | 6H-CC | 7H-CC | 57.45 | 67.13 | 62.29 | 4.84 | 59.83 | 70.51 | 65.17 | 5.34 |
| P | 1171C | FO *Globorotalia puncticulata* | 5.3 | 6H-CC | 7H-CC | 57.45 | 67.13 | 62.29 | 4.84 | 59.83 | 70.51 | 65.17 | 5.34 |
| D | 1171C | LO *Actinocyclus ingens* var. *ovalis* | 6.3 | 6H-CC | 7H-CC | 57.45 | 67.13 | 62.29 | 4.84 | 59.83 | 70.51 | 65.17 | 5.34 |
| P | 1171C | FO *Globorotalia conomiozea* | 6.9 | 6H-CC | 7H-CC | 57.45 | 67.13 | 62.29 | 4.84 | 59.83 | 70.51 | 65.17 | 5.34 |
| P | 1171C | LO *Paragloborotalia nympha* | 10.1 | 7H-CC | 8H-CC | 67.13 | 75.33 | 71.23 | 4.10 | 70.51 | 80.71 | 75.61 | 5.10 |
| N | 1171C | LO *Coccolithus miopelagicus* | 10.9 | 13X-CC | 14X-CC | 115.72 | 123.49 | 119.61 | 3.89 | 122.40 | 130.17 | 126.29 | 3.88 |
| P | 1171C | LO *Paragloborotalia mayeri* | 11.4 | 10H-CC | 11H-CC | 94.40 | 104.12 | 99.26 | 4.86 | 100.62 | 111.06 | 105.84 | 5.22 |
| D | 1171C | LO *Denticulopsis praedimorpha* | 11.5 | 13X-CC | 14X-CC | 115.72 | 123.49 | 119.61 | 3.89 | 122.40 | 130.17 | 126.29 | 3.88 |
| D | 1171C | LO *Nitzschia denticuloides* | 11.7 | 13X-CC | 14X-CC | 115.72 | 123.49 | 119.61 | 3.89 | 122.40 | 130.17 | 126.29 | 3.88 |
| N | 1171C | LO *Cyclocargolithus floridanus* | 11.9 | 17X-CC | 18X-CC | 150.18 | 162.93 | 156.56 | 6.38 | 156.86 | 169.61 | 163.24 | 6.38 |
| P | 1171C | FO *Paragloborotalia mayeri* | 12.1 | 16X-CC | 17X-CC | 139.66 | 150.18 | 144.92 | 5.26 | 146.34 | 156.86 | 151.60 | 5.26 |
| D | 1171C | LO *Proboscia barboi* | 12.5 | 14X-CC | 15X-CC | 123.49 | 134.45 | 128.97 | 5.48 | 130.17 | 141.13 | 135.65 | 5.48 |
| R | 1171C | LAO *Cyrtocapsella tetrapera* | 12.5 | 14X-CC | 15X-CC | 123.49 | 134.45 | 128.97 | 5.48 | 130.17 | 141.13 | 135.65 | 5.48 |
| D | 1171C | LO *Actinocyclus ingens* var. *nodus* | 12.7 | 14X-CC | 15X-CC | 123.49 | 134.45 | 128.97 | 5.48 | 130.17 | 141.13 | 135.65 | 5.48 |
| D | 1171C | FO *Actinocyclus ingens* var. *nodus* | 14.4 | 21X-CC | 22X-CC | 190.11 | 198.93 | 194.52 | 4.41 | 196.79 | 205.61 | 201.20 | 4.41 |
| D | 1171C | LO *Cavitatus (Synedra) jouseanus* | 14.6 | 22X-CC | 23X-CC | 198.93 | 210.12 | 204.53 | 5.60 | 205.61 | 216.8 | 211.21 | 5.60 |
| P | 1171C | FO *Orbulina suturalis* | 15.1 | 20X-CC | 21X-CC | 181.10 | 190.11 | 185.61 | 4.51 | 187.78 | 196.79 | 192.29 | 4.51 |
| R | 1171C | FO *Lychnocanoma nipponica* | 15.7 | 19X-CC | 20X-CC | 172.76 | 181.10 | 176.93 | 4.17 | 179.44 | 187.78 | 183.61 | 4.17 |
| P | 1171C | FO *Praeorbulina curva* | 16.3 | 21X-CC | 22X-CC | 190.11 | 198.93 | 194.52 | 4.41 | 196.79 | 205.61 | 201.20 | 4.41 |
| R | 1171C | LO *Cenosphaera coronata* | 16.7 | 22X-CC | 23X-CC | 198.93 | 210.12 | 204.53 | 5.60 | 205.61 | 216.8 | 211.21 | 5.60 |
| N | 1171C | FO *Calcidiscus premacintyrei* | 17.4 | 22X-CC | 23X-CC | 198.93 | 210.12 | 204.53 | 5.60 | 205.61 | 216.8 | 211.21 | 5.60 |

# Table T13 (continued).

| Group | Hole | Bioevent | Age (Ma) | Interval (cm) Top | Bottom | Depth (mbsf) Top | Bottom | Mean (mbsf) | +/– | Top (mcd) | Bottom (mcd) | Mean (mcd) | +/– |
|---|---|---|---|---|---|---|---|---|---|---|---|---|---|
| P | 1171C | FO *Globigerinoides trilobus* | 18.8 | 22X-CC | 23X-CC | 198.93 | 210.12 | 204.53 | 5.60 | 205.61 | 216.80 | 211.21 | 5.60 |
| P | 1171C | FO *Globoturborotalita connecta* | 20.9 | 23X-CC | 24X-CC | 210.12 | 219.74 | 214.93 | 4.81 | 216.80 | 226.42 | 221.61 | 4.81 |
| D | 1171C | LO *Rocella gelida* | 22.5 | 25X-CC | 26X-CC | 228.48 | 237.56 | 233.02 | 4.54 | 235.16 | 244.24 | 239.70 | 4.54 |
| P | 1171C | FO *Globoturborotalita woodi* | 22.6 | 25X-CC | 26X-CC | 228.48 | 237.56 | 233.02 | 4.54 | 235.16 | 244.24 | 239.70 | 4.54 |
| N | 1171C | LO *Reticulofenestra bisecta* | 23.9 | 28X-CC | 29X-CC | 253.79 | 264.83 | 259.31 | 5.52 | 260.47 | 271.51 | 265.99 | 5.52 |
| D | 1171C | FO *Rocella gelida* | 26.5 | 29X-CC | 30X-CC | 264.83 | 272.87 | 268.85 | 4.02 | 271.51 | 279.55 | 275.53 | 4.02 |
| P | 1171C | LO *Subbotina angiporoides* | 30.0 | 29X-CC | 30X-CC | 264.83 | 272.87 | 268.85 | 4.02 | 271.51 | 279.55 | 275.53 | 4.02 |
| D | 1171C | FO *Rocella vigilans* (small) | 30.2 | 30X-CC | 31X-CC | 272.87 | 274.43 | 273.65 | 0.78 | 279.55 | 281.11 | 280.33 | 0.78 |
| D | 1171C | FO *Cavitatus (Synedra) jouseanus* | 30.6 | 30X-CC | 31X-CC | 272.87 | 274.43 | 273.65 | 0.78 | 279.55 | 281.11 | 280.33 | 0.78 |
| C | 1171C | LO *Areosphaeridium diktyoplokum* | 33.3 | 30X-CC | 31X-CC | 272.87 | 274.43 | 273.65 | 0.78 | 279.55 | 281.11 | 280.33 | 0.78 |
| R | 1171D | FO *Cyrtocapsella tetrapera* | 23.6 | 2R-CC | 3R-CC | 260.68 | 271.34 | 266.01 | 5.33 | 268.80 | 281.10 | 274.95 | 6.15 |
| N | 1171D | LO *Chiasmolithus altus* | 26.0 | 3R-3, 2 | 3R-3, 20 | 269.62 | 269.80 | 269.71 | 0.09 | 279.40 | 279.60 | 279.50 | 0.10 |
| D | 1171D | FO *Rocella gelida* | 26.5 | 2R-CC | 3R-CC | 260.68 | 271.34 | 266.01 | 5.33 | 268.80 | 281.10 | 274.95 | 6.15 |
| D | 1171D | FO *Rocella vigilans* (small) | 30.24 | 2R-CC | 3R-CC | 260.68 | 271.34 | 266.01 | 5.33 | 268.80 | 281.10 | 274.95 | 6.15 |
| D | 1171D | FO *Cavitatus (Synedra) jouseanus* | 30.62 | 2R-CC | 3R-CC | 260.68 | 271.34 | 266.01 | 5.33 | 268.80 | 281.10 | 274.95 | 6.15 |
| N | 1171D | LO *Isthmolithus recurvus* | 31.80 | 3R-3, 20 | 3R-CC | 269.80 | 271.39 | 270.60 | 0.80 | 279.60 | 281.10 | 280.40 | 0.80 |
| N | 1171D | LO *Reticulofenestra umbilica* | 32.3 | 3R-3, 20 | 3R-CC | 271.30 | 280.60 | 276.00 | 4.60 | 279.60 | 281.10 | 280.40 | 0.80 |
| N | 1171D | LO *Reticulofenestra oamaruensis* | 33.70 | 3R-3, 20 | 3R-CC | 268.80 | 271.36 | 270.10 | 1.30 | 279.60 | 281.10 | 280.40 | 0.80 |
| N | 1171D | LO *Reticulofenestra reticulata* | 35.0 | 4R-CC | 5R-CC | 280.60 | 287.50 | 284.10 | 3.50 | 290.40 | 297.30 | 293.80 | 3.50 |
| N | 1171D | FO *Isthmolithus recurvus* | 36.0 | 4R-CC | 5R-CC | 280.60 | 287.50 | 284.10 | 3.40 | 290.40 | 297.30 | 293.90 | 3.40 |
| C | 1171D | FCO *Alterbidinium distinctum* | 37.0 | 4R-CC | 5R-CC | 280.59 | 287.53 | 284.06 | 3.47 | 290.37 | 297.31 | 293.84 | 3.47 |
| C | 1171D | LO *Cerebrocysta bartonensis* | 38.6 | 6R-CC | 7R-CC | 295.26 | 302.30 | 298.78 | 3.52 | 305.04 | 312.08 | 308.56 | 3.52 |
| C | 1171D | LAO *Enneadocysta partridgei* | 39.5 | 15R-CC | 17R-CC | 374.35 | 398.40 | 386.38 | 12.03 | 384.13 | 408.18 | 396.16 | 12.03 |
| N | 1171D | LO *Chiasmolithus solitus* | 40.4 | 6R-CC | 7R-1, 25 | 300.70 | 300.30 | 295.30 | 5.00 | 300.70 | 310.40 | 305.50 | 4.90 |
| N | 1171D | FO *Reticulofenestra reticulata* | 42.0 | 6R-CC | 7R-1, 25 | 300.70 | 300.30 | 295.30 | 5.00 | 300.70 | 310.40 | 305.50 | 4.90 |
| C | 1171D | FO *Cerebrocysta bartonensis* | 43.0 | 29R-CC | 35R-CC | 516.79 | 573.86 | 545.33 | 28.54 | 526.57 | 583.64 | 555.11 | 28.54 |
| C | 1171D | FAO *Enneadocysta partridgei* | 43.0 | 29R-CC | 35R-CC | 516.79 | 573.86 | 545.33 | 28.54 | 526.57 | 583.64 | 555.11 | 28.54 |
| N | 1171D | FO *Reticulofenestra umbilica* | 43.7 | 25R-CC | 26R-CC | 476.80 | 488.00 | 482.40 | 5.60 | 486.60 | 497.80 | 492.20 | 5.60 |
| C | 1171D | LO *Membranophoridium perforatum* | 46.3 | 29R-CC | 35R-CC | 516.79 | 573.86 | 545.33 | 28.54 | 526.57 | 583.64 | 555.11 | 28.54 |
| C | 1171D | LO *Hystrichokolpoma spinosa* | 47.0 | 35R-CC | 40R-CC | 573.86 | 622.70 | 598.28 | 24.42 | 583.64 | 632.48 | 608.06 | 24.42 |
| C | 1171D | LO *Charlesdowniea edwardsii* | 48.0 | 40R-CC | 44R-CC | 622.70 | 660.71 | 641.71 | 19.01 | 632.48 | 670.49 | 651.49 | 19.01 |
| C | 1171D | LO *Charlesdowniea coleothrypta* | 48.5 | 40R-CC | 44R-CC | 622.70 | 660.71 | 641.71 | 19.01 | 632.48 | 670.49 | 651.49 | 19.01 |
| C | 1171D | FO *Pyxidinopsis waipawaense* | 49.5 | 44R-CC | 50R-CC | 660.71 | 718.48 | 689.60 | 28.89 | 670.49 | 728.26 | 699.38 | 28.89 |
| C | 1171D | FO *Charlesdowniea coleothrypta* | 50.3 | 44R-CC | 50R-CC | 660.71 | 718.48 | 689.60 | 28.89 | 670.49 | 728.26 | 699.38 | 28.89 |
| C | 1171D | FO *Charlesdowniea edwardsii* | 50.3 | 44R-CC | 50R-CC | 660.71 | 718.48 | 689.60 | 28.89 | 670.49 | 728.26 | 699.38 | 28.89 |
| C | 1171D | FO *Areosphaeridium diktyoplokum* | 51.7 | 50R-CC | 56R-CC | 718.48 | 771.40 | 744.94 | 26.46 | 728.26 | 781.18 | 754.72 | 26.46 |
| C | 1171D | FO *Membranophoridium perforatum* | 53.0 | 50R-CC | 56R-CC | 718.48 | 771.40 | 744.94 | 26.46 | 728.26 | 781.18 | 754.72 | 26.46 |
| C | 1171D | LO *Dracodinium waipawaense* | 53.2 | 60R-CC | 70R-CC | 814.60 | 908.07 | 861.34 | 46.74 | 824.38 | 917.85 | 871.12 | 46.74 |
| C | 1171D | FO *Dracodinium waipawaense* | 53.5 | 70R-CC | 71R-CC | 908.07 | 920.20 | 914.14 | 6.07 | 917.85 | 928.90 | 923.38 | 5.52 |
| C | 1171D | FO *Hystrichokolpoma spinosa* | 53.5 | 70R-CC | 71R-CC | 908.07 | 920.20 | 914.14 | 6.07 | 917.85 | 928.90 | 923.38 | 5.52 |
| C | 1171D | FO *Deflandrea phosphoriticacpx* | 55.0 | 72R-CC | 73R-CC | 920.20 | 939.51 | 929.86 | 9.66 | 939.07 | 949.29 | 944.18 | 5.11 |

Notes: Mean depth is the midpoint between the top and bottom sample of the event interval. D = diatom, R = radiolarian, N = nannofossil, P = planktonic foraminifer, C = dinocyst. LO = last occurrence, FO = first occurrence, LCO = last consistent occurrence, FCO = first consistent occurrence, LAO = last abundant occurrence, FAO = first abundant occurrence. This table is also available in **ASCII format.**

**Table T14.** Magnetostratigraphic results, Site 1171.

| Chron/Subchron | Age (Ma) | Depth (mbsf) |
|---|---|---|
| Hole 1171C, 0-36 mbsf: | | |
| Onset C1n | 12.6 | 0.78 |
| Termination C1r.1n | 14.9 | 0.99 |
| Onset C1r.1n | 16.5 | 1.07 |
| Termination C2n | 24 | 1.77 |
| Onset C2n | 26 | 1.95 |
| Termination C2An.1n | 31.75 | 2.58 |
| Onset C2An.1n | 34.5 | 3.04 |
| Termination C2An.2n | 35.6 | 3.11 |
| Hole 1171C, 80-135 mbsf: | | |
| Termination C5n.1n | 80 | 9.74 |
| Onset C5n.1n | 82.5 | 9.90 |
| Termination C5n.2n | 83.5 | 9.92 |
| Onset C5n.2n | 107.75 | 10.95 |
| Termination C5r.1n | 109.5 | 11.05 |
| Onset C5r.1n | 113 | 11.11 |
| Termination C5r.2n | 123 | 11.48 |
| Termination C5An.1n | 129.75 | 11.94 |
| Onset C5An.1n | 130.6 | 12.08 |
| Termination C5An.2n | 133.4 | 12.18 |
| Onset C5An.2n | 134.5 | 12.40 |
| Hole 1171C, 155-170 mbsf: | | |
| Termination C5ACn | 156 | 13.70 |
| Onset C5ACn | 159.35 | 14.08 |
| Termination C5ADn | 161.3 | 14.18 |
| Onset C5ADn | 167.2 | 14.61 |
| Hole 1171C, 200-225 mbsf: | | |
| Termination C6n | 207.2 | 19.05 |
| Onset C6n | 223.5 | 20.13 |

**Table T15.** Composite depth section, Site 1171.

| Hole, core | Depth (mbsf) | Offset (m) | Depth (mcd) |
|---|---|---|---|
| **189-1171A-** | | | |
| 1H | 0.0 | 0.00 | 0.00 |
| 2H | 7.1 | 0.74 | 7.84 |
| 3H | 16.6 | 0.56 | 17.16 |
| 4H | 26.1 | 1.18 | 27.28 |
| 5H | 35.6 | 1.90 | 37.50 |
| 6H | 45.1 | 2.26 | 47.36 |
| 7H | 54.6 | 3.56 | 58.16 |
| 8H | 64.1 | 4.70 | 68.80 |
| 9H | 73.6 | 5.44 | 79.04 |
| 10H | 83.1 | 5.88 | 88.98 |
| 11H | 92.6 | 6.76 | 99.36 |
| 12H | 102.1 | 6.74 | 108.84 |
| 13X | 111.6 | 6.74 | 118.34 |
| 14X | 114.8 | 6.74 | 121.54 |
| **189-1171B-** | | | |
| 1H | 0.0 | 0.12 | 0.12 |
| 2H | 4.3 | 0.34 | 4.64 |
| 3H | 13.8 | 0.10 | 13.90 |
| 4H | 23.3 | 1.06 | 24.36 |
| 5H | 32.8 | 1.22 | 34.02 |
| 6H | 42.3 | 2.06 | 44.36 |
| 7H | 51.8 | 2.90 | 54.70 |
| 8H | 61.3 | 3.36 | 64.66 |
| 9H | 70.8 | 4.66 | 75.46 |
| 10H | 80.3 | 6.28 | 86.58 |
| 11H | 89.8 | 6.98 | 96.78 |
| 12H | 99.3 | 6.88 | 106.18 |
| **189-1171C-** | | | |
| 1H | 0.0 | 0.44 | 0.44 |
| 2H | 9.5 | 0.74 | 10.24 |
| 3H | 19.0 | 0.02 | 19.02 |
| 4H | 28.5 | 0.34 | 28.84 |
| 5H | 38.0 | 1.60 | 39.60 |
| 6H | 47.5 | 2.38 | 49.88 |
| 7H | 57.0 | 3.38 | 60.38 |
| 8H | 66.5 | 5.38 | 71.88 |
| 9H | 76.0 | 5.40 | 81.40 |
| 10H | 85.5 | 6.22 | 91.72 |
| 11H | 95.0 | 6.94 | 101.94 |
| 12X | 104.5 | 6.68 | 111.18 |
| 13X | 110.2 | 6.68 | 116.88 |
| 14X | 115.2 | 6.68 | 121.88 |

**Table T16.** Splice tie points, Site 1171.

| Hole, core, section, interval (cm) | Depth (mbsf) | Depth (mcd) | | Hole, core, section, interval (cm) | Depth (mbsf) | Depth (mcd) |
|---|---|---|---|---|---|---|
| 189- | | | | 189- | | |
| 1171A-1H-4, 112 | 5.62 | 5.62 | Tie to | 1171C-1H-4, 68 | 5.18 | 5.62 |
| 1171C-1H-7, 6 | 9.00 | 9.44 | Tie to | 1171A-2H-2, 10 | 8.70 | 9.44 |
| 1171A-2H-6, 106 | 15.66 | 16.40 | Tie to | 1171B-3H-2, 100 | 16.30 | 16.40 |
| 1171B-3H-3, 90 | 17.70 | 17.80 | Tie to | 1171A-3H-1, 64 | 17.24 | 17.80 |
| 1171A-3H-5, 72 | 23.32 | 23.88 | Tie to | 1171C-3H-4, 36 | 23.86 | 23.88 |
| 1171C-3H-5, 92 | 25.92 | 25.94 | Tie to | 1171B-4H-2, 8 | 24.88 | 25.94 |
| 1171B-4H-6, 8 | 30.88 | 31.94 | Tie to | 1171C-4H-3, 10 | 31.60 | 31.94 |
| 1171C-4H-4, 140 | 34.40 | 34.74 | Tie to | 1171B-5H-1, 72 | 33.52 | 34.74 |
| 1171B-5H-4, 10 | 37.40 | 38.62 | Tie to | 1171A-5H-1, 112 | 36.72 | 38.62 |
| 1171A-5H-3, 122 | 39.82 | 41.72 | Tie to | 1171C-5H-2, 62 | 40.12 | 41.72 |
| 1171C-5H-6, 118 | 46.68 | 48.28 | Tie to | 1171A-6H-1, 92 | 46.02 | 48.28 |
| 1171A-6H-6, 46 | 53.06 | 55.32 | Tie to | 1171B-7H-1, 62 | 52.42 | 55.32 |
| 1171B-7H-4, 18 | 56.48 | 59.38 | Tie to | 1171A-7H-1, 122 | 55.82 | 59.38 |
| 1171A-7H-6, 28 | 62.38 | 65.94 | Tie to | 1171B-8H-1, 128 | 62.58 | 65.94 |
| 1171B-8H-6, 92 | 69.72 | 73.08 | Tie to | 1171A-8H-4, 114 | 68.38 | 73.08 |
| 1171A-8H-7, 8 | 71.82 | 76.52 | Tie to | 1171B-9H-1, 106 | 71.86 | 76.52 |
| 1171B-9H-4, 144 | 76.74 | 81.40 | Tie to | 1171A-9H-2, 86 | 75.96 | 81.40 |
| 1171A-9H-5, 122 | 80.82 | 86.26 | Tie to | 1171C-9H-4, 36 | 80.86 | 86.26 |
| 1171C-9H-6, 90 | 84.40 | 89.80 | Tie to | 1171A-10H-1, 82 | 83.92 | 89.80 |
| 1171A-10H-6, 74 | 91.34 | 97.22 | Tie to | 1171C-10H-4, 100 | 91.00 | 97.22 |
| 1171C-10H-5, 128 | 92.78 | 99.00 | Tie to | 1171B-11H-2, 72 | 92.02 | 99.00 |
| 1171B-11H-4, 6 | 94.36 | 101.34 | Tie to | 1171A-11H-2, 48 | 94.58 | 101.34 |
| 1171A-11H-6, 16 | 100.26 | 107.02 | Tie to | 1171B-12H-1, 84 | 100.14 | 107.02 |
| 1171B-12H-3, 144 | 103.74 | 110.62 | Tie to | 1171A-12H-2, 28 | 103.88 | 110.62 |
| 1171A-12H-6, 96 | 110.56 | 117.30 | | | | |

**Table T17.** Values for inorganic carbon, calcium carbonate, total carbon, total organic carbon, total nitrogen, total sulfur, and hydrogen in sediments, Site 1171. (**See table notes.** Continued on next three pages.)

| Hole, core, section | Depth (mbsf) | IC (wt%) | CaCO$_3$ (wt%) | TC (wt%) | TOC (wt%) | N (wt%) | S (wt%) | H (mg HC/g) |
|---|---|---|---|---|---|---|---|---|
| 189-1171A- | | | | | | | | |
| 1H-1 | 0.72 | 10.93 | 91.01 | 11.05 | 0.12 | 0.02 | NA | 0.14 |
| 1H-3 | 3.72 | 11.14 | 92.76 | 11.71 | 0.57 | 0.02 | NA | 0.13 |
| 1H-5 | 6.72 | 11.29 | 94.06 | 11.31 | 0.02 | 0.01 | NA | 0.08 |
| 2H-1 | 7.82 | 10.84 | 90.33 | 11.23 | 0.39 | 0.02 | NA | 0.09 |
| 2H-3 | 10.82 | 10.45 | 87.01 | 11.62 | 1.17 | 0.02 | NA | 0.14 |
| 2H-5 | 13.82 | 11.14 | 92.81 | 11.05 | 0.00 | 0.03 | NA | 0.16 |
| 3H-1 | 17.32 | 11.37 | 94.70 | 10.94 | 0.00 | 0.01 | NA | 0.15 |
| 3H-3 | 20.32 | 11.12 | 92.61 | 10.91 | 0.00 | 0.02 | NA | 0.13 |
| 3H-5 | 23.32 | 10.29 | 85.73 | 10.00 | 0.00 | 0.02 | NA | 0.22 |
| 4H-1 | 26.82 | 10.75 | 89.54 | 10.50 | 0.00 | 0.01 | NA | 0.14 |
| 4H-3 | 29.82 | 10.70 | 89.15 | 11.07 | 0.37 | 0.01 | NA | 0.16 |
| 4H-5 | 32.82 | 10.76 | 89.63 | 10.75 | 0.00 | 0.01 | NA | 0.14 |
| 5H-1 | 36.32 | 10.82 | 90.11 | 10.82 | 0.00 | 0.01 | NA | 0.14 |
| 5H-3 | 39.32 | 10.87 | 90.57 | 11.31 | 0.43 | 0.01 | NA | 0.07 |
| 5H-5 | 42.32 | 11.45 | 95.38 | 11.44 | 0.00 | 0.01 | NA | 0.06 |
| 6H-1 | 45.82 | 11.51 | 95.85 | 11.82 | 0.31 | 0.01 | NA | 0.07 |
| 6H-3 | 48.82 | 11.52 | 95.96 | 11.34 | 0.00 | 0.02 | NA | 0.07 |
| 6H-5 | 51.82 | 11.41 | 95.07 | 11.39 | 0.00 | 0.01 | NA | 0.05 |
| 7H-1 | 55.32 | 11.39 | 94.85 | 11.29 | 0.00 | 0.02 | NA | 0.07 |
| 7H-3 | 58.32 | 11.53 | 96.03 | 11.94 | 0.41 | 0.01 | NA | 0.04 |
| 7H-5 | 61.32 | 11.32 | 94.34 | 11.80 | 0.48 | 0.00 | NA | 0.06 |
| 8H-1 | 64.82 | 11.16 | 93.00 | 11.36 | 0.20 | 0.01 | NA | 0.05 |
| 8H-3 | 66.46 | 11.21 | 93.38 | 11.61 | 0.40 | 0.01 | NA | 0.07 |
| 8H-5 | 69.46 | 11.20 | 93.34 | 11.14 | 0.00 | 0.01 | NA | 0.08 |
| 9H-1 | 74.32 | 10.95 | 91.23 | 10.86 | 0.00 | 0.02 | NA | 0.12 |
| 9H-3 | 77.32 | 11.34 | 94.49 | 11.12 | 0.00 | 0.01 | NA | 0.08 |
| 9H-6 | 81.82 | 11.36 | 94.61 | 11.51 | 0.15 | 0.01 | NA | 0.06 |
| 10H-1 | 83.82 | 11.29 | 94.07 | 11.29 | 0.00 | 0.01 | NA | 0.08 |
| 10H-3 | 86.82 | 11.63 | 96.87 | 11.78 | 0.15 | 0.01 | NA | 0.05 |
| 10H-5 | 89.82 | 11.39 | 94.91 | 11.82 | 0.43 | 0.01 | NA | 0.05 |
| 11H-1 | 93.32 | 11.42 | 95.13 | 11.72 | 0.30 | 0.01 | NA | 0.07 |
| 11H-3 | 96.32 | 11.17 | 93.08 | 11.23 | 0.05 | 0.00 | NA | 0.09 |
| 11H-5 | 99.32 | 11.54 | 96.14 | 11.66 | 0.12 | 0.01 | NA | 0.04 |
| 12H-1 | 102.82 | 11.59 | 96.51 | 11.81 | 0.22 | 0.01 | NA | 0.06 |
| 12H-3 | 105.82 | 11.40 | 94.96 | 11.10 | 0.00 | 0.00 | NA | 0.07 |
| 12H-5 | 108.82 | 10.39 | 86.51 | 11.82 | 1.44 | 0.01 | NA | 0.05 |
| 13X-1 | 112.32 | 11.41 | 95.02 | 11.81 | 0.40 | 0.02 | NA | 0.41 |
| 14X-1 | 115.52 | 11.53 | 96.02 | 11.71 | 0.18 | 0.00 | NA | 0.04 |
| 14X-3 | 118.52 | 10.69 | 89.03 | 11.16 | 0.47 | 0.02 | NA | 0.07 |
| 189-1171C- | | | | | | | | |
| 13X-1 | 110.92 | 11.40 | 94.99 | NA | NA | NA | NA | NA |
| 13X-3 | 113.92 | 11.36 | 94.63 | 11.27 | 0.00 | 0.00 | NA | 0.07 |
| 14X-1 | 115.92 | 11.53 | 96.08 | NA | NA | NA | NA | NA |
| 14X-3 | 118.92 | 11.41 | 95.01 | 11.35 | 0.00 | 0.00 | NA | 0.08 |
| 14X-5 | 121.92 | 11.43 | 95.17 | NA | NA | NA | NA | NA |
| 15X-1 | 125.52 | 11.33 | 94.37 | NA | NA | NA | NA | NA |
| 15X-3 | 128.52 | 11.47 | 95.57 | 11.49 | 0.02 | 0.00 | NA | 0.07 |
| 15X-5 | 131.52 | 11.31 | 94.23 | NA | NA | NA | NA | NA |
| 16X-1 | 135.22 | 11.34 | 94.46 | NA | NA | NA | NA | NA |
| 16X-3 | 138.22 | 11.39 | 94.86 | 11.32 | 0.00 | 0.01 | NA | 0.06 |
| 17X-1 | 144.82 | 11.42 | 95.11 | NA | NA | NA | NA | NA |
| 17X-3 | 147.82 | 11.27 | 93.84 | 11.10 | 0.00 | 0.00 | NA | 0.10 |
| 18X-1 | 154.42 | 11.25 | 93.68 | NA | NA | NA | NA | NA |
| 18X-3 | 157.42 | 11.52 | 95.94 | 11.55 | 0.04 | 0.00 | NA | 0.06 |
| 18X-5 | 160.42 | 11.49 | 95.70 | NA | NA | NA | NA | NA |
| 19X-1 | 164.02 | 11.14 | 92.79 | NA | NA | NA | NA | NA |
| 19X-3 | 167.02 | 11.35 | 94.55 | 11.20 | 0.00 | 0.01 | NA | 0.08 |
| 19X-5 | 170.02 | 11.45 | 95.37 | NA | NA | NA | NA | NA |
| 20X-1 | 173.62 | 11.30 | 94.10 | NA | NA | NA | NA | NA |
| 20X-3 | 176.62 | 11.13 | 92.72 | 11.01 | 0.00 | 0.01 | NA | 0.07 |
| 20X-5 | 179.62 | 11.29 | 94.04 | NA | NA | NA | NA | NA |
| 21X-1 | 182.92 | 11.36 | 94.66 | NA | NA | NA | NA | NA |
| 21X-3 | 185.92 | 11.00 | 91.64 | 11.21 | 0.20 | 0.01 | NA | 0.13 |
| 21X-5 | 188.92 | 10.83 | 90.21 | NA | NA | NA | NA | NA |

**Table T17 (continued).**

| Hole, core, section | Depth (mbsf) | IC (wt%) | CaCO₃ (wt%) | TC (wt%) | TOC (wt%) | N (wt%) | S (wt%) | H (mg HC/g) |
|---|---|---|---|---|---|---|---|---|
| 22X-1 | 192.52 | 11.17 | 93.01 | NA | NA | NA | NA | NA |
| 22X-3 | 195.52 | 10.88 | 90.67 | 10.95 | 0.06 | 0.00 | NA | 0.11 |
| 22X-5 | 198.52 | 10.84 | 90.29 | NA | NA | NA | NA | NA |
| 23X-1 | 202.26 | 11.02 | 91.80 | NA | NA | NA | NA | NA |
| 23X-3 | 205.22 | 11.41 | 95.07 | 11.29 | 0.00 | 0.01 | NA | 0.08 |
| 23X-5 | 208.22 | 11.16 | 92.95 | NA | NA | NA | NA | NA |
| 24X-1 | 211.82 | 11.19 | 93.21 | NA | NA | NA | NA | NA |
| 24X-3 | 214.82 | 11.31 | 94.19 | 11.18 | 0.00 | 0.01 | NA | 0.08 |
| 24X-5 | 217.82 | 11.26 | 93.78 | NA | NA | NA | NA | NA |
| 25X-1 | 221.40 | 11.23 | 93.50 | NA | NA | NA | NA | NA |
| 25X-3 | 224.40 | 11.28 | 93.94 | 11.21 | 0.00 | 0.01 | NA | 0.08 |
| 25X-5 | 227.42 | 11.13 | 92.73 | NA | NA | NA | NA | NA |
| 26X-1 | 231.21 | 10.89 | 90.74 | NA | NA | NA | NA | NA |
| 26X-3 | 234.03 | 11.09 | 92.37 | 11.04 | 0.00 | 0.01 | NA | 0.10 |
| 26X-5 | 236.98 | 11.02 | 91.76 | NA | NA | NA | NA | NA |
| 27X-1 | 240.37 | 11.05 | 92.03 | NA | NA | NA | NA | NA |
| 27X-3 | 243.29 | 10.26 | 85.50 | 10.71 | 0.45 | 0.01 | NA | 0.13 |
| 27X-5 | 246.35 | 10.95 | 91.18 | NA | NA | NA | NA | NA |
| 28X-1 | 249.62 | 10.81 | 90.09 | NA | NA | NA | NA | NA |
| 28X-3 | 252.62 | 10.77 | 89.72 | 10.79 | 0.02 | 0.01 | NA | 0.13 |
| 29X-1 | 259.30 | 10.11 | 84.19 | NA | NA | NA | NA | NA |
| 29X-3 | 262.22 | 10.20 | 84.95 | 10.47 | 0.27 | 0.01 | 0.07 | 0.16 |
| 30X-1 | 268.85 | 9.31 | 77.52 | 9.56 | 0.25 | 0.01 | 0.00 | 0.22 |
| 30X-3 | 271.87 | 8.90 | 74.13 | 9.20 | 0.30 | 0.01 | 0.00 | 0.21 |
| 189-1171D- | | | | | | | | |
| 3R-1 | 266.69 | 9.28 | 77.31 | 9.30 | 0.02 | 0.00 | 0.03 | 0.22 |
| 3R-3 | 269.60 | 0.05 | 0.41 | 0.09 | 0.04 | 0.02 | 0.00 | 0.88 |
| 4R-1 | 276.21 | 0.84 | 6.96 | NA | NA | NA | NA | NA |
| 4R-3 | 279.21 | 0.95 | 7.90 | 1.39 | 0.44 | 0.06 | 1.24 | 0.90 |
| 5R-1 | 285.80 | 0.37 | 3.04 | 0.84 | 0.47 | 0.04 | 1.12 | 1.01 |
| 6R-1 | 293.80 | 0.05 | 0.38 | 0.16 | 0.11 | 0.02 | 0.05 | 0.62 |
| 7R-1 | 300.40 | 0.00 | 0.00 | 2.18 | NA | 0.05 | 0.75 | 0.87 |
| 8R-1 | 305.42 | 1.79 | 14.87 | 2.25 | 0.47 | 0.05 | 0.75 | 0.86 |
| 9R-1 | 314.71 | 1.22 | 10.16 | NA | NA | NA | NA | NA |
| 9R-3 | 317.70 | 0.04 | 0.34 | 0.34 | 0.30 | 0.03 | 0.67 | 0.91 |
| 10R-1 | 324.30 | 0.17 | 1.42 | NA | NA | NA | NA | NA |
| 10R-3 | 327.30 | 0.19 | 1.61 | 0.74 | 0.55 | 0.04 | 0.74 | 0.96 |
| 15R-1 | 372.40 | 0.44 | 3.68 | 0.97 | 0.53 | 0.04 | 1.98 | 0.57 |
| 16R-1 | 382.00 | 0.29 | 2.39 | 0.86 | 0.57 | 0.04 | 2.48 | 0.51 |
| 17R-1 | 391.61 | 0.56 | 4.70 | NA | NA | NA | NA | NA |
| 17R-3 | 394.60 | 0.39 | 3.22 | 0.89 | 0.50 | 0.07 | 0.93 | 0.57 |
| 19R-1 | 410.82 | 2.06 | 17.16 | NA | NA | NA | NA | NA |
| 19R-3 | 413.82 | 2.19 | 18.24 | 2.49 | 0.30 | 0.03 | 0.64 | 0.39 |
| 19R-5 | 416.88 | 7.73 | 64.40 | NA | NA | NA | NA | NA |
| 20R-1 | 420.40 | 0.34 | 2.83 | NA | NA | NA | NA | NA |
| 20R-3 | 423.40 | 0.02 | 0.19 | 1.81 | 1.78 | 0.10 | 2.55 | 0.62 |
| 20R-5 | 426.40 | 0.04 | 0.31 | NA | NA | NA | NA | NA |
| 22R-1 | 439.60 | 0.18 | 1.48 | NA | NA | NA | NA | NA |
| 22R-3 | 442.60 | 0.14 | 1.15 | 0.72 | 0.58 | 0.05 | 1.32 | 0.47 |
| 22R-5 | 445.61 | 0.54 | 4.46 | NA | NA | NA | NA | NA |
| 23R-1 | 449.20 | 0.12 | 1.02 | NA | NA | NA | NA | NA |
| 23R-3 | 452.20 | 0.22 | 1.80 | 1.05 | 0.84 | 0.08 | 1.57 | 0.48 |
| 24R-1 | 458.80 | 0.11 | 0.92 | NA | NA | NA | NA | NA |
| 24R-3 | 461.80 | 0.09 | 0.73 | 0.75 | 0.67 | 0.05 | 2.25 | 0.48 |
| 25R-1 | 468.50 | 0.02 | 0.18 | NA | NA | NA | NA | NA |
| 25R-3 | 471.50 | 0.02 | 0.15 | 1.57 | 1.55 | 0.12 | 3.29 | 0.64 |
| 25R-5 | 474.50 | 0.02 | 0.17 | NA | NA | NA | NA | NA |
| 26R-1 | 478.10 | 0.02 | 0.14 | NA | NA | NA | NA | NA |
| 26R-3 | 481.10 | 0.03 | 0.28 | 1.40 | 1.37 | 0.11 | 2.95 | 0.63 |
| 26R-5 | 484.10 | 0.13 | 1.08 | NA | NA | NA | NA | NA |
| 27R-1 | 487.70 | 0.07 | 0.59 | NA | NA | NA | NA | NA |
| 27R-3 | 490.70 | 0.06 | 0.53 | 1.10 | 1.04 | 0.05 | 1.97 | 0.59 |
| 27R-5 | 493.70 | 0.21 | 1.75 | NA | NA | NA | NA | NA |
| 28R-1 | 497.31 | 0.99 | 8.27 | NA | NA | NA | NA | NA |
| 28R-3 | 500.31 | 0.59 | 4.93 | 1.36 | 0.77 | 0.06 | 0.83 | 0.42 |
| 28R-5 | 503.30 | 0.47 | 3.91 | NA | NA | NA | NA | NA |
| 29R-1 | 507.00 | 0.27 | 2.23 | NA | NA | NA | NA | NA |
| 29R-3 | 510.00 | 0.16 | 1.37 | 0.76 | 0.59 | 0.05 | 0.61 | 0.39 |
| 29R-5 | 513.00 | 0.47 | 3.87 | NA | NA | NA | NA | NA |

**Table T17 (continued).**

| Hole, core, section | Depth (mbsf) | IC (wt%) | CaCO$_3$ (wt%) | TC (wt%) | TOC (wt%) | N (wt%) | S (wt%) | H (mg HC/g) |
|---|---|---|---|---|---|---|---|---|
| 30R-1 | 516.61 | 0.56 | 4.65 | NA | NA | NA | NA | NA |
| 30R-3 | 519.41 | 0.31 | 2.60 | 0.78 | 0.47 | 0.04 | 0.98 | 0.48 |
| 30R-5 | 522.41 | 0.50 | 4.12 | NA | NA | NA | NA | NA |
| 31R-1 | 526.21 | 0.57 | 4.71 | NA | NA | NA | NA | NA |
| 31R-2 | 527.71 | 1.08 | 8.96 | 1.68 | 0.60 | 0.04 | 0.69 | 0.49 |
| 31R-4 | 530.71 | 0.99 | 8.25 | NA | NA | NA | NA | NA |
| 32R-1 | 535.81 | 1.35 | 11.25 | NA | NA | NA | NA | NA |
| 32R-5 | 541.82 | 2.44 | 20.30 | 1.19 | 0.00 | 0.00 | 0.40 | 0.41 |
| 33R-1 | 545.51 | 1.29 | 10.78 | NA | NA | NA | NA | NA |
| 33R-3 | 548.50 | 0.07 | 0.55 | 0.53 | 0.47 | 0.04 | 0.87 | 0.41 |
| 33R-5 | 551.50 | 0.28 | 2.29 | NA | NA | NA | NA | NA |
| 34R-1 | 555.11 | 0.59 | 4.95 | NA | NA | NA | NA | NA |
| 34R-3 | 558.11 | 0.91 | 7.60 | 1.33 | 0.42 | 0.04 | 0.51 | 0.50 |
| 34R-5 | 561.13 | 2.54 | 21.18 | NA | NA | NA | NA | NA |
| 35R-1 | 564.71 | 1.34 | 11.16 | NA | NA | NA | NA | NA |
| 35R-3 | 567.71 | 0.50 | 4.17 | 0.79 | 0.29 | 0.03 | 0.31 | 0.49 |
| 35R-5 | 570.70 | 0.29 | 2.43 | NA | NA | NA | NA | NA |
| 36R-1 | 574.31 | 0.82 | 6.82 | NA | NA | NA | NA | NA |
| 36R-3 | 577.31 | 0.96 | 8.00 | 1.28 | 0.32 | 0.03 | 0.28 | 0.43 |
| 36R-5 | 580.31 | 1.45 | 12.10 | NA | NA | NA | NA | NA |
| 37R-1 | 583.91 | 0.56 | 4.68 | NA | NA | NA | NA | NA |
| 37R-3 | 586.91 | 0.73 | 6.08 | 1.11 | 0.38 | 0.04 | 0.64 | 0.42 |
| 37R-5 | 589.91 | 0.69 | 5.73 | NA | NA | NA | NA | NA |
| 38R-1 | 593.61 | 0.59 | 4.89 | NA | NA | NA | NA | NA |
| 38R-3 | 596.62 | 1.68 | 14.01 | 2.11 | 0.43 | 0.04 | 0.43 | 0.47 |
| 38R-5 | 599.61 | 1.25 | 10.41 | NA | NA | NA | NA | NA |
| 39R-1 | 603.21 | 1.36 | 11.36 | NA | NA | NA | NA | NA |
| 39R-3 | 606.21 | 1.13 | 9.45 | 1.63 | 0.50 | 0.05 | 0.69 | 0.52 |
| 39R-5 | 609.21 | 0.73 | 6.06 | NA | NA | NA | NA | NA |
| 40R-1 | 612.81 | 0.77 | 6.37 | NA | NA | NA | NA | NA |
| 40R-3 | 615.80 | 0.48 | 4.02 | 1.00 | 0.52 | 0.05 | 0.61 | 0.56 |
| 40R-5 | 618.80 | 0.08 | 0.68 | NA | NA | NA | NA | NA |
| 41R-1 | 622.40 | 0.32 | 2.68 | NA | NA | NA | NA | NA |
| 41R-3 | 625.40 | 0.10 | 0.84 | 0.68 | 0.58 | 0.05 | 0.46 | 0.54 |
| 41R-5 | 628.40 | 0.14 | 1.14 | NA | NA | NA | NA | NA |
| 42R-1 | 632.01 | 0.69 | 5.76 | NA | NA | NA | NA | NA |
| 42R-3 | 635.01 | 0.98 | 8.14 | 1.58 | 0.60 | 0.05 | 0.73 | 0.64 |
| 42R-5 | 638.01 | 1.44 | 11.97 | NA | NA | NA | NA | NA |
| 43R-1 | 641.62 | 1.67 | 13.88 | NA | NA | NA | NA | NA |
| 43R-3 | 644.62 | 1.77 | 14.73 | 2.01 | 0.24 | 0.04 | 0.16 | 0.41 |
| 43R-5 | 647.61 | 1.28 | 10.66 | NA | NA | NA | NA | NA |
| 44R-1 | 651.32 | 1.87 | 15.61 | NA | NA | NA | NA | NA |
| 44R-3 | 654.32 | 1.62 | 13.49 | 1.92 | 0.30 | 0.04 | 0.17 | 0.43 |
| 44R-5 | 657.32 | 1.97 | 16.41 | NA | NA | NA | NA | NA |
| 45R-1 | 660.92 | 2.30 | 19.19 | 2.78 | 0.47 | 0.04 | 0.23 | 0.51 |
| 46R-1 | 670.52 | 1.82 | 15.16 | NA | NA | NA | NA | NA |
| 46R-3 | 673.52 | 1.81 | 15.11 | 2.37 | 0.55 | 0.04 | 0.19 | 0.53 |
| 46R-5 | 676.52 | 2.12 | 17.65 | NA | NA | NA | NA | NA |
| 47R-1 | 680.22 | 1.77 | 14.76 | NA | NA | NA | NA | NA |
| 47R-3 | 681.94 | 2.71 | 22.54 | 3.27 | 0.56 | 0.03 | 0.10 | 0.50 |
| 47R-5 | 684.93 | 1.77 | 14.71 | NA | NA | NA | NA | NA |
| 48R-1 | 689.91 | 0.88 | 7.30 | NA | NA | NA | NA | NA |
| 48R-3 | 692.90 | 0.20 | 1.63 | 0.55 | 0.36 | 0.05 | 0.72 | 0.53 |
| 48R-5 | 695.90 | 0.22 | 1.81 | NA | NA | NA | NA | NA |
| 49R-3 | 701.52 | 0.15 | 1.21 | 0.40 | 0.25 | 0.05 | 0.16 | 0.52 |
| 49R-5 | 704.53 | 0.56 | 4.70 | NA | NA | NA | NA | NA |
| 50R-1 | 709.10 | 0.09 | 0.73 | NA | NA | NA | NA | NA |
| 50R-3 | 712.10 | 0.26 | 2.19 | 0.99 | 0.73 | 0.05 | 0.27 | 0.59 |
| 50R-5 | 715.10 | 0.00 | 0.00 | NA | NA | NA | NA | NA |
| 51R-1 | 718.70 | 0.17 | 1.45 | NA | NA | NA | NA | NA |
| 51R-3 | 721.70 | 0.12 | 1.00 | 0.47 | 0.35 | 0.05 | 0.14 | 0.56 |
| 51R-5 | 724.70 | 0.31 | 2.58 | NA | NA | NA | NA | NA |
| 52R-1 | 728.31 | 0.89 | 7.39 | NA | NA | NA | NA | NA |
| 52R-3 | 731.30 | 0.09 | 0.72 | 0.73 | 0.65 | 0.10 | 0.67 | 0.57 |
| 52R-5 | 734.30 | 0.12 | 0.98 | NA | NA | NA | NA | NA |
| 53R-1 | 737.90 | 0.47 | 3.94 | NA | NA | NA | NA | NA |
| 53R-3 | 740.90 | 0.06 | 0.47 | 0.84 | 0.79 | 0.08 | 0.72 | 0.59 |
| 53R-5 | 743.90 | 0.19 | 1.57 | NA | NA | NA | NA | NA |
| 54R-1 | 747.51 | 0.52 | 4.29 | NA | NA | NA | NA | NA |

**Table T17 (continued).**

| Hole, core, section | Depth (mbsf) | IC (wt%) | CaCO$_3$ (wt%) | TC (wt%) | TOC (wt%) | N (wt%) | S (wt%) | H (mg HC/g) |
|---|---|---|---|---|---|---|---|---|
| 54R-3 | 750.50 | 0.33 | 2.74 | 0.91 | 0.58 | 0.06 | 0.31 | 0.56 |
| 54R-5 | 753.50 | 0.10 | 0.86 | NA | NA | NA | NA | NA |
| 55R-1 | 757.10 | 0.39 | 3.21 | NA | NA | NA | NA | NA |
| 55R-3 | 760.10 | 0.48 | 4.03 | 1.10 | 0.62 | 0.09 | 0.15 | 0.56 |
| 55R-5 | 763.10 | 0.17 | 1.42 | NA | NA | NA | NA | NA |
| 56R-1 | 766.70 | 0.25 | 2.12 | NA | NA | NA | NA | NA |
| 56R-3 | 769.70 | 0.47 | 3.87 | 0.97 | 0.51 | 0.10 | 0.27 | 0.54 |
| 57R-1 | 776.31 | 0.57 | 4.76 | NA | NA | NA | NA | NA |
| 57R-3 | 779.30 | 0.04 | 0.36 | 0.67 | 0.63 | 0.08 | 0.43 | 0.55 |
| 58R-1 | 785.90 | 0.03 | 0.25 | NA | NA | NA | NA | NA |
| 58R-3 | 788.90 | 0.03 | 0.26 | 0.51 | 0.47 | 0.09 | 0.46 | 0.59 |
| 58R-5 | 791.90 | 0.03 | 0.28 | NA | NA | NA | NA | NA |
| 59R-1 | 795.50 | 0.08 | 0.67 | NA | NA | NA | NA | NA |
| 59R-3 | 798.50 | 0.03 | 0.27 | 0.51 | 0.48 | 0.08 | 0.36 | 0.56 |
| 59R-5 | 801.51 | 1.14 | 9.48 | NA | NA | NA | NA | NA |
| 60R-1 | 805.10 | 0.03 | 0.27 | NA | NA | NA | NA | NA |
| 60R-3 | 808.10 | 0.04 | 0.30 | 0.66 | 0.62 | 0.08 | 0.62 | 0.57 |
| 60R-5 | 811.10 | 0.03 | 0.24 | NA | NA | NA | NA | NA |
| 61R-1 | 814.70 | 0.03 | 0.27 | NA | NA | NA | NA | NA |
| 61R-3 | 817.70 | 0.04 | 0.35 | 0.71 | 0.67 | 0.11 | 0.64 | 0.57 |
| 61R-5 | 820.70 | 0.03 | 0.25 | NA | NA | NA | NA | NA |
| 62R-1 | 824.30 | 0.03 | 0.22 | NA | NA | NA | NA | NA |
| 62R-3 | 827.30 | 0.02 | 0.17 | 0.93 | 0.91 | 0.11 | 0.55 | 0.66 |
| 62R-5 | 830.30 | 0.02 | 0.17 | NA | NA | NA | NA | NA |
| 63R-1 | 833.90 | 0.00 | 0.00 | NA | NA | NA | NA | NA |
| 63R-3 | 836.90 | 0.03 | 0.26 | 0.69 | 0.66 | 0.10 | 0.96 | 0.58 |
| 63R-5 | 839.90 | 0.03 | 0.25 | NA | NA | NA | NA | NA |
| 64R-1 | 843.50 | 0.02 | 0.19 | NA | NA | NA | NA | NA |
| 64R-3 | 846.50 | 0.03 | 0.28 | 1.22 | 1.19 | 0.16 | 1.56 | 0.66 |
| 64R-5 | 849.50 | 0.10 | 0.84 | NA | NA | NA | NA | NA |
| 65R-1 | 853.10 | 0.05 | 0.43 | NA | NA | NA | NA | NA |
| 65R-3 | 856.10 | 0.03 | 0.26 | 0.72 | 0.69 | 0.11 | 0.90 | 0.68 |
| 65R-5 | 859.10 | 0.04 | 0.29 | NA | NA | NA | NA | NA |
| 66R-1 | 862.70 | 0.04 | 0.32 | NA | NA | NA | NA | NA |
| 66R-3 | 865.70 | 0.04 | 0.31 | 0.77 | 0.73 | 0.11 | 0.97 | 0.67 |
| 66R-5 | 868.70 | 0.04 | 0.32 | NA | NA | NA | NA | NA |
| 67R-1 | 872.30 | 0.02 | 0.17 | NA | NA | NA | NA | NA |
| 67R-3 | 875.30 | 0.04 | 0.33 | 0.91 | 0.87 | 0.09 | 1.04 | 0.52 |
| 67R-5 | 878.30 | 0.02 | 0.19 | NA | NA | NA | NA | NA |
| 68R-2 | 883.20 | 0.05 | 0.42 | NA | NA | NA | NA | NA |
| 68R-3 | 884.70 | 0.05 | 0.44 | 0.63 | 0.58 | 0.07 | 0.81 | 0.62 |
| 68R-6 | 888.70 | 0.16 | 1.34 | NA | NA | NA | NA | NA |
| 69R-1 | 891.30 | 0.02 | 0.17 | NA | NA | NA | NA | NA |
| 69R-3 | 894.30 | 0.04 | 0.37 | 1.31 | 1.26 | 0.13 | 0.79 | 0.62 |
| 69R-5 | 897.30 | 0.03 | 0.26 | NA | NA | NA | NA | NA |
| 70R-1 | 900.90 | 0.02 | 0.19 | NA | NA | NA | NA | NA |
| 70R-5 | 906.90 | 0.00 | 0.00 | 1.58 | NA | 0.14 | 1.34 | 0.67 |
| 71R-1 | 910.50 | 0.12 | 1.01 | NA | NA | NA | NA | NA |
| 71R-2 | 912.01 | 1.10 | 9.18 | NA | NA | NA | NA | NA |
| 71R-3 | 913.50 | 0.25 | 2.09 | 1.29 | 1.04 | 0.16 | 1.21 | 0.62 |
| 72R-1 | 920.20 | 0.04 | 0.36 | NA | NA | NA | NA | NA |
| 72R-3 | 923.20 | 0.00 | 0.00 | 1.42 | NA | 0.11 | 2.00 | 0.55 |
| 72R-5 | 926.20 | 0.05 | 0.38 | NA | NA | NA | NA | NA |
| 73R-1 | 929.90 | 0.10 | 0.84 | NA | NA | NA | NA | NA |
| 73R-3 | 932.90 | 0.05 | 0.45 | 1.21 | 1.16 | 0.11 | 1.43 | 0.59 |
| 73R-5 | 935.90 | 0.05 | 0.42 | NA | NA | NA | NA | NA |
| 75R-1 | 949.21 | 0.60 | 4.98 | NA | NA | NA | NA | NA |
| 75R-3 | 952.20 | 0.07 | 0.57 | 0.89 | 0.82 | 0.11 | 1.48 | 0.60 |

Notes: IC = inorganic carbon, CaCO$_3$ = calcium carbonate, TC = total carbon, TOC = total organic carbon, N = total nitrogen, S = total sulfur, H = hydrogen. NA = not analyzed.

**Table T18.** Results of Rock-Eval analyses on sediments, Site 1171. (**See table notes.** Continued on next page.)

| Hole, core, section | Depth (mbsf) | $T_{max}$ (°C) | $S_1$ | $S_2$ | $S_3$ | TOC (%) | HI | OI |
|---|---|---|---|---|---|---|---|---|
| **189-1171A-** | | | | | | | | |
| 1H-4 | 4.50 | 440 | 0.02 | 0.06 | 0.64 | 0.01 | 600 | 6400 |
| 2H-4 | 11.60 | NA | 0.03 | 0.06 | 0.67 | 0.01 | 600 | 6700 |
| 3H-4 | 21.10 | 459 | 0.03 | 0.14 | 0.82 | 0.02 | 700 | 4100 |
| 4H-4 | 30.60 | 597 | 0.02 | 0.05 | 1.20 | 0.02 | 250 | 6000 |
| 5H-4 | 40.10 | NA | 0.03 | 0.00 | 0.45 | 0.00 | NA | NA |
| 6H-4 | 49.60 | NA | 0.01 | 0.00 | 0.41 | 0.01 | 0 | 4100 |
| 7H-4 | 59.10 | 451 | 0.02 | 0.02 | 0.52 | 0.01 | 200 | 5200 |
| 8H-4 | 67.24 | NA | 0.01 | 0.00 | 0.44 | 0.00 | NA | NA |
| 9H-4 | 78.10 | NA | 0.01 | 0.00 | 0.48 | 0.01 | 0 | 4750 |
| 10H-4 | 87.60 | 398 | 0.01 | 0.03 | 0.46 | 0.00 | NA | NA |
| 11H-4 | 97.10 | NA | 0.02 | 0.00 | 0.42 | 0.01 | 0 | 4400 |
| 12H-4 | 106.60 | 302 | 0.02 | 0.01 | 0.46 | 0.00 | NA | NA |
| 13X-1 | 111.60 | 382 | 0.04 | 0.01 | 0.41 | 0.01 | 0 | 4500 |
| 13X-1 | 113.30 | 341 | 0.03 | 0.01 | 0.53 | 0.01 | 100 | 5300 |
| 14X-3 | 117.80 | NA | 0.05 | 0.00 | 0.36 | 0.01 | 0 | 1750 |
| **189-1171C-** | | | | | | | | |
| 16X-3 | 137.50 | 345 | 0.03 | 0.01 | 0.38 | 0.01 | 200 | 3800 |
| 17X-4 | 148.60 | 302 | 0.05 | 0.01 | 0.40 | 0.01 | 100 | 4000 |
| 18X-4 | 158.20 | 451 | 0.07 | 0.11 | 0.61 | 0.02 | 550 | 3050 |
| 19X-4 | 168.50 | 347 | 0.07 | 0.01 | 0.48 | 0.01 | 100 | 4800 |
| 20X-4 | 177.40 | NA | 0.02 | 0.00 | 0.42 | 0.01 | 0 | 4150 |
| 21X-4 | 186.70 | 438 | 0.05 | 0.13 | 0.72 | 0.03 | 433 | 2400 |
| 22X-4 | 196.30 | 461 | 0.02 | 0.09 | 0.56 | 0.02 | 450 | 2800 |
| 23X-4 | 206.00 | 325 | 0.02 | 0.01 | 0.58 | 0.01 | 100 | 5800 |
| 24X-4 | 215.60 | 344 | 0.03 | 0.02 | 0.42 | 0.01 | 200 | 4200 |
| 25X-4 | 225.20 | 301 | 0.02 | 0.01 | 0.41 | 0.01 | 100 | 4100 |
| 26X-4 | 235.55 | NA | 0.03 | 0.00 | 0.57 | 0.01 | 0 | 5700 |
| 27X-4 | 244.10 | 377 | 0.01 | 0.01 | 0.46 | 0.00 | NA | NA |
| 28X-4 | 253.00 | NA | 0.00 | 0.00 | 0.82 | 0.00 | NA | NA |
| 29X-4 | 263.00 | 338 | 0.01 | 0.02 | 0.47 | 0.01 | 200 | 4700 |
| 30X-3 | 271.10 | NA | 0.00 | 0.00 | 0.58 | 0.02 | 0 | 2900 |
| 31X-1 | 273.50 | NA | 0.00 | 0.00 | 0.38 | 0.00 | NA | NA |
| **189-1171D-** | | | | | | | | |
| 1R-2 | 249.10 | NA | 0.00 | 0.00 | 0.67 | 0.01 | 0 | 3100 |
| 2R-2 | 258.50 | 500 | 0.01 | 0.08 | 0.93 | 0.03 | 266 | 3100 |
| 3R-2 | 268.10 | NA | 0.00 | 0.00 | 0.70 | 0.01 | 0 | 7000 |
| 4R-2 | 277.70 | NA | 0.01 | 0.00 | 1.36 | 0.08 | 0 | 1700 |
| 5R-1 | 285.80 | 480 | 0.09 | 0.71 | 1.05 | 0.24 | 295 | 437 |
| 6R-1 | 293.80 | 490 | 0.01 | 0.31 | 0.30 | 0.12 | 206 | 245 |
| 7R-2 | 301.60 | 412 | 0.09 | 0.84 | 0.96 | 0.28 | 300 | 342 |
| 8R-2 | 306.90 | 436 | 0.05 | 0.72 | 1.52 | 0.16 | 509 | 1148 |
| 9R-2 | 316.20 | 400 | 0.06 | 0.38 | 1.06 | 0.09 | 422 | 1177 |
| 10R-4 | 328.80 | 415 | 0.23 | 1.17 | 0.56 | 0.27 | 433 | 207 |
| 11R-CC | 334.02 | 425 | 0.08 | 0.74 | 0.41 | 0.31 | 238 | 132 |
| 12R-CC | 343.50 | 417 | 0.05 | 0.57 | 0.54 | 0.32 | 178 | 168 |
| 13R-CC | 353.20 | 420 | 0.06 | 0.61 | 0.89 | 0.37 | 164 | 240 |
| 14R-1 | 362.80 | 404 | 0.06 | 0.79 | 1.34 | 0.27 | 292 | 496 |
| 14R-2 | 363.00 | 594 | 0.05 | 0.12 | 0.10 | 0.03 | 400 | 333 |
| 15R-2 | 373.60 | 584 | 0.10 | 1.55 | 0.48 | 0.36 | 430 | 133 |
| 16R-4 | 383.50 | 594 | 0.05 | 1.05 | 0.63 | 0.32 | 328 | 196 |
| 17R-CC | 396.10 | 500 | 0.05 | 1.14 | 0.96 | 0.25 | 486 | 432 |
| 18R-4 | 401.22 | 423 | 0.03 | 0.64 | 1.09 | 0.23 | 278 | 473 |
| 18R-4 | 401.23 | NA | NA | NA | NA | NA | NA | NA |
| 19R-CC | 415.30 | 419 | 0.04 | 0.27 | 0.91 | 0.20 | 135 | 455 |
| 20R-4 | 424.90 | 504 | 0.07 | 1.38 | 0.91 | 0.54 | 318 | 284 |
| 21R-2 | 430.00 | 423 | 0.07 | 2.39 | 0.88 | 1.21 | 197 | 73 |
| 21R-3 | 430.30 | NA | NA | NA | NA | NA | NA | NA |
| 22R-4 | 444.10 | 442 | 0.06 | 1.32 | 1.00 | 0.49 | 269 | 204 |
| 23R-4 | 450.70 | 593 | 0.05 | 0.99 | 0.55 | 0.32 | 309 | 171 |
| 24R-4 | 461.80 | 418 | 0.06 | 2.42 | 0.57 | 0.89 | 308 | 103 |
| 25R-4 | 473.00 | 420 | 0.07 | 1.50 | 0.46 | 0.39 | 384 | 117 |
| 26R-4 | 482.60 | 419 | 0.06 | 2.49 | 0.48 | 0.97 | 255 | 51 |
| 27R-4 | 492.20 | 420 | 0.05 | 3.14 | 0.49 | 1.17 | 268 | 41 |
| 27R-4 | 497.40 | NA | 0.00 | 0.00 | 2.22 | 0.37 | 0 | 600 |
| 28R-4 | 501.80 | 421 | 0.04 | 2.45 | 0.64 | 0.74 | 331 | 86 |
| 29R-4 | 511.50 | 420 | 0.06 | 2.63 | 1.05 | 0.76 | 346 | 138 |

**Table T18 (continued).**

| Hole, core, section | Depth (mbsf) | $T_{max}$ (°C) | $S_1$ | $S_2$ | $S_3$ | TOC (%) | HI | OI |
|---|---|---|---|---|---|---|---|---|
| 30R-4 | 520.91 | 454 | 0.08 | 1.12 | 0.91 | 0.10 | 1120 | 910 |
| 31R-4 | 530.70 | 460 | 0.06 | 1.80 | 0.83 | 0.45 | 400 | 184 |
| 32R-4 | 540.30 | 453 | 0.60 | 4.06 | 0.45 | 0.65 | 624 | 69 |
| 33R-4 | 550.00 | 425 | 0.05 | 0.55 | 0.72 | 0.29 | 189 | 248 |
| 34R-4 | 559.60 | 424 | 0.10 | 1.09 | 0.53 | 0.37 | 294 | 143 |
| 35R-4 | 569.20 | 423 | 0.03 | 0.50 | 0.70 | 0.27 | 185 | 259 |
| 36R-4 | 578.80 | 426 | 0.03 | 0.46 | 0.85 | 0.29 | 158 | 293 |
| 37R-4 | 588.40 | 423 | 0.04 | 0.43 | 0.89 | 0.25 | 172 | 356 |
| 38R-4 | 598.10 | 422 | 0.04 | 0.47 | 0.44 | 0.27 | 174 | 162 |
| 39R-4 | 607.70 | 425 | 0.04 | 1.07 | 0.55 | 0.38 | 281 | 144 |
| 40R-4 | 617.30 | 427 | 0.05 | 0.27 | 0.55 | 0.29 | 93 | 189 |
| 41R-4 | 626.90 | 552 | 0.05 | 0.42 | 0.52 | 0.26 | 161 | 200 |
| 42R-4 | 636.50 | NA | NA | NA | NA | NA | NA | NA |
| 43R-4 | 646.10 | 476 | 0.03 | 0.30 | 0.90 | 0.21 | 158 | 509 |
| 44R-4 | 655.80 | NA | NA | NA | NA | NA | NA | NA |
| 45R-3 | 663.90 | 491 | 0.05 | 0.07 | 0.79 | 0.10 | 70 | 790 |
| 46R-3 | 673.50 | 539 | 0.05 | 0.12 | 1.04 | 0.11 | 109 | 945 |
| 47R-4 | 683.41 | 411 | 0.04 | 0.11 | 0.63 | 0.04 | 275 | 1575 |
| 48R-4 | 694.40 | 595 | 0.09 | 0.67 | 0.96 | 0.19 | 352 | 505 |
| 49R-4 | 703.02 | 516 | 0.05 | 0.18 | 0.75 | 0.13 | 142 | 696 |
| 50R-4 | 713.60 | 573 | 0.08 | 0.28 | 1.06 | 0.14 | 200 | 757 |
| 51R-4 | 723.20 | 533 | 0.10 | 0.37 | 0.67 | 0.21 | 185 | 330 |
| 52R-4 | 732.80 | 595 | 0.06 | 0.63 | 0.75 | 0.23 | 273 | 326 |
| 53R-4 | 742.40 | NA | NA | NA | NA | NA | NA | NA |
| 54R-4 | 752.00 | 489 | 0.04 | 0.21 | 0.66 | 0.16 | 131 | 412 |
| 55R-4 | 761.60 | 421 | 0.07 | 0.37 | 0.90 | 0.23 | 160 | 391 |
| 56R-3 | 769.70 | 529 | 0.01 | 0.44 | 0.58 | 0.25 | 176 | 232 |
| 57R-3 | 779.30 | 368 | 0.00 | 0.31 | 0.39 | 0.26 | 119 | 150 |
| 58R-4 | 790.40 | 577 | 0.44 | 13.60 | 0.54 | 1.41 | 957 | 38 |
| 59R-4 | 800.00 | NA | 0.02 | 0.00 | 0.69 | 0.34 | 0 | 198 |
| 60R-4 | 809.60 | 593 | 0.05 | 3.02 | 0.50 | 0.83 | 363 | 60 |
| 61R-4 | 819.20 | 588 | 0.03 | 0.45 | 0.48 | 0.67 | 67 | 71 |
| 62R-4 | 828.80 | 571 | 0.01 | 0.28 | 0.38 | 0.57 | 50 | 65 |
| 63R-4 | 838.40 | 590 | 0.40 | 3.57 | 0.56 | 0.69 | 517 | 81 |
| 65R-4 | 857.60 | NA | 0.10 | 0.00 | 0.79 | 0.54 | 0 | 146 |
| 66R-4 | 867.20 | 530 | 0.15 | 0.66 | 0.48 | 0.70 | 94 | 68 |
| 67R-4 | 876.80 | 540 | 0.13 | 0.41 | 0.81 | 0.60 | 68 | 135 |
| 68R-4 | 886.20 | 593 | 0.13 | 0.26 | 0.71 | 0.31 | 83 | 229 |
| 69R-4 | 895.80 | NA | 0.00 | 0.00 | 0.18 | 1.05 | 0 | 17 |
| 70R-4 | 905.40 | 427 | 0.13 | 5.78 | 0.85 | 1.82 | 317 | 46 |
| 71R-4 | 915.00 | 325 | 0.08 | 0.02 | 0.70 | 1.02 | 1 | 66 |
| 72R-4 | 924.70 | 456 | 0.14 | 1.28 | 0.61 | 0.73 | 175 | 83 |
| 73R-4 | 934.40 | 444 | 0.25 | 3.87 | 0.87 | 1.09 | 355 | 79 |
| 74R-CC | 939.50 | 593 | 0.15 | 1.60 | 0.74 | 0.78 | 205 | 94 |
| 75R-4 | 953.70 | 423 | 0.15 | 0.91 | 2.81 | 1.17 | 77 | 240 |

Notes: $T_{max}$ = temperature (°C) of maximum hydrocarbon generation from kerogen. $S_1$ = volatile hydrocarbons, $S_2$ = kerogen-derived hydrocarbons, $S_3$ = organic $CO_2$ from kerogen. TOC = total organic carbon obtained by Rock-Eval analysis. HI = hydrogen index, OI = oxygen index. NA = not analyzed.

**Table T19.** Headspace gas composition, Site 1171.

| Hole, core, section | Depth (mbsf) | $C_1$ (ppmv) | $C_2$ (ppmv) | $C_3$ (ppmv) |
|---|---|---|---|---|
| **189-1171A-** | | | | |
| 1H-4 | 4.50 | 17 | 1 | NA |
| 2H-4 | 11.60 | 49 | 3 | NA |
| 3H-4 | 21.10 | 3 | 0 | NA |
| 4H-4 | 30.60 | 8 | 0 | NA |
| 5H-4 | 40.10 | 3 | 0 | NA |
| 6H-4 | 49.60 | 3 | 0 | NA |
| 7H-4 | 59.10 | 3 | 0 | NA |
| 8H-4 | 67.24 | 20 | 1 | NA |
| 9H-4 | 78.10 | 16 | 1 | NA |
| 10H-4 | 87.60 | 15 | 1 | NA |
| 11H-4 | 97.10 | 16 | 1 | NA |
| 12H-4 | 106.60 | 3 | 0 | NA |
| 13X-1 | 111.60 | 3 | 0 | NA |
| 14X-3 | 117.80 | 3 | 0 | NA |
| **189-1171C-** | | | | |
| 16X-3 | 137.50 | 3 | NA | NA |
| 17X-4 | 148.60 | 4 | NA | NA |
| 18X-4 | 158.20 | 3 | NA | NA |
| 20X-4 | 177.40 | 5 | NA | NA |
| 21X-4 | 186.70 | 2 | NA | NA |
| 22X-4 | 196.30 | 2 | NA | NA |
| 23X-4 | 206.00 | 3 | NA | NA |
| 24X-4 | 215.60 | 4 | NA | NA |
| 25X-4 | 225.20 | 4 | NA | NA |
| 27X-4 | 244.10 | 3 | NA | NA |
| 28X-4 | 253.00 | 3 | NA | NA |
| 29X-4 | 263.00 | 6 | NA | NA |
| 30X-3 | 271.10 | 5 | NA | NA |
| 31X-1 | 273.50 | 5 | NA | NA |
| **189-1171D-** | | | | |
| 1R-2 | 249.10 | 25 | 2 | 0 |
| 2R-2 | 258.50 | 6 | 0 | 0 |
| 3R-2 | 268.10 | 7 | 0 | 0 |
| 4R-2 | 277.70 | 4 | 0 | 0 |
| 5R-1 | 285.80 | 5 | 0 | 0 |
| 6R-1 | 293.80 | 4 | 0 | 0 |
| 7R-2 | 301.60 | 3 | 0 | 0 |
| 8R-2 | 306.90 | 2 | 0 | 0 |
| 9R-2 | 316.20 | 11 | 0 | 0 |
| 10R-4 | 328.80 | 2 | 0 | 0 |
| 11R-CC | 334.02 | 2 | 0 | 0 |
| 12R-CC | 343.50 | 4 | 0 | 0 |
| 13R-CC | 353.20 | 393 | 0 | 0 |
| 14R-1 | 362.80 | 14 | 0 | 0 |
| 15R-2 | 373.60 | 5 | 0 | 0 |
| 16R-2 | 383.50 | 2 | 0 | 0 |
| 17R-4 | 396.10 | 2 | 0 | 0 |
| 18R-CC | 401.22 | 3 | 0 | 0 |
| 19R-4 | 415.30 | 4 | 0 | 0 |
| 20R-4 | 424.90 | 3 | 0 | 0 |
| 21R-CC | 430.00 | 2 | 0 | 0 |
| 22R-4 | 444.10 | 3 | 0 | 0 |
| 23R-2 | 450.70 | 3 | 0 | 0 |
| 24R-3 | 461.80 | 2 | 0 | 0 |
| 25R-4 | 473.00 | 2 | 0 | 0 |
| 26R-4 | 482.60 | 2 | 0 | 0 |
| 27R-4 | 492.20 | 37688 | 314 | 78 |
| 28R-4 | 501.80 | 17144 | 150 | 29 |
| 29R-4 | 511.50 | 11570 | 115 | 33 |
| 30R-4 | 520.91 | 25058 | 189 | 40 |
| 30R-4 | 520.91 | 19913 | 173 | 29 |
| 31R-4 | 530.70 | 14907 | 150 | 49 |
| 31R-4 | 530.70 | 10339 | 136 | 64 |
| 32R-4 | 540.30 | 15770 | 122 | 23 |

| Hole, core, section | Depth (mbsf) | $C_1$ (ppmv) | $C_2$ (ppmv) | $C_3$ (ppmv) |
|---|---|---|---|---|
| 33R-4 | 550.00 | 7658 | 69 | 13 |
| 33R-4 | 550.00 | 18601 | 183 | 36 |
| 34R-4 | 559.60 | 7429 | 71 | 15 |
| 34R-4 | 559.60 | 18966 | 190 | 46 |
| 35R-4 | 569.20 | 10250 | 106 | 0 |
| 35R-4 | 569.20 | 6116 | 44 | 7 |
| 36R-4 | 578.80 | 7907 | 61 | 9 |
| 36R-4 | 578.80 | 6213 | 63 | 0 |
| 37R-4 | 588.40 | 6480 | 68.3 | 0 |
| 37R-4 | 588.40 | 13001 | 105 | 16 |
| 38R-4 | 598.10 | 13716 | 117 | 20 |
| 39R-4 | 607.70 | 13424 | 131 | 29 |
| 40R-4 | 617.30 | 13424 | 131 | 29 |
| 41R-4 | 626.90 | 14818 | 132 | 25 |
| 42R-4 | 636.50 | 20119 | 160 | 27 |
| 43R-4 | 646.10 | 46395 | 374 | 74 |
| 44R-4 | 655.80 | 51668 | 454 | 106 |
| 44R-4 | 655.80 | 5110 | 62 | 0 |
| 45R-3 | 663.90 | 37184 | 180 | 49 |
| 45R-3 | 663.90 | 43475 | 320 | 53 |
| 46R-3 | 673.50 | 27402 | 212 | 34 |
| 47R-4 | 683.41 | 39873 | 209 | 69 |
| 47R-4 | 683.41 | 37112 | 297 | 54 |
| 48R-4 | 694.40 | 24562 | 237 | 53 |
| 48R-4 | 694.40 | 12816 | 148 | 23 |
| 49R-4 | 703.02 | 9397 | 113 | 3 |
| 49R-4 | 703.02 | 10107 | 95 | 14 |
| 50R-4 | 713.60 | 11635 | 125 | 27 |
| 50R-4 | 713.60 | 5308 | 75 | 0 |
| 51R-4 | 723.20 | 2157 | 32 | 0 |
| 51R-4 | 723.20 | 5777 | 86 | 25 |
| 52R-4 | 732.80 | 8767 | 142 | 46 |
| 52R-4 | 732.80 | 5801 | 111 | 24 |
| 53R-4 | 742.40 | 7826 | 122 | 21 |
| 53R-4 | 742.40 | 14868 | 193 | 52 |
| 54R-4 | 752.00 | 14651 | 188 | 48 |
| 54R-4 | 752.00 | 5395 | 91 | 6 |
| 55R-4 | 761.60 | 6587 | 127 | 44 |
| 55R-4 | 761.60 | 10694 | 180 | 69 |
| 56R-3 | 769.70 | 14864 | 192 | 54 |
| 57R-3 | 779.30 | 18385 | 514 | 285 |
| 58R-4 | 790.40 | 15700 | 352 | 156 |
| 59R-4 | 800.00 | 30344 | 558 | 235 |
| 60R-4 | 809.60 | 37385 | 766 | 280 |
| 61R-4 | 819.20 | 13166 | 620 | 407 |
| 62R-4 | 828.80 | 22672 | 453 | 156 |
| 63R-4 | 838.40 | 30461 | 486 | 420 |
| 63R-4 | 838.40 | 8766 | 206 | 85 |
| 65R-4 | 857.60 | 59259 | 829 | 641 |
| 65R-4 | 857.60 | 63531 | 1335 | 489 |
| 66R-4 | 867.20 | 26371 | 830 | 484 |
| 66R-4 | 867.20 | 20395 | 543 | 498 |
| 67R-4 | 876.80 | 10508 | 316 | 259 |
| 67R-4 | 876.80 | 14490 | 485 | 254 |
| 68R-4 | 886.20 | 16917 | 479 | 259 |
| 69R-4 | 895.80 | 20262 | 809 | 398 |
| 70R-4 | 905.40 | 24180 | 2115 | 1383 |
| 71R-4 | 915.00 | 25549 | 1404 | 850 |
| 72R-4 | 924.70 | 21104 | 779 | 452 |
| 73R-4 | 934.40 | 17129 | 747 | 343 |
| 74R-CC | 939.50 | 3168 | 292 | 251 |
| 75R-4 | 953.70 | 4947 | 286 | 174 |
| 75R-4 | 953.70 | 26352 | 1012 | 1172 |

Notes: $C_1$ = methane, $C_2$ = ethane, $C_3$ = propane. ppmv = parts per million by volume. NA = not analyzed.

**Table T20.** Interstitial water data, Site 1171.

| Core, section, interval (cm) | Depth (mbsf) | pH | Alkalinity (mM) | Salinity | Cl⁻ (mM) | SO₄²⁻ (mM) | Na⁺ (mM) | Mg²⁺ (mM) | Ca²⁺ (mM) | K⁺ (mM) | H₄SiO₄⁰ (μM) | NH₄⁺ (μM) | Sr²⁺ (μM) | Li⁺ (μM) |
|---|---|---|---|---|---|---|---|---|---|---|---|---|---|---|
| 189-1171A- | | | | | | | | | | | | | | |
| 1H-1, 145-150 | 1.45 | 7.64 | 3.07 | 34.5 | 554 | 26.8 | 465 | 51.3 | 10.3 | 10.0 | 468 | 10 | 117 | 21 |
| 2H-3, 145-150 | 11.55 | 7.53 | 4.19 | 34.5 | 557 | 24.5 | 466 | 47.8 | 11.3 | 10.0 | 661 | 114 | 283 | 18 |
| 3H-3, 145-150 | 21.05 | 7.51 | 4.35 | 34.0 | 561 | 23.9 | 472 | 47.3 | 11.4 | 9.8 | 699 | 196 | 342 | 17 |
| 4H-3, 145-150 | 30.55 | 7.43 | 4.61 | 35.0 | 558 | 24.0 | 477 | 46.1 | 11.5 | 9.7 | 749 | 263 | 376 | 17 |
| 5H-3, 145-150 | 40.05 | 7.44 | 4.57 | 35.0 | 562 | 22.7 | 471 | 45.9 | 11.9 | 9.9 | 714 | 321 | 409 | 18 |
| 6H-3, 145-150 | 49.55 | 7.44 | 4.97 | 35.0 | 564 | 22.3 | 480 | 44.5 | 11.4 | 9.4 | 734 | 352 | 419 | 20 |
| 7H-3, 145-150 | 59.05 | 7.48 | 5.13 | 36.0 | 562 | 22.7 | 476 | 44.6 | 11.7 | 9.3 | 705 | 421 | 416 | 22 |
| 8H-3, 140-150 | 67.14 | 7.17 | 4.74 | 35.0 | 562 | 22.4 | 478 | 44.9 | 11.7 | 9.1 | 770 | 454 | 414 | 22 |
| 9H-3, 140-150 | 78.00 | 7.20 | 4.81 | 35.0 | 561 | 22.6 | 477 | 45.5 | 11.7 | 9.0 | 861 | 509 | 419 | 22 |
| 10H-3, 140-150 | 87.50 | 7.39 | 5.15 | 35.0 | 560 | 23.4 | 474 | 44.9 | 12.3 | 8.6 | 856 | 514 | 412 | 23 |
| 11H-3, 140-150 | 97.00 | 7.37 | 4.97 | 35.0 | 561 | 22.1 | 468 | 45.0 | 11.9 | 8.5 | 865 | 468 | 407 | 24 |
| 14X-2, 140-150 | 117.70 | 7.40 | 5.47 | 34.5 | 561 | 21.3 | 466 | 45.1 | 12.0 | 8.4 | 819 | 565 | 391 | 24 |
| 189-1171C- | | | | | | | | | | | | | | |
| 17X-3, 140-150 | 148.50 | 7.45 | 5.10 | 34.5 | 558 | 21.2 | 473 | 43.6 | 11.7 | 8.1 | 848 | 625 | 384 | 31 |
| 20X-3, 140-150 | 177.30 | 7.42 | 5.40 | 34.5 | 557 | 20.8 | 469 | 43.5 | 11.9 | 7.8 | 972 | 710 | 380 | 33 |
| 23X-3, 140-150 | 205.90 | 7.42 | 5.47 | 34.0 | 556 | 21.1 | 476 | 43.0 | 11.6 | 7.8 | 920 | 733 | 362 | 36 |
| 26X-3, 140-150 | 234.70 | 7.44 | 5.26 | 34.0 | 556 | 19.5 | 466 | 42.3 | 11.8 | 7.5 | 968 | 763 | 358 | 41 |
| 29X-3, 140-150 | 262.90 | 7.46 | 5.30 | 34.0 | 554 | 18.3 | 461 | 40.5 | 11.8 | 7.4 | 981 | 864 | 352 | 50 |
| 189-1171D- | | | | | | | | | | | | | | |
| 2R-1, 140-150 | 258.40 | 7.44 | 5.06 | 34.0 | 555 | 19.5 | 493 | 40.2 | 11.3 | 7.5 | 946 | 891 | 356 | 48 |
| 9R-1, 140-150 | 316.10 | 7.44 | 7.21 | 32.0 | 557 | 5.8 | 484 | 34.4 | 10.5 | 6.1 | 1065 | 965 | 340 | 79 |
| 16R-1, 140-150 | 383.40 | 7.56 | 5.81 | 31.0 | 548 | 1.7 | 474 | 29.6 | 10.3 | 4.7 | 667 | 1062 | 291 | 121 |
| 19R-3, 140-150 | 415.20 | 7.63 | 4.10 | 31.0 | 547 | 1.5 | 474 | 27.4 | 10.5 | 4.4 | 633 | 1085 | 286 | 134 |
| 22R-3, 135-150 | 443.95 | 7.66 | 6.02 | 31.0 | 547 | 1.4 | 480 | 26.5 | 11.5 | 4.7 | 585 | 1155 | 275 | 156 |
| 25R-3, 135-150 | 472.85 | 7.62 | 5.25 | 30.5 | 544 | 1.5 | 484 | 24.4 | 11.1 | 4.1 | 541 | 1287 | 264 | 166 |
| 28R-3, 140-150 | 501.70 | 7.69 | 4.57 | 31.0 | 551 | 2.1 | 487 | 23.7 | 11.2 | 4.0 | 516 | 1321 | 257 | 183 |
| 31R-3, 135-150 | 530.55 | 8.24 | 2.61 | 31.0 | 550 | 0.8 | 493 | 21.2 | 10.6 | 3.9 | 175 | 1549 | 260 | 212 |
| 34R-3, 135-150 | 559.45 | 8.22 | 1.92 | 30.0 | 544 | 1.7 | 487 | 21.2 | 10.8 | 3.3 | 137 | 1453 | NM | NM |
| 37R-3, 135-150 | 588.25 | NM | NM | 30.0 | 548 | 2.4 | 496 | 19.0 | 10.9 | 3.4 | 115 | 1871 | 248 | 285 |
| 40R-3, 135-150 | 617.15 | 8.22 | 1.53 | 30.0 | 524 | 0.0 | 465 | 19.1 | 11.3 | 2.4 | 135 | 1515 | 245 | 322 |
| 43R-3, 135-150 | 645.95 | NM | NM | 28.0 | 512 | 0.0 | 459 | 17.7 | 11.7 | 2.4 | 91 | 1540 | 228 | 345 |
| 46R-2, 135-150 | 673.35 | NM | NM | 27.0 | 488 | 0.0 | 438 | 16.5 | 11.5 | 1.9 | 95 | 1477 | 213 | 369 |
| 49R-3, 135-150 | 702.87 | NM | NM | 28.0 | 495 | 0.0 | 445 | 15.1 | 10.0 | 1.8 | 85 | 1653 | 231 | 399 |
| 52R-3, 135-150 | 732.65 | 8.39 | 2.15 | 27.0 | 489 | 0.0 | 448 | 12.9 | 10.6 | 1.8 | 95 | 1669 | 223 | 436 |
| 55R-3, 135-150 | 761.45 | NM | NM | 28.0 | 514 | 0.0 | 472 | 12.4 | 9.4 | 1.9 | 111 | 1939 | 224 | 475 |
| 58R-3, 135-150 | 790.25 | NM | NM | 27.0 | 486 | 0.0 | 451 | 11.7 | 8.6 | 1.6 | 117 | 1827 | 220 | 489 |
| 61R-3, 135-150 | 819.05 | NM | NM | 28.0 | 509 | 0.0 | 484 | 11.4 | 7.6 | 1.9 | 111 | 2154 | 210 | 520 |
| 64R-3, 135-150 | 847.85 | 8.07 | 11.59 | 28.0 | 504 | 0.0 | 480 | 10.0 | 7.3 | 1.8 | 127 | 2381 | 203 | 547 |
| 67R-3, 135-150 | 876.65 | NM | NM | 28.0 | 498 | 0.0 | 479 | 9.2 | 6.5 | 1.8 | 117 | 2343 | 201 | 584 |
| 70R-3, 135-150 | 905.25 | NM | NM | 29.0 | 503 | 1.0 | 492 | 9.7 | 6.8 | 2.0 | 161 | 2430 | 178 | 603 |
| 73R-3, 135-150 | 934.25 | NM | NM | NM | 497 | 0.0 | 472 | 7.8 | 5.6 | 1.7 | NM | 3043 | NM | NM |

Note: NM = not measured.

**Table T21.** *P*-wave velocities measured at discrete intervals, Site 1171. (**See table notes.** Continued on next two pages.)

| Core, section, interval (cm) | Depth (mbsf) | PWS1 (km/s) | PWS3 (km/s) | Core, section, interval (cm) | Depth (mbsf) | PWS1 (km/s) | PWS3 (km/s) | Core, section, interval (cm) | Depth (mbsf) | PWS1 (km/s) | PWS3 (km/s) |
|---|---|---|---|---|---|---|---|---|---|---|---|
| 189-1171A- | | | | 11H-4, 48.6 | 97.59 | 1.640 | 1.632 | 22X-3, 48.6 | 195.29 | 1.589 | 1.633 |
| 1H-1, 81.9 | 0.82 | | 1.681 | 11H-5, 49.6 | 99.10 | 1.615 | 1.630 | 22X-4, 49.5 | 196.79 | 1.599 | 1.636 |
| 1H-2, 56.6 | 2.07 | | 1.676 | 11H-6, 49.6 | 100.60 | 1.587 | 1.609 | 22X-5, 48.1 | 198.28 | 1.582 | 1.641 |
| 1H-3, 55.3 | 3.55 | | 1.649 | 11H-7, 49.7 | 102.10 | 1.577 | 1.608 | 23X-1, 83.9 | 202.34 | 1.580 | |
| 1H-4, 50.5 | 5.01 | | 1.617 | 12H-1, 43.4 | 102.53 | 1.582 | 1.611 | 23X-2, 49.0 | 203.49 | 1.572 | 1.616 |
| 1H-5, 28.0 | 6.28 | | 1.608 | 12H-2, 47.8 | 104.08 | 1.573 | 1.600 | 23X-3, 48.1 | 204.98 | 1.632 | 1.684 |
| 2H-3, 63.8 | 10.74 | | 1.676 | 12H-3, 48.1 | 105.58 | 1.639 | 1.620 | 23X-4, 53.9 | 206.54 | 1.600 | 1.655 |
| 2H-4, 54.5 | 12.15 | | 1.693 | 12H-4, 50.7 | 107.11 | 1.586 | 1.605 | 23X-5, 52.1 | 208.02 | 1.633 | 1.649 |
| 2H-5, 91.6 | 14.02 | | 1.676 | 12H-5, 48.6 | 108.59 | 1.596 | 1.634 | 23X-6, 49.4 | 209.49 | 1.653 | 1.650 |
| 2H-6, 36.5 | 14.97 | | 1.650 | 12H-6, 48.6 | 110.09 | 1.559 | 1.587 | 24X-1, 50.2 | 211.60 | 1.617 | 1.627 |
| 3H-1, 55.2 | 17.15 | | 1.644 | 13X-1, 48.3 | 112.08 | | 1.622 | 24X-3, 83.9 | 214.94 | | 1.690 |
| 3H-2, 59.4 | 18.69 | | 1.612 | 13X-1, 48.9 | 112.09 | 1.651 | | 24X-4, 64.3 | 216.24 | | 1.673 |
| 3H-3, 42.4 | 20.02 | | 1.641 | 14X-1, 49.7 | 115.30 | 1.626 | 1.608 | 24X-5, 54.5 | 217.65 | | 1.686 |
| 3H-4, 48.3 | 21.58 | | 1.644 | 14X-2, 48.9 | 116.79 | | 1.616 | 24X-6, 43.7 | 219.04 | | 1.670 |
| 3H-5, 46.9 | 23.07 | | 1.626 | 14X-3, 48.4 | 118.28 | 1.625 | 1.640 | 25X-1, 50.0 | 221.20 | 1.604 | 1.623 |
| 4H-1, 80.2 | 26.90 | | 1.620 | 14X-4, 49.7 | 119.80 | | 1.668 | 25X-2, 42.2 | 222.62 | | 1.666 |
| 4H-2, 50.4 | 28.10 | 1.583 | 1.645 | | | | | 25X-3, 64.1 | 224.34 | | 1.694 |
| 4H-4, 49.8 | 31.10 | 1.597 | | 189-1171C- | | | | 25X-4, 72.4 | 225.92 | | 1.635 |
| 4H-5, 50.1 | 32.60 | 1.595 | | 13X-1, 49.3 | 110.69 | | 1.601 | 25X-5, 31.2 | 227.01 | | 1.687 |
| 4H-6, 50.5 | 34.10 | 1.595 | | 13X-2, 49.9 | 112.20 | 1.601 | 1.629 | 26X-1, 33.1 | 230.63 | | 1.652 |
| 4H-5, 50.7 | 32.61 | | 1.648 | 13X-3, 49.5 | 113.69 | 1.593 | | 26X-2, 61.6 | 232.42 | | 1.709 |
| 5H-1, 50.7 | 36.11 | | 1.613 | 13X-3, 49.7 | 113.70 | | 1.631 | 26X-2, 73.2 | 232.53 | | 1.636 |
| 5H-2, 50.7 | 37.61 | 1.585 | 1.602 | 13X-4, 49.5 | 115.19 | 1.576 | 1.612 | 26X-3, 48.9 | 233.79 | | 1.673 |
| 5H-3, 49.6 | 39.10 | 1.600 | 1.657 | 14X-1, 43.5 | 115.64 | | 1.599 | 26X-4, 113.1 | 235.93 | | 1.707 |
| 5H-4, 49.8 | 40.60 | | 1.697 | 14X-1, 49.8 | 115.70 | 1.616 | 1.589 | 26X-5, 54.7 | 236.85 | | 1.682 |
| 5H-6, 50.6 | 43.61 | 1.676 | 1.739 | 14X-2, 50.0 | 117.20 | 1.625 | | 26X-5, 63.8 | 236.94 | | 1.701 |
| 6H-1, 49.9 | 45.60 | 1.600 | 1.703 | 14X-3, 50.1 | 118.70 | 1.594 | 1.636 | 27X-1, 80.8 | 240.41 | | 1.694 |
| 6H-2, 49.2 | 47.09 | 1.683 | | 14X-4, 49.5 | 120.19 | 1.646 | 1.655 | 27X-2, 36.2 | 241.46 | | 1.683 |
| 6H-2, 49.6 | 47.10 | | 1.683 | 14X-5, 50.7 | 121.71 | | 1.637 | 27X-3, 44.9 | 243.05 | | 1.671 |
| 6H-3, 49.9 | 48.60 | | 1.654 | 14X-5, 50.0 | 121.70 | 1.607 | | 27X-4, 61.4 | 244.71 | | 1.681 |
| 6H-4, 50.1 | 50.10 | | 1.674 | 15X-1, 49.9 | 125.30 | 1.616 | 1.637 | 27X-5, 96.5 | 246.57 | | 1.683 |
| 6H-5, 50.9 | 51.61 | | 1.788 | 15X-2, 50.1 | 126.80 | 1.589 | 1.616 | 28X-1, 89.8 | 249.80 | | 1.663 |
| 6H-6, 50.2 | 53.10 | | 1.622 | 15X-3, 50.4 | 128.30 | 1.621 | | 28X-2, 61.1 | 251.01 | | 1.746 |
| 7H-1, 49.9 | 55.10 | 1.597 | 1.626 | 15X-3, 51.2 | 128.31 | | 1.618 | 28X-3, 46.7 | 252.37 | | 1.758 |
| 7H-2, 49.6 | 56.60 | 1.593 | 1.663 | 15X-4, 50.1 | 129.80 | 1.592 | 1.627 | 29X-1 101.0 | 259.51 | | 1.729 |
| 7H-3, 50.1 | 58.10 | 1.615 | 1.658 | 15X-5, 49.9 | 131.30 | 1.625 | 1.656 | 29X-2, 54.6 | 260.55 | | 1.649 |
| 7H-4, 49.2 | 59.59 | 1.587 | 1.625 | 15X-6, 50.0 | 132.80 | 1.600 | 1.644 | 29X-2, 69.5 | 260.70 | | 1.714 |
| 7H-5, 50.0 | 61.10 | 1.592 | 1.634 | 16X-1, 78.2 | 135.28 | 1.642 | 1.674 | 29X-2, 75.7 | 260.76 | | 1.701 |
| 7H-6, 50.8 | 62.61 | 1.573 | 1.611 | 16X-2, 53.9 | 136.54 | 1.646 | 1.694 | 30X-1, 53.8 | 268.64 | | 1.694 |
| 8H-1, 50.4 | 64.60 | 1.593 | | 16X-3, 48.6 | 137.99 | 1.590 | 1.642 | 30X-2, 46.5 | 270.07 | | 1.739 |
| 8H-1, 51.1 | 64.61 | | 1.656 | 17X-1, 53.7 | 144.64 | | 1.691 | 30X-3, 35.9 | 271.46 | | 1.715 |
| 8H-3, 37.7 | 66.12 | | 1.620 | 17X-2, 60.0 | 146.20 | 1.644 | | 30X-CC, 24.6 | 272.99 | | 3.729 |
| 8H-4, 50.1 | 67.74 | 1.561 | 1.614 | 17X-2, 84.9 | 146.45 | | 1.645 | 31X-1, 19.5 | 273.70 | | 3.328 |
| 8H-5, 49.4 | 69.23 | 1.564 | | 17X-3, 52.0 | 147.62 | 1.602 | 1.646 | 31X-1, 57.3 | 274.07 | | 1.705 |
| 8H-5, 49.9 | 69.24 | | 1.617 | 17X-4, 47.9 | 149.08 | | 1.669 | | | | |
| 8H-6, 50.0 | 70.74 | 1.572 | 1.623 | 18X-1, 40.5 | 154.10 | | 1.666 | 189-1171D- | | | |
| 8H-7, 38.5 | 72.13 | 1.653 | 1.712 | 18X-2, 65.0 | 155.85 | 1.635 | | 1R-1, 63.5 | 248.24 | | 1.690 |
| 9H-2, 50.1 | 75.60 | 1.588 | 1.678 | 18X-2, 75.3 | 155.95 | | 1.669 | 1R-1, 102.4 | 248.62 | | 1.653 |
| 9H-3, 50.0 | 77.10 | 1.619 | 1.665 | 18X-3, 49.7 | 157.20 | 1.671 | 1.674 | 1R-2, 20.3 | 249.30 | | 1.723 |
| 9H-4, 49.4 | 78.59 | 1.587 | | 18X-4, 45.8 | 158.66 | 1.631 | 1.682 | 2R-1, 87.3 | 257.87 | | 1.727 |
| 9H-4, 50.3 | 78.60 | | 1.661 | 18X-5, 50.7 | 160.21 | | 1.701 | 2R-2, 27.3 | 258.77 | | 1.742 |
| 9H-5, 50.1 | 80.10 | 1.582 | 1.646 | 18X-6, 49.1 | 161.69 | | 1.702 | 2R-2, 49.3 | 258.99 | | 1.727 |
| 9H-6, 49.4 | 81.59 | 1.600 | | 19X-2, 53.1 | 165.33 | 1.604 | 1.655 | 2R-2, 75.2 | 259.25 | | 1.715 |
| 9H-6, 49.9 | 81.60 | | 1.658 | 19X-3, 49.6 | 166.80 | 1.619 | 1.631 | 2R-2, 113.2 | 259.63 | | 1.796 |
| 10H-1, 50.2 | 83.60 | 1.602 | | 19X-4, 49.9 | 168.30 | 1.625 | 1.640 | 3R-1, 100.0 | 267.60 | | 1.756 |
| 10H-1, 51.0 | 83.61 | | 1.615 | 19X-5, 49.3 | 169.79 | 1.623 | 1.675 | 3R-2, 64.3 | 268.74 | | 1.758 |
| 10H-2, 49.9 | 85.10 | 1.629 | | 19X-6, 48.5 | 171.29 | 1.616 | 1.682 | 3R-3, 16.5 | 269.77 | | 1.753 |
| 10H-2, 50.7 | 85.11 | | 1.633 | 20X-1, 50.1 | 173.40 | 1.630 | 1.673 | 3R-3, 34.2 | 269.94 | | 3.647 |
| 10H-3, 48.6 | 86.59 | 1.596 | 1.604 | 20X-2, 22.1 | 174.62 | 1.593 | 1.627 | 3R-3, 53.1 | 270.13 | | 3.502 |
| 10H-4, 50.6 | 88.11 | 1.585 | 1.626 | 20X-4, 48.4 | 177.88 | 1.612 | 1.652 | 3R-3, 71.3 | 270.31 | | 1.699 |
| 10H-5, 49.4 | 89.59 | 1.620 | | 20X-5, 48.5 | 179.38 | 1.752 | 1.657 | 3R-3, 88.3 | 270.48 | | 2.823 |
| 10H-5, 49.7 | 89.60 | | 1.653 | 21X-1, 80.1 | 183.00 | 1.624 | 1.644 | 3R-3, 104.2 | 270.64 | | 2.926 |
| 10H-6, 50.0 | 91.10 | 1.597 | | 21X-2, 63.9 | 184.34 | 1.612 | 1.641 | 3R-4, 19.7 | 270.96 | | 2.981 |
| 10H-6, 50.9 | 91.11 | | 1.652 | 21X-3, 49.6 | 185.70 | 1.581 | 1.628 | 4R-1, 43.8 | 276.64 | | 1.628 |
| 11H-1, 50.0 | 93.10 | 1.608 | | 21X-4, 54.5 | 187.24 | 1.642 | 1.645 | 4R-2, 44.2 | 278.14 | | 1.659 |
| 11H-1, 50.8 | 93.11 | | 1.618 | 21X-5, 49.9 | 188.70 | 1.619 | 1.653 | 4R-3, 42.8 | 279.63 | | 1.653 |
| 11H-2, 49.7 | 94.60 | 1.607 | 1.635 | 22X-1, 49.4 | 192.29 | | 1.676 | 5R-1, 45.2 | 286.25 | | 1.644 |
| 11H-3, 49.7 | 96.10 | 1.612 | 1.657 | 22X-2, 49.8 | 193.8 | 1.626 | 1.662 | 5R-1, 63.6 | 286.44 | | 3.204 |

**Table T21 (continued).**

| Core, section, interval (cm) | Depth (mbsf) | PWS1 (km/s) | PWS3 (km/s) | Core, section, interval (cm) | Depth (mbsf) | PWS1 (km/s) | PWS3 (km/s) | Core, section, interval (cm) | Depth (mbsf) | PWS1 (km/s) | PWS3 (km/s) |
|---|---|---|---|---|---|---|---|---|---|---|---|
| 5R-2, 29.8 | 287.10 | | 1.660 | 27R-4, 42.0 | 492.62 | | 1.834 | 39R-6, 60.7 | 611.31 | | 1.882 |
| 5R-2, 50.7 | 287.31 | | 2.859 | 27R-5, 48.0 | 494.18 | | 1.856 | 40R-1, 52.0 | 613.32 | | 2.007 |
| 6R-1, 36.6 | 294.17 | | 3.045 | 27R-6, 46.0 | 495.66 | | 1.873 | 40R-5, 40.0 | 619.20 | | 2.063 |
| 6R-1, 114.1 | 294.94 | | 1.716 | 27R-7, 14.0 | 496.84 | | 1.864 | 40R-6, 27.0 | 620.57 | | 1.940 |
| 7R-1, 61.3 | 301.01 | | 1.617 | 28R-1, 62.5 | 497.92 | | 1.882 | 40R-7, 52.0 | 622.32 | | 1.993 |
| 7R-2, 27.3 | 301.87 | | 1.626 | 28R-2, 62.0 | 499.42 | | 1.901 | 41R-1, 25.0 | 622.65 | | 1.973 |
| 8R-1, 53.4 | 305.93 | | 1.618 | 28R-3, 35.0 | 500.65 | | 1.788 | 41R-3, 87.0 | 626.27 | | 1.934 |
| 8R-1, 129.7 | 306.70 | | 1.636 | 28R-3, 118.0 | 501.48 | | 1.943 | 41R-4, 26.0 | 627.16 | | 1.960 |
| 8R-2, 32.9 | 307.23 | | 1.619 | 28R-4, 98.0 | 502.78 | | 1.866 | 41R-5, 42.0 | 628.82 | | 1.946 |
| 9R-1, 49.2 | 315.19 | | 1.616 | 28R-5, 54.0 | 503.84 | | 1.841 | 42R-1, 82.0 | 632.82 | | 1.856 |
| 9R-2, 83.8 | 317.04 | | 1.609 | 28R-6, 48.0 | 505.28 | | 1.899 | 42R-2, 92.0 | 634.42 | | 1.917 |
| 9R-2, 131.3 | 317.51 | | 1.643 | 29R-1, 50.0 | 507.50 | | 1.957 | 42R-3, 54.0 | 635.54 | | 1.970 |
| 9R-3, 33.4 | 318.03 | | 1.643 | 29R-2, 37.0 | 508.87 | | 1.835 | 42R-4, 75.0 | 637.25 | | 1.917 |
| 10R-1, 49.2 | 324.79 | | 1.616 | 29R-3, 38.0 | 510.38 | | 1.821 | 42R-5, 52.0 | 638.52 | | 1.889 |
| 10R-2, 69.9 | 326.50 | | 1.610 | 29R-4, 37.0 | 511.87 | | 1.877 | 42R-6, 40.0 | 639.90 | | 1.921 |
| 10R-3, 45.1 | 327.75 | | 1.585 | 29R-5, 94.0 | 513.94 | | 1.909 | 43R-1, 99.0 | 642.59 | | 1.804 |
| 10R-4, 46.2 | 329.26 | | 1.592 | 29R-6, 12.0 | 514.62 | | 1.955 | 43R-2, 34.0 | 643.44 | | 2.008 |
| 10R-5, 21.9 | 330.52 | | 1.595 | 30R-1, 84.0 | 517.44 | | 1.829 | 43R-3, 93.0 | 645.53 | | 1.925 |
| 11R, CC, 2.0 | 333.92 | | 3.324 | 30R-2, 90.0 | 518.81 | | 1.888 | 43R-4, 119.0 | 647.29 | | 2.222 |
| 12R, CC, 2.0 | 343.52 | | 1.947 | 30R-3, 77.0 | 520.18 | | 2.164 | 43R-5, 114.0 | 648.74 | | 1.953 |
| 13R, CC, 6.0 | 353.26 | | 1.940 | 30R-4, 72.0 | 521.63 | | 2.052 | 43R-6, 96.0 | 650.06 | | 1.972 |
| 14R-1, 6.3 | 362.86 | | 2.664 | 31R-1, 34.0 | 526.54 | | 2.233 | 44R-1, 100.0 | 652.30 | | 1.939 |
| 15R-1, 42.8 | 372.83 | | 1.647 | 31R-3, 97.0 | 530.17 | | 1.958 | 44R-2, 105.0 | 653.85 | | 1.922 |
| 15R-2, 37.4 | 373.97 | | 1.714 | 31R-4, 30.0 | 531.00 | | 1.948 | 44R-3, 98.0 | 655.28 | | 1.883 |
| 15R-CC, 9.1 | 374.24 | | 3.131 | 31R-4, 119.0 | 531.89 | | 2.130 | 44R-4, 121.0 | 657.01 | | 1.981 |
| 16R-2, 80.6 | 384.31 | | 1.797 | 31R-5, 83.0 | 533.03 | | 2.303 | 44R-6, 106.0 | 659.86 | | 1.894 |
| 16R-2, 94.2 | 384.44 | | 1.700 | 32R-1, 52.0 | 536.32 | | 1.974 | 45R-1, 130.0 | 662.20 | | 1.705 |
| 17R-1, 65.2 | 392.25 | | 1.686 | 32R-1, 90.0 | 536.70 | | 1.998 | 45R-2, 39.0 | 662.79 | | 1.891 |
| 17R-2, 50.9 | 393.61 | | 1.823 | 32R-2, 81.0 | 537.30 | | 1.905 | 45R-3, 35.0 | 664.25 | | 1.934 |
| 17R-3, 61.6 | 395.22 | | 1.820 | 32R-3, 92.0 | 539.72 | | 1.946 | 45R-4, 45.0 | 664.99 | | 1.943 |
| 17R-4, 70.4 | 396.80 | | 1.776 | 32R-4, 104.0 | 541.34 | | 2.028 | 46R-1, 123.0 | 671.73 | | 1.908 |
| 19R-1, 84.8 | 411.65 | | 1.625 | 32R-5, 105.0 | 542.85 | | 2.115 | 46R-2, 114.0 | 673.14 | | 1.914 |
| 19R-2, 48.7 | 412.79 | | 1.802 | 33R-1, 97.0 | 546.47 | | 1.875 | 46R-3, 37.0 | 673.87 | | 1.952 |
| 19R-2, 77.3 | 413.07 | | 1.701 | 33R-2, 83.0 | 547.83 | | 2.279 | 46R-4, 103.0 | 676.03 | | 1.912 |
| 19R-3, 61.0 | 414.41 | | 1.774 | 33R-3, 90.0 | 549.40 | | 1.884 | 46R-5, 111.0 | 677.61 | | 1.934 |
| 19R-3, 97.0 | 414.77 | | 1.930 | 33R-4, 92.0 | 550.92 | | 1.921 | 47R-1, 81.0 | 681.01 | | 2.043 |
| 19R-3, 105.5 | 414.86 | | 3.273 | 33R-5, 55.0 | 552.05 | | 1.932 | 47R-3, 42.0 | 682.33 | | 1.986 |
| 19R-5, 33.3 | 417.13 | | 1.790 | 33R-6, 76.0 | 553.76 | | 2.037 | 47R-4, 86.0 | 684.27 | | 1.987 |
| 19R-5, 66.1 | 417.46 | | 4.072 | 34R-1, 7.0 | 555.17 | | 1.919 | 47R-5, 87.0 | 685.78 | | 1.976 |
| 20R-1, 53.9 | 420.94 | | 2.060 | 34R-2, 73.0 | 557.33 | | 1.938 | 47R-6, 25.0 | 686.66 | | 4.114 |
| 20R-2, 45.3 | 422.35 | | 1.710 | 34R-3, 66.0 | 558.76 | | 1.914 | 47R-6, 104.0 | 687.45 | | 1.916 |
| 20R-3, 50.8 | 423.91 | | 1.722 | 34R-4, 85.0 | 560.45 | | 1.915 | 48R-1, 19.0 | 690.09 | | 1.943 |
| 20R-4, 46.8 | 425.37 | | 1.772 | 34R-5, 60.0 | 561.70 | | 1.963 | 48R-1, 100.0 | 690.90 | | 4.309 |
| 20R-6, 25.8 | 428.16 | | 1.755 | 34R-6, 109.0 | 563.69 | | 1.964 | 48R-2, 25.0 | 691.65 | | 1.899 |
| 22R-1, 97.0 | 440.57 | | 1.783 | 35R-1, 94.0 | 565.60 | | 1.947 | 48R-3, 106.0 | 693.96 | | 1.946 |
| 22R-2, 62.0 | 441.72 | | 1.769 | 35R-2, 103.0 | 567.23 | | 1.956 | 48R-4, 96.0 | 695.36 | | 2.001 |
| 22R-3, 57.0 | 443.17 | | 1.758 | 35R-4, 111.0 | 570.31 | | 1.900 | 48R-5, 51.0 | 696.41 | | 2.055 |
| 22R-4, 75.0 | 444.85 | | 1.771 | 35R-5, 88.0 | 571.58 | | 2.066 | 49R-1, 30.0 | 699.80 | | 2.009 |
| 22R-5, 40.0 | 446.00 | | 1.748 | 35R-6, 75.0 | 572.95 | | 1.923 | 49R-2, 44.0 | 700.46 | | 1.878 |
| 22R-6, 63.0 | 447.73 | | 1.740 | 36R-1, 102.0 | 575.32 | | 1.988 | 49R-6, 44.0 | 706.46 | | 1.964 |
| 23R-1, 10.5 | 449.30 | | 1.750 | 36R-2, 93.0 | 576.73 | | 2.045 | 50R-2, 116.0 | 711.76 | | 1.990 |
| 23R-1, 53.0 | 449.73 | | 1.792 | 36R-3, 92.0 | 578.22 | | 2.059 | 50R-4, 43.0 | 714.03 | | 1.997 |
| 23R-3, 66.0 | 452.86 | | 1.802 | 36R-4, 80.0 | 579.60 | | 2.155 | 50R-5, 21.0 | 715.31 | | 1.927 |
| 24R-2, 108.0 | 461.38 | | 1.769 | 36R-5, 57.0 | 580.87 | | 1.998 | 50R-6, 14.0 | 716.74 | | 2.001 |
| 24R-4, 5.0 | 463.35 | | 1.820 | 36R-6, 82.0 | 582.62 | | 2.051 | 51R-1, 17.0 | 718.87 | | 1.891 |
| 25R-1, 82.0 | 469.32 | | 1.785 | 37R-1, 109.0 | 584.99 | | 2.020 | 51R-2, 17.0 | 720.37 | | 1.891 |
| 25R-3, 21.0 | 471.71 | | 1.789 | 37R-2, 124.0 | 586.64 | | 1.993 | 51R-4, 117.0 | 724.37 | | 2.061 |
| 25R-4, 76.0 | 473.76 | | 1.856 | 37R-3, 115.0 | 588.05 | | 2.080 | 52R-1, 51.0 | 728.81 | | 1.944 |
| 25R-5, 92.0 | 475.42 | | 1.797 | 37R-4, 61.0 | 589.01 | | 2.002 | 52R-4, 73.0 | 733.53 | | 2.352 |
| 25R-6, 62.0 | 476.62 | | 1.809 | 37R-6, 31.0 | 591.71 | | 2.072 | 52R-5, 53.0 | 734.83 | | 2.287 |
| 26R-1, 38.0 | 478.48 | | 1.806 | 38R-1, 25.0 | 593.85 | | 1.943 | 55R-1, 84.0 | 757.94 | | 2.068 |
| 26R-2, 27.0 | 479.87 | | 1.799 | 38R-3, 36. | 596.96 | | 1.969 | 55R-2, 107.0 | 759.67 | | 1.943 |
| 26R-3, 44.0 | 481.54 | | 1.808 | 38R-4, 28.0 | 598.38 | | 1.994 | 58R-1, 103.0 | 786.93 | | 2.196 |
| 26R-4, 119.0 | 483.79 | | 1.811 | 38R-7, 31.0 | 602.91 | | 2.003 | 58R-2, 83.0 | 788.23 | | 2.107 |
| 26R-5, 27.0 | 484.37 | | 1.816 | 39R-1, 56.4 | 603.76 | | 2.280 | 58R-4, 97.0 | 791.37 | | 2.191 |
| 26R-6, 105.0 | 486.65 | | 1.827 | 39R-2, 132.4 | 606.02 | | 1.867 | 58R-7, 27.0 | 795.17 | | 2.196 |
| 27R-1, 40.0 | 488.10 | | 1.849 | 39R-3, 23.3 | 606.43 | | 1.923 | 59R-2, 29.0 | 797.29 | | 2.783 |
| 27R-2, 72.0 | 489.92 | | 1.863 | 39R-4, 45.6 | 608.16 | | 1.904 | 59R-2, 116.0 | 798.16 | | 2.194 |
| 27R-3, 28.0 | 490.98 | | 1.862 | 39R-5, 36.2 | 609.56 | | 1.957 | 59R-3, 68.0 | 799.18 | | 4.541 |

**Table T21 (continued).**

| Core, section, interval (cm) | Depth (mbsf) | PWS1 (km/s) | PWS3 (km/s) |
|---|---|---|---|
| 59R-3, 123.0 | 799.73 | | 2.225 |
| 59R-4, 122.0 | 801.22 | | 2.181 |
| 59R-6, 12.0 | 803.12 | | 2.258 |
| 60R-1, 119.0 | 806.29 | | 2.100 |
| 60R-3, 131.0 | 809.41 | | 2.132 |
| 60R-4, 111.0 | 810.71 | | 2.220 |
| 60R-5, 117.0 | 812.27 | | 4.405 |
| 61R-1, 17.0 | 814.87 | | 2.224 |
| 61R-4, 113.0 | 820.33 | | 2.106 |
| 62R-1, 23.0 | 824.53 | | 2.174 |
| 62R-4, 72.0 | 829.52 | | 2.188 |
| 62R-6, 62.0 | 832.42 | | 2.236 |
| 63R-1, 65.0 | 834.55 | | 2.268 |
| 63R-4, 108.0 | 839.48 | | 2.222 |
| 63R-6, 32.0 | 841.72 | | 2.145 |
| 64R-1, 108.0 | 844.58 | | 2.228 |
| 64R-4, 43.0 | 848.43 | | 2.147 |
| 65R-1, 42.0 | 853.52 | | 2.079 |
| 65R-4, 38.0 | 857.98 | | 2.170 |
| 66R-1, 97.0 | 863.67 | | 2.461 |
| 66R-4, 74.0 | 867.94 | | 2.309 |
| 66R-6, 7.0 | 870.27 | | 2.334 |
| 67R-1, 40.0 | 872.70 | | 2.171 |
| 67R-4, 42.0 | 877.22 | | 2.301 |
| 68R-1, 145.0 | 883.15 | | 5.241 |
| 69R-1, 38.0 | 891.68 | | 2.420 |
| 69R-3, 122.0 | 895.52 | | 2.444 |
| 71R-2, 45.0 | 912.45 | | 2.238 |
| 71R-3, 122.0 | 914.72 | | 2.268 |
| 71R-5, 130.0 | 917.80 | | 2.249 |
| 72R-1, 43.0 | 920.63 | | 2.360 |
| 72R-3, 63.0 | 923.83 | | 2.237 |
| 72R-5, 116.0 | 927.36 | | 2.310 |
| 72R-6, 17.0 | 927.87 | | 2.316 |
| 73R-1, 120.0 | 931.10 | | 2.402 |
| 73R-2, 126.0 | 932.66 | | 2.286 |
| 73R-5, 126.0 | 937.16 | | 2.421 |
| 75R-2, 67.0 | 951.37 | | 4.035 |
| 75R-2, 118.0 | 951.88 | | 2.433 |
| 75R-4, 60.0 | 954.30 | | 2.417 |

Notes: All *P*-wave velocities measured at discrete intervals. PSW1 = measured along the core, PSW3 = measured across the core (Hamilton frame). Blank = no data.

**Table T22.** Thermal conductivity measured on whole-core sections, Hole 1171A.

| Core, section, interval (cm) | Depth (mbsf) | Thermal conductivity (W/[m·K]) |
|---|---|---|
| 189-1171A- | | |
| 1H-3, 75 | 3.75 | 1.056 |
| 2H-3, 75 | 10.85 | 1.034 |
| 3H-3, 75 | 20.35 | 1.103 |
| 4H-3, 75 | 29.85 | 1.002 |
| 5H-3, 75 | 39.35 | 1.105 |
| 6H-3, 75 | 48.85 | 1.201 |
| 7H-3, 75 | 58.35 | 1.181 |
| 8H-3, 75 | 66.49 | 1.170 |
| 9H-3, 70 | 77.30 | 1.133 |
| 10H-3, 75 | 86.85 | 1.125 |
| 11H-3, 75 | 96.35 | 1.118 |
| 12H-3, 75 | 105.85 | 1.118 |

**Table T23.** Undrained shear strength from miniature vane-shear measurements, Hole 1171A.

| Core, section, interval (cm) | Depth (mbsf) | Undrained shear strength (kPa) | Core, section, interval (cm) | Depth (mbsf) | Undrained shear strength (kPa) |
|---|---|---|---|---|---|
| 189-1171A- | | | 7H-5, 99.3 | 61.59 | 18.074 |
| 1H-1, 122.4 | 1.22 | 6.099 | 7H-6, 99.9 | 63.10 | 13.972 |
| 1H-3, 116.2 | 4.16 | 11.310 | 8H-1, 87.4 | 64.97 | 12.419 |
| 1H-4, 93.7 | 5.44 | 23.064 | 8H-3, 86.8 | 66.61 | 20.292 |
| 1H-5, 80.8 | 6.81 | 11.310 | 8H-4, 99.2 | 68.23 | 11.754 |
| 2H-3, 85.2 | 10.95 | 8.871 | 8H-5, 98.9 | 69.73 | 8.316 |
| 2H-4, 103.6 | 12.64 | 17.631 | 8H-6, 98.9 | 71.23 | 16.744 |
| 2H-5, 117.5 | 14.27 | 15.191 | 8H-7, 88.2 | 72.62 | 20.625 |
| 2H-6, 78.4 | 15.38 | 13.639 | 9H-2, 99.0 | 76.09 | 22.953 |
| 3H-1, 103.9 | 17.64 | 4.657 | 9H-3, 99.2 | 77.59 | 3.437 |
| 3H-2, 95.7 | 19.06 | 17.742 | 9H-4, 99.4 | 79.09 | 5.101 |
| 3H-3, 91.5 | 20.51 | 10.534 | 9H-5, 99.2 | 80.59 | 7.651 |
| 3H-4, 121.5 | 22.32 | 4.435 | 9H-6, 99.0 | 82.09 | 35.040 |
| 3H-5, 96.0 | 23.56 | 17.076 | 10H-1, 100.1 | 84.10 | 11.532 |
| 4H-1, 129.3 | 28.57 | 24.506 | 10H-2, 99.8 | 85.60 | 5.433 |
| 4H-2, 86.1 | 29.64 | 2.883 | 10H-3, 98.4 | 87.08 | 2.329 |
| 4H-3, 99.3 | 30.09 | 20.957 | 10H-4, 100.3 | 88.60 | 3.327 |
| 4H-4, 99.6 | 31.60 | 20.847 | 10H-5, 98.8 | 90.09 | 11.532 |
| 4H-5, 99.8 | 33.10 | 22.510 | 10H-6, 100.0 | 91.60 | 8.871 |
| 4H-6, 100.3 | 34.60 | 11.199 | 11H-1, 99.9 | 93.60 | 10.645 |
| 5H-1, 99.8 | 36.60 | 9.203 | 11H-2, 98.7 | 95.09 | 8.316 |
| 5H-2, 100.0 | 38.10 | 9.536 | 11H-3, 98.9 | 96.59 | 7.651 |
| 5H-3, 99.0 | 39.59 | 8.871 | 11H-4, 101.2 | 98.11 | 4.103 |
| 5H-4, 98.9 | 41.09 | 12.863 | 11H-5, 100.9 | 99.61 | 9.647 |
| 5H-5, 99.8 | 42.60 | 8.649 | 11H-6, 100.6 | 101.11 | 5.877 |
| 5H-6, 100.4 | 44.10 | 22.621 | 11H-7, 62.2 | 102.22 | 9.314 |
| 6H-1, 99.0 | 46.09 | 16.300 | 12H-1, 101.4 | 103.11 | 9.758 |
| 6H-2, 98.7 | 47.59 | 7.097 | 12H-2, 100.6 | 104.61 | 8.982 |
| 6H-3, 98.9 | 49.09 | 6.099 | 12H-3, 100.7 | 106.11 | 4.325 |
| 6H-4, 99.2 | 50.59 | 8.871 | 12H-4, 90.9 | 107.51 | 10.201 |
| 6H-5, 100.0 | 52.10 | 12.197 | 12H-5, 104.4 | 109.14 | 10.201 |
| 6H-6, 99.3 | 53.59 | 17.409 | 12H-6, 68.5 | 110.29 | 9.425 |
| 7H-1, 99.6 | 55.60 | 15.746 | 14X-1, 100.9 | 115.81 | 1.552 |
| 7H-2, 99.5 | 57.10 | 7.429 | 14X-2, 101.1 | 117.31 | 2.994 |
| 7H-3, 99.5 | 58.60 | 16.965 | 14X-3, 100.4 | 118.80 | 5.655 |
| 7H-4, 98.4 | 60.08 | 16.411 | 14X-4, 98.8 | 120.29 | 8.871 |

**Table T24.** Index properties measured at discrete intervals, Site 1171. (Continued on next four pages.)

| Core, section, interval (cm) | Depth (mbsf) | Water content (wt%) | | Density (g/cm$^3$) | | | Porosity (%) | Void ratio |
|---|---|---|---|---|---|---|---|---|
| | | Bulk | Dry | Bulk | Dry | Grain | | |
| 189-1171A- | | | | | | | | |
| 1H-1, 70.0-72.0 | 0.70 | 42.3 | 73.4 | 1.600 | 0.922 | 2.724 | 66.1 | 1.953 |
| 1H-2, 70.0-72.0 | 2.20 | 45.4 | 83.2 | 1.549 | 0.846 | 2.705 | 68.7 | 2.199 |
| 1H-3, 70.0-72.0 | 3.70 | 38.6 | 62.8 | 1.663 | 1.021 | 2.737 | 62.7 | 1.680 |
| 1H-4, 70.0-72.0 | 5.20 | 39.9 | 66.4 | 1.632 | 0.981 | 2.693 | 63.6 | 1.745 |
| 1H-5, 70.0-72.0 | 6.70 | 38.1 | 61.6 | 1.664 | 1.029 | 2.705 | 62.0 | 1.628 |
| 2H-1, 70.0-72.0 | 7.80 | 39.5 | 65.4 | 1.639 | 0.991 | 2.700 | 63.3 | 1.723 |
| 2H-3, 70.0-72.0 | 10.80 | 41.5 | 70.9 | 1.605 | 0.939 | 2.685 | 65.0 | 1.860 |
| 2H-4, 61.0-63.0 | 12.21 | 37.6 | 60.1 | 1.676 | 1.047 | 2.717 | 61.5 | 1.596 |
| 2H-5, 70.0-72.0 | 13.80 | 47.1 | 89.0 | 1.527 | 0.808 | 2.716 | 70.2 | 2.361 |
| 2H-6, 70.0-72.0 | 15.30 | 40.3 | 67.5 | 1.624 | 0.970 | 2.686 | 63.9 | 1.769 |
| 3H-1, 70.0-72.0 | 17.30 | 42.1 | 72.7 | 1.593 | 0.922 | 2.675 | 65.5 | 1.900 |
| 3H-2, 70.0-72.0 | 18.80 | 42.8 | 74.8 | 1.582 | 0.905 | 2.671 | 66.1 | 1.951 |
| 3H-3, 70.0-72.0 | 20.30 | 44.2 | 79.1 | 1.571 | 0.877 | 2.719 | 67.7 | 2.100 |
| 3H-4, 70.0-72.0 | 21.80 | 42.4 | 73.6 | 1.601 | 0.922 | 2.734 | 66.3 | 1.965 |
| 3H-5, 70.0-72.0 | 23.30 | 46.6 | 87.3 | 1.528 | 0.816 | 2.677 | 69.5 | 2.282 |
| 4H-1, 70.0-72.0 | 26.80 | 46.5 | 87.0 | 1.525 | 0.815 | 2.652 | 69.3 | 2.253 |
| 4H-2, 70.0-72.0 | 28.30 | 46.5 | 86.8 | 1.539 | 0.824 | 2.730 | 69.8 | 2.313 |
| 4H-3, 70.0-72.0 | 29.80 | 43.9 | 78.3 | 1.573 | 0.882 | 2.709 | 67.4 | 2.071 |
| 4H-4, 70.0-72.0 | 31.30 | 43.6 | 77.2 | 1.576 | 0.889 | 2.697 | 67.0 | 2.033 |
| 4H-5, 70.0-72.0 | 32.80 | 42.4 | 73.6 | 1.603 | 0.923 | 2.744 | 66.4 | 1.974 |
| 4H-6, 70.0-72.0 | 34.30 | 40.9 | 69.2 | 1.612 | 0.953 | 2.676 | 64.4 | 1.810 |
| 5H-1, 70.0-72.0 | 36.30 | 35.2 | 54.3 | 1.699 | 1.101 | 2.647 | 58.4 | 1.403 |
| 5H-2, 70.0-72.0 | 37.80 | 37.7 | 60.6 | 1.662 | 1.035 | 2.671 | 61.2 | 1.580 |
| 5H-3, 70.0-72.0 | 39.30 | 30.9 | 44.6 | 1.792 | 1.239 | 2.693 | 54.0 | 1.174 |
| 5H-4, 70.0-72.0 | 40.80 | 36.6 | 57.7 | 1.695 | 1.075 | 2.724 | 60.5 | 1.534 |
| 5H-5, 70.0-72.0 | 42.30 | 29.8 | 42.5 | 1.821 | 1.277 | 2.721 | 53.1 | 1.131 |
| 5H-6, 70.0-72.0 | 43.80 | 30.6 | 44.1 | 1.801 | 1.250 | 2.706 | 53.8 | 1.165 |
| 6H-1, 70.0-72.0 | 45.80 | 33.0 | 49.2 | 1.760 | 1.180 | 2.724 | 56.7 | 1.309 |
| 6H-2, 70.0-72.0 | 47.30 | 38.2 | 61.9 | 1.661 | 1.025 | 2.701 | 62.0 | 1.634 |
| 6H-3, 70.0-72.0 | 48.80 | 34.5 | 52.6 | 1.734 | 1.136 | 2.731 | 58.4 | 1.404 |
| 6H-4, 70.0-72.0 | 50.30 | 33.9 | 51.2 | 1.733 | 1.146 | 2.684 | 57.3 | 1.342 |
| 6H-5, 70.0-72.0 | 51.80 | 32.3 | 47.7 | 1.760 | 1.192 | 2.676 | 55.5 | 1.246 |
| 6H-6, 70.0-72.0 | 53.30 | 35.1 | 54.0 | 1.715 | 1.113 | 2.701 | 58.8 | 1.425 |
| 7H-1, 70.0-72.0 | 55.30 | 35.4 | 54.8 | 1.712 | 1.106 | 2.708 | 59.2 | 1.448 |
| 7H-2, 70.0-72.0 | 56.80 | 35.0 | 53.9 | 1.721 | 1.118 | 2.718 | 58.9 | 1.431 |
| 7H-3, 70.0-72.0 | 58.30 | 30.6 | 44.1 | 1.796 | 1.247 | 2.691 | 53.7 | 1.158 |
| 7H-4, 70.0-72.0 | 59.80 | 33.1 | 49.5 | 1.749 | 1.170 | 2.692 | 56.6 | 1.302 |
| 7H-5, 70.0-72.0 | 61.30 | 35.6 | 55.2 | 1.703 | 1.097 | 2.686 | 59.1 | 1.448 |
| 7H-6, 70.0-72.0 | 62.80 | 34.9 | 53.6 | 1.710 | 1.113 | 2.666 | 58.2 | 1.394 |
| 8H-1, 70.0-72.0 | 64.80 | 35.3 | 54.6 | 1.700 | 1.100 | 2.659 | 58.6 | 1.418 |
| 8H-3, 70.0-72.0 | 66.44 | 37.0 | 58.6 | 1.684 | 1.062 | 2.708 | 60.8 | 1.550 |
| 8H-4, 70.0-72.0 | 67.94 | 38.3 | 62.1 | 1.663 | 1.026 | 2.715 | 62.2 | 1.646 |
| 8H-5, 70.0-72.0 | 69.44 | 36.7 | 57.9 | 1.695 | 1.074 | 2.732 | 60.7 | 1.545 |
| 8H-6, 70.0-72.0 | 70.94 | 33.7 | 50.8 | 1.748 | 1.160 | 2.727 | 57.5 | 1.351 |
| 9H-1, 70.0-72.0 | 74.30 | 46.0 | 85.2 | 1.537 | 0.830 | 2.680 | 69.0 | 2.230 |
| 9H-3, 70.0-72.0 | 77.30 | 35.6 | 55.3 | 1.697 | 1.092 | 2.666 | 59.0 | 1.441 |
| 9H-5, 70.0-72.0 | 80.30 | 34.7 | 53.2 | 1.728 | 1.128 | 2.727 | 58.6 | 1.418 |
| 10H-1, 70.0-72.0 | 83.80 | 38.9 | 63.8 | 1.644 | 1.004 | 2.678 | 62.5 | 1.668 |
| 10H-3, 70.0-72.0 | 86.80 | 33.6 | 50.7 | 1.762 | 1.169 | 2.778 | 57.9 | 1.375 |
| 10H-5, 70.0-72.0 | 89.80 | 36.9 | 58.5 | 1.688 | 1.065 | 2.719 | 60.8 | 1.554 |
| 11H-1, 70.0-72.0 | 93.30 | 36.0 | 56.3 | 1.702 | 1.089 | 2.714 | 59.9 | 1.492 |
| 11H-3, 70.0-72.0 | 96.30 | 39.2 | 64.5 | 1.637 | 0.995 | 2.666 | 62.7 | 1.679 |
| 11H-5, 70.0-72.0 | 99.30 | 35.3 | 54.6 | 1.706 | 1.104 | 2.679 | 58.8 | 1.427 |
| 12H-1, 70.0-72.0 | 102.80 | 34.4 | 52.5 | 1.734 | 1.137 | 2.728 | 58.3 | 1.399 |
| 12H-3, 70.0-72.0 | 105.80 | 37.3 | 59.6 | 1.672 | 1.048 | 2.685 | 61.0 | 1.563 |
| 12H-5, 70.0-72.0 | 108.80 | 35.4 | 54.7 | 1.706 | 1.103 | 2.684 | 58.9 | 1.434 |
| 13X-1, 70.0-72.0 | 112.30 | 39.3 | 64.8 | 1.643 | 0.997 | 2.699 | 63.1 | 1.707 |
| 14X-1, 70.0-72.0 | 115.50 | 34.9 | 53.6 | 1.720 | 1.120 | 2.706 | 58.6 | 1.415 |
| 14X-3, 70.0-72.0 | 118.50 | 43.3 | 76.4 | 1.578 | 0.895 | 2.692 | 66.8 | 2.009 |
| 189-1171C- | | | | | | | | |
| 13X-1, 70.0-72.0 | 110.90 | 38.3 | 62.0 | 1.657 | 1.023 | 2.689 | 62.0 | 1.629 |
| 13X-3, 70.0-72.0 | 113.90 | 36.0 | 56.3 | 1.695 | 1.084 | 2.689 | 59.7 | 1.479 |
| 14X-1, 70.0-72.0 | 115.90 | 34.6 | 53.0 | 1.743 | 1.139 | 2.776 | 59.0 | 1.436 |
| 14X-3, 70.0-72.0 | 118.90 | 37.4 | 59.7 | 1.682 | 1.053 | 2.731 | 61.4 | 1.593 |
| 14X-5, 70.0-72.0 | 121.90 | 42.5 | 74.1 | 1.585 | 0.911 | 2.668 | 65.9 | 1.930 |

**Table T24 (continued).**

| Core, section, interval (cm) | Depth (mbsf) | Water content (wt%) | | Density (g/cm$^3$) | | | Porosity (%) | Void ratio |
|---|---|---|---|---|---|---|---|---|
| | | Bulk | Dry | Bulk | Dry | Grain | | |
| 15X-1, 70.0-72.0 | 125.50 | 37.9 | 61.1 | 1.674 | 1.039 | 2.733 | 62.0 | 1.631 |
| 15X-3, 70.0-72.0 | 128.50 | 36.7 | 58.0 | 1.688 | 1.068 | 2.704 | 60.5 | 1.531 |
| 15X-5, 70.0-72.0 | 131.50 | 40.6 | 68.4 | 1.620 | 0.962 | 2.690 | 64.2 | 1.796 |
| 16X-1, 70.0-72.0 | 135.20 | 42.6 | 74.3 | 1.590 | 0.912 | 2.697 | 66.2 | 1.957 |
| 16X-3, 70.0-72.0 | 138.20 | 39.0 | 64.0 | 1.643 | 1.002 | 2.679 | 62.6 | 1.674 |
| 17X-1, 70.0-72.0 | 144.80 | 38.7 | 63.1 | 1.658 | 1.017 | 2.722 | 62.7 | 1.678 |
| 17X-3, 70.0-72.0 | 147.80 | 37.2 | 59.3 | 1.690 | 1.061 | 2.753 | 61.5 | 1.595 |
| 18X-1, 70.0-72.0 | 154.40 | 38.4 | 62.3 | 1.654 | 1.019 | 2.682 | 62.0 | 1.632 |
| 18X-3, 70.0-72.0 | 157.40 | 41.4 | 70.7 | 1.624 | 0.952 | 2.773 | 65.7 | 1.913 |
| 18X-5, 70.0-72.0 | 160.40 | 42.2 | 72.9 | 1.600 | 0.925 | 2.715 | 65.9 | 1.934 |
| 18X-7, 40.0-42.0 | 162.60 | 37.8 | 60.7 | 1.670 | 1.039 | 2.705 | 61.6 | 1.604 |
| 19X-1, 70.0-72.0 | 164.00 | 38.2 | 61.8 | 1.657 | 1.024 | 2.682 | 61.8 | 1.619 |
| 19X-3, 70.0-72.0 | 167.00 | 39.7 | 65.9 | 1.647 | 0.993 | 2.750 | 63.9 | 1.769 |
| 19X-5, 70.0-72.0 | 170.00 | 36.3 | 56.9 | 1.699 | 1.083 | 2.720 | 60.2 | 1.512 |
| 20X-1, 70.0-72.0 | 173.60 | 38.2 | 61.8 | 1.666 | 1.030 | 2.720 | 62.2 | 1.642 |
| 20X-3, 70.0-72.0 | 176.60 | 40.2 | 67.2 | 1.629 | 0.974 | 2.701 | 63.9 | 1.773 |
| 20X-5, 70.0-72.0 | 179.60 | 38.9 | 63.7 | 1.641 | 1.003 | 2.663 | 62.4 | 1.656 |
| 21X-1, 70.0-72.0 | 182.90 | 36.2 | 56.7 | 1.694 | 1.081 | 2.693 | 59.9 | 1.491 |
| 21X-3, 70.0-72.0 | 185.90 | 38.1 | 61.4 | 1.670 | 1.034 | 2.726 | 62.1 | 1.635 |
| 21X-5, 70.0-72.0 | 188.90 | 38.7 | 63.2 | 1.651 | 1.012 | 2.691 | 62.4 | 1.660 |
| 22X-1, 70.0-72.0 | 192.50 | 37.7 | 60.5 | 1.669 | 1.040 | 2.696 | 61.4 | 1.592 |
| 22X-3, 70.0-72.0 | 195.50 | 45.0 | 81.9 | 1.569 | 0.863 | 2.782 | 69.0 | 2.226 |
| 22X-5, 70.0-72.0 | 198.50 | 34.7 | 53.0 | 1.726 | 1.128 | 2.711 | 58.4 | 1.404 |
| 23X-1, 73.0-75.0 | 202.23 | 38.9 | 63.7 | 1.664 | 1.016 | 2.764 | 63.2 | 1.720 |
| 23X-3, 70.0-72.0 | 205.20 | 38.2 | 61.9 | 1.669 | 1.031 | 2.737 | 62.3 | 1.655 |
| 23X-5, 70.0-72.0 | 208.20 | 40.9 | 69.3 | 1.615 | 0.954 | 2.688 | 64.5 | 1.818 |
| 24X-1, 70.0-72.0 | 211.80 | 37.4 | 59.9 | 1.678 | 1.050 | 2.718 | 61.4 | 1.589 |
| 24X-3, 70.0-72.0 | 214.80 | 36.6 | 57.8 | 1.694 | 1.073 | 2.726 | 60.6 | 1.540 |
| 24X-5, 70.0-72.0 | 217.80 | 39.9 | 66.5 | 1.642 | 0.986 | 2.745 | 64.1 | 1.783 |
| 25X-1, 70.0-72.0 | 221.40 | 35.7 | 55.6 | 1.712 | 1.100 | 2.731 | 59.7 | 1.482 |
| 25X-3, 70.0-72.0 | 224.40 | 37.5 | 59.9 | 1.673 | 1.047 | 2.698 | 61.2 | 1.577 |
| 25X-5, 70.0-72.0 | 227.40 | 36.7 | 58.0 | 1.688 | 1.069 | 2.704 | 60.5 | 1.530 |
| 26X-1, 89.0-91.0 | 231.19 | 34.9 | 53.5 | 1.716 | 1.118 | 2.688 | 58.4 | 1.404 |
| 26X-3, 71.0-73.0 | 234.01 | 35.5 | 55.0 | 1.709 | 1.103 | 2.703 | 59.2 | 1.451 |
| 26X-5, 67.0-69.0 | 236.97 | 36.6 | 57.8 | 1.696 | 1.075 | 2.732 | 60.7 | 1.543 |
| 27X-1, 75.0-77.0 | 240.35 | 34.3 | 52.1 | 1.720 | 1.131 | 2.664 | 57.6 | 1.356 |
| 27X-3, 68.0-70.0 | 243.28 | 34.3 | 52.2 | 1.733 | 1.138 | 2.715 | 58.1 | 1.385 |
| 27X-5, 74.0-76.0 | 246.34 | 35.8 | 55.7 | 1.708 | 1.097 | 2.720 | 59.7 | 1.480 |
| 28X-1, 69.0-71.0 | 249.59 | 34.4 | 52.4 | 1.722 | 1.130 | 2.680 | 57.8 | 1.372 |
| 28X-3, 70.0-72.0 | 252.60 | 43.4 | 76.6 | 1.565 | 0.886 | 2.628 | 66.3 | 1.966 |
| 29X-1, 70.0-72.0 | 259.20 | 38.6 | 62.8 | 1.649 | 1.013 | 2.675 | 62.1 | 1.640 |
| 29X-3, 70.0-72.0 | 262.20 | 40.8 | 68.9 | 1.609 | 0.953 | 2.651 | 64.1 | 1.782 |
| 30X-1, 73.0-75.0 | 268.83 | 36.8 | 58.2 | 1.669 | 1.055 | 2.636 | 60.0 | 1.498 |
| 30X-3, 73.0-75.0 | 271.83 | 38.0 | 61.2 | 1.655 | 1.027 | 2.658 | 61.4 | 1.588 |
| 189-1171D- | | | | | | | | |
| 3R-1, 70.0-72.0 | 267.30 | 38.4 | 62.3 | 1.632 | 1.006 | 2.590 | 61.2 | 1.576 |
| 3R-3, 70.0-72.0 | 270.30 | 37.0 | 58.8 | 1.701 | 1.071 | 2.783 | 61.5 | 1.598 |
| 4R-1, 70.0-72.0 | 276.90 | 55.6 | 125.5 | 1.376 | 0.610 | 2.422 | 74.8 | 2.967 |
| 4R-3, 70.0-72.0 | 279.90 | 56.9 | 131.9 | 1.375 | 0.593 | 2.513 | 76.4 | 3.236 |
| 5R-1, 49.0-51.0 | 286.29 | 54.1 | 117.7 | 1.399 | 0.643 | 2.460 | 73.9 | 2.828 |
| 6R-1, 51.0-53.0 | 294.31 | 11.7 | 13.3 | 2.154 | 1.902 | 2.524 | 24.6 | 0.327 |
| 7R-1, 65.0-67.0 | 301.05 | 58.5 | 140.9 | 1.334 | 0.554 | 2.324 | 76.2 | 3.198 |
| 8R-1, 70.0-72.0 | 306.10 | 59.3 | 145.8 | 1.339 | 0.545 | 2.431 | 77.6 | 3.462 |
| 9R-1, 70.0-72.0 | 315.40 | 51.4 | 105.9 | 1.422 | 0.691 | 2.415 | 71.4 | 2.497 |
| 9R-3, 70.0-72.0 | 318.40 | 38.0 | 61.3 | 1.647 | 1.021 | 2.628 | 61.1 | 1.573 |
| 10R-1, 75.0-77.0 | 325.05 | 55.1 | 122.5 | 1.351 | 0.607 | 2.221 | 72.7 | 2.656 |
| 10R-3, 70.0-72.0 | 328.00 | 57.6 | 135.7 | 1.340 | 0.568 | 2.302 | 75.3 | 3.050 |
| 15R-1, 73.0-75.0 | 373.13 | 31.8 | 46.7 | 1.709 | 1.165 | 2.487 | 53.2 | 1.135 |
| 16R-1, 70.0-72.0 | 382.70 | 33.7 | 50.9 | 1.696 | 1.124 | 2.547 | 55.8 | 1.265 |
| 17R-1, 76.0-78.0 | 392.36 | 35.7 | 55.5 | 1.645 | 1.058 | 2.482 | 57.4 | 1.346 |
| 17R-3, 70.0-72.0 | 395.30 | 30.6 | 44.1 | 1.743 | 1.209 | 2.526 | 52.1 | 1.089 |
| 19R-1, 89.0-91.0 | 411.69 | 30.6 | 44.1 | 1.744 | 1.210 | 2.529 | 52.1 | 1.090 |
| 19R-3, 70.0-72.0 | 414.50 | 30.4 | 43.7 | 1.743 | 1.213 | 2.514 | 51.7 | 1.072 |
| 19R-5, 70.0-72.0 | 417.50 | 13.7 | 15.9 | 2.158 | 1.862 | 2.621 | 28.9 | 0.407 |
| 20R-1, 70.0-72.0 | 421.10 | 26.3 | 35.7 | 1.829 | 1.348 | 2.544 | 47.0 | 0.888 |
| 20R-3, 70.0-72.0 | 424.10 | 27.7 | 38.4 | 1.829 | 1.322 | 2.620 | 49.6 | 0.982 |
| 20R-5, 69.0-71.0 | 427.09 | 27.9 | 38.6 | 1.845 | 1.331 | 2.673 | 50.2 | 1.008 |
| 22R-1, 70.0-72.0 | 440.30 | 32.9 | 49.1 | 1.700 | 1.140 | 2.516 | 54.7 | 1.207 |

**Table T24 (continued).**

| Core, section, interval (cm) | Depth (mbsf) | Water content (wt%) | | Density (g/cm³) | | | Porosity (%) | Void ratio |
|---|---|---|---|---|---|---|---|---|
| | | Bulk | Dry | Bulk | Dry | Grain | | |
| 22R-3, 70.0-72.0 | 443.30 | 32.3 | 47.6 | 1.714 | 1.161 | 2.523 | 54.0 | 1.174 |
| 22R-5, 70.0-72.0 | 446.30 | 35.5 | 54.9 | 1.651 | 1.066 | 2.487 | 57.2 | 1.334 |
| 23R-1, 67.0-69.0 | 449.87 | 32.3 | 47.6 | 1.690 | 1.145 | 2.449 | 53.2 | 1.139 |
| 23R-3, 70.0-72.0 | 452.90 | 31.8 | 46.7 | 1.736 | 1.184 | 2.572 | 54.0 | 1.173 |
| 24R-1, 72.0-74.0 | 459.52 | 35.4 | 54.7 | 1.658 | 1.072 | 2.508 | 57.3 | 1.340 |
| 24R-3, 66.0-68.0 | 462.46 | 33.9 | 51.3 | 1.684 | 1.113 | 2.517 | 55.8 | 1.260 |
| 25R-1, 68.0-70.0 | 469.18 | 30.4 | 43.6 | 1.757 | 1.224 | 2.556 | 52.1 | 1.089 |
| 25R-3, 70.0-72.0 | 472.20 | 29.8 | 42.3 | 1.774 | 1.247 | 2.573 | 51.6 | 1.064 |
| 25R-5, 70.0-72.0 | 475.20 | 30.4 | 43.7 | 1.745 | 1.214 | 2.520 | 51.8 | 1.076 |
| 26R-1, 70.0-72.0 | 478.80 | 30.0 | 42.9 | 1.755 | 1.229 | 2.531 | 51.5 | 1.060 |
| 26R-3, 70.0-72.0 | 481.80 | 31.2 | 45.4 | 1.728 | 1.188 | 2.511 | 52.7 | 1.114 |
| 26R-5, 70.0-72.0 | 484.80 | 35.4 | 54.9 | 1.663 | 1.074 | 2.530 | 57.6 | 1.356 |
| 27R-1, 77.0-79.0 | 488.47 | 32.5 | 48.1 | 1.733 | 1.170 | 2.598 | 55.0 | 1.221 |
| 27R-3, 70.0-72.0 | 491.40 | 27.8 | 38.6 | 1.805 | 1.302 | 2.557 | 49.1 | 0.963 |
| 27R-5, 70.0-72.0 | 494.40 | 28.1 | 39.0 | 1.771 | 1.274 | 2.475 | 48.5 | 0.943 |
| 28R-1, 70.0-72.0 | 498.00 | 38.6 | 63.0 | 1.609 | 0.987 | 2.515 | 60.7 | 1.547 |
| 28R-3, 70.0-72.0 | 501.00 | 31.7 | 46.4 | 1.725 | 1.179 | 2.527 | 53.4 | 1.144 |
| 28R-4, 70.0-72.0 | 502.50 | 32.3 | 47.6 | 1.704 | 1.154 | 2.493 | 53.7 | 1.160 |
| 28R-5, 70.0-72.0 | 504.00 | 35.6 | 55.3 | 1.663 | 1.071 | 2.539 | 57.8 | 1.371 |
| 29R-1, 70.0-72.0 | 507.70 | 34.7 | 53.1 | 1.635 | 1.068 | 2.393 | 55.4 | 1.241 |
| 29R-3, 70.0-72.0 | 510.70 | 33.3 | 49.9 | 1.675 | 1.118 | 2.453 | 54.4 | 1.194 |
| 29R-5, 70.0-72.0 | 513.70 | 32.0 | 47.1 | 1.716 | 1.167 | 2.515 | 53.6 | 1.155 |
| 30R-1, 70.0-72.0 | 517.30 | 31.5 | 46.1 | 1.716 | 1.174 | 2.491 | 52.9 | 1.121 |
| 30R-3, 70.0-72.0 | 520.11 | 30.4 | 43.6 | 1.783 | 1.241 | 2.635 | 52.9 | 1.123 |
| 30R-5, 70.0-72.0 | 523.11 | 28.4 | 39.6 | 1.808 | 1.295 | 2.594 | 50.1 | 1.004 |
| 31R-1, 70.0-72.0 | 526.90 | 31.1 | 45.1 | 1.765 | 1.216 | 2.623 | 53.6 | 1.156 |
| 31R-2, 70.0-72.0 | 528.40 | 24.0 | 31.6 | 1.935 | 1.470 | 2.690 | 45.3 | 0.829 |
| 31R-4, 70.0-72.0 | 531.40 | 22.3 | 28.6 | 1.954 | 1.519 | 2.641 | 42.5 | 0.739 |
| 32R-1, 70.0-72.0 | 536.50 | 24.3 | 32.1 | 1.916 | 1.450 | 2.660 | 45.5 | 0.834 |
| 32R-4, 70.0-72.0 | 541.00 | 26.1 | 35.3 | 1.907 | 1.410 | 2.740 | 48.5 | 0.943 |
| 32R-5, 70.0-72.0 | 542.50 | 22.7 | 29.4 | 1.945 | 1.503 | 2.646 | 43.2 | 0.761 |
| 33R-1, 70.0-72.0 | 546.20 | 24.6 | 32.7 | 1.931 | 1.456 | 2.718 | 46.4 | 0.867 |
| 33R-3, 70.0-72.0 | 549.20 | 21.4 | 27.2 | 2.021 | 1.589 | 2.748 | 42.2 | 0.730 |
| 33R-5, 70.0-72.0 | 552.20 | 24.0 | 31.6 | 1.936 | 1.471 | 2.694 | 45.4 | 0.831 |
| 34R-1, 70.0-72.0 | 555.80 | 22.1 | 28.4 | 1.961 | 1.527 | 2.648 | 42.3 | 0.734 |
| 34R-3, 70.0-72.0 | 558.80 | 26.5 | 36.0 | 1.894 | 1.392 | 2.728 | 49.0 | 0.959 |
| 34R-5, 70.0-72.0 | 561.80 | 21.2 | 26.9 | 2.018 | 1.590 | 2.732 | 41.8 | 0.719 |
| 35R-1, 70.0-72.0 | 565.40 | 24.3 | 32.1 | 1.924 | 1.456 | 2.682 | 45.7 | 0.842 |
| 35R-3, 70.0-72.0 | 568.40 | 22.3 | 28.7 | 1.977 | 1.537 | 2.698 | 43.0 | 0.755 |
| 35R-5, 70.0-72.0 | 571.40 | 21.8 | 27.9 | 1.999 | 1.563 | 2.720 | 42.5 | 0.740 |
| 36R-1, 70.0-72.0 | 575.00 | 22.5 | 29.0 | 1.944 | 1.506 | 2.629 | 42.7 | 0.746 |
| 36R-3, 70.0-72.0 | 578.00 | 22.0 | 28.3 | 1.975 | 1.540 | 2.679 | 42.5 | 0.739 |
| 36R-5, 70.0-72.0 | 581.00 | 24.3 | 32.0 | 1.930 | 1.462 | 2.693 | 45.7 | 0.842 |
| 37R-1, 70.0-72.0 | 584.60 | 24.9 | 33.2 | 1.911 | 1.435 | 2.681 | 46.5 | 0.869 |
| 37R-3, 70.0-72.0 | 587.60 | 23.2 | 30.2 | 1.950 | 1.497 | 2.684 | 44.2 | 0.793 |
| 37R-5, 70.0-72.0 | 590.60 | 23.2 | 30.2 | 1.949 | 1.497 | 2.681 | 44.1 | 0.790 |
| 38R-1, 70.0-72.0 | 594.30 | 25.4 | 34.0 | 1.920 | 1.432 | 2.735 | 47.6 | 0.910 |
| 38R-3, 70.0-72.0 | 597.30 | 23.1 | 30.0 | 1.964 | 1.511 | 2.711 | 44.3 | 0.794 |
| 38R-5, 70.0-72.0 | 600.30 | 24.7 | 32.7 | 1.930 | 1.454 | 2.716 | 46.5 | 0.868 |
| 39R-1, 70.0-72.0 | 603.90 | 25.3 | 33.8 | 1.903 | 1.422 | 2.682 | 47.0 | 0.886 |
| 39R-3, 72.0-74.0 | 606.92 | 23.3 | 30.4 | 1.972 | 1.512 | 2.745 | 44.9 | 0.816 |
| 39R-5, 69.0-71.0 | 609.89 | 21.9 | 28.0 | 2.006 | 1.567 | 2.742 | 42.8 | 0.750 |
| 40R-1, 70.0-72.0 | 613.50 | 23.8 | 31.2 | 1.926 | 1.468 | 2.657 | 44.8 | 0.810 |
| 40R-3, 70.0-72.0 | 616.50 | 28.0 | 39.0 | 1.851 | 1.332 | 2.701 | 50.7 | 1.027 |
| 40R-4, 23.0-25.0 | 617.53 | 23.3 | 30.3 | 1.963 | 1.506 | 2.719 | 44.6 | 0.805 |
| 40R-5, 70.0-72.0 | 619.50 | 23.1 | 30.1 | 1.935 | 1.488 | 2.642 | 43.7 | 0.776 |
| 41R-1, 70.0-72.0 | 623.10 | 22.3 | 28.6 | 1.988 | 1.545 | 2.721 | 43.2 | 0.761 |
| 41R-3, 70.0-72.0 | 626.10 | 22.8 | 29.5 | 1.972 | 1.522 | 2.714 | 43.9 | 0.783 |
| 41R-5, 70.0-72.0 | 629.10 | 24.0 | 31.6 | 1.978 | 1.503 | 2.802 | 46.3 | 0.864 |
| 42R-1, 70.0-72.0 | 632.70 | 25.4 | 34.0 | 1.917 | 1.431 | 2.726 | 47.5 | 0.905 |
| 42R-3, 70.0-72.0 | 635.70 | 24.8 | 33.0 | 1.940 | 1.459 | 2.752 | 47.0 | 0.886 |
| 42R-5, 70.0-72.0 | 638.70 | 24.7 | 32.8 | 1.946 | 1.466 | 2.760 | 46.9 | 0.883 |
| 43R-1, 70.0-72.0 | 642.30 | 24.9 | 33.1 | 1.939 | 1.457 | 2.754 | 47.1 | 0.890 |
| 43R-3, 70.0-72.0 | 645.30 | 24.4 | 32.3 | 1.953 | 1.476 | 2.760 | 46.5 | 0.869 |
| 43R-5, 70.0-72.0 | 648.30 | 23.6 | 30.9 | 1.979 | 1.513 | 2.780 | 45.6 | 0.838 |
| 44R-1, 70.0-72.0 | 652.00 | 21.8 | 27.8 | 2.010 | 1.572 | 2.744 | 42.7 | 0.745 |
| 44R-3, 71.0-73.0 | 655.01 | 24.9 | 33.2 | 1.931 | 1.449 | 2.735 | 47.0 | 0.887 |
| 44R-5, 70.0-72.0 | 658.00 | 20.9 | 26.5 | 2.027 | 1.602 | 2.737 | 41.5 | 0.708 |

**Table T24 (continued).**

| Core, section, interval (cm) | Depth (mbsf) | Water content (wt%) | | Density (g/cm³) | | | Porosity (%) | Void ratio |
|---|---|---|---|---|---|---|---|---|
| | | Bulk | Dry | Bulk | Dry | Grain | | |
| 45R-1, 70.0-72.0 | 661.60 | 23.5 | 30.8 | 1.960 | 1.499 | 2.729 | 45.1 | 0.821 |
| 45R-4, 70.0-72.0 | 665.24 | 21.4 | 27.2 | 2.025 | 1.592 | 2.761 | 42.4 | 0.735 |
| 46R-1, 70.0-72.0 | 671.20 | 23.1 | 30.1 | 1.983 | 1.524 | 2.759 | 44.7 | 0.810 |
| 46R-3, 70.0-72.0 | 674.20 | 24.0 | 31.6 | 1.969 | 1.496 | 2.781 | 46.2 | 0.859 |
| 46R-5, 70.0-72.0 | 677.20 | 23.2 | 30.2 | 1.973 | 1.516 | 2.739 | 44.7 | 0.807 |
| 47R-1, 70.0-72.0 | 680.90 | 26.1 | 35.3 | 1.906 | 1.409 | 2.736 | 48.5 | 0.942 |
| 47R-3, 70.0-72.0 | 682.61 | 19.1 | 23.6 | 2.082 | 1.684 | 2.754 | 38.8 | 0.635 |
| 47R-5, 70.0-72.0 | 685.61 | 22.2 | 28.5 | 2.019 | 1.571 | 2.790 | 43.7 | 0.776 |
| 48R-1, 70.0-72.0 | 690.60 | 19.7 | 24.6 | 2.071 | 1.662 | 2.767 | 39.9 | 0.664 |
| 48R-3, 70.0-72.0 | 693.60 | 19.2 | 23.8 | 2.083 | 1.683 | 2.764 | 39.1 | 0.643 |
| 48R-5, 70.0-72.0 | 696.60 | 19.7 | 24.6 | 2.057 | 1.651 | 2.737 | 39.7 | 0.658 |
| 49R-3, 70.0-72.0 | 702.22 | 19.7 | 24.6 | 2.060 | 1.654 | 2.742 | 39.7 | 0.658 |
| 49R-5, 70.0-72.0 | 705.22 | 20.8 | 26.3 | 2.037 | 1.613 | 2.752 | 41.4 | 0.705 |
| 49R-7, 70.0-72.0 | 708.22 | 19.6 | 24.4 | 2.048 | 1.646 | 2.709 | 39.2 | 0.646 |
| 50R-1, 73.0-75.0 | 709.83 | 20.5 | 25.8 | 2.127 | 1.690 | 2.948 | 42.7 | 0.744 |
| 50R-3, 73.0-75.0 | 712.83 | 21.3 | 27.0 | 2.016 | 1.588 | 2.731 | 41.9 | 0.720 |
| 50R-5, 70.0-72.0 | 715.80 | 21.6 | 27.6 | 1.996 | 1.565 | 2.703 | 42.1 | 0.728 |
| 51R-1, 70.0-72.0 | 719.40 | 18.6 | 22.8 | 2.096 | 1.706 | 2.754 | 38.0 | 0.614 |
| 51R-3, 73.0-75.0 | 722.43 | 22.1 | 28.4 | 1.988 | 1.548 | 2.713 | 42.9 | 0.752 |
| 51R-5, 70.0-72.0 | 725.40 | 19.4 | 24.0 | 2.048 | 1.651 | 2.697 | 38.8 | 0.633 |
| 52R-1, 72.0-74.0 | 729.02 | 18.5 | 22.6 | 2.085 | 1.700 | 2.724 | 37.6 | 0.602 |
| 52R-3, 69.0-71.0 | 731.99 | 19.3 | 24.0 | 2.084 | 1.680 | 2.771 | 39.4 | 0.649 |
| 52R-5, 69.0-71.0 | 734.99 | 19.6 | 24.5 | 2.065 | 1.659 | 2.748 | 39.6 | 0.656 |
| 53R-1, 70.0-72.0 | 738.60 | 18.2 | 22.3 | 2.148 | 1.756 | 2.843 | 38.2 | 0.619 |
| 53R-3, 73.0-75.0 | 741.63 | 22.5 | 29.0 | 1.970 | 1.527 | 2.690 | 43.2 | 0.762 |
| 53R-5, 70.0-72.0 | 744.60 | 19.0 | 23.4 | 2.072 | 1.679 | 2.725 | 38.4 | 0.623 |
| 54R-1, 72.0-74.0 | 748.22 | 17.5 | 21.2 | 2.114 | 1.745 | 2.729 | 36.1 | 0.564 |
| 54R-3, 74.0-76.0 | 751.24 | 19.1 | 23.7 | 2.073 | 1.676 | 2.735 | 38.7 | 0.632 |
| 54R-5, 74.0-76.0 | 754.24 | 16.4 | 19.6 | 2.168 | 1.812 | 2.778 | 34.8 | 0.533 |
| 55R-1, 70.0-72.0 | 757.80 | 21.2 | 27.0 | 2.049 | 1.613 | 2.806 | 42.5 | 0.739 |
| 55R-3, 70.0-72.0 | 760.80 | 16.8 | 20.2 | 2.150 | 1.788 | 2.765 | 35.3 | 0.547 |
| 55R-5, 70.0-72.0 | 763.80 | 17.0 | 20.5 | 2.121 | 1.761 | 2.717 | 35.2 | 0.543 |
| 56R-1, 70.0-72.0 | 767.40 | 18.6 | 22.9 | 2.109 | 1.716 | 2.783 | 38.3 | 0.622 |
| 56R-3, 70.0-72.0 | 770.40 | 17.3 | 21.0 | 2.287 | 1.891 | 3.085 | 38.7 | 0.632 |
| 57R-2, 69.0-71.0 | 778.49 | 17.6 | 21.3 | 2.171 | 1.789 | 2.851 | 37.2 | 0.593 |
| 58R-1, 70.0-72.0 | 786.60 | 16.6 | 19.9 | 2.137 | 1.782 | 2.726 | 34.6 | 0.530 |
| 58R-3, 70.0-72.0 | 789.60 | 16.9 | 20.4 | 2.135 | 1.773 | 2.741 | 35.3 | 0.546 |
| 58R-5, 70.0-72.0 | 792.60 | 16.5 | 19.7 | 2.159 | 1.803 | 2.764 | 34.8 | 0.533 |
| 59R-1, 70.0-72.0 | 796.20 | 19.8 | 24.7 | 2.066 | 1.657 | 2.759 | 39.9 | 0.665 |
| 59R-3, 70.0-72.0 | 799.20 | 21.1 | 26.8 | 2.032 | 1.602 | 2.759 | 41.9 | 0.722 |
| 59R-5, 70.0-72.0 | 802.20 | 20.1 | 25.1 | 2.058 | 1.645 | 2.757 | 40.4 | 0.677 |
| 60R-1, 70.0-72.0 | 805.80 | 18.0 | 21.9 | 2.084 | 1.709 | 2.697 | 36.6 | 0.578 |
| 60R-3, 70.0-72.0 | 808.80 | 16.3 | 19.5 | 2.164 | 1.811 | 2.764 | 34.5 | 0.526 |
| 60R-5, 70.0-72.0 | 811.80 | 15.4 | 18.2 | 2.190 | 1.853 | 2.762 | 32.9 | 0.490 |
| 61R-1, 70.0-72.0 | 815.40 | 15.9 | 19.0 | 2.167 | 1.822 | 2.750 | 33.7 | 0.509 |
| 61R-3, 61.0-63.0 | 818.31 | 15.8 | 18.8 | 2.153 | 1.812 | 2.717 | 33.3 | 0.499 |
| 61R-5, 70.0-72.0 | 821.40 | 17.4 | 21.1 | 2.105 | 1.738 | 2.710 | 35.9 | 0.559 |
| 62R-1, 70.0-72.0 | 825.00 | 15.5 | 18.4 | 2.192 | 1.851 | 2.775 | 33.3 | 0.499 |
| 62R-3, 70.0-72.0 | 828.00 | 18.4 | 22.5 | 2.079 | 1.697 | 2.707 | 37.3 | 0.595 |
| 62R-5, 70.0-72.0 | 831.00 | 16.3 | 19.5 | 2.137 | 1.789 | 2.711 | 34.0 | 0.516 |
| 63R-1, 70.0-72.0 | 834.60 | 15.8 | 18.7 | 2.195 | 1.849 | 2.792 | 33.8 | 0.510 |
| 63R-3, 69.0-71.0 | 837.59 | 16.2 | 19.3 | 2.155 | 1.806 | 2.739 | 34.1 | 0.517 |
| 63R-5, 70.0-72.0 | 840.60 | 21.6 | 27.5 | 2.025 | 1.588 | 2.769 | 42.6 | 0.743 |
| 64R-1, 68.0-70.0 | 844.18 | 19.2 | 23.8 | 2.075 | 1.676 | 2.744 | 38.9 | 0.637 |
| 64R-5, 70.0-72.0 | 850.20 | 16.9 | 20.4 | 2.146 | 1.783 | 2.763 | 35.5 | 0.550 |
| 65R-1, 70.0-72.0 | 853.80 | 22.2 | 28.6 | 2.009 | 1.562 | 2.770 | 43.6 | 0.773 |
| 65R-3, 70.0-72.0 | 856.80 | 15.0 | 17.7 | 2.211 | 1.879 | 2.783 | 32.5 | 0.481 |
| 66R-1, 70.0-72.0 | 863.40 | 14.3 | 16.7 | 2.211 | 1.895 | 2.742 | 30.9 | 0.447 |
| 66R-3, 70.0-72.0 | 866.40 | 15.2 | 18.0 | 2.199 | 1.864 | 2.770 | 32.7 | 0.486 |
| 66R-5, 70.0-72.0 | 869.40 | 14.1 | 16.4 | 2.220 | 1.907 | 2.748 | 30.6 | 0.441 |
| 67R-1, 70.0-72.0 | 873.00 | 15.5 | 18.3 | 2.156 | 1.822 | 2.703 | 32.6 | 0.484 |
| 67R-3, 70.0-72.0 | 876.00 | 16.1 | 19.2 | 2.162 | 1.815 | 2.748 | 34.0 | 0.514 |
| 67R-5, 69.0-71.0 | 878.99 | 16.1 | 19.2 | 2.171 | 1.821 | 2.767 | 34.2 | 0.520 |
| 68R-2, 70.0-72.0 | 883.90 | 14.7 | 17.3 | 2.181 | 1.860 | 2.711 | 31.4 | 0.458 |
| 68R-2, 125.0 127.0 | 884.45 | 15.4 | 18.3 | 2.192 | 1.854 | 2.769 | 33.1 | 0.494 |
| 68R-6, 70.0-72.0 | 889.40 | 16.2 | 19.4 | 2.158 | 1.807 | 2.747 | 34.2 | 0.520 |
| 69R-1, 70.0-72.0 | 892.00 | 14.2 | 16.5 | 2.196 | 1.885 | 2.707 | 30.4 | 0.436 |
| 69R-3, 70.0-72.0 | 895.00 | 14.2 | 16.6 | 2.212 | 1.897 | 2.739 | 30.7 | 0.443 |

**Table T24 (continued).**

| Core, section, interval (cm) | Depth (mbsf) | Water content (wt%) | | Density (g/cm$^3$) | | | Porosity (%) | Void ratio |
|---|---|---|---|---|---|---|---|---|
| | | Bulk | Dry | Bulk | Dry | Grain | | |
| 69R-5, 70.0-72.0 | 898.00 | 14.6 | 17.1 | 2.191 | 1.872 | 2.720 | 31.2 | 0.453 |
| 70R-1, 69.0-71.0 | 901.59 | 17.3 | 20.9 | 2.107 | 1.744 | 2.704 | 35.5 | 0.551 |
| 70R-3, 70.0-72.0 | 904.60 | 19.6 | 24.3 | 2.045 | 1.645 | 2.700 | 39.1 | 0.642 |
| 70R-5, 70.0-72.0 | 907.60 | 18.2 | 22.2 | 2.080 | 1.702 | 2.697 | 36.9 | 0.585 |
| 71R-1, 70.0-72.0 | 911.20 | 19.7 | 24.5 | 2.051 | 1.647 | 2.719 | 39.4 | 0.651 |
| 71R-2, 70.0-72.0 | 912.70 | 14.5 | 17.0 | 2.225 | 1.902 | 2.778 | 31.5 | 0.461 |
| 71R-3, 70.0-72.0 | 914.20 | 13.7 | 15.9 | 2.242 | 1.935 | 2.763 | 30.0 | 0.428 |
| 72R-1, 70.0-72.0 | 920.90 | 13.7 | 15.9 | 2.218 | 1.914 | 2.721 | 29.6 | 0.421 |
| 72R-3, 70.0-72.0 | 923.90 | 13.4 | 15.5 | 2.259 | 1.955 | 2.780 | 29.7 | 0.422 |
| 72R-5, 70.0-72.0 | 926.90 | 13.6 | 15.7 | 2.229 | 1.926 | 2.735 | 29.6 | 0.420 |
| 73R-1, 70.0-72.0 | 930.60 | 13.5 | 15.7 | 2.253 | 1.947 | 2.774 | 29.8 | 0.424 |
| 73R-5, 70.0-72.0 | 936.60 | 15.7 | 18.6 | 2.165 | 1.826 | 2.732 | 33.2 | 0.496 |
| 75R-1, 70.0-72.0 | 949.90 | 15.7 | 18.7 | 2.184 | 1.841 | 2.770 | 33.6 | 0.505 |
| 75R-3, 70.0-72.0 | 952.90 | 17.9 | 21.8 | 2.111 | 1.733 | 2.747 | 36.9 | 0.585 |